Substantive Evidence of Initial Habitation in the Remote Pacific:

Archaeological Discoveries at Unai Bapot in Saipan, Mariana Islands

Mike T. Carson
Hsiao-chun Hung

Access Archaeology

Archaeopress Access Archaeology

About Access Archaeology

Access Archaeology offers a different publishing model for specialist academic material that might traditionally prove commercially unviable, perhaps due to its sheer extent or volume of colour content, or simply due to its relatively niche field of interest.

All *Access Archaeology* publications are available in open-access e-pdf format and in (on-demand) print format. The open-access model supports dissemination in areas of the world where budgets are more severely limited, and also allows individual academics from all over the world the chance to access the material privately, rather than relying solely on their university or public library. Print copies, nevertheless, remain available to individuals and institutions who need or prefer them.

The material is professionally refereed, but not peer reviewed. Copy-editing takes place prior to submission of the work for publication and is the responsibility of the author. Academics who are able to supply print-ready material are not charged any fee to publish (including making the material available in open-access). In some instances the material is type-set in-house and in these cases a small charge is passed on for layout work.

This model works for us as a publisher because we are able to publish specialist work with relatively little editorial investment. Our core effort goes into promoting the material, both in open-access and print, where *Access Archaeology* books get the same level of attention as our core peer-reviewed imprint by being included in marketing e-alerts, print catalogues, displays at academic conferences and more, supported by professional distribution worldwide.

Open-access allows for greater dissemination of the academic work than traditional print models, even lithographic printing, could ever hope to support. It is common for a new open-access e-pdf to be downloaded several hundred times in its first month since appearing on our website. Print sales of such specialist material would take years to match this figure, if indeed it ever would.

By printing 'on-demand', meanwhile, (or, as is generally the case, maintaining minimum stock quantities as small as two), we are able to ensure orders for print copies can be fulfilled without having to invest in great quantities of stock in advance. The quality of such printing has moved forward radically, even in the last few years, vastly increasing the fidelity of images (highly important in archaeology) and making colour printing more economical.

Access Archaeology is a vehicle that allows us to publish useful research, be it a PhD thesis, a catalogue of archaeological material or data, in a model that does not cost more than the income it generates.

This model may well evolve over time, but its ambition will always remain to publish archaeological material that would prove commercially unviable in traditional publishing models, without passing the expense on to the academic (author or reader).

Archaeopress Access Archaeology

Substantive Evidence of Initial Habitation in the Remote Pacific:

Archaeological Discoveries at Unai Bapot in Saipan, Mariana Islands

Mike T. Carson
Hsiao-chun Hung

Access Archaeology

Archaeopress Access Archaeology

Archaeopress Publishing Ltd
Gordon House
276 Banbury Road
Oxford OX2 7ED

www.archaeopress.com

ISBN 978 1 78491 665 7
ISBN 978 1 78491 666 4 (e-Pdf)

Table of Contents

Chapter 1 Unai Bapot and Earliest Remote Oceanic Settlement 1

Chapter 2 Project Context and Questions 4

Physical Environment 4

Land Use 6

Archaeological Setting 7

2005 Investigation 9

Role of the 2016 Investigation 19

Chapter 3 Investigative Procedures 20

Chapter 4 New Findings: Stratigraphy and Dating 33

Radiocarbon Dating and Marine Reservoir Correction 33

Datable Materials within Calcrete 39

An Alternative Marine Reservoir Proposal? 39

Current Investigation 40

Layer VIII 43

Layer VII 43

Layer VI-B 46

Layer VI-A 47

Layer V 48

Layer IV 50

Layer III-B 50

Layer III-A 51

Layer II 51

Layer I 51

Chapter 5 New Findings: Overall Archaeological Contents 52

Chapter 6 New Findings: Traces of Structural Features 80

Layer VII, Features G, H, I, and Post Moulds 81

Layer VI-B, Features D, E, and F 86

Layer VI-A, Feature C 87

Layer V, Features A and B 91

Chapter 7 New Findings: Pottery Artefacts 93

Layer VII Pottery 95

Layer VI-B Pottery 99

Layer VI-A Pottery 102

Layer V Pottery ... 105
Layer IV Pottery ... 110
Layer III-B Pottery ... 111
Layer III-A Pottery ... 114
Layer II Pottery ... 115
Layer I Pottery ... 117
Chapter 8 New Findings: Non-Pottery Artefacts ... 120
Adzes ... 120
Stone Flakes, Fragments, and Raw Materials ... 127
Pounders and Grinding Basins ... 133
Slingstone Fragment ... 136
Polished Balls ... 136
Fishing Gear ... 137
Sea Urchin Spine Abraders ... 140
Shell Discs ... 141
Shell Bands ... 145
Shell Circlets ... 146
Shell Rings ... 147
Cypraea sp. Shell Beads ... 148
Conus spp. and Other Small Round Shell Beads ... 149
Shell Pendants ... 154
Shell Ear Ornaments ... 156
Drilled Turbo spp. Shells ... 157
Drilled and Cut Cypraea spp. Shells ... 159
Smoothed-edge Bivalve Shell Objects ... 160
Drilled Shark Tooth ... 162
Bevelled Shell Triangle ... 162
"Corkscrew" Shell ... 163
Edge-worked Nacreous Bivalve Shells ... 164
Worked Nacreous Shell Debitage ... 165
Chapter 9 New Findings: Midden of Animal Food Remains ... 167
Shellfish Remains ... 167
Animal Bones ... 169
Chapter 10 Answering the Initial Research Questions ... 172
Chapter 11 Larger Research Implications ... 174
References ... 176

List of Tables

Table 1. Summary of traditional cultural materials recovered from the 2005 test pits, TU-1 and -2, Layers I-A (youngest) through IV-A (oldest)....12

Table 2. Radiocarbon dating results from 2005, using updated marine reservoir correction and calibration curves. 18

Table 3. Stratigraphic layer descriptions, as observed in October 2016....32

Table 4. Paired charcoal and Anadara sp. shells validating a ΔR of -49±61 in the Mariana Islands....35

Table 5. Results of radiocarbon dating. 41

Table 6. Summary of archaeological material from the October 2016 excavation....56

List of Figures

Figure 1. Position of the Mariana Islands in the Asia-Pacific region, noting the cross-regional settlement chronology. 1

Figure 2. Known earliest settlement sites of 1500–1100 B.C. in the Mariana Islands....2

Figure 3. Study area, shown on an enlarged (1:5000 scale) portion of 2005 satellite image of Saipan. 4

Figure 4. Updated contour map of the study area, showing surface remains, prior excavations, and renewed excavations....5

Figure 5. Megalithic latte remains on cleared site surface in 2005, view to east....10

Figure 6. Portion of broken lusong grinding mortar in 2005, view to north....10

Figure 7. Profile of TU-2 from 2005 excavation, view to west....11

Figure 8. Examples of excavated pottery with reconstructed vessel shapes in stratigraphic order, according to the 2005 test pit findings....14

Figure 9. Samples of excavated stone, shell, and bone tools from 2005 findings. 15

Figure 10. Samples of shell and coral ornaments from 2005 findings....16

Figure 11. Chronological trends in marine shellfish remains from 2005 findings. 17

Figure 12. Hand-clearing of the vegetation cover, while preparing the 4 by 4 m excavation area....21

Figure 13. Outline of the 4 by 4 m excavation area, ready to begin excavation....21

Figure 14. Excavation in process of the uppermost stratigraphic layer, in the designated Quadrant 1 of the northeast portion of the excavation area. 22

Figure 15. Exposing the entire excavation area, Quadrants 1 through 4, at 20 cm depth within Layer I. 22

Figure 16. Continued exposure of stratigraphic layers by hand-controlled excavation....23

Figure 17. Loading buckets for fine-mesh sieving. 23

Figure 18. Carrying buckets to a sieving station. 24

Figure 19. Fine-mesh sieving in progress at station 1 of 2....24

Figure 20. Fine-mesh sieving in progress at station 2 of 2..25
Figure 21. Exposing a heated-rock feature as a discrete unit within the stratigraphic context. 25
Figure 22. Collection of sedimentary samples for analysis of possible palaeo-botanical materials. 27
Figure 23. Flotation of sediment samples in progress. 27
Figure 24. Processing of the excavated materials, involving washing, separation of material categories, and thorough drying in preparation for recording of counts, weights, and detailed descriptions. 28
Figure 25. Stratigraphy exposed at end of October 2016 excavation, showing Quadrant 2, view to southeast...30
Figure 26. Stratigraphic profile, according to observations in October 2016. 31
Figure 27. Approximate reconstructions of the site setting during earliest settlement periods as compared to the modern conditions. 33
Figure 28. Sample Beta-448701 of Anadara sp. shell in dorsal (left) and ventral (right) views, from Feature G of Layer VII, prior to radiocarbon dating by Beta Analytic. 34
Figure 29. Samples Beta-448702 (left) and Beta-452141 (right) from Feature G of Layer VII, containing insufficient carbon for radiocarbon dating. 37
Figure 30. Sample Beta-453138 from Feature H of Layer VII. Left image shows the whole sample, removed by trowel from the feature...38
Figure 31. Charcoal and ash within Feature G of Layer VII, during excavation, view to south. 38
Figure 32. Plan view of Layer VII..44
Figure 33. Examples of earliest artefacts from the 2005 and 2016 excavations at Unai Bapot. Scale bars are in 1-cm increments...45
Figure 34. Plan view of Layer VI-B. 46
Figure 35. Plan view of Layer VI-A. 48
Figure 36. Plan view of Layer V. 49
Figure 37. Raw counts of pottery fragments and grams of marine shell per layer. 53
Figure 38. Approximate concentrations of numbers of pottery fragments and grams of marine shell per 100 litres of excavated sediment in each layer..54
Figure 39. Distribution of major artefact categories in stratigraphic layers. 55
Figure 40. Near base of pit of Feature G in Layer VII, during excavation in Quadrant 2, view to south-southeast...82
Figure 41. Closer view near base of Feature G in Layer VII, during excavation in Quadrant 2, view downward to south. 82
Figure 42. Initial exposure of heated-rock hearths of Features H and I in Layer VII, during excavation in Quadrant 3, view to southwest. 83
Figure 43. Pedestalled portions of heated-rock hearths of Features H and I in Layer VII, during excavation in Quadrant 3, view down to north. 83
Figure 44. Post moulds, after excavation near base of Layer VII, view to south. Scale bars are in 20-cm increments..84

Figure 45. Post moulds, after excavation near base of Layer VII, view down to southeast. 85
Figure 46. Post moulds P-3-1 (right), P-3-2 (partial in top center), and P-3-3 (lower left) in Quadrant 3, after excavation near base of Layer VII, view to north-northwest. 85
Figure 47. Exposure of heated-rock hearth of Feature D in Layer VI-B, during excavation in Quadrant 4, view down to north. 86
Figure 48. Initial exposure of heated-rock hearths of Features E and F in Layer VI-B, during excavation in Quadrant 1, view down to north. 87
Figure 49. Initial exposure of pottery concentration at top of Feature C in Layer VI-A, during excavation in Quadrant 3, view down to west. 88
Figure 50. Pedestalled portion of heated-rock hearth of Feature C in Layer VI-A, during excavation in Quadrant 3, view down to west. 88
Figure 51. Preserved portion of carinated red-slipped bowl in partially pedestalled heated-rock hearth of Feature C in Layer VI-A, during excavation of Quadrant 3, view to east.............................89
Figure 52. Detail of preserved portion of carinated red-slipped bowl in heated-rock hearth of Feature C in Layer VI-A, during excavation of Quadrant 3, view down to east...89
Figure 53. Fire-reddened and hardened ashy matrix at the base of Feature C, during excavation in Quadrant 3, view down to west. 90
Figure 54. Sample Beta-448705 from Feature C of Layer VI-A. 90
Figure 55. Initial exposure of heated-rock hearth of Feature A in Layer V, during excavation in Quadrants 3 and 4, view to west. 91
Figure 56. Pedestalled portions of heated-rock hearth of Feature A in Layer V, during excavation in Quadrants 3 and 4, view to west. 92
Figure 57. Pedestalled surface of pit of Feature B in Layer V, during excavation in Quadrant 3, view to southeast..92
Figure 58. Overall chronological trends in major categories of pottery. 94
Figure 59. Pieces of a carinated bowl with everted lip, two pieces shown in two views, recovered from Layer VII. 96
Figure 60. Pieces of a round-shouldered bowl with everted lip, recovered from Layer VII.....................96
Figure 61. Rim fragments of nearly straight-sided bowls, with slight outcurving, recovered from Layer VII. 97
Figure 62. Rare examples of flat-cornered base fragments, recovered from Layer VII. 98
Figure 63. Decorated pottery fragment, recovered from Feature G of Layer VII....................................98
Figure 64. Comparison of red-slipped (left) versus blackware (right) everted rims, recovered from Layer VII...98
Figure 65. Pieces of carinated red-slipped bowl, recovered from Layer VI-B. 99
Figure 66. Fragment of round-shouldered bowl, recovered from Layer VI-B. 100
Figure 67. Fragments of blackware rims, broken from everted (upper) and nearly straight-sided (lower) variants, recovered from Layer VI-B...100
Figure 68. Rims broken from slightly incurved bowls, recovered from Layer VI-B. 100

Figure 69. Decorated blackware rim, recovered from Layer VI-B. 101
Figure 70. Decorated blackware carination, with partly retained white lime infill, recovered from Feature D of Layer VI-B...101
Figure 71. Paddle-impressed pottery fragment, recovered from Layer VI-B. 101
Figure 72. Examples of fragments from everted-rim bowls, with varying degree of sharply carinated to rounded profile, recovered from Layer VI-A. 102
Figure 73. Rim of slightly incurved bowl, recovered from Layer VI-A..103
Figure 74. Decorated red-slipped pottery fragments, with traces of white lime infill, recovered from Layer VI-A. 103
Figure 75. Decorated blackware fragments, with traces of white lime infill, broken from carinated bowl, recovered from Quandrant 3 in Layer VI-A...104
Figure 76. Drilled potsherd, shown in exterior (left) and interior (right views), recovered from Layer VI-A. 104
Figure 77. Fragments of carinated red-slipped bowl with everted rim, recovered from Layer V. 106
Figure 78. Fragment of very small carinated red-slipped bowl with everted rim, recovered from Layer V. 106
Figure 79. Rim of narrow straight-sided cup, recovered from Layer V. 106
Figure 80. Rare example of circle-stamped red-slipped handle, with traces of white lime infill, shown in three views, recovered from Layer V. 107
Figure 81. Portion of very small circle- stamped red-slipped pottery, shown in three views, recovered from Layer V. 107
Figure 82. Two red-slipped pottery fragments, with curvilinear garlands and circles, retaining traces of white lime infill, recovered from Layer V..108
Figure 83. Two red-slipped rims, decorated over the lip, showing row of circles (left) and row of half-circles (right), recovered from Layer V...108
Figure 84. Red-slipped pottery fragment, modified by notching of the rim, recovered from Layer VI-A......108
Figure 85. Fragments of red-slipped bowl with everted rim, recovered from Layer IV. 109
Figure 86. Examples of narrow straight-sided cup (upper) and large flat-based pan (lower), recovered from Layer IV. 109
Figure 87. Bold-line incised pottery rim fragment, recovered from Layer IV.......................................110
Figure 88. Variations of narrow cups, recovered from Layer III-B. 111
Figure 89. Variations of thick-walled, flat-bottomed pans, recovered from Layer III-B. 112
Figure 90. Example of surface-roughened red-slipped large bowl fragment, with circle-stamped lip, recovered from Layer III-B. 113
Figure 91. Variations of circle-stamped lip pieces, recovered from Layer III-B....................................113
Figure 92. Rim fragments of narrow straight-sided cup, recovered from Layer III-A............................114
Figure 93. Conjoined rim and base fragments of a shallow flat-bottomed pan, recovered from Layer III-A. ...114
Figure 94. Rim of red-slipped slightly incurved bowl, recovered from Layer III-A................................115
Figure 95. Rim of thick-walled, non-slipped, slightly incurved bowl, recovered from Layer III-A..........115
Figure 96. Decorated lip pieces, recovered from Layer III-A..115

Figure 97. Rims from straight-sided cups, recovered from Layer II. 116
Figure 98. Examples of rim and base fragments of two different pans, recovered from Layer II. 116
Figure 99. Thick incurving rims pieces, recovered from Layer II. 117
Figure 100. Variations of thick incurving rims pieces, recovered from Layer I. 118
Figure 101. Example of thick straight-sided rim, recovered from Layer I. 118
Figure 102. Decorated portions of upward-facing lips of rim fragments, recovered from Layer I..........118
Figure 103. Exceptionally thickened rim piece, shown in four views, recovered from Layer I. 119
Figure 104. Unusual cornered piece, recovered from Layer I. Scale bars are in 1-cm increments. 119
Figure 105. Stratigraphic distribution of adzes (whole, partial, and pre-form varieties) of different material categories. 121
Figure 106. Polished chert adzes from Layer VI-B (upper left) and Layer VI-B (lower right), shown in two views. 122
Figure 107. Broken tip of polished chert adze or chisel, shown in three views, recovered from Layer VI-A. 123
Figure 108. Chert adze pre-form, recovered from Layer VI-A. 123
Figure 109. Tridacna sp. adze fragment (upper row, two views) and pre-form (lower row, two views), recovered from Layer III-B. 124
Figure 110. Tridacna sp. adze fragment (upper row, two views) and pre-form (lower row, two views), recovered from Layer III-B. 125
Figure 111. Terebra sp. shell adze or chisel (upper row, two views) from Layer III-A and broken Conus sp. shell adze (lower row, two views) from Layer I. 126
Figure 112. Stratigraphic distribution of stone flakes and raw materials, shown in values of raw counts per stratigraphic layer. 128
Figure 113. Stratigraphic distribution of chert flakes, flakes with polish, and adze-related materials, shown in values of raw counts per stratigraphic layer. 129
Figure 114. Examples of chert flakes. 130
Figure 115. Examples of volcanic stone flakes. 131
Figure 116. Examples of limestone flakes. 132
Figure 117. Examples of limestone crystal raw materials, recovered from Layer VI-A. 133
Figure 118. Fragment of limestone grinding stone, shown in two views, recovered from Layer I. 134
Figure 119. Limestone pounder fragment from Layer VI-B (lower row) and complete pounder from Layer VI-A (upper row), shown in two views each. 134
Figure 120. Two limestone pounder fragments, shown in two views per row, recovered from Layer IV. 135
Figure 121. Volcanic stone pounder fragment, shown in two views, recovered from Layer I. 135
Figure 122. Fragment of limestone slingstone, shown in two views, recovered from Layer I. 136
Figure 123. Ball of limestone from Layer III-A (left) and another of polished probable Tridacna sp. shell from Layer VI-A (right). 136
Figure 124. Broken net weight made of Asaphis sp. shell, shown in two views, recovered from Layer VI-A....137

Figure 125. Net weight made of limestone crystal, shown in three views, recovered from Feature B in Layer V. 138
Figure 126. Nacreous shell fishing hook pieces, recovered from Layer VI-B. 138
Figure 127. Nacreous shell fishing hook pieces, recovered from layers IV-A through II. 139
Figure 128. Sea urchin spine abraders, recovered from lower layers. 140
Figure 129. Sea urchin spine abraders, recovered from middle and upper layers. 141
Figure 130. Examples of different categories of shell ornaments, recovered from 2016 excavation. 142
Figure 131. Conus spp. shell disc pieces from Layers VII and VI-B. 143
Figure 132. Conus spp. shell disc pieces from Layer VI-A. 144
Figure 133. Spondylus sp. shell disc, shown in two views, recovered from Layer I. 144
Figure 134. Shell band fragments. 145
Figure 135. Shell circlet fragments, each shown in two views. 146
Figure 136. Larger-diameter shell ring fragments. 147
Figure 137. Smaller-diameter shell rings. 147
Figure 138. Cypraea sp. shell bead pieces. 148
Figure 139. Conus spp. shell beads in process, shown in two views each, recovered from Layer VII. 149
Figure 140. Conus spp. and possibly other taxa of shell beads, recovered from Layer VII. 150
Figure 141. Conus spp. shell beads in process, shown in two views each, recovered from Layer VI-B. 151
Figure 142. Conus spp. and possibly other taxa of shell beads, recovered from Layer VII. 151
Figure 143. Conus sp. shell bead in process, shown in two views, recovered from Layer VI-A. 152
Figure 144. Conus spp. and possibly other taxa of shell beads, recovered from Layer VI-A. 152
Figure 145. Conus spp. and possibly other taxa of shell beads, recovered from Layer V. 153
Figure 146. Conus spp. and possibly other taxa of shell beads, recovered from Layer IV. 153
Figure 147. Conus spp. and possibly other taxa of shell beads, recovered from Layer III-B. 153
Figure 148. Conus sp. shell pendant, shown in four views, recovered From Layer VII. 154
Figure 149. Fragment of nacreous shell pendant, shown in two views, recovered From Layer IV. 155
Figure 150. Elongate shell pendant, shown in two views, recovered From Layer III-B. 155
Figure 151. Shell ear ornament, shown in two views, recovered From Layer VI-B. 156
Figure 152. Two nearly identically shaped ear ornament fragments, recovered from Layer II. 157
Figure 153. Complete probable lime container, made of Turbo sp. shell, shown in three views, recovered from Layer II. 158
Figure 154. Fragment of drilled Turbo sp. shell, recovered from Layer VI-B. 158
Figure 155. Pieces of drilled and cut Cypraea spp. shells. 159
Figure 156. Two smoothed-edge shell artefacts of probable Anadara sp. shell, shown in three views each, recovered from Layer VI-B. 160

Figure 157. Two smoothed-edge shell artifacts of probable Anadara sp. shell, shown in three views each, recovered from Layer VI-A. 161

Figure 158. Smoothed-edge shell artefact of nacreous shell, shown in two views, recovered from Layer V. 161

Figure 159. Fragment of drilled shark tooth (upper) and another unmodified fragment (lower), shown in three views, recovered from Layer IV....................162

Figure 160. Bevelled nacreous shell triangle, shown in three views, recovered from Layer VII. 163

Figure 161. "Corkscrew" shaped Terebra sp. shell artefact, recovered from Layer IV. 163

Figure 162. Thoroughly edge-worked nacreous shell, shown in two views, recovered from Feature I within Layer VII. 164

Figure 163. Edge-worked Isognomon sp. shell, shown in two views, recovered from Layer VI-A. 165

Figure 164. Examples of pieces of worked nacreous shell. Item at lower right was from Layer VI-B. All other items were from Layer VI-A. 166

Figure 165. Major chronological trends in marine shellfish remains, based on collections from Quadrant 1. 168

Figure 166. Example of nearly complete Haliotis sp. shell, shown in dorsal (left) and ventral (right) views, recovered from Layer VII. 169

Figure 167. Stratigraphic distribution of vertebrate animal bones, shown in raw counts per stratigraphic layer. 170

Preface

This book discloses the latest excavation findings of October 2016 at Unai Bapot in Saipan, accounting for the evidence of one of the oldest known habitation sites in the entire region of Remote Oceania, dating just prior to 1500 B.C. Given the significance of the findings, the raw data are presented here in detail as a source of primary information. Other studies will continue and may yet be published elsewhere, and meanwhile the primary datasets are shared in this comprehensive synthesis.

The current results have been possible with funding granted by the Australian Research Council (DP140100384) and the Chiang Ching-kuo Foundation (RG017-P-13, 2014–2016). This project had been a long time in development, prompted by a renewed interest in 2005. Other archaeologists had worked at the site since the 1920s, and a project in 2005 aimed to nominate the site in the U.S. National Register of Historic Places. The 2005 effort verified the deep stratigraphic layers and ancient dating of the site, and eventually funding was secured as noted for more research at last conducted in 2016.

The 2016 investigation at Unai Bapot was performed in partnership with the Historic Preservation Office of the Commonwealth of the Northern Mariana Islands, with special thanks owed to Mertie Kani, John Diego Palacios, and Jim Pruitt for their professional support and for contributing to the field excavation, along with other staff members Lufo Babauta, Jose Jesus Fitial, Jennifer Sablan, Juan Salas, and Abraham Tenorio. A number of Saipan residents worked with us during the excavation, including Lufo Babauta Junior, John Castro, Cassius Fitial, Erik Kani, and Angel Palacios. We are blessed that Hiro Kurashina, Peter Bellwood, Scott Russell, Rebecca Stephenson, and Zhenhua Deng participated in the field excavation and offered advice toward the success of the project. Collaborations with Larisa Ford, Brian Leon Guerrero, Emily Sablan, Jeried Calaor, and Kyle Ngiratregd at the U.S. Fish and Wildlife Service enhanced this project. Scott Russell, Eulalia Arriola, and Honora Tenorio at the Northern Mariana Islands Humanities Council enabled productive community outreach and sharing of information at public lectures and news interviews.

Chapter 1

Unai Bapot and Earliest Remote Oceanic Settlement

Excavation during October 2016 unearthed the buried palaeo-seashore layers of the oldest so far known habitation in Remote Oceania, specifically at Unai Bapot in Saipan of the Mariana Islands (Figures 1 and 2). Radiocarbon dating now has been confirmed at 1697–1531 B.C. for the oldest cultural layers situated at the palaeo-seashore, followed by dating of the next overlaying stratigraphic unit at 1437–1288 B.C. These results validated the prior findings from two small test pits in 2005, wherein two cross-confirming radiocarbon dates had indicated a pre-1500 B.C. age (Carson 2008, 2014a), as compared to the preceding reports of vaguely pre-dating 1000 B.C. (Bonhomme and Craib 1987; Marck 1978; Ward and Craib 1985). Another excavation in 2008 documented a layer of a stable backbeach dated around 1100 B.C., with inconclusive results from only a small sample window into the deeper and older layers (Clark et al. 2010), such that the newest discoveries have resolved a long-standing problem in refining the dating and context of the site's initial habitation.

The apparent dating at Unai Bapot was slightly earlier than so far has been verified at any other first-settlement site in the Mariana Islands and indeed in the entire Remote Oceanic region, thus attracting attention for clarifying the timing and context of a major episode in human inhabitation of a large part of the globe. Even without accepting the dating specifically at Unai Bapot, a number of other sites dating close to 1500 B.C. have distinguished the Marianas as the place of initial cultural settlement of Remote Oceania (Carson and Kurashina 2012), made possible by the world's longest ocean-crossing migration of its time, exceeding 2000 km (Craib 1999; Hung et al. 2011). The first Marianas settlement certainly pre-dated the next attested cultural horizon in other parts of Remote Oceania around 1100 B.C. in Southern Melanesia and West Polynesia (Denham et al. 2012). The singular instance of oldest dating at Unai Bapot potentially could re-direct and re-focus research of this rarely captured view of first human contact in a previously uninhabited region of the world.

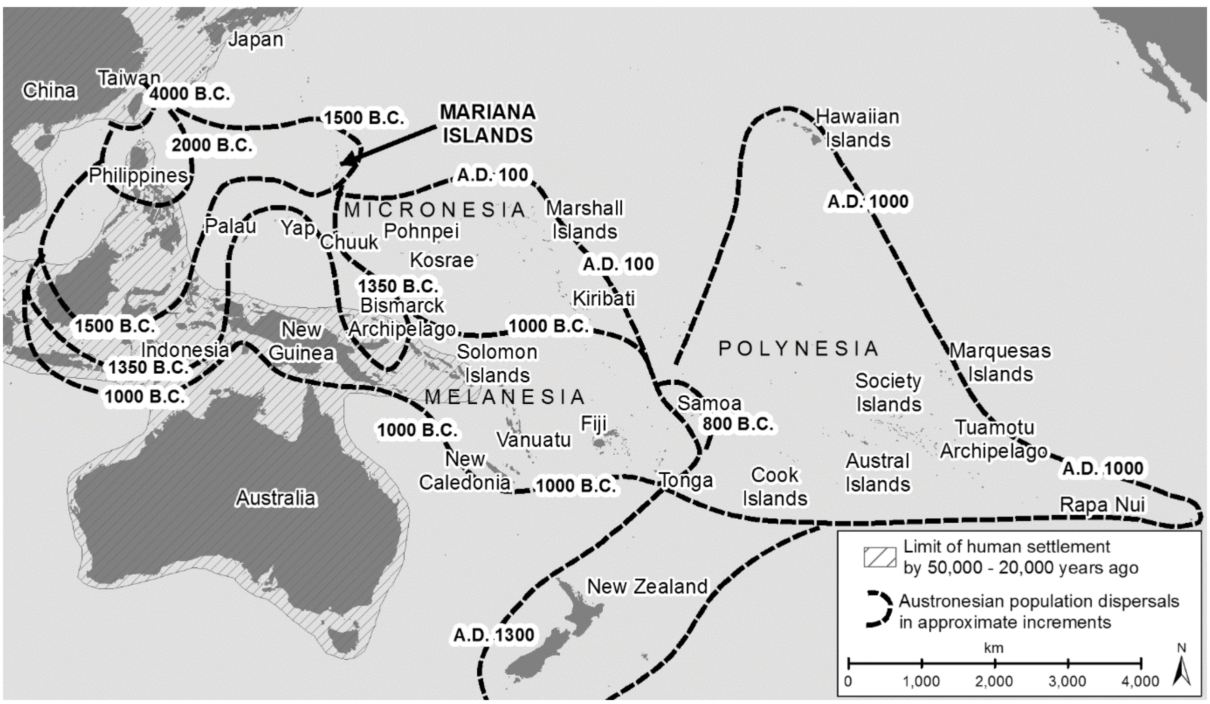

FIGURE 1. POSITION OF THE MARIANA ISLANDS IN THE ASIA-PACIFIC REGION, NOTING THE CROSS-REGIONAL SETTLEMENT CHRONOLOGY.

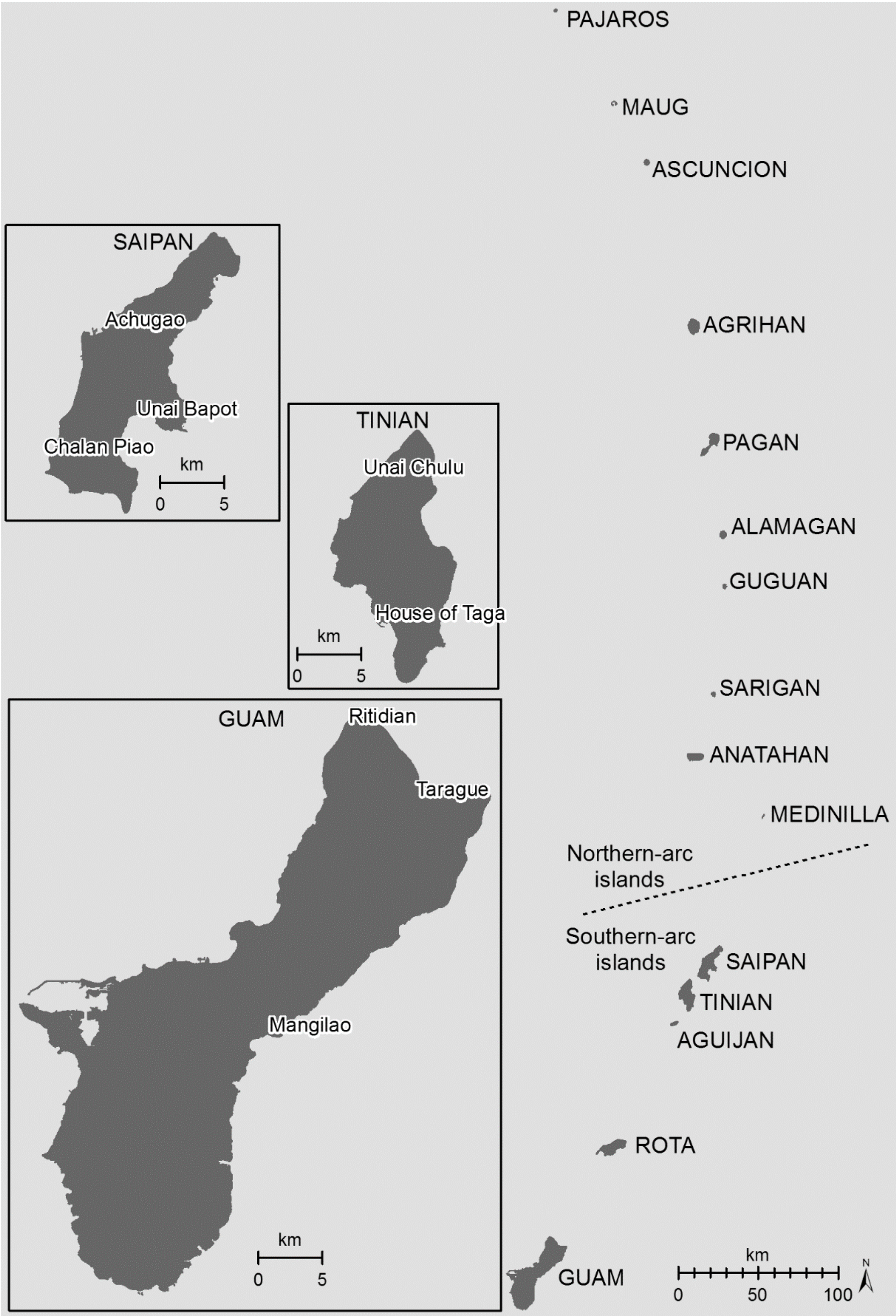

FIGURE 2. KNOWN EARLIEST SETTLEMENT SITES OF 1500–1100 B.C. IN THE MARIANA ISLANDS.

A critical review of Marianas first-settlement dating had concluded initial cultural presence at a number of sites of separate islands absolutely by 1500 B.C., with the possibility of discovering slightly older material in cases that have not yet been validated (Carson 2014a; Carson and Kurashina 2012). One of those prospective pre-1500 B.C. candidates was at Unai Bapot, hence the continued research with new results as reported here. Other acknowledged pre-1500 B.C. possibilities referred to the older-extending portions of radiocarbon date ranges at a few sites, as well as the palaeo-environmental indicators of initial anthropogenic impacts. Most recently at the Ritidian Site in Guam, the initial pottery-bearing horizon in one location was documented in a palaeo-lagoon bed of *Halimeda* sp. algal bioclasts directly dated at 2122–1734 B.C., overlain by the next cultural layer dated at 1456–1096 B.C. (Carson 2017a, 2017b).

The ancient contexts of first-settlement sites have been more thoroughly understood within the last decade of research in the Marianas, and this new knowledge has allowed more productive re-investigation at sites such as Unai Bapot. These oldest sites contained distinctive red-slipped pottery and other artefacts in ancient shoreline-oriented residential habitations, definitely pre-dating 1100 B.C. and therefore associated with a period of higher sea level during the mid-Holocene highstand (Dickinson 2000, 2003; Kayanne et al. 1993). Investigations at the Ritidian Site in Guam have illustrated the ancient lagoon and associated habitats that had existed within and around the first-settlement sites at 1500 B.C. (Carson 2012a, 2017a, 2017b). A large-format excavation at House of Taga in Tinian has exposed more than 90 sq m of the ancient living surface, with post moulds and stonework features along the ancient shoreline of 1500 B.C. (Carson 2014a; Carson and Hung 2015).

The newest (October 2016) excavation at Unai Bapot uncovered an area of 4 by 4 m (16 sq m), thus constituting so far the largest single contiguous excavation at the site, officially listed in the U.S. National Register of Historic Places as the Bapot Latte Site (SP-1-0013) was concerned with the buried cultural layers at the site. An investigation in 2005 had provided updated mapping and recording of numerous stone ruins and artefacts on the surface, a 1-m contour map of the site area, and two 1 by 2 m test excavations in support of a nomination of the site to the National Register of Historic Places (Carson 2005; Carson and Welch 2005). The new 2016 excavation therefore could focus on expanding knowledge of the subsurface layers, building on the prior documentation.

The research project entailed excavation during October 2016, followed by data analysis through January 2017. The research team consisted of Dr. Mike T. Carson and Dr. Hsiao-chun Hung as co-directors and investigators. The team worked closely with the Historic Preservation Office (HPO) of the Commonwealth of the Northern Mariana Islands (CNMI). Training opportunities were provided for staff members of HPO, including the excavation and processing of artefacts for analysis. Additionally, partnership with the U.S. Fish and Wildlife Service supported training opportunities for staff from the Guam National Wildlife Refuge. Furthermore, the CNMI Humanities Council coordinated public outreach in a series of open lecture presentations, news media reports, and site visits during and after the investigation.

All work tasks conformed to the "Content, Format, and Submission Standards for Final Reports of Archaeological Projects in the CNMI." This work also complied with pertinent sections of the National Historic Preservation Act (NHPA) and associated 36 Code of Federal Regulations (CFR) Part 800, as well as with CNMI Public Law 3-39. Toward ensuring these standards and regulations, the involvement of the CNMI HPO was critical.

Here we present the knowledge gained from investigating at Unai Bapot, working toward a new understanding of the initial cultural inhabitation of the ancient seashores of the Remote Oceanic region, evidently beginning just prior to 1500 B.C. and then continuing in a long sequence thereafter. Following this introductory chapter (Chapter 1), the presentation is structured to address the project context (Chapter 2), investigative procedures (Chapter 3), material findings (Chapters 4 through 9), and implications of the new discoveries (Chapters 10 and 11). The raw data are disclosed in full detail to substantiate the most robust interpretations and to withstand future interrogations of the findings.

Chapter 2

Project Context and Questions

The project concerned the Bapot Latte Site (SP-1-0013), situated within an area covering approximately 500 sq m in Laulau, along the east coast of Saipan in the CNMI (Figures 3 and 4). The key portion of interest was in the range of 80 to 135 m from the shoreline and 4.6 to 8 m above sea level. The 2016 hand-controlled excavation concentrated within a 4 by 4 m area, around the elevation of 4.8–5.2 m, according to the updated 2016 contour elevation map.

Physical Environment

The research area was in Unai Bapot at the north end of Laulau Bay (also known as Magicienne Bay or as Bahia Laolao), on the southeast coast of Saipan. The embayment today measures just over 3 km wide where it opens to the ocean, and it is about 2.5 km along its seaward-landward axis. A narrow strip of reef formation is found in the waters near the project area, in the most sheltered portion of the bay, where it receives the least pounding surf.

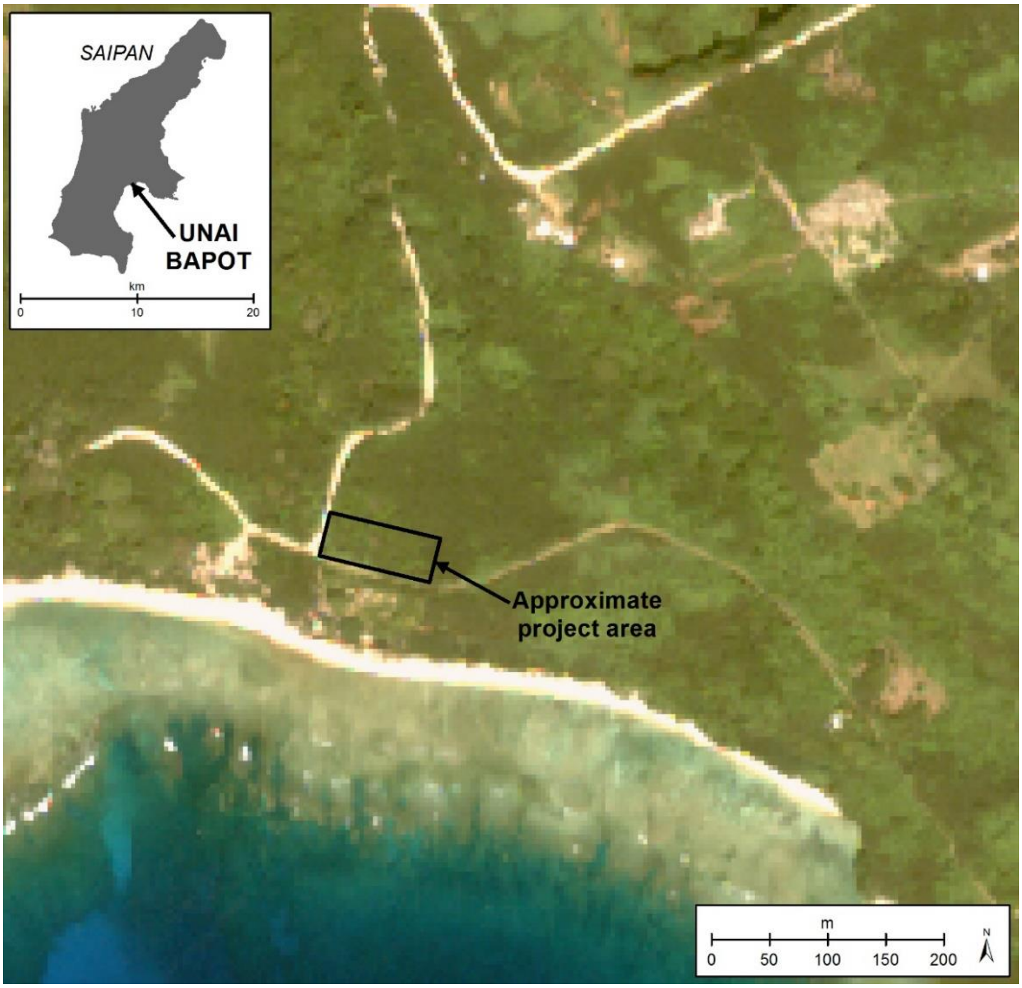

FIGURE 3. STUDY AREA, SHOWN ON AN ENLARGED (1:5000 SCALE) PORTION OF 2005 SATELLITE IMAGE OF SAIPAN. BASE IMAGE WAS OBTAINED FROM ONLINE DATABASE OF THE U.S. NATIONAL OCEANIC AND ATMOSPHERIC ADMINISTRATION (NOAA).

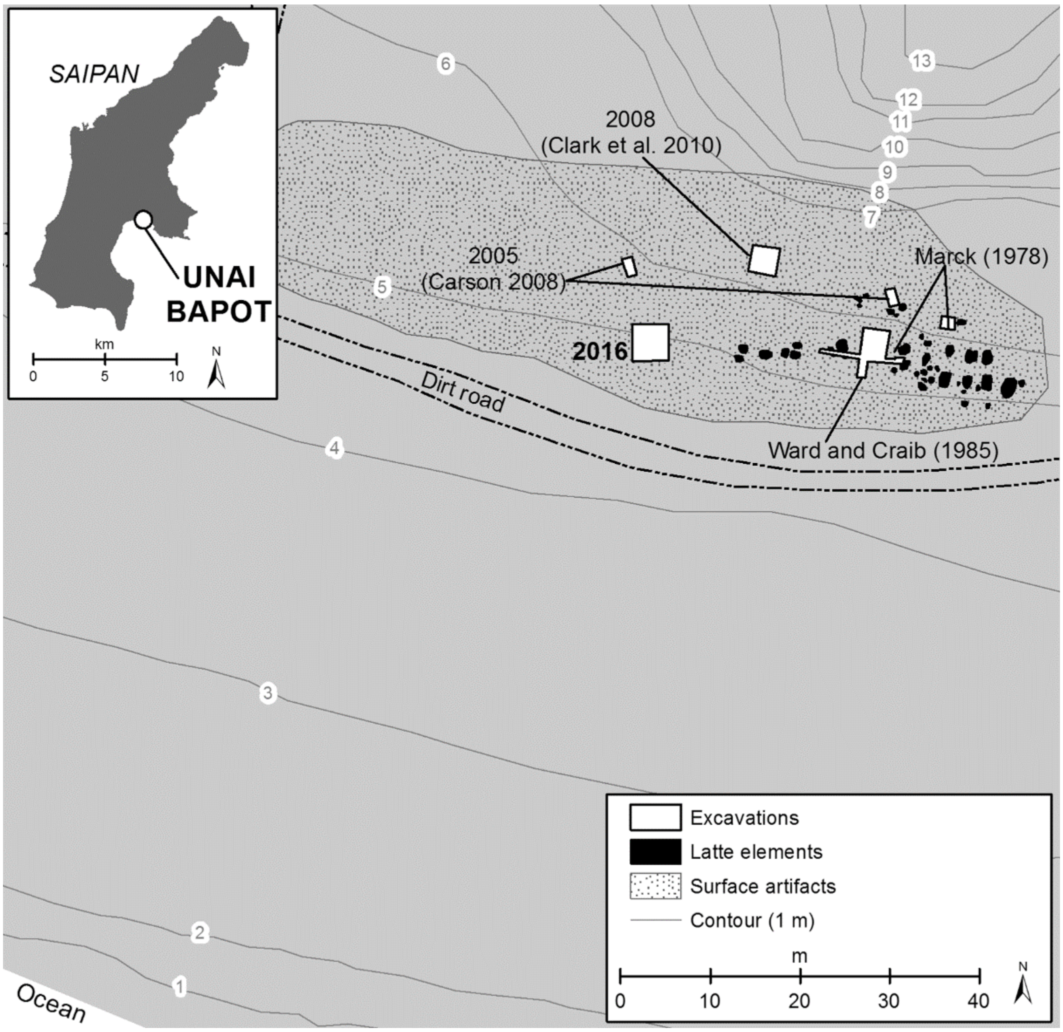

FIGURE 4. UPDATED CONTOUR MAP OF THE STUDY AREA, SHOWING SURFACE REMAINS, PRIOR EXCAVATIONS, AND RENEWED EXCAVATIONS.

Site SP-1-0013 is situated near the base of a colluvial slope, at the landward (north) margin of a slender coastal plain of calcareous beach sand. The colluvial slope rises to a steep, raised coral limestone formation of the island's core. The same arrangement of landforms characterises most of the Laulau Bay area, dissected by a number of stream drainages. At least two streams drain into the Bapot area.

A soil survey (Young 1989) has classified the slope deposits near the project area into two categories: 1) Kagman clay, 0 to 5 percent slopes; and 2) Chinen clay loam, 0 to 5 percent slopes. These deposits are considered suitable for general crop growth and most land use practices (Young 1989:25, 37).

At present, the vegetation cover at Unai Bapot includes invasive grasses, weeds, and mixed trees such as coconut (*Cocos nucifera*), *tangantangan* (*Leucaena leucocephala*), *Hibiscus tiliaceus*, and others. No endangered species have been reported in this area.

Overlapping with the time of initial human settlement in the region, a mid-Holocene high sea level stand (approximately 3000 through 1100 B.C.) created a remarkably different coastal morphology than exists today. In Saipan, the highstand was on average 1.65 ± 0.2 m above the present sea level, although some local variations may reflect Holocene deformation of the island associated with active faulting (Dickinson

2000). In the Laulau Bay area, emergent palaeoshoreline features vary from 1.5 m to 1.8 m above present sea level, progressively higher toward the north end of the bay and measured as 1.8 ± 0.2 m specifically nearest to the project area at Unai Bapot (Dickinson 2000:741–742). A figure of 1.8 ± 0.2 m has been verified as generally applicable throughout most areas of Guam, Tinian, and Saipan according to direct measurements and dating of buried coral formations and palaeo-lagoon deposits (Carson 2011, 2014b).

The environmental setting of the project area indicates at least three favourable circumstances for human settlement, including: 1) access to a variety of marine habitats and resources near a protected portion of a bay; 2) availability of fresh water from stream drainages; and 3) slope deposits suitable for general crop growth. Although significant environmental changes undoubtedly occurred during the span of human settlement in the region, the aforementioned three key factors were constantly present in variable forms during the past few thousand years.

Land Use

The following summary of land use history refers to six major time periods, based on a prior overview of the history and historic resources of the Laulau area (Russell 1987).

1) During the prehistoric period (pre-1668), "the Unai Bapot and Unai Laulau areas were attractive to the earliest island settlers because they offered relatively fertile land, intermittent fresh water sources and access to protected offshore marine resources" (Russell 1987:5). The earliest land use probably involved coastal settlement and an emphasis on marine resources. The use of inland areas for plant food production appears to have intensified over time. In this view, the project area likely contains evidence of several periods of human habitation.

2) The Spanish period (1668–1899) witnessed several important social changes in the region, under the increasing influence of Spanish priests and military presence. Russell (1987:7–8) noted: "The first priest to visit Saipan, Fr. Medina, landed at the village of Obyan in 1670 from which he and two secular companions walked northward to Laulau. The three then proceeded to an interior village called Cao, which may have been located above Laulau." This report indicated that the general vicinity of the project area supported some form of settlement around 1670. However, by 1700, as a result of introduced diseases and forced resettlement of the Chamorro population to Guam by the Spanish, Saipan's population was reduced to a small remnant. No records indicate people living in the Laulau area during the remainder of the Spanish period.

In July 1858, the British frigate Magicienne anchored at Laulau Bay, and a party landed apparently at Unai Bapot (Driver 1987:23–24; Russell 1987:10–11). Russell (1987:11) suggested that the place-name Bapot may have derived from this historical event, because the word Bapot is glossed as "Ship – large with engine" (Topping et al. 1975:28) as in reference to a steamship like Magicienne that incidentally gave Laulau Bay its alternate name of Magicienne Bay. At that time, the Bapot area likely was not a major population centre, as it was observed to supported thick tree growth without mention of a formal village.

3) During the short-lived German period (1899–1914), Germany formally possessed the Northern Marianas. At this time, the "energetic administrator, Georg Fritz, was anxious to begin developing the islands so they would be economically self-sufficient" (Russell 1987:12).

Fritz abandoned plans for harbour improvements at Laulau, opting instead to focus on Tanapag. For the Laulau area, land use alterations included: a) a road to connect Laulau with Garapan; and b) a copra plantation emplaced over the site of an abandoned Chamorro settlement (Russell 1987:12–13).

4) The Japanese administration (1914–1941) brought widespread land use changes to Saipan. Initial attempts had failed to establish a sugar industry, but a revitalised effort beginning in 1922 was successful (Russell 1987:13–14). Four plantations operated in Saipan, and several villages blossomed around these centres. At that time, Laulau appears to have been one of a few rural agglomerations, consisting of "concentrations of farm families in settlements not large enough to be considered major villages" (Russell 1987:15). Meanwhile, the older German roads were improved, and a narrow-gauge railway was constructed around the island.

5) Although brief in terms of years, the World War II period (1941–1945) had dramatic effects. At first, little if any war-related activities occurred in Saipan. In early 1944, "the Japanese high command launched a desperate program to turn Saipan into an impregnable fortress" (Russell 1987:19). Laulau Bay was particularly important, because "its relatively protected beaches fronting a deep water bay were possible American landing zones and required defensive positions. Indeed, the two beaches were given code names by the American invasion planners; Unai Laulau was designated Purple One and Unai Bapot as Purple Two" (Russell 1987:22).

In June 1944, American forces bombarded most of Saipan for several days, followed by slow advance across the island from initial landings in the south (Russell 1987:25–41). Fortifications at Laulau eventually were overtaken and secured, along with positions throughout the island. No such fortifications are known to exist specifically within the current research area at Unai Bapot, but some remnants may exist in whole or in ruins in other locations at Laulau.

6) The post-war period (post-1945) has included an increasing pace of land development in Saipan. Following repatriation of Japanese and Okinawan immigrants in 1946, "a few native farms were opened in the Laulau area" (Russell 1987:41). Based on observations in 1949, Spoehr (1957:45) reported that the Laulau area was planted in maize, coconut, and bananas. Small-scale homesteads and farms were occupied in the area over the next few decades. Limited development for modern housing and resorts has occurred since the 1990s.

Since the time of Scott Russell's (1987) overview as summarised here, the project vicinity has supported a number of newer land-use patterns. The immediate surroundings have become Public Land in the CNMI, and the specific footprint of the "Bapot Latte Site" has been nominated in the U.S. National Register of Historic Places (Carson 2005). A few private house lots have been developed with new structures or re-modelling of older structures, for instance directly seaward (south) of the designated site area. A diving area has been maintained to the west.

Archaeological Setting

Archaeological investigations in the Laulau area have been intermittent since the 1920s. As part of a Marianas region-wide survey during the early 1920s, Hans Hornbostel examined a set of drawings on the interior walls of caves at Laulau (Hornbostel 1925). Working with Hornbostel's records, Laura Thompson (1932:20) noted: "These drawings are reported to have been executed with white pigment." Hornbostel (1925) mentioned the stone ruins of *latte* house sites in the general area.

In 1949, Alexander Spoehr conducted archaeological survey and excavations in several parts of Saipan, Tinian, and Rota. Concerning the Laulau area, Spoehr (1957:31) documented a "Laulau Site" and a "Bapot Site." The current project at Site SP-1-0013 appears to coincide with the "Bapot Site."

Spoehr (1957:31) described the "Laulau Site":

> There is an extensive village area back of the beach on Magicienne Bay. This site was undisturbed by military operations and was partially excavated.

At this site, Spoehr (1957:43–58) mapped the remnant pillars and capital stones of several *latte* sets, and he excavated both at the *latte* and in a nearby rockshelter. The excavations revealed hearths and other possible activity areas associated with the ancient *latte* houses. The rockshelter contained burial remains, along with a range of pottery types.

Spoehr (1957:31) described the "Bapot Site":

> North and east along the shores of Magicienne Bay there is a coastal terrace about 100 yards wide. The soil is good and there is easy access to reef and offshore fishing. This area is the site of three clusters of *latte* houses: Bapot I consists of two, Bapot II of four, and Bapot III of five. All have been disturbed by defensive trenching by the Japanese military forces, while a road also cuts across the former occupation area. Sherds are distributed throughout the area. It is probable that the area once contained numerous house sites.

The current research site appears to coincide with the central portion of "Bapot I." Spoehr did not conduct any further work at Bapot. Instead, the work at the "Laulau Site" served to characterise the archaeological resources of the general area.

In 1977–1978, Jeffrey Marck undertook excavation of an area between two *latte* sets at the Bapot site. The main excavation was 3 m by 3 m, and it terminated upon reaching culturally sterile sands at depths varying from 1.9 m to 2.2 m below the present ground surface (Marck 1978:16). The excavation recovered more than 12,000 pieces of pottery from different recognised stratigraphic layers, along with an appreciable amount of shellfish and other food remains. Two samples of charcoal produced dates of approximately 1000 B.C., but the contexts were unclear in relation to the specific archaeological layers of the site.

The initial excavations at Bapot indicated a more or less continuous use of the beach area at least since 1000 B.C. if not earlier. In principle, a number of changes in the archaeological assemblage could be traced through the stratigraphic sequence. In particular, the exceptionally high density of pottery presents an excellent opportunity to examine chronological change.

In 1979, Ross Cordy conducted brief surface surveys of the coastal plain and stream beds in the Bapot area, with the goal to examine settlement patterns in the region. Cordy (1979a, 1979b, 1979c) inferred a late population expansion into the island interior, around the same time when people occupied at least three foci of coastal settlement around *latte* structures.

In 1985, Graeme Ward and John Craib re-excavated the Bapot site, aiming to document the surface features and stratigraphy in more detail than was recorded previously. A 2 by 2 m excavation terminated close to 3.5 m below the present ground surface. Bonhomme and Craib (1987:99) reported a series of radiocarbon dates from different stratigraphic layers, confirming initial occupation of the site at least as early as 1000 B.C. and continuing more or less uninterrupted thereafter. This work clearly established the importance of the site for archaeological investigations in the region. Although a preliminary report was filed (Ward and Craib 1985), a final report for the project has not yet been produced.

In 1986–1987, Michael Graves conducted a surface survey with limited subsurface testing in the Laulau area, intending to locate, record, and evaluate archaeological resources prior to anticipated land development. According to Russell (1987:54), "Graves' work identified significant archaeological resources, including previously unrecorded *latte* sets and rockshelters and extensive Japanese World War II defensive positions." In 2005, Graves recalled that the work at Bapot was not a major focus of the survey and that the coastal portion of Bapot appeared to have been heavily disturbed by World War II Japanese trenches and other fortifications (Michael W. Graves, personal communication to Mike T. Carson, 2005). A formal report for this work has not yet been developed.

Based on a review of available documents and a brief field reconnaissance in 1991, Tomonari-Tuggle (1991) synthesised the archaeological and historic resources in the Laulau area. Referring in general to coastal deposits such as in the current project area at Bapot, Tomonari-Tuggle (1991:34) recommended test excavations:

> Cultural material, including *Latte* and pre-*Latte* Period sherds, shell, basalt mortars, and disturbed *latte* capstones and shafts, occurs at Unai Laolao and Unai Bapot. However, extensive damage through wartime Japanese defensive preparations has been documented at the latter area. The primary purpose of testing will be to determine the location and extent of intact portions of the coastal occupations.

Olmo (1992a, 1992b) conducted archaeological surface survey with limited subsurface testing along the central portion of the coast of Laulau Bay. The northeast end of this survey work overlapped with the westernmost portion of the Bapot site complex. In the Bapot area generally, although not specifically in the current research area, Olmo (1992a) reported:

a) a rockshelter (T37);
b) a surface scatter of potsherds and stone tools (T56);
c) the ruins of an early or middle 20th century house (T89);
d) a concrete slab (T90);
e) a concentration of two concrete slabs (T91);
f) another concrete slab (T92);
g) a well complex (T93);
h) a casemate fragment (T95);
i) a *latte* set probably coincident with Spoehr's (1957:31) "Bapot 3" area (T124A);
j) a rockshelter (T124B);
k) another rockshelter (T124C);
l) one more rockshelter (T124D); and
m) a surface scatter and *latte* set (T127)

2005 Investigation

The 2005 investigation was designed for gathering sufficient information to nominate the site in the U.S. National Register of Historic Places (Carson 2005; Carson and Welch 2005). Toward the project goal, the site was cleared and mapped in detail, and two test pits were excavated at 1 by 2 m each. The excavations proved to contain several cultural layers, with the lowest and oldest dating to 1500 B.C. or perhaps earlier (Carson 2008).

The surface-visible components of the site included *latte* remains, a wide scatter of potsherds, and few marine shell fragments (Figures 5 and 6; see also Figure 4). A broken *lusong* (food-grinding mortar) was observed in secondary context. These findings indicated a late pre-Spanish activity area, post-dating A.D. 1000. The primary activity area was mostly about 90 to 110 m from the modern shoreline. This area corresponded to one in a series of abandoned coastal *latte* villages described by Spoehr (1957:31) as the Bapot complex.

The *latte* remains included two clusters of fallen columns and capitals of quarried limestone. The western cluster had been disturbed by World War II activities and post-war clean-up efforts, but the eastern cluster retained all of its original elements. Prior to abandonment, the columns would have been upright and topped by the capitals, supporting house structures as described in general by Laguana et al. (2012) and by Thompson (1940).

FIGURE 5. MEGALITHIC *LATTE* REMAINS ON CLEARED SITE SURFACE IN 2005, VIEW TO EAST. SCALE BARS ARE IN 20-CM INCREMENTS.

FIGURE 6. PORTION OF BROKEN *LUSONG* GRINDING MORTAR IN 2005, VIEW TO NORTH. SCALE BARS ARE IN 20-CM INCREMENTS.

The widespread potsherds on the surface included fragments of undecorated, thick, coarse, large vessels typical of the *latte* period post-dating A.D. 1000 (Carson 2012). The pottery scatter reflected a slightly larger habitation zone than just the *latte* remnants.

The Unai Bapot site was especially valuable for its intact subsurface deposits and clear stratigraphy in its deepest and earliest components, apparently due to its setting in the most protected part of a sheltered embayment. Unlike other beach sites in exposed high-energy environments, the subsurface occupation layers at Unai Bapot have escaped massive disturbance or obliteration by several centuries of cultural and natural formation processes. Additionally beneficial for the preservation of the site's lower layers, their depth was beneath the impacts of the World War II and post-war intrusions. Especially in its deepest and oldest components, Unai Bapot showed separate stratigraphic layers with good preservation of archaeological contents.

In 2005, two test units (TU-1 and -2) disclosed a deep stratigraphic sequence of seven distinct layers with minor internal variations (Figure 7). Cultural materials were encountered as deep as 190 cm in TU-1 and 220 cm in TU-2. The assemblage was remarkable for its range of pottery and other artefacts, especially in the earliest cultural layers (Table 1). The findings from 2005 were encouraging, yet the test pits of 1 by 2 m each allowed only limited conclusions.

Although the upper portion of the site deposit had been disturbed, the lower portion remained intact. The uppermost layer (I-A) contained 20th Century disturbance, evident in World War II shrapnel, modern bottle glass, and other materials. The abrupt lower boundary of Layer I-A suggested partial disturbance (and perhaps truncation) of the upper portion of the underlying Layer II-A. In all other cases, gradual or diffuse layer boundaries indicated continued occupation with gradual change in sedimentation and minimal disturbance of pre-existing deposits. Nonetheless, portions of older living surfaces tended to become incorporated in successive occupation layers, mixing a certain amount of sediment and constituent material (such as pottery, shell, etc.) across the gradual and diffuse layer boundaries.

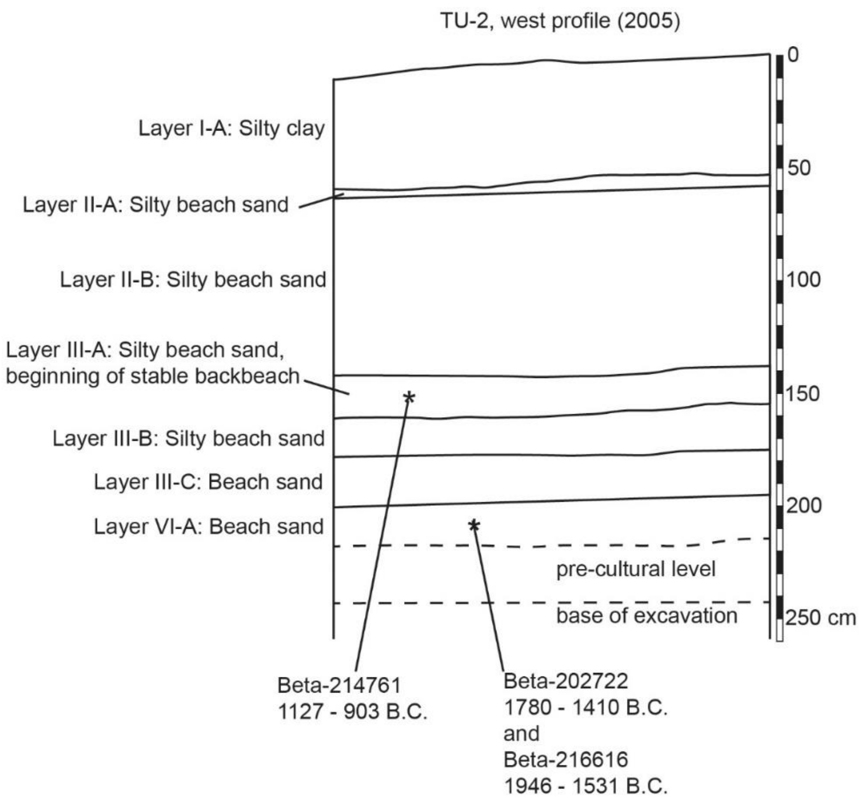

FIGURE 7. PROFILE OF TU-2 FROM 2005 EXCAVATION, VIEW TO WEST.

TABLE 1. SUMMARY OF TRADITIONAL CULTURAL MATERIALS RECOVERED FROM THE 2005 TEST PITS, TU-1 AND -2, LAYERS I-A (YOUNGEST) THROUGH IV-A (OLDEST). NUMBERS ARE WHOLE COUNTS. NUMBERS IN PARENTHESES ARE SQ CM FOR POTSHERDS AND TOTAL GRAMS FOR ALL OTHER ITEMS.

Material	I-A	II-A	II-B	III-A	III-B	III-C	IV-A
Pottery							
Non-slipped, undecorated	1167 (6639)	80 (415)	308 (1615)	36 (103)			
Non-slipped, decorated	14 (123)		5 (47)	7 (23)			
Redware, undecorated	64 (218)	40 (139)	960 (3431)	713 (1495)	1229 (2416)	1712 (3469)	1727 (3224)
Redware, decorated				1 (4)	3 (40)	2 (75)	
Blackware, undecorated	1 (2)			13 (41)	47 (136)	95 (294)	71 (205)
Blackware, decorated	1 (3)		3 (17)		4 (28)	7 (24)	
Flaked material							
Volcanic stone	14 (318)	5 (11)	1 (3)		1 (24)	2 (14)	
Chert	26 (149)	1 (19)	28 (90)	7 (24)	5 (34)	10 (58)	8 (28)
Quartz			2 (34)	1 (7)	1 (15)	1 (1)	
Marine shell	11 (58)	1 (2)				2 (5)	
Tools							
Slingstone	1 (34)		1 (71)		1 (37)		
Adze	1 (97)		1 (42)		3 (127)	2 (24)	
Spear point	1 (1)		3 (4)				
Fishing hook	1 (<1)		2 (1)				

Material	I-A	II-A	II-B	III-A	III-B	III-C	IV-A
Lime container		1 (63)					
Abrader			1 (3)				
Cut shell							2 (9)
Ornaments							
Shell bead	1 (<1)		3 (2)	2 (<1)	1 (14)	1 (2)	
Shell armlet			1 (5)				
Shell pendant					1 (<1)	1 (1)	
Coral pendant							1 (1)
Modified shell						1 (1)	
Faunal remains							
Shellfish remains	1205 (2950)	320 (907)	3874 (8946)	1313 (3227)	1254 (3117)	1280 (3076)	1063 (1995)
Fish bone	2 (1)		10 (12)				
Bird bone	1 (<1)		3 (1)		1 (<1)	9 (2.2)	3 (1)
Human bone	1 (1)		2 (2)	1 (2)			
Unidentified bone	4 (7)		4 (1)	1 (<1)	2 (12)	6 (4)	

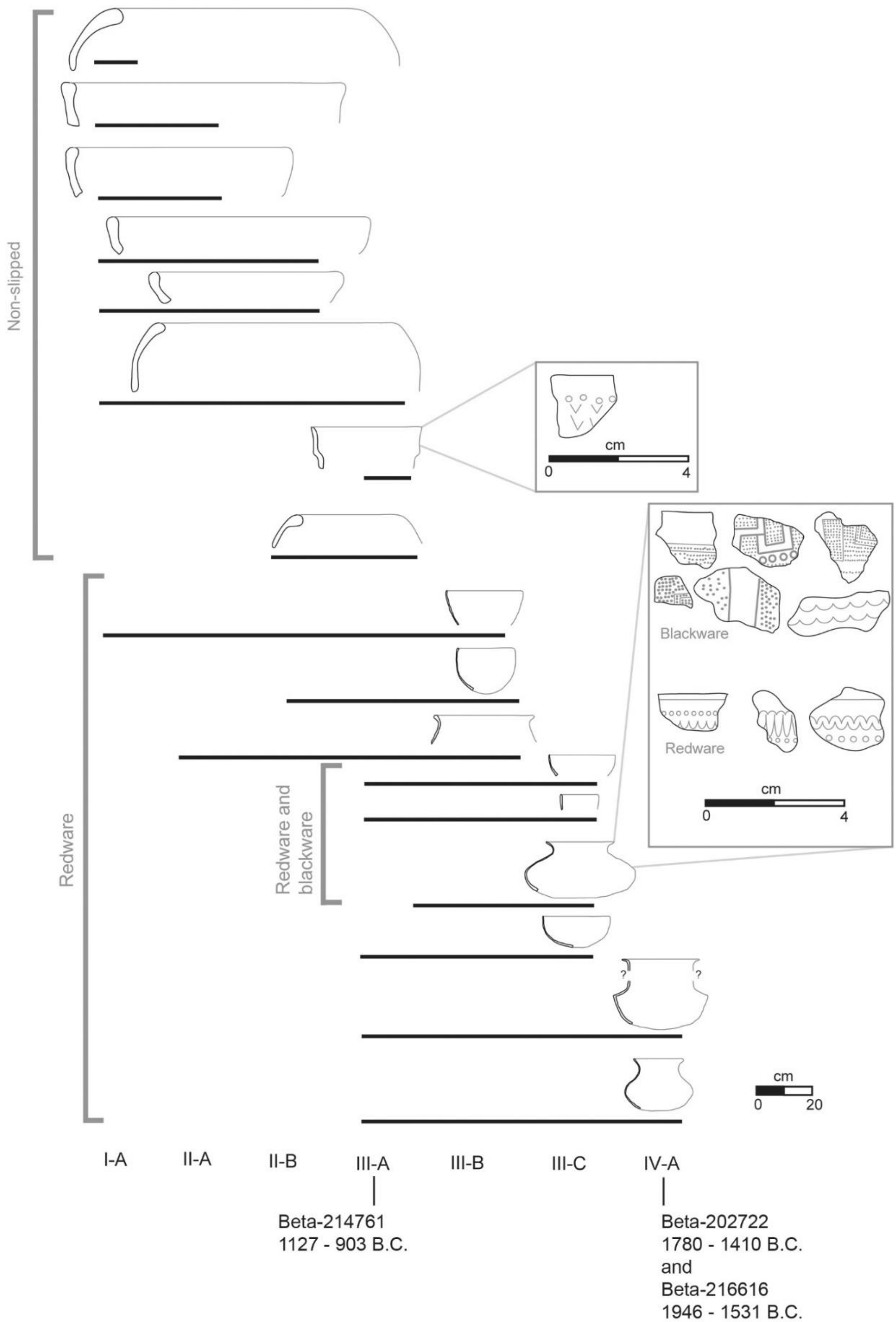

FIGURE 8. EXAMPLES OF EXCAVATED POTTERY WITH RECONSTRUCTED VESSEL SHAPES IN STRATIGRAPHIC ORDER, ACCORDING TO THE 2005 TEST PIT FINDINGS. HORIZONTAL BLACK BARS BENEATH ITEMS INDICATE DURATION OF PRESENCE IN OCCUPATION LAYERS AT UNAI BAPOT. IN THIS DIAGRAM, LAYER I-A (LEFT) WAS THE YOUNGEST, AND LAYER IV-A (RIGHT) WAS THE OLDEST.

FIGURE 9. SAMPLES OF EXCAVATED STONE, SHELL, AND BONE TOOLS FROM 2005 FINDINGS. TOP ROW: LEFT, BEACH ROCK PROBABLE NET SINKER FROM LAYER III-B IN TU-1; RIGHT, LIMESTONE SLINGSTONE FROM LAYER II-B IN TU-2. SECOND ROW: LEFT, THREE PIECES OF BONE SPEAR POINT FROM LAYER II-B IN TU-1; RIGHT, LIME CONTAINER OF *TURBO* SP. SHELL FORM LAYER II-A IN TU-2. THIRD ROW: LEFT, *CONUS* SP. SHELL ADZE FROM LAYER I-A IN TU-2; RIGHT, TWO FRAGMENTS OF POLISHED CHERT ADZE FROM LAYER III-C IN TU-1. BOTTOM ROW: LEFT TO RIGHT, FISHING HOOK FRAGMENTS FROM LAYER II-B IN TU-1 AND TU-2 AND POSSIBLE MANUFACTURING DEBRIS FROM LAYER IV-A IN TU-2.

FIGURE 10. SAMPLES OF SHELL AND CORAL ORNAMENTS FROM 2005 FINDINGS. TOP ROW: SAMPLE OF *CONUS* SPP. SHELLS IN VARIABLE FORMS AND MANUFACTURING STAGES. SECOND ROW: LEFT, PENDANT OF NACREOUS MARINE SHELL FROM LAYER III-B IN TU-2; MIDDLE, PENDANT OF NACREOUS MARINE SHELL FROM LAYER III-C IN TU-2; RIGHT, ARMLET FRAGMENT OF *CONUS* SP. SHELL FROM LAYER II-B IN TU-1. BOTTOM ROW: LEFT, MODIFIED *ANADARA* SP. SHELL FROM LAYER III-C IN TU-2; RIGHT, UNIQUE CORAL PENDANT FROM LAYER IV-A IN TU-2.

Since 2005, other research in the Marianas region has clarified about the layer of hardened sand as documented near the base of the excavation at Unai Bapot. It now is classified as calcrete (Carson and Peterson 2011). Moreover, a methodology was developed to remove large blocks, dissolve in light acid, halt the acid reaction in distilled water, and then identify any constituent remaining artifacts and midden.

The details of the 2005 excavations have been reported elsewhere (Carson 2005, 2008) and not reiterated here. The site has shown almost every major type of pottery and other artefact in the known prehistoric ceramic sequence for the Mariana Islands, found in stratigraphic order (Figures 8, 9, and 10). Additionally, the shellfish remains revealed chronological change along with the artefact sequence, further linked with the chronology of changing sea level, coastal ecology, and cultural harvesting (Figure 11).

In 2005, dating of the earliest occupation at Unai Bapot was confirmed by two radiocarbon dates of burned *Anadara antiquata* shells in a single localised discard pile in Layer IV-A (Table 2). The two dating results overlapped significantly in the range of 1780–1531 B.C., thus calling attention to a pre-1500 B.C. age of the site's lowest cultural layer. The two individual dating results have been calibrated at 1780–1410 B.C. and at 1916–1531 B.C.

Since the time of the 2005 research, new advancements have been possible with refining the localised marine reservoir correction for radiocarbon dating of shells and specifically of *Anadara* sp. shells. The new correction value has been calculated as -49±61 years, instead of a prior rough estimate of +75±35 years. This new calculation is based on three different pairings of charcoal specimens with *Anadara* sp. shells at the Ritidian Site in Guam (Carson 2010, 2017a, 2017b), further corroborated with more paired samples at House of Taga in Tinian (Carson 2014a), and now with another pairing at Unai Bapot reported later here. The most current radiocarbon calibrations curves have included refinements over-riding the older calibrations for both terrestrial land marine curves (Reimer et al. 2013), and calibration programs such as OxCal have been updated accordingly (Bronk Ramsey and Lee 2013).

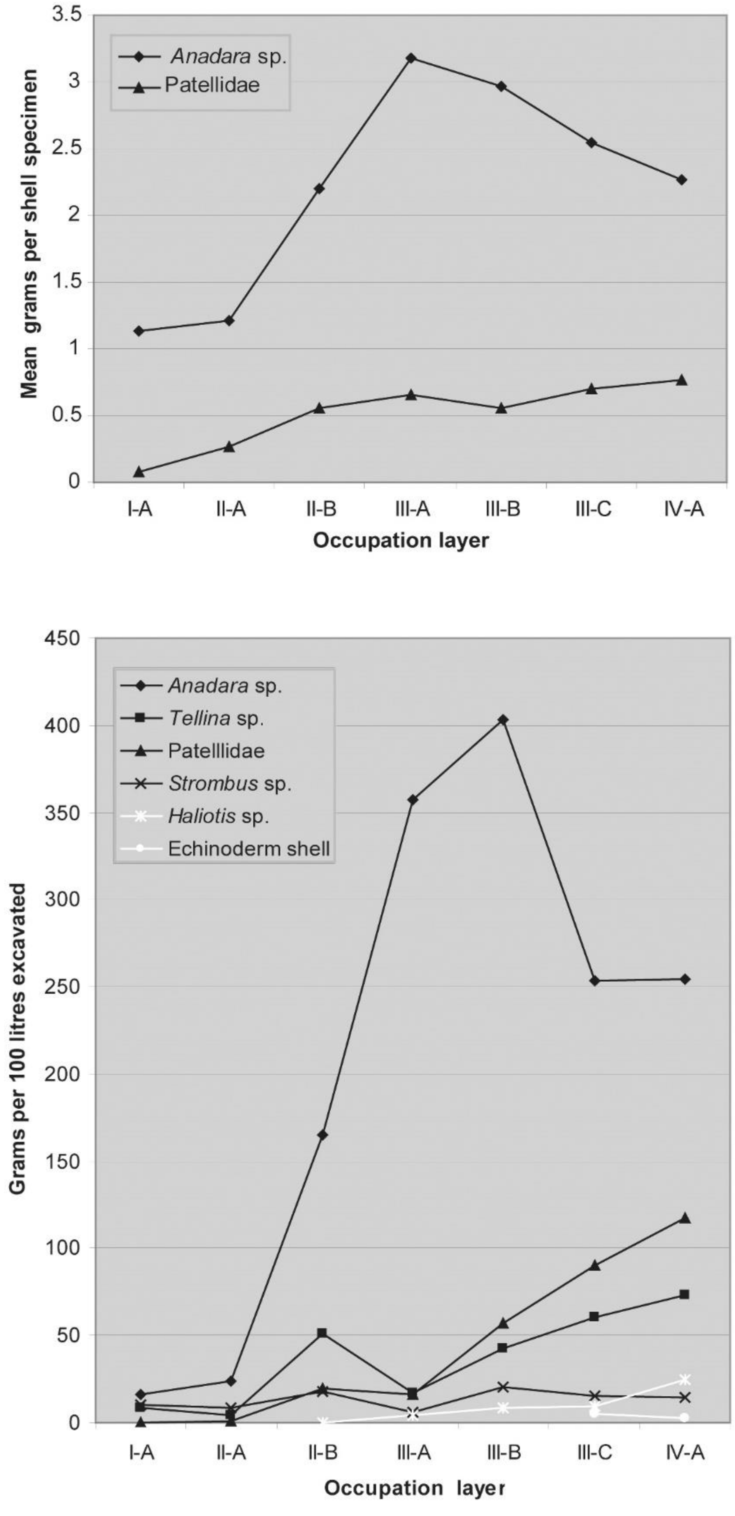

FIGURE 11. CHRONOLOGICAL TRENDS IN MARINE SHELLFISH REMAINS FROM 2005 FINDINGS. TOP: MEAN GRAMS PER SHELL SPECIMEN OF *ANADARA* SP. AND PATELLIDAE IN TU-2, LAYERS I-A (YOUNGEST) THROUGH IV-A (OLDEST). BOTTOM: GRAMS OF KEY SHELLFISH TAXA PER 100 LITRES EXCAVATED IN TU-2, LAYERS I-A (YOUNGEST) THROUGH IV-A (OLDEST).

TABLE 2. RADIOCARBON DATING RESULTS FROM 2005, USING UPDATED MARINE RESERVOIR CORRECTION AND CALIBRATION CURVES.

Beta Sample #	Provenience	Measured Radiocarbon Age	$^{13}C/^{12}C$ Ratio (‰)	Conventional Radiocarbon Age	Marine Reservoir Correction*	Calibrated Date Range (2 Sigma)**
214761	TU-2, Layer III-A, combustion feature, charcoal flecks	2850 ± 40 B.P.	-25.8	2840 ± 40 B.P.	Not applicable	1127–903 B.C. (95.4%)
202722	TU-2, Layer IV-A, localised discard pile, *Anadara* sp. shell	3210 ± 40 B.P.	- 1.5	3590 ± 40 B.P.	-49±61	1780–1410 B.C. (95.4%)
216616	TU-2, Layer IV-A, localised discard pile, *Anadara* sp. shell	3320 ± 50 B.P.	-1.1	3710 ± 50 B.P.	-49±61	1946–1531 B.C. (95.4%)

* = Marine reservoir correction (ΔR) of -49±61 follows the calculation specifically for *Anadara* sp. shells paired with charcoal specimens at multiple sites as reported later here in detail, using the Deltar software online software package (Reimer and Reimer 2017).

** = Calibrations were by the OxCal program (Bronk Ramsey and Lee 2013), using the INTCAL13 and MARINE13 calibration curves (Reimer et al. 2013).

A sample of charcoal from a small firepit in the fourth occupation layer (III-A in the 2005 layer designations) yielded a calibrated radiocarbon date of 1127–903 B.C. (see Table 2). This sample post-dated the abundant redware and blackware pottery characterising the earliest site components, and it immediately pre-dated a change in the marine shellfish assemblage reflecting the initial stages of sea-level drawdown and loss of mangrove habitat. The beginning of regional sea-level drawdown overall has been noticed around 1100 B.C.

After the 2005 excavation, a follow-up 3 by 3 m (9 sq m) excavation was initiated by Carson in 2008, in partnership with Geoffrey Clark at the Australian National University, for the purpose of learning more about the earliest cultural layer and dating at the site. After the excavation reached 50 cm depth, Clark assumed the responsibilities of the project, so far reported in a summary publication (Clark et al. 2010), with plans of a Ph.D. study by Olaf Winter under Clark's supervision not yet completed as of 2017. In its lower depth, the 2008 excavation narrowed considerably less than the initial 3 by 3 m, and therefore Clark et al. (2010) by default focused on the middle to upper layers with preserved charcoal post-dating 1100 B.C. In this way, the deepest and oldest layers were documented only partially and with unanswered questions.

In the absence of different new information about the deepest and oldest cultural layers at the Bapot Site, the pre-existing 2005 results have indicated a dating at least as early as 1500 B.C. but still needing further confirmation or refinement. Meanwhile, the early dating has played a key role in establishing the first-settlement context of the Marianas overall (Carson and Kurashina 2012). The Marianas dating in general has re-opened cross-regional research about population movements and dispersals between Island Southeast Asia and Remote Oceania (Hung et al. 2011).

Role of the 2016 Investigation

According to the foregoing review of the project context, the Bapot Latte Site (Site SP-1-0013) contains a deep subsurface layer that could be one of the earliest cultural deposits in the Marianas, and the surface of the site supports a set of *latte* structures dating to the later traditional Chamorro period prior to the impacts of Spanish imperialism. The site contains abundant pottery and other cultural materials in deep, stratified deposits dating at least as early as 1500 B.C.

The limits of the 2005 project did not allow pursuit of the site's full research potential, and therefore the new 2016 excavation could be more productive toward these goals. The new excavation allowed: a) recovery of a greater volume of material; b) clarity of site dating; and c) more detailed studies, given funding from the Australian Research Council, awarded to the project investigators.

The 2016 investigation addressed five primary research questions:

1) What was the date of initial human presence at this site? A larger excavation of 4 by 4 m provided the best way to answer this question, as it allowed recovery of more volume of datable material from the deepest and oldest cultural layer. Especially now with more refined correction values and calibration curves for radiocarbon dating than had been possible in 2005, the dating could concluded more precisely and reliably. Additionally, statistical probabilities could be calculated by obtaining dating samples from stratigraphic positions above and below the specific points of interest.

2) How did the oldest layer at Unai Bapot relate to the dating of other earliest settlement sites in the Mariana Islands? Now with substantially more dating results from other sites than had been available in 2005, this question could be addressed more productively. With the new excavation and more precise and reliable dating at Unai Bapot, the dating results could be compared most effectively with the results so far known at other sites of the region.

3) What was the ecological context of the site during different time intervals? The results from 2005 were sufficient to outline the general characteristics of a changing coastal environment, coordinated with a chronology of the food remains, cultural artefacts, and other factors. A more refined chronology now has been possible, along with greater clarity of the ancient coastal ecological context, as enabled by new information and techniques that had not been available in 2005. Of particular significance have been the new advancements in regional knowledge of ancient sea level, coastal environments, and cultural chronology (Carson 2014a, 2014b, 2016).

4) What was the cultural setting at the site during different time intervals? The 2005 results were reasonable for identifying the range of artefacts and midden during broadly defined time periods, but the new 2016 investigation has obtained greater clarity and precision. The two test pits from 2005 in total were only 4 sq m, and a new large-format excavation of 16 sq m has increased the ability to characterise the archaeological assemblages during each time interval. Additionally, a more refined chronological sequence has allowed finer-scale identification of how the artefacts and midden changed through time at the site.

5) What can be ascertained of spatial patterns of site use during different time intervals? The new excavation uncovered 16 sq m, wherein it revealed spatial patterning that was not identifiable in the prior 2005 excavations of much smaller size. Of special interest were the arrangements of hearth features, post moulds, and pits within their associated cultural layers. Also of interest were the patterns in concentrations of different types of artefacts and food remains across the exposed excavation area. This information importantly was identified within each cultural layer and associated time period.

Chapter 3

Investigative Procedures

The October 2016 excavation opened an area of 4 by 4 m (16 q m), well within the limits of the permitted proposal of a maximum of 6 by 6 m (36 sq m). The expected depth of cultural deposits was about 2–3 m, and indeed the excavation terminated at 2.05/2.15 m on the underlying coral limestone. The specific location of the excavation was intended for a position at a slightly lower elevation than had been targeted by the 2005 excavations, such that a buried cultural layer at 2 m depth would have been situated closer along the paleo-shoreline prior to 1100 B.C.

Given the importance of knowing the elevation of sedimentary units relative to present and ancient sea level, the site's contour map was revised in October 2016, according to redundant cross-checked elevation measurements over the course of three weeks at the site. The updated contour map (see Figure 4) may be considered accurate with a margin of ± 20 cm. It shows mostly the same shape of the terrain as in the prior 2005 map, but the absolute elevations now have been updated. The 2005 contour map (Carson and Welch 2005) was based on the elevations as recorded in the U.S. Geological Survey (USGS) topographic series map, with only limited access in 2005 to the directly associated shoreline for cross-checking the elevation above sea level. In October 2016, access was available directly to the shoreline on a daily basis for cross-checking of elevations, resulting in the updated map.

The updated contour map helped to solve a question about the absolute elevations of the buried layers as documented in the prior 2005 excavations. In the 2005 excavations, the lowest cultural layers resembled a context of an unstable beachfront, and such a context should have been situated within 1 m of the ancient seashore. The prior elevation estimates, however, would have suggested a higher absolute elevation that called for further investigation.

With the CNMI HPO staff, a location around the corrected estimate of 4 m elevation was hand-cleared of the modern vegetation (Figure 12). The hand-clearing did not displace the plant roots or any sedimentary material, with the goal of leaving the sedimentary units intact for careful hand-controlled excavation. As already noted, the local vegetation did not include any endangered or threatened species, and furthermore the spatial extent did not create a negative effect on the habitat of local animal life. As of December 2016, the vegetation already was re-growing.

The block area was divided into equal-sized quadrants of 2 by 2 m each, further subdivided into 1 by 1 m units (Figure 13). Provenience was recorded for each quadrant and with notation of the subdivided units, but ultimately the major relevant information was discerned within the quadrant designations.

Excavations proceeded by artificial levels of 20 cm or less, within natural strata (Figures 14, 15, and 16). The natural strata constituted the primary units of analysis, but the internal artificial divisions of levels were necessary to ensure proper recognition of minor differences in sedimentary matrix and material contents. In some cases, a single lithostratigraphic unit could be identified by its overall sedimentary characteristics (e.g., colour, texture, consistence, etc.), yet internal differences could be noticed as sub-units within a layer (designated as A versus B) in terms of its sediment composition, artefacts, and midden.

All contents were screened through 2-mm wire mesh, such that artefacts and midden as small as 2 mm were recovered (Figures 17 through 20). A field catalogue recorded the provenience information for each bag of material. Fragile items, such as delicate shell objects and small fragments of animal bones, were bagged separately to avoid inadvertent damage.

Where subsurface features were encountered, they were recorded by scaled plan and section maps, text descriptions, and photographs before and after excavation. They were treated as individual stratigraphic units for the purposes of provenience and catalog reference (Figure 21).

FIGURE 12. HAND-CLEARING OF THE VEGETATION COVER, WHILE PREPARING THE 4 BY 4 M EXCAVATION AREA. JOSE JESUS FITIAL IS AT THE FRONT LEFT. HSIAO-CHUN HUNG IS WALKING IN THE BACKGROUND. IN THE MIDDLE GROUND, FROM LEFT TO RIGHT, ARE JUAN SALAS AND ABRAHAM TENORIO.

FIGURE 13. OUTLINE OF THE 4 BY 4 M EXCAVATION AREA, READY TO BEGIN EXCAVATION. THE PERIMETER WAS MARKED BY ORANGE ROPE, TIED TO WOODEN STAKES AT THE CORNERS. PINK FLAGGING CLARIFIED THE CORNER POINTS OF THE FOUR QUADRANTS FOR EASE OF VISUAL IDENTIFICATION, ALTHOUGH MEASUREMENTS ALWAYS WERE MADE FOR EACH QUADRANT AND SUB-UNIT. FROM LEFT TO RIGHT ARE JOSE JESUS FITIAL, ABRAHAM TENORIO, HSIAO-CHUN HUNG, AND JUAN SALAS.

FIGURE 14. EXCAVATION IN PROCESS OF THE UPPERMOST STRATIGRAPHIC LAYER, IN THE DESIGNATED QUADRANT 1 OF THE NORTHEAST PORTION OF THE EXCAVATION AREA. THE SEDIMENT WAS FILLED INTO MEASURED BUCKETS FOR FINE-MESH SIEVING. HSIAO-CHUN HUNG AT THE FRONT RIGHT. ABRAHAM TENORIO IS AT THE CENTRE RIGHT. JOSE JESUS FITIAL AT THE CENTRE BACK.

FIGURE 15. EXPOSING THE ENTIRE EXCAVATION AREA, QUADRANTS 1 THROUGH 4, AT 20 CM DEPTH WITHIN LAYER I. LUFO BABAUTA IS STANDING AT THE CENTRE FRONT. SITTING IN THE CENTRE GROUND, FROM LEFT TO RIGHT, ARE ANGLES PALACIOS, JOSE JESUS FITIAL, AND ABRAHAM TENORIO. IN THE FAR BACKGROUND, FROM LEFT TO RIGHT, ARE JENNIFER SABLAN, MERTIE KANI, AND JUAN SALAS.

FIGURE 16. CONTINUED EXPOSURE OF STRATIGRAPHIC LAYERS BY HAND-CONTROLLED EXCAVATION. THE EXCAVATION PROFILES HOW A SUCCESSION OF LITHOSTRATIGRAPHIC LAYERS, IN PROGRESS ABOUT HALF-WAY THROUGH THE EXCAVATION. LUFO BABAUTA IS STANDING IN THE CENTRE BACK. IN THE FRONT, LEFT TO RIGHT, ARE ANGLES PALACIOS AND JOSE JESUS FITIAL.

FIGURE 17. LOADING BUCKETS FOR FINE-MESH SIEVING. MERTIE KANI IS AT THE FRONT LEFT, PREPARING TO LIFT A BUCKET. JENNIFER SABLAN IS AT THE FRONT RIGHT, USING A SHOVEL. IN THE MIDDLE GROUND, LEFT TO RIGHT, ARE JUAN SALAS, ABRAHAM TENORIO, AND JOSE JESUS FITIAL. HSIAO-CHUN HUNG IS IN THE FAR BACKGROUND.

FIGURE 18. CARRYING BUCKETS TO A SIEVING STATION. ABRAHAM TENORIO CARRIES TWO BUCKETS.

FIGURE 19. FINE-MESH SIEVING IN PROGRESS AT STATION 1 OF 2. LEFT TO RIGHT ARE JOHN DIEGO PALACIOS, ERIK KANI, AND HSIAO-CHUN HUNG.

FIGURE 20. FINE-MESH SIEVING IN PROGRESS AT STATION 2 OF 2. JUAN SALAS PREPARES FOR SIEVING.

FIGURE 21. EXPOSING A HEATED-ROCK FEATURE AS A DISCRETE UNIT WITHIN THE STRATIGRAPHIC CONTEXT. ANGEL PALACIOS IS AT THE CENTRE LEFT. LUFO BABAUTA IS AT THE CENTRE TO UPPER RIGHT. JOHN CASTRO IS AT THE LOWER RIGHT.

Where charcoal concentrations or other datable materials were encountered in situ, their locations were point-plotted and photographed prior to removal. These samples were assigned individual catalogue numbers.

Excavations continued to the depth of the underlying coral limestone, discovered directly beneath the lowest cultural deposit. This discovery confirmed that the excavation had reached the base of the archaeological layers, without missing any older cultural deposit in this particular location.

No human burial features were encountered during the excavation. Plans of action had been discussed with the CNMI HPO regarding how to proceed with burial findings, but no such procedures were needed in this case of not discovering any human burial features.

The exposed profile of the total excavation area was recorded by photography and by scaled 1:10 illustration. The profile illustrations identified the stratigraphic units, and they indicated the portions of subsurface features present in the profiles. As has been mentioned, all subsurface features were documented thoroughly, regardless of position inside or outside one of the arbitrary border profiles of the block excavation.

Small samples (10 g or less) were retrieved for each recorded stratigraphic layer and also at standard 20-cm intervals in a column in each exposed profile. Under controlled and even conditions, these samples were described in terms of colour and texture, then discarded. Observations of consistence, matrix, and lower boundary were recorded in the field.

Additional samples of sedimentary layers were collected for examination of possible preserved ancient botanical remains. This work will continue through 2017 and potentially into 2018 by Dr. Deng Zhen-hua at the Institute of Geology and Geophysics, Chinese Academy of Sciences, in Beijing, China. Samples of 10 g or less were collected from the stratigraphic profile (Figure 22), and then larger samples of 30 litres were collected from each layer. Those larger samples of sediments were floated in water and passed through a micro-fibre screen to recover any possible pieces of preserved plant parts that could be less than 1 mm in size (Figure 23). Those smaller samples were retained inside their sedimentary matrix for identifying different varieties of preserved plant parts. As of June 2017, the analysis has been proceeding with microscope at 30x or greater magnification.

At the completion of the excavations, CNMI HPO supervised the back-filling, performed by backhoe. The CNMI HPO staff supervised the backhoe activity, in order to ensure that the site was not adversely affected.

The materials from the excavations have undergone standard analysis almost entirely locally in Saipan (Figure 24), but some of the materials needed to be exported temporarily to the Micronesian Area Research Center, University of Guam. Prior to leaving Saipan, a complete field catalogue list was copied for the CNMI HPO, with a formal request for temporary export of the material for scientific analysis.

The recovered contents were washed and then separated by material category (e.g., bone, shell, stone, pottery, etc.). The materials in each category were counted, weighed, and described. More detailed analyses proceeded as appropriate for each material type.

Pottery artefacts were described in terms of basic physical attributes. These attributes included sherd size (sq cm), thickness (mm), weight (g), vessel part (rim, shoulder, body, base, etc.), edge condition (angular or rounded), primary non-plastic inclusion (calcareous, volcanic, or mixed), manufacturing evidence (slab-built, coiled, finger impressions, anvil marks, etc.), surface treatment (wiped, burnished, slipped, etc.), decorative techniques (incision, combing, relief, notching, etc.), and decorative motifs (identifiable design shapes). Photographs and illustrations were recorded of the representative specimens, with attempts to reconstruct vessel forms whenever possible. The results were compared with established pottery types of the region.

FIGURE 22. COLLECTION OF SEDIMENTARY SAMPLES FOR ANALYSIS OF POSSIBLE PALAEO-BOTANICAL MATERIALS. DENG ZHEN-HUA COLLECTS THE SAMPLES HERE.

FIGURE 23. FLOTATION OF SEDIMENT SAMPLES IN PROGRESS. THE LIGHT-WEIGHT PLANT MATERIALS FLOATED TO THE SURFACE OF THE WATER, AND THE CONSTITUENTS AT THE WATER'S SURFACE THEN WERE PASSED THROUGH A MICRO-FIBRE FILTER FOR COMPLETE RETENTION. HSIAO-CHUN HUNG IS STANDING IN THE CENTRE LEFT. SITTING, LEFT TO RIGHT, ARE JENNIFER SABLAN, CASSIUS FITIAL, AND ANGEL PALACIOS.

FIGURE 24. PROCESSING OF THE EXCAVATED MATERIALS, INVOLVING WASHING, SEPARATION OF MATERIAL CATEGORIES, AND THOROUGH DRYING IN PREPARATION FOR RECORDING OF COUNTS, WEIGHTS, AND DETAILED DESCRIPTIONS. MERTIE KANI IS AT THE LEFT, ORGANISING MATERIALS FOR DRYING. JUAN SALAS IS AT THE RIGHT, WASHING MATERIALS.

Stone and shell artefacts were measured, counted, and weighed separately. Photographs were recorded of the representative specimens. Objects were compared with others from known ethnographic and archaeological collections.

Marine shellfish remains were analysed from one of the excavation quadrants (Quadrant 1), thus constituting a 25% sample of the total. The shellfish remains were separated into categories of Genus whenever possible, using a Mariana Islands marine shellfish collection. All resulting categories were counted and weighed. Artificially modified shells were treated as artefacts, while non-modified specimens were treated as elements of food remains.

Non-human bones were separated in taxonomic classes of fish, bird, and turtle. All resulting categories were counted and weighed. Further analysis may yet be performed for more detailed results. None of the animal bones showed indications of having been fashioned into artefacts, and instead they all resembled food remains.

Radiocarbon dating was conducted at Beta Analytic Laboratories in Miami. All samples of charcoal and of marine shell were processed for isotope ratio correction. Accelerated mass spectrometry (AMS) was performed to supply precise age ranges.

For all materials, provenience information was retained to enable analysis of possible spatial patterns and chronological trends. This information was necessary to address the project's central substantive research questions.

All artefacts by law belong to the CNMI Museum. Temporarily and pending approval by the CNMI HPO, some but not all of the newly excavated materials were exported for detailed studies at the Micronesian

Area Research Center, University of Guam. Whenever requested, the materials will be available to return to the CNMI Museum in Saipan.

The project involved opportunities for the staff of CNMI HPO to gain and improve technical skills first-hand in terms of excavation, managing materials, and processing the findings for analysis. Additionally, members of the U.S. Fish and Wildlife Service (USFWS) participated in a portion of the excavation, with a goal of building future partnerships between USFWS and CNMI HPO. The CNMI HPO staff included Mertie Kani, Lufo Babauta, Jose Jesus Fitial, John Diego Palacios, James Pruitt, Jennifer Sablan, Juan Salas, and Abraham Tenorio. The USFWS staff included Jeried Calaor, Brian Leon Guerrero, Kyle Ngiriatregd, and Emily Sablan with authorised travel from their regular assignments at the Ritidian Unit of Guam National Wildlife Refuge (GNWR). Further opportunities were provided for Saipan residents Lufo Babauta Junior, John Castro, Angel Palacios, Cassius Fitial, and Erik Kani to gain certified working experience.

Chapter 4

New Findings: Stratigraphy and Dating

The excavation revealed seven major sedimentary units containing cultural material, designated Layer I (the first layer encountered at the top) through VII (the last layer encountered at the bottom) with internal divisions in some cases of minor differences in the constituent matrix (Table 3; Figures 25 and 26). For instance, Layers III and VI showed internal differentiation from their top to bottom portions, sub-divided into III-A and III-B and into VI-A and VI-B. The underlying limestone technically constituted another layer (Layer VIII), albeit a non-cultural unit.

As observed in October 2016, the site stratigraphy overall accorded with the layers as identified in 2005, but two factors contributed to finer distinctions and a few localised differences. First, the 2016 observations were based on more information, given the ability to examine the sedimentary characteristics across a large contiguous area of 4 by 4 m, as compared to the limited windows of narrow 1 by 2 m test pits in 2005. Second, the October 2016 excavation targeted a slightly lower absolute elevation, closer to sea level and farther downslope (south), where the sedimentary units had formed differently than had occurred in the slightly landward (north) situations of the 2005 test pits.

In chronological order, the layer units began with Layer VIII as the oldest prior to cultural presence in the area, followed by a sequence ending with Layer I as the youngest still in formation today. Each discernable layer had formed over a length of some centuries, as seen in both radiocarbon dating and in the associated pottery, other artefacts, and shellfish remains. These indicators in concert pointed to the date range for the deposition of artefacts and food remains within their associated layers.

FIGURE 25. STRATIGRAPHY EXPOSED AT END OF OCTOBER 2016 EXCAVATION, SHOWING QUADRANT 2, VIEW TO SOUTHEAST. SCALE BARS ARE IN 20-CM INCREMENTS.

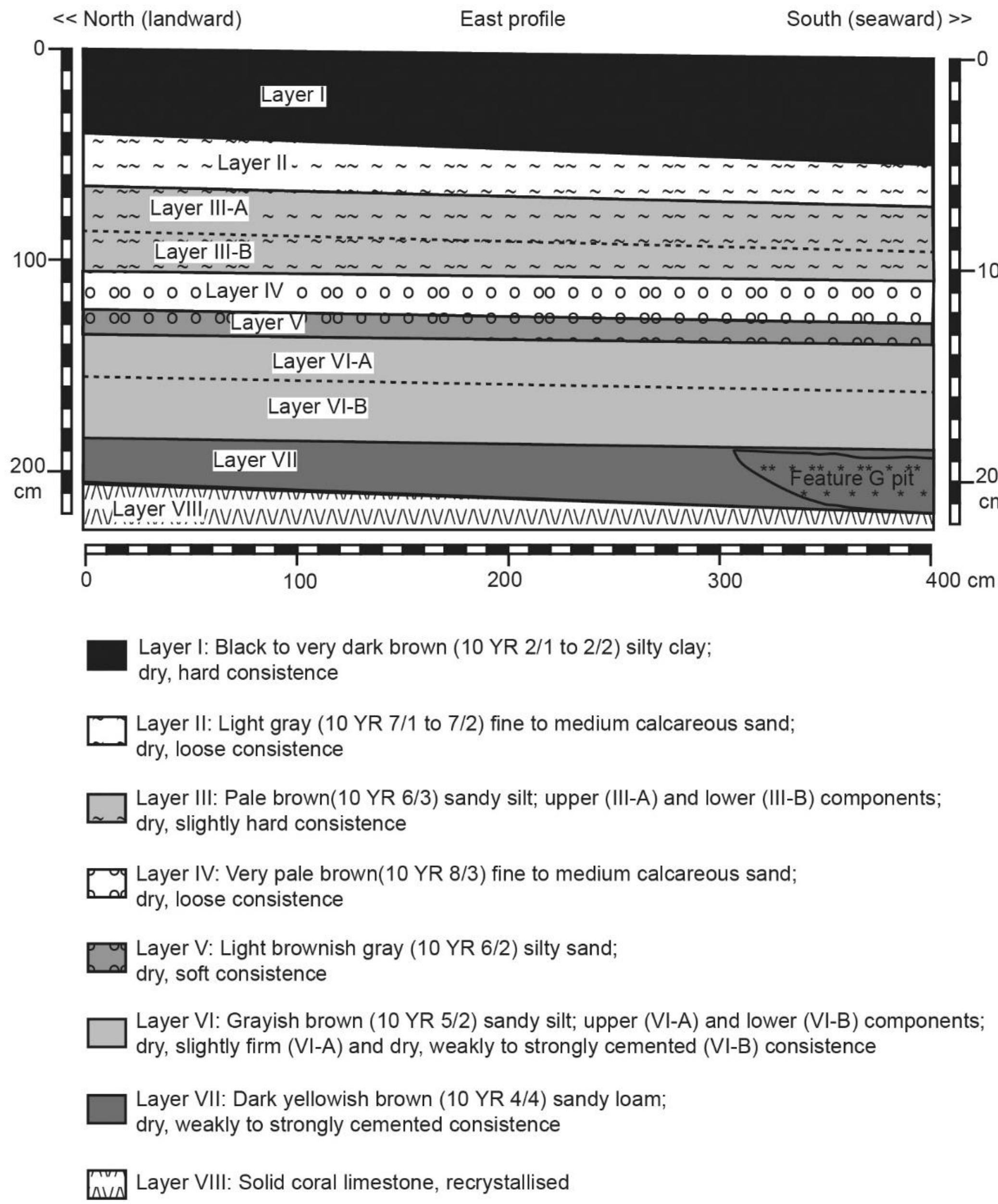

FIGURE 26. STRATIGRAPHIC PROFILE, ACCORDING TO OBSERVATIONS IN OCTOBER 2016.

By coordinating the sedimentary units with their date ranges and associated ancient sea level conditions, the site context can be reconstructed for different time periods (Figure 27). These reconstructions may be considered accurate within ±20 cm elevations. The time periods may yet be refined, and so far the most attention has been given to the earliest settlement contexts prior to 1100 B.C.

The date ranges of each layer were based on radiocarbon dating within the context of the established chronology of Marianas regional cultural material. The regional archaeological chronology has been formulated on the basis of radiocarbon dating of the kinds of artefacts and midden found in several sites across the Mariana Islands (Carson 2016). The region-wide chronology inherently involves gradational boundaries that can be slightly older or younger in one site or another, thus allowing for site-specific variation. The findings at Bapot can be situated within this overall region-wide framework, while still recognising the site-specific uniqueness as encountered in the 2016 excavation.

TABLE 3. STRATIGRAPHIC LAYER DESCRIPTIONS, AS OBSERVED IN OCTOBER 2016.

Layer Designation	Unit Description	Approximate Dating
I 0–40/50 cm	Black to very dark brown (10 YR 2/1 to 2/2) silty clay; 50% pebble and cobble matrix; dry, hard consistence; very abrupt lower boundary	A.D. 1000 through A.D. 1700
II 40/50–65/70 cm	Light gray (10 YR 7/1 to 7/2)fine to medium calcareous sand; less than 5% pebble matrix; dry, loose consistence; abrupt lower boundary	A.D. 500 through A.D. 1000
III-A 65/70–85/90 cm	Pale brown (10 YR 6/3) slightly sandy silt; 20% pebble and cobble matrix; dry, slightly hard consistence; gradual lower boundary	A.D. 100 through A.D. 500
III-B 85/90–105 cm	Pale brown to yellowish brown (10 YR 6/3 to 6/4) sandy silt; 20% pebble and cobble matrix; dry, slightly hard consistence; abrupt lower boundary	500 B.C. through A.D. 100
IV 105–125 cm	Very pale brown (10 YR 8/3) fine to medium calcareous sand; 10% pebble matrix; dry, loose consistence; abrupt lower boundary	700 B.C. to 500 B.C.
V 125–135 cm	Light brownish gray (10 YR 6/2) silty sand; 30% pebble and cobble matrix; dry, soft consistence; clear lower boundary	1100 B.C. through 700 B.C.
VI-A 135–155 cm	Grayish brown (10 YR 5/2) slightly sandy silt; 20% pebble and cobble matrix; dry, slightly firm consistence; gradual lower boundary	1500 B.C. through 1100 B.C.
VI-B 155–185 cm	Grayish brown (10 YR 5/2) sandy silt; intermittent lensing of light gray (10 YR 7/1 to 7/2) fine to medium calcareous sand; 20% pebble and cobble matrix; dry, weakly to strongly cemented consistence; abrupt lower boundary	Approximately 1500 B.C. and possibly earlier
VII 185–205/215 cm	Dark yellowish brown (10 YR 4/4) sandy loam; 10% pebble and cobble matrix; dry, weakly to strongly cemented consistence; very abrupt lower boundary	Approximately 1500 B.C. and possibly earlier
VIII 205/215+	Solid coral limestone, recrystallised	Prior to 3000 B.C.

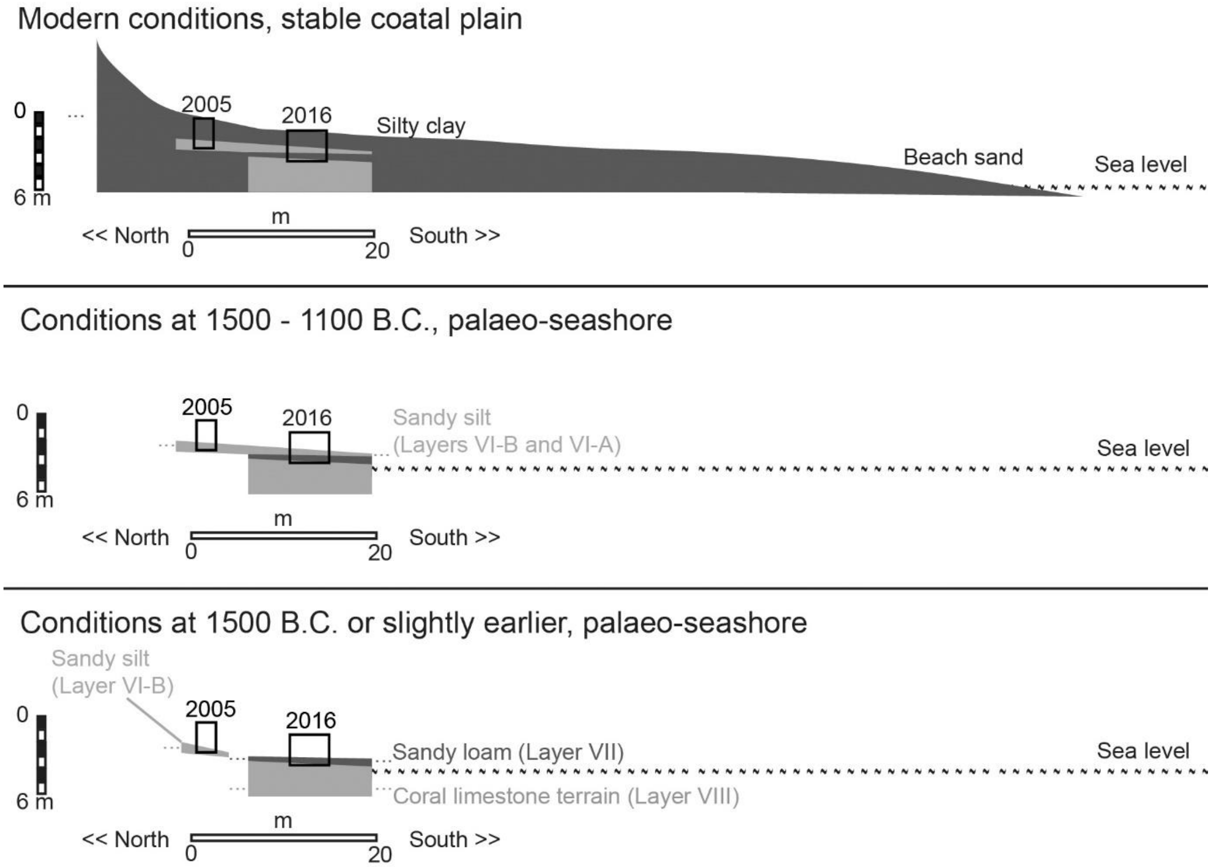

FIGURE 27. APPROXIMATE RECONSTRUCTIONS OF THE SITE SETTING DURING EARLIEST SETTLEMENT PERIODS AS COMPARED TO THE MODERN CONDITIONS.

The 2016 excavation benefitted from new knowledge about the regional sea-level history, parallel findings at other early-period sites, and advancements in radiocarbon dating since the time of the 2005 test pits at Unai Bapot. Other site excavations in Guam and Tinian, south of Saipan within the Mariana Islands, have shown that the oldest habitations were situated on palaeo-seashores close to 1500 B.C., specifically in unstable former beachfronts, lagoon zones, or near-tidal habitats (Carson 2014a, 2014b; Carson and Hung 2015). Additionally informative, buried surfaces of ancient shorelines with and without archaeological deposits have been documented in several locations, in total clarifying where to search for similar sites, how to obtain reliable radiocarbon dating, and how to interpret their ancient contexts (Carson 2011, 2016).

Radiocarbon Dating and Marine Reservoir Correction

Radiocarbon dating successfully assigned measured ages in an otherwise relative-order sequence of stratigraphic layers. The stratigraphic positions alone could reveal the sequence of oldest through youngest components of the site, and then radiocarbon dating could provide specific ages for the materials inside those identified layers. Additional knowledge of chronology of meanwhile was available, such as knowing the approximate ages of geological formations, pottery categories, and other aspects of the archaeological layers.

Worldwide, paired samples of marine shell and charcoal specimens generally provide different radiocarbon dates, due to older carbon in the world's oceans, and therefore a marine calibration curve was developed to make the results inter-comparable. Currently, the calibration set of MARINE13 for marine samples provides high-resolution matching the terrestrial calibration curve of INTCAL13 for charcoal and other terrestrial samples (Reimer et al. 2013). These calibration curves now allow for inter-comparability of results that had not been possible some decades previously.

With the globally established marine calibration curve, further refinement is possible to account for locally specific variations in marine carbon or even specifically in the effects of localised carbon on certain shellfish taxa. This specific correction is known as the marine reservoir correction or ΔR. This correction factor can be ascertained by pairing marine and terrestrial samples from the same contexts, then measuring their variance from the global calibration curves (Reimer and Reimer 2013).

A marine reservoir correction (ΔR) of -49±61 specifically for *Anadara* sp. bivalves (Figure 28) enabled more confidence for dating the oldest site layers in palaeo-seashore contexts, where poorly preserved charcoal often has been unreliable for radiocarbon dating (Table 4). This calculation was based on five different pairings of *Anadara* sp. shells with charcoal in secure contexts, most importantly including one such pairing in a hearth feature of Unai Bapot as presented here. The specific pairing in this case at Unai Bapot actually produced a ΔR of -90±48, which would produce slightly older ages for other unpaired *Anadara* sp. shells than seen in the overall pooled ΔR of -49±61. Nonetheless, the overall pooled value can be appreciated as more conservative and preferable to account for possible variations.

The new ΔR of -49±61 for five different secure-context pairings is strongly aligned with a prior calculation of -44±41 based on two paired samples at the Ritidian Site in Guam (Carson 2010). The five individual pairings produced ΔR values of -70±80 at Ritidian in Guam, 1±56 again at Ritidian, -56±66 once more at Ritidian, -28±48 at House of Taga in Tinian, and now -90±48 at Unai Bapot in Saipan (see Table 4). The results all cross-corroborated each other significantly, proving the validity of the pooled ΔR of -49±61 across multiple contexts, different ages, and three separate islands.

FIGURE 28. SAMPLE BETA-448701 OF *ANADARA* SP. SHELL IN DORSAL (LEFT) AND VENTRAL (RIGHT) VIEWS, FROM FEATURE G OF LAYER VII, PRIOR TO RADIOCARBON DATING BY BETA ANALYTIC. SCALE BARS ARE IN 1-CM INCREMENTS.

TABLE 4. PAIRED CHARCOAL AND *ANADARA* SP. SHELLS VALIDATING A ΔR OF -49±61 IN THE MARIANA ISLANDS.

Context	Beta-#	Material	δ13C (‰)	δ18O (‰)	Conventional Age (years BP)	Marine Reservoir Correction (ΔR)*	2-Sigma Calibration (calendar years)**
Ritidian, Guam, Stable backbeach layer, 90–100 cm (Carson 2010)	263449	*Anadara* sp. shell	+2.1	Not measured	2810±40	-70±80	867–412 B.C. (95.4%)
Ritidian, Guam, Stable backbeach layer, 92 cm (Carson 2010)	263448	Carbonised *Cocos nucifera* (coconut) endocarp	-24.5	-	2510±40	Not applciable	796–509 B.C. (95.4%)
Ritidian, Guam, Stable backbeach layer, 105–110 cm (Carson 2010)	239578	*Anadara* sp. shell	+1.5	Not measured	3140±40	1±56	1165–806 B.C. (95.4%)
Ritidian, Guam, Stable backbeach layer, 98–105 cm (Carson 2010)	239577	Carbonised *Cocos nucifera* (coconut) endocarp	-25.4	-	2810±40	Not measured	1073–1066 B.C. (0.7%); 1057–843 B.C. (94.7%)
Ritidian, Guam, Stable backbeach layer, 80 cm (Carson 2017a, 2017b)	424685	*Anadara* sp. shell	-1.2	-2.1	2870±30	-56±66	788–420 B.C. (95.4%)
Ritidian, Guam, Stable backbeach layer, pit	433372	Charcoal	-26.3	-	2470±30	Not applicable	768–476 B.C. (92.4%); 464–453 B.C. (1.2%);

Context	Beta-#	Material	δ13C (‰)	δ18O (‰)	Conventional Age (years BP)	Marine Reservoir Correction (ΔR)*	2-Sigma Calibration (calendar years)**
feature from origin at 80 cm (Carson 2017a, 2017b)							445–431 B.C. (1.8%)
House of Taga, Tinian, Hearth Feature A, 170 cm (Carson 2014a)	316283	*Anadara* sp. shell	0	Not measured	3390±30	-28±48	1481–1190 B.C. (95.4%)
House of Taga, Tinian, Hearth Feature A, 170 cm (Carson 2014a)	313866	Charcoal, narrow twigs	-30.1	-	3070±30	Not applicable	1413–1266 B.C. (95.4%)
Feature C hearth, originating from Layer VI-A (this study, Table 5)	461342	*Anadara* sp. shell	+0.2	-1.1	3370±30	-90±48	1522–1230 B.C. (95.4%)
Feature C hearth, originating from Layer VI-A (this study, Table 5)	448705	Charcoal	-25.9	Not measured	3110±30	Not applicable	1437–1288 B.C. (95.4%)
TOTAL POOLED						**-49±61**	

* = Marine reservoir corrections were calculated with the Deltar online software package (Reimer and Reimer 2017).

** = Calibrations were by the OxCal program (Bronk Ramsey and Lee 2013), using the INTCAL13 and MARINE13 calibration curves (Reimer et al. 2013).

The evidently reliable ΔR for *Anadara* sp. shells has been particularly useful due to the fact that they dominated the site middens at palaeo-seashore sites, near their preferred habitats of mangroves, seagrass beds, and other shallow-water settings. Consistent with this kind of ancient environmental setting, the rather minimal ΔR of -49±61 indicated that the shells contained carbon in near-equilibrium with the ancient sea surface, in other words not significantly divergent from the modeled global marine calibration curve (Reimer et al. 2013). Moreover, the isotope ratios have been measured consistently within similar parameters for δ13C and for δ18O whenever available, without any irregularities or anomalies that otherwise could suggest a problem with the shell material.

In any case, *Anadara* sp. shells proved to be reliable for dating the contexts paired with charcoal as old as 1437–1288 B.C. specifically at Unai Bapot (see Table 4), although older components of the same palaeo-seashore sites did not retain sufficient carbon for cross-checking with the *Anadara* sp. shells dating back to 1500 B.C. or earlier. Given the apparent problems of finding reliably datable charcoal in the oldest palaeo-seashore layers, the ΔR of -49±61 has been based on paired samples in definite features and other convincing contexts of slightly younger age. Now with independent validation at multiple sites, this ΔR calculation has become one of the most robustly proven in the Pacific Oceanic region.

Unlike the abundantly preserved *Anadara* sp. shells throughout the palaeo-seashore habitation layers, observed concentrations of charcoal and ash have retained insufficient carbon for reliable dating in the deepest and oldest portions of the former near-tidal or subtidal zones (Figures 29, 30, and 31). Charcoal samples have been successful for dating the ancient habitation contexts back to approximately 1300 B.C. in their landward portions or middle-upper zones of their stratigraphy, but so far they have not been effective for dating the first instances of pottery-bearing horizons, dated instead by *Anadara* sp. shells about 200 years older. From both the 2005 and 2016 excavations at Unai Bapot, samples of 500–2000 mg of apparent charcoal from the lowest cultural layers were shown to contain less than 5 mg of actual carbon after acid-wash pre-treatment, and the stringent protocols at Beta Analytic found insufficient carbon for reliable dating of those residual samples of 5 mg or less.

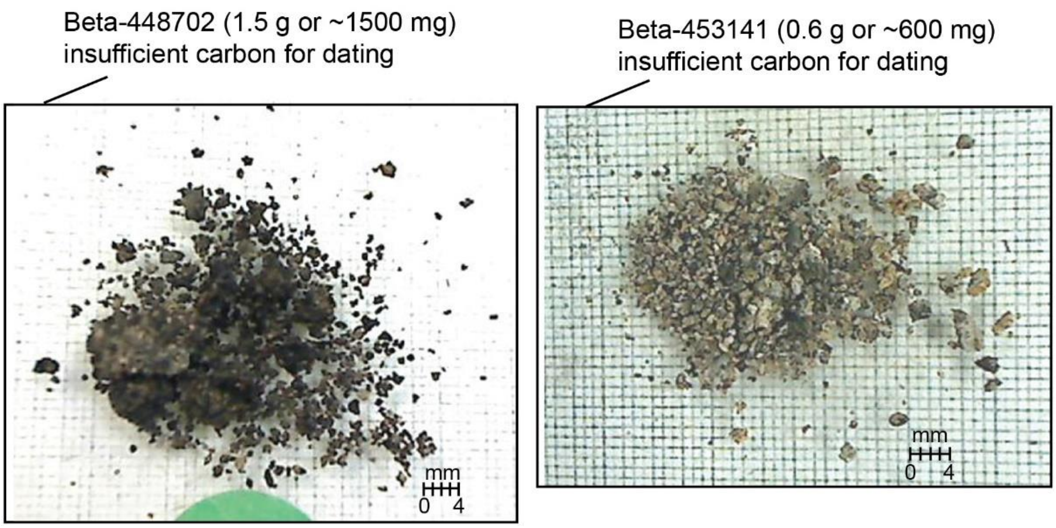

FIGURE 29. SAMPLES BETA-448702 (LEFT) AND BETA-452141 (RIGHT) FROM FEATURE G OF LAYER VII, CONTAINING INSUFFICIENT CARBON FOR RADIOCARBON DATING. IMAGES WERE PROVIDED BY BETA ANALYTIC LABORATORY.

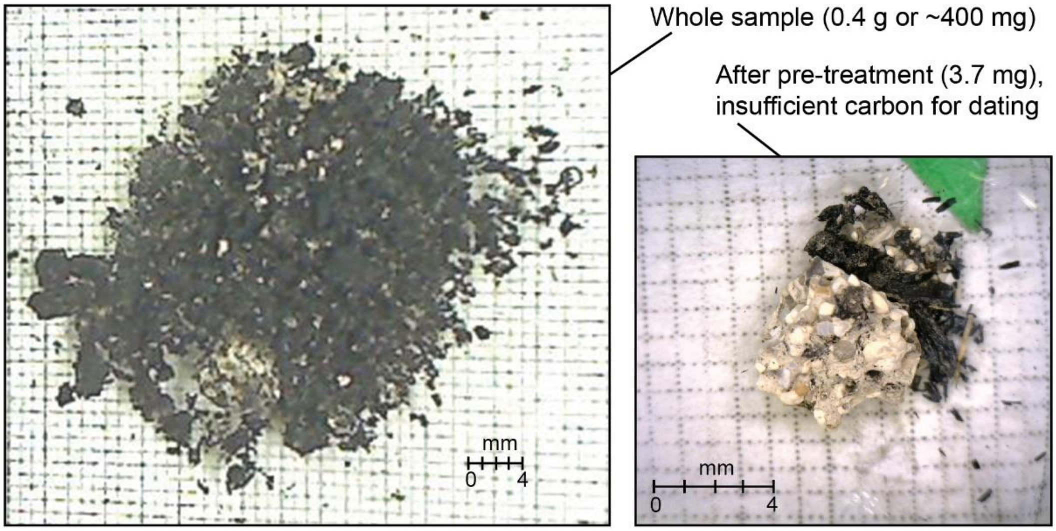

FIGURE 30. SAMPLE BETA-453138 FROM FEATURE H OF LAYER VII. LEFT IMAGE SHOWS THE WHOLE SAMPLE, REMOVED BY TROWEL FROM THE FEATURE. RIGHT IMAGE SHOWS THE REMAINING FRACTION AFTER PRE-TREATMENT OF ACID WASH TO REMOVE POTENTIAL CONTAMINANTS, RETAINING INSUFFICIENT CARBON FOR RADIOCARBON DATING. IMAGES WERE PROVIDED BY BETA ANALYTIC LABORATORY.

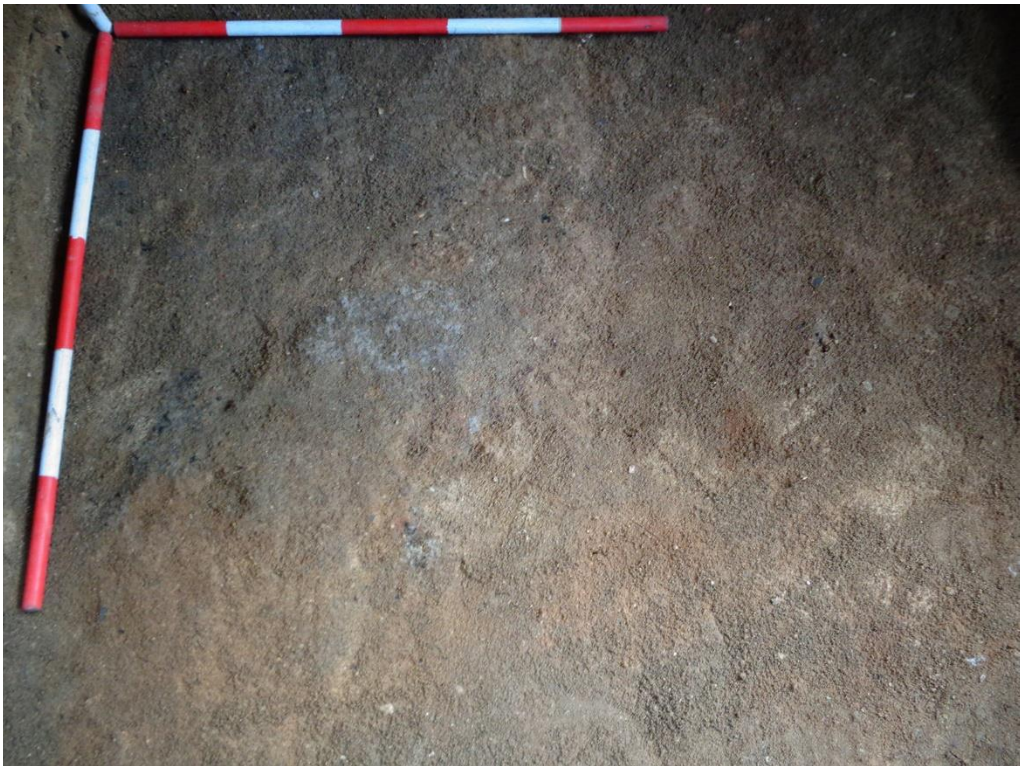

FIGURE 31. CHARCOAL AND ASH WITHIN FEATURE G OF LAYER VII, DURING EXCAVATION, VIEW TO SOUTH. SCALE BARS ARE IN 20-CM INCREMENTS.

Datable Materials within Calcrete

Furthermore in regards to the radiocarbon dating, the Bapot Site revealed an additional problem of cemented sand likely affecting the naturally porous charcoal particles. As will be described in detail here in the presentation of the site stratigraphy, the lower sedimentary units had been cemented into calcrete (Carson and Peterson 2011). Charcoal found above the calcrete zone consistently was datable with results of approximately 1100 B.C. and proceeding in stratigraphic order from there. Charcoal within the calcrete zone, even from dense concentrations of hearths and other features as described here, yielded insufficient carbon for dating.

An Alternative Marine Reservoir Proposal?

The calculated ΔR of -49±61 has been forced to contend with an alternative ΔR of +218±68 proposed by Petchey et al. (2017), but we argue that the radically different proposal suffers from poor context of the charcoal particles that were used as pairings for the marine shells. The alternative ΔR of +218±68 was based on *Anadara* sp. shells paired with charcoal from approximate 10-cm depth intervals of an excavation previously reported by Clark et al. (2010), qualitatively different from the multi-site and context-oriented details supporting the ΔR of -49±61 (see Table 4). The vastly different ΔR values cannot both be accurate, so either one or the other must have been affected by an anomalous factor.

Petchey et al. (2017) suggested that the curiously high ΔR value of +218±68 may have been caused by a hardwater effect uniquely on the deepest *Anadara* sp. shells at Unai Bapot, but we surmise that the ΔR calculation in itself was erroneous. In order for Petchey et al. (2017) to validate their claim, other independent evidence would need to demonstrate that the shells in question were affected by old carbon responsible for the ΔR value of +218±68, while in fact all of the other successful pairings of *Anadara* sp. shells at Ritidian, House of Taga, and now at Unai Bapot consistently showed results confirming the ΔR of -49±61. Actual evidence of a hardwater effect or other in-built old age at Unai Bapot has not been reported, and instead contrary evidence has been discovered as outlined here.

1. ΔR of -49±61 has been proven accurate in repeated instances of paired samples in secured contexts, including a pairing from a hearth feature at the Bapot Site itself as old as 1437–1288 B.C. (see Table 4). These pairings cannot be rejected on any reasonable basis.

2. Petchey et al. (2017) neglected the fact that the nine charcoal particles originally dated by Clark et al. (2010) from 150 through 260 cm depth all returned dates clustered around 1100 B.C., despite their distribution in 110 cm of vertical stratigraphy, crossing different sedimentary contexts, pottery associations, shell midden compositions, and other indicators of significant chronological change. Based on the contextual evidence alone, the materials in the lower layers should pre-date 1100 B.C. Given the newest successful pairing of *Anadara* sp. shell with charcoal in a hearth at 1437–1288 B.C., the lowest cultural layers should pre-date this age range.

3. Instead of pairing *Anadara* sp. shells with charcoal from the most secure middle to upper stratigraphic contexts, for instance around 150 cm depth, Petchey et al. (2017) paired *Anadara* sp. shells with charcoal exclusively from the lowest depths of 230–260 cm, where our current investigations have shown that reliably datable charcoal is either quite scarce or else entirely absent.

4. The pairings by Petchey et al. (2017) actually were in three different depth intervals, and each 10-cm depth grouping produced its own unique ΔR value without overall agreement. The ΔR thus varied as 282±44 at 230–240 cm, as 186±50 at 240–250 cm, and as 147±49 at 250–260 cm. The results from any one given context therefore disagreed with the results from the other reported contexts, such that they could not support a confident pooled value. Even if the results are pooled with their evident disagreement, then the resulting value should be 205±48 instead of the proposal

of 218±68. In contrast, all of the pairings for producing the ΔR of -49±61 were in strong agreement with each other (see Table 4).

5. Regardless of whatever ΔR is being proposed, *Anadara* sp. shells from Unai Bapot have produced radiocarbon dates progressively older with depth, as described here for the 2016 excavation and corroborated by a prior investigation (Bonhomme and Craib 1987). In other words, the *Anadara* sp. shell dating follows the different stratigraphic contexts, unlike the uniform dating of charcoal across 110 cm of stratigraphy as obtained by Clark et al. (2010).

6. The charcoal particles within the calcrete zone at Bapot appear to have been affected by a cementation process and perhaps other factors, such that they are not credible as the basis to calculate a different ΔR. As revealed through the 2016 investigation, reliably datable carbon had been severely depleted from charcoal samples in the lower layers.

7. The upper-dated charcoal samples all were from a stable backbeach layer, situated stratigraphically above the calcrete zone, dated at 1100 B.C., and therefore this upper layer most likely was the source of either intrusive carbon or the actual charcoal particles filtering downward into the lower and older chronostratigraphic units of the palaeo-shoreline context. These effects may have been accentuated by the downward settling of water during the calcrete formation process.

8. The unusually high ΔR value of +218±68 (or more properly of +205±48) signifies a problem with the source material being dated, and so far the charcoal appears to be the problem instead of the shells that have not shown any indication of in-built old age, contaminated carbon, or unusual isotope ratios.

Current Investigation

The artefacts and midden will be presented later, but first the radiocarbon dating results are disclosed here as part of describing the site's stratigraphic sequence (Table 5). The dating samples were retrieved from the secure contexts of features such as hearths and pits, with the least likelihood of having been disturbed or contaminated by material of different age. All samples were analysed at Beta Analytic Laboratory in Miami, Florida, with strict protocols of pre-treatment to remove contaminants.

Through time, the site setting transformed in its physical structure and ecology, as indicated by the sedimentary units and corroborated by the shellfish remains. The older layers revealed the closest association with an ancient shoreline setting, beginning with the coral of Layer VIII that had formed sub-tidally. The younger layers overall show increasing amounts of terrigenous silt and clay, at first mixed with beach sand matrix but eventually involving the entirely terrestrial accumulation of silty clay of Layer I as seen today.

Here we present the stratigraphic layers in chronological order, with emphasis on their formation processes, dated parameters, and cultural contents. The lowest cultural layers definitely pre-dated 1100 B.C. and referred to an older period of higher sea level and different coastal ecology. The middle and upper layers revealed the formation of a stable backbeach and eventually the inland margin of a coastal plain as seen today.

TABLE 5. RESULTS OF RADIOCARBON DATING.

Context	Beta-#	Material	13C/12C ratio (‰)	δ18O (‰)	Conventional Age (years BP)	Marine Reservoir Correction (ΔR)*	2-Sigma Calibration (calendar years)**
Equivalent of Layer V, hearth feature (Carson 2008)	214761	Charcoal flecks	-25.8	-	2840±40	Not applicable	1127–903 B.C. (95.4%)
Feature A hearth, originating from Layer V	448704	Charcoal	-26.1	-	2870±30	Not applicable	1127–931 B.C. (95.4%)
Feature A hearth, originating from Layer V	453139	Charcoal	-22.9	-	2930±30	Not applicable	1220–1025 B.C. (95.4%)
Feature B pit, originating from Layer V	453140	Charcoal flecks	Not reported	-	2960±30	Not applicable	1263–1056 B.C. (95.4%)
Feature C hearth, originating from Layer VI-A	448705	Charcoal	-25.9	-	3110±30	Not applicable	1437–1288 B.C. (95.4%)
Feature C hearth, originating from Layer VI-A	461342	*Anadara* sp. shell	+0.2	-1.5	3370±30	-90±48	1522–1230 B.C. (95.4%)
Feature E hearth, originating from Layer VI-B	448703	Insufficient carbon	-	-	-	-	-
Feature E hearth, originating from Layer VI-B	461341	*Anadara* sp. shell	-0.1	-1.1	3530±30	-49±61	1697–1368 B.C. (95.4%)
Equivalent of Layer VI-B, ash discard pile (Carson 2008)	215936	Insufficient carbon	-	-	-	-	-

Context	Beta-#	Material	13C/12C ratio (‰)	δ18O (‰)	Conventional Age (years BP)	Marine Reservoir Correction (ΔR)*	2-Sigma Calibration (calendar years)**
Equivalent of Layer VI-B, ash discard pile (Carson 2008)	214762	Insufficient carbon	-	-	-	-	-
Equivalent of Layer VI-B, ash discard pile (Carson 2008)	202722	*Anadara* sp. shell	-1.5	Not measured	3590±40	-49±61	1780–1410 B.C. (95.4%)
Equivalent of Layer VI-B, ash discard pile (Carson 2008)	216616	*Anadara* sp. shell	-1.1	Not measured	3710±50	-49±61	1946–1531 B.C. (95.4%)
Feature H hearth, originating from Layer VII	453138	Insufficient carbon	-	-	-	-	-
Feature G pit, originating from Layer VII	453141	Insufficient carbon	-	-	-	-	-
Feature G pit, originating from Layer VII	448702	Insufficient carbon	-	-	-	-	-
Feature G pit, originating from Layer VII	448701	*Anadara* sp. shell	-1.4	-1.7	3600±30	-49±61	1780–1425 B.C.

* = Marine reservoir correction follows the calculations specifically for *Anadara* sp. shells paired with charcoal specimens at the Ritidian Site in Guam (Carson 2010).

** = Calibrations were by the OxCal program (Bronk Ramsey and Lee 2013), using the INTCAL13 and MARINE13 calibration curves (Reimer et al. 2013).

Layer VIII

Layer VIII consisted of coral limestone that must have formed in a sub-tidal context and definitely pre-dated the deposition of the superimposed Layer VII. The coral most likely had formed during the last time of a sea level at such an elevation, perhaps 130,000–115,000 years ago during the last Interglacial Period (Kopp et al. 2009). At 2.05–2.15 m depth beneath today's ground surface of 4.8–5.2 m elevation, the coral of Layer VIII would have been about 0.85–1.35 m above the Mid-Holocene sea level, hence it must have been already uplifted as an exposed rocky shore above sea level by 3000 B.C. When opened by a hammer strike, the coral's interior structure showed that it had been re-crystallised and had absorbed later-aged clay particles and other materials. This kind of re-crystallisation generally is seen in Pleistocene or older formations, and it is rare in the mid-Holocene corals of the Marianas.

Layer VII

The sandy loam of Layer VII had formed only at a low elevation near the palaeo-seashore at Unai Bapot, not seen in any of the prior excavations in slightly landward locations. Its composition suggested a mucky soft-sediment unit, consistent with a repeatedly wet near-tidal zone according to its measured elevation. The silt and clay of the loam consisted of fine-sized particles of apparently decomposed organic matter. The sand included water-rounded calcareous grains and water-rounded fine to coarse gravel of broken shells and coral, indicative of proximate origins on a beach or shallow sea floor.

Within Layer VII, two heated-rock hearths, one large pit feature, and 18 post moulds signified definite cultural activity during the time when the sandy loam still was in process of formation (Figure 32). Some of the sandy loam of Layer VII must have existed prior to the downward cutting of the features into the soft sediment. The sandy loam continued to accumulate and cover the features. The perimeters and bases of the hearths showed fire-hardening and reddening of the adjacent sandy loam. Some of the post moulds may have intruded downward from later layers, yet their top portions all were observed within Layer VII.

The large pit feature provided an *Anadara* sp. shell with a date of 1780–1425 B.C. (Beta-448701), while two charcoal samples (500 and 1500 mg) from the same pit feature retained insufficient carbon for dating. From a hearth feature, a charcoal concentration of 2000 mg retained less than 5 mg of actual carbon after the standard acid wash to remove contaminants. The same problem occurred with other apparent charcoal concentrations from the next stratigraphic unit of Layer VI-B, thus indicating that the charcoal in the oldest layers had been rendered unreliable for radiocarbon dating.

Artefacts from Layer VII were typical of first-settlement sites in the Marianas pre-dating 1100 B.C. and specifically matching with the prior 2005 findings at Unai Bapot (Figure 33). Thin-walled earthenware pottery vessels were made in the forms of red-slipped or black-burnished bowls, often with sharp carinations, and generally 20 cm or less in diameter. Finely decorated pottery was extremely rare, consistent with the observations in less than 1% of other site assemblages. Polished adzes were made of chert, not yet sourced geochemically but commonly found in the early-period site layers. Beads and other body ornaments were made of varied shells.

The shellfish midden of Layer VII reflected cultural harvesting primarily from a shallow-water mucky zone, but people must have accessed rocky exposure habitats as well. As seen in every known early habitation site of the region, *Anadara* sp. clamshells comprised by far the most dominant component, and they most likely lived within a shallow-water mangrove or seagrass bed directly adjacent to the site. Meanwhile, numerically lesser but nonetheless significant amounts of rock-clinging shellfish taxa included *Haliotis* sp. (abalone), *Patelloida* spp. (limpets), sea urchin, and chiton that must have lived on roughly horizontal rocky surfaces of limestone or coral reef. *Haliotis* sp. shells so far have been documented only in Unai Bapot's earliest cultural layers and no other archaeological instance in the Marianas, thus revealing more about the unique character of this palaeo-seashore habitation.

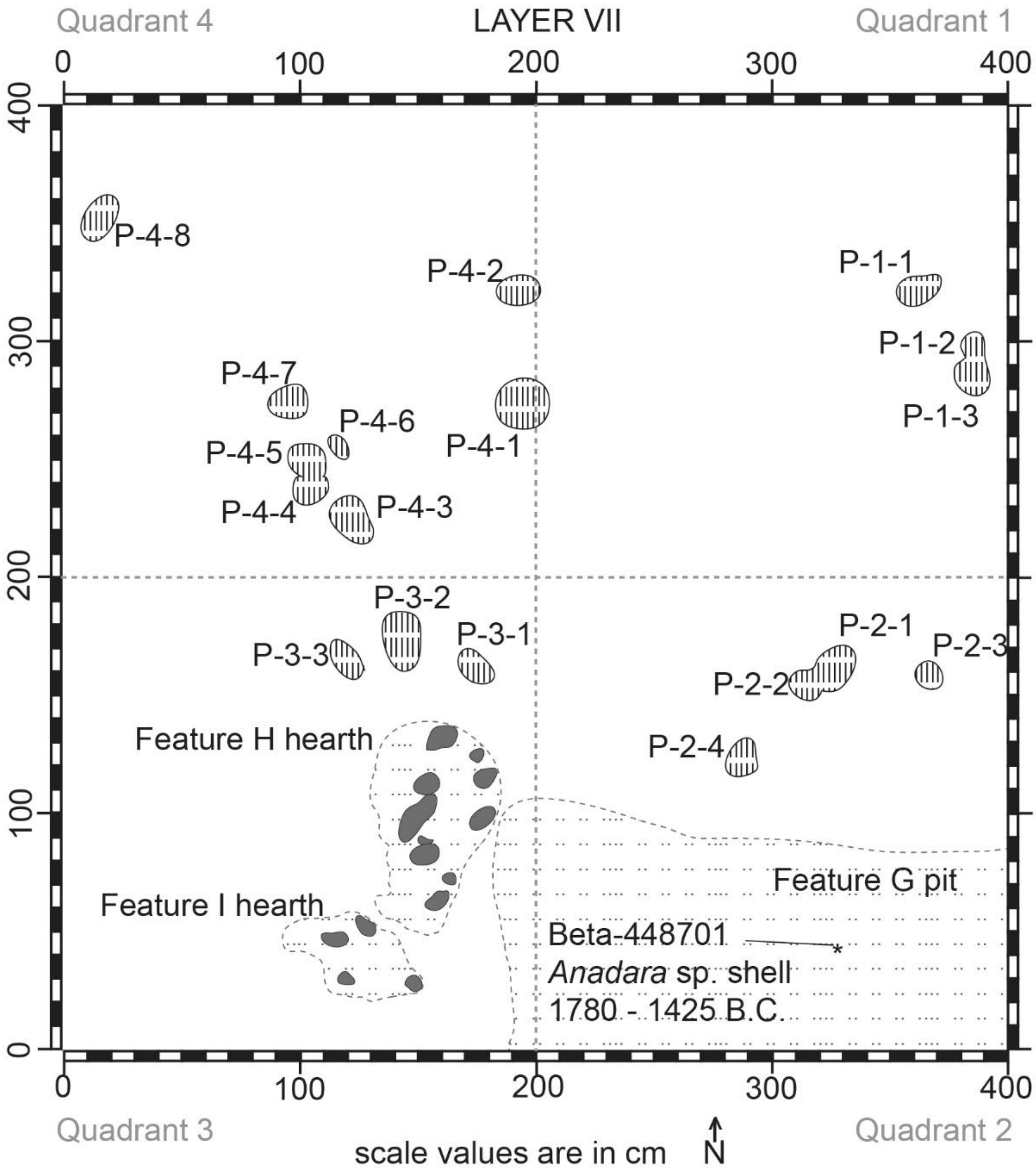

FIGURE 32. PLAN VIEW OF LAYER VII.

At some time after Layer VII had formed, its sandy component was cemented into calcrete. The cementation process affected Layers VII and VI-B, so it must have occurred after both of those layers were buried and positioned at a depth where water could settle and create cementation with the carbonate clasts (Carson and Peterson 2011). Pieces of broken artefacts and midden were encased within the calcrete that formed around them, occurring at a time post-dating their deposition and when draining rainwater had interacted with the carbonates in the buried sedimentary unit.

The cementation in Layers VII and VI-B definitely involved the downward settling of water into a certain depth, likely affecting charcoal particles that otherwise might have been useful for radiocarbon dating. First of all, charcoal flecks easily could be displaced vertically, and isolated occurrences must be regarded skeptically in comparison to the more secure contexts of hearths, pits, or other structural features. Second but equally important, the cementation process itself as a chemical reaction may have affected the constituent charcoal. In the rare instances of finding apparent charcoal concentrations at this depth, the samples retained only a miniscule amount of actual carbon as noted here (less than 1% of the whole samples), insufficient for radiocarbon dating even with the capacities of accelerator mass spectrometry (AMS). Even if sufficient carbon had been retained, then the vastly reduced amount of carbon would signal a warning of an unreliable sample material. As for the *Anadara* sp. shells, they did not exhibit any extraordinary isotope ratios or other indications outside expectations, and their dating proceeded normally. Furthermore, the hard bivalves generally would be more resistant against infiltration of contaminants, as compared to the porous nature of charcoal.

FIGURE 33. EXAMPLES OF EARLIEST ARTEFACTS FROM THE 2005 AND 2016 EXCAVATIONS AT UNAI BAPOT. SCALE BARS ARE IN 1-CM INCREMENTS.

1 = TWO CONJOINED PIECES OF CARINATED RED-SLIPPED BOWL FRAGMENTS, 2016. 2 = ONE PIECE OF DECORATED POTTERY, 2016. 3 = FOUR PIECES OF DECORATED POTTERY, 2005. 4 = TWO NACREOUS SHELL PENDANTS, 2005. 5 = THREE *CYPRAEA* SP. SHELL BEADS, 2016. 6 = SHELL ORNAMENT, POSSIBLE EAR RING, 2016. 7 = SHELL FISHING HOOK, ENCASED IN CEMENTED SAND, 2016. 8 = FOUR SHELL DISCS IN VARIABLE STAGES OF MANUFACTURE, TWO VIEWS EACH, 2016. 9 = POLISHED CHERT ADZE FRAGMENTS, 2005. 10 = TWO POLISHED CHERT ADZES, 2016.

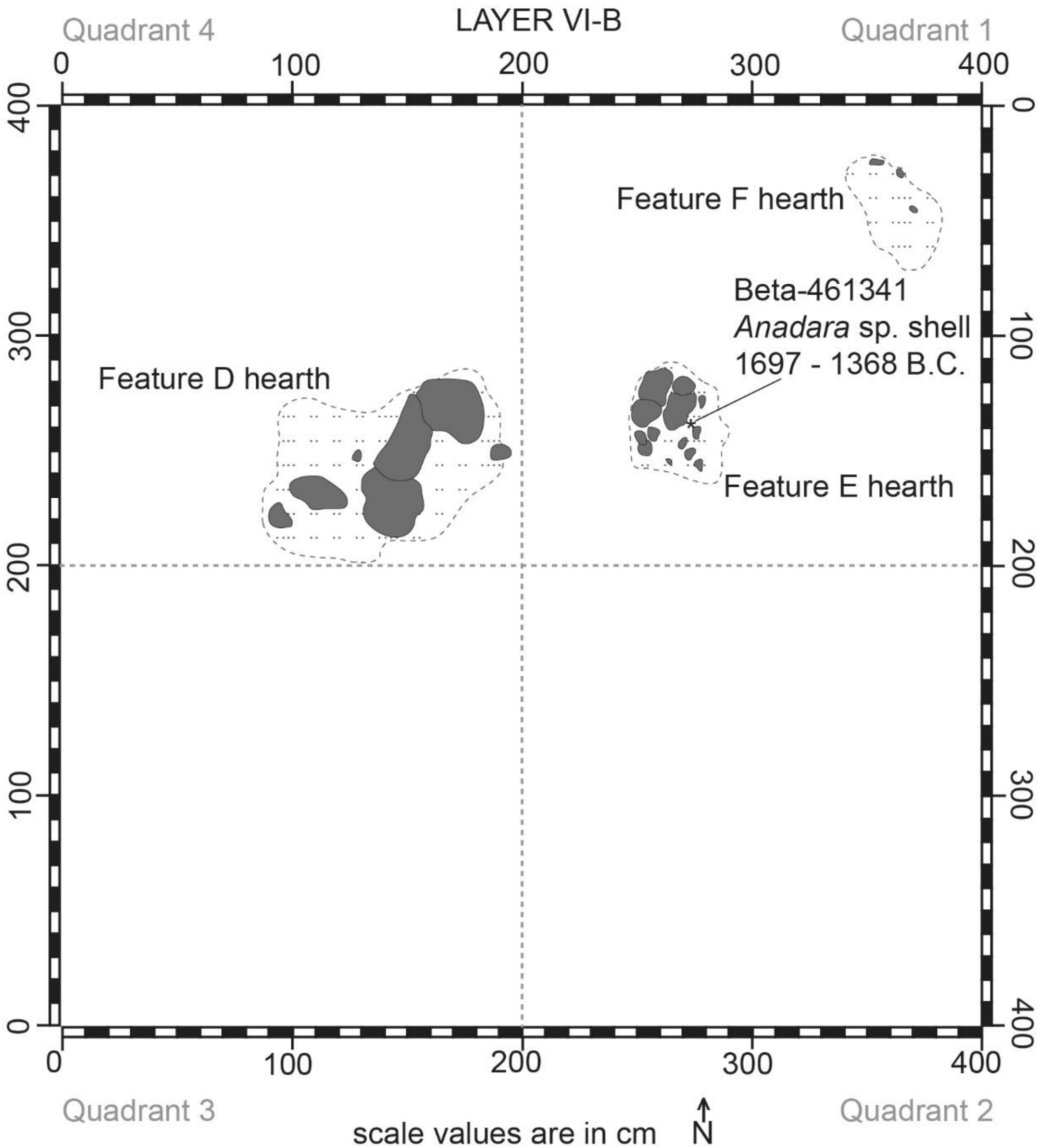

FIGURE 34. PLAN VIEW OF LAYER VI-B.

Layer VI-B

The sandy silt of Layer VI was recognised as a buried palaeosol unit, consisting of lower (VI-B) and upper (VI-A) parts, internally distinguished by a gradual boundary interface. Most likely due to the ancient soil-formation process, the upper (VI-A) portion contained more silt and organic material, whereas the lower (VI-B) portion contained more calcareous sand. The cementation process of making calcrete affected the lower (VI-B) but not the upper (VI-A) portion.

A hearth feature in Layer VI-B yielded charcoal that could not be dated by radiocarbon, but an *Anadara* sp. shell produced a calibrated date of 1697–1368 B.C. (Beta-461341) (Figure 34). This date range was slightly later than the dating for the underlying Layer VII, but the two dating results overlapped significantly at 1697–1425 B.C. In this case, the chronological difference may have been minimal between the two separate chronostratigraphic units.

In terms of their artefacts and midden contents, Layers VI-B and VI-A were very much similar with each other, and furthermore they showed no significant difference from the findings in the underlying Layer VII. All three of these layers referred to a context of a palaeo-seashore during the end of the Mid-Holocene highstand, and they pre-dated the beginning of a stable backbeach in next super-imposed unit of Layer V around 1100 B.C. Likewise, they referred to a continuous usage of the same artefact traditions and harvesting of the same shellfish resources as seen since the initiation of cultural presence at the site, showing clear compositional change only later in Layer V.

Layer VI-B represented the layer of initial cultural habitation in the more landward portion of the site, for instance in the portion exposed through the 2005 test pits. This more landward locale was positioned 1–1.3 m higher than the 2016 excavation area, and it was separated from the extent of the near-tidal sandy loam of Layer VII. From this landward portion of Layer VI-B, a small ash pile yielded two *Anadara* sp. shells with cross-supporting radiocarbon dates calibrated at 1946–1531 B.C. (Beta-216616) and 1780–1410 B.C. (Beta-202722).

The landward portion of Layer VI-B (excavated in 2005) may have existed prior to the seaward portion (excavated in 2016), instead closer in age to the occurrence of Layer VII. The two landward dating samples of Layer VI-B overlapped at 1780–1531 B.C., strongly compatible with the dating of the exclusively seaward Layer VII at 1780–1425 B.C. Definitely post-dating Layer VII, however, the seaward portion of Layer VI-B was dated at 1697–1368 B.C. as shown here.

The time difference between the stratigraphic components of Layers VII and VI-B was small, in fact occurring within the error range of radiocarbon dating precision. If the collective results from Layers VII and VI-B are taken together, then all can be seen as overlapping at 1697–1531 B.C. and thus demonstrating a pre-1500 B.C. age for these two lowest cultural layers. More accurately in accordance with their contexts, however, the individual dating results refer to slightly different points in a longer extended range, given an oldest instance at 1946–1531 B.C. and a youngest at 1697–1368 B.C.

Within the area of the 2016 excavation, a definite chronostratigraphic order was observable for Layers VII, VI-B, and VI-A. Superimposed patterns of features revealed that the same space was used differentially through time. For example, hearths in Layers VI-B and VI-A were positioned over the locations of older post moulds and other features in Layer VII. Nonetheless, the three layers exhibited continuity of artefacts, midden, and palaeo-seashore context pre-dating 1100 B.C.

Layer VI-A

Radiocarbon dating provided a calibrated age of 1437–1288 B.C. (Beta-448705) for charcoal in a hearth of Layer VI-A (Figure 35), representing so far the oldest dated charcoal at Unai Bapot. The same hearth contained an *Anadara* sp. shell dated at 1522–1230 B.C. (Beta-461342), thus providing the oldest radiocarbon pairing of charcoal and shell in the Mariana Islands. In the more landward test pits of 2005, the stratigraphic equivalent of Layer VI-A had been within the calcrete zone where charcoal was considered unreliable for radiocarbon dating. In the 2016 excavation area, Layer VI-A was above the calcrete.

The dating samples were obtained from a heated-rock hearth that contained about 20–25% of an earthenware bowl. This particular discovery exhibited the diagnostic indicators of early-period pottery in the Marianas, made with thin walls, everted lip over a carinated shoulder, red slip, and opening of about 20 cm diameter. Other findings from this layer were consistent with the artifacts and midden generally pre-dating 1100 B.C.

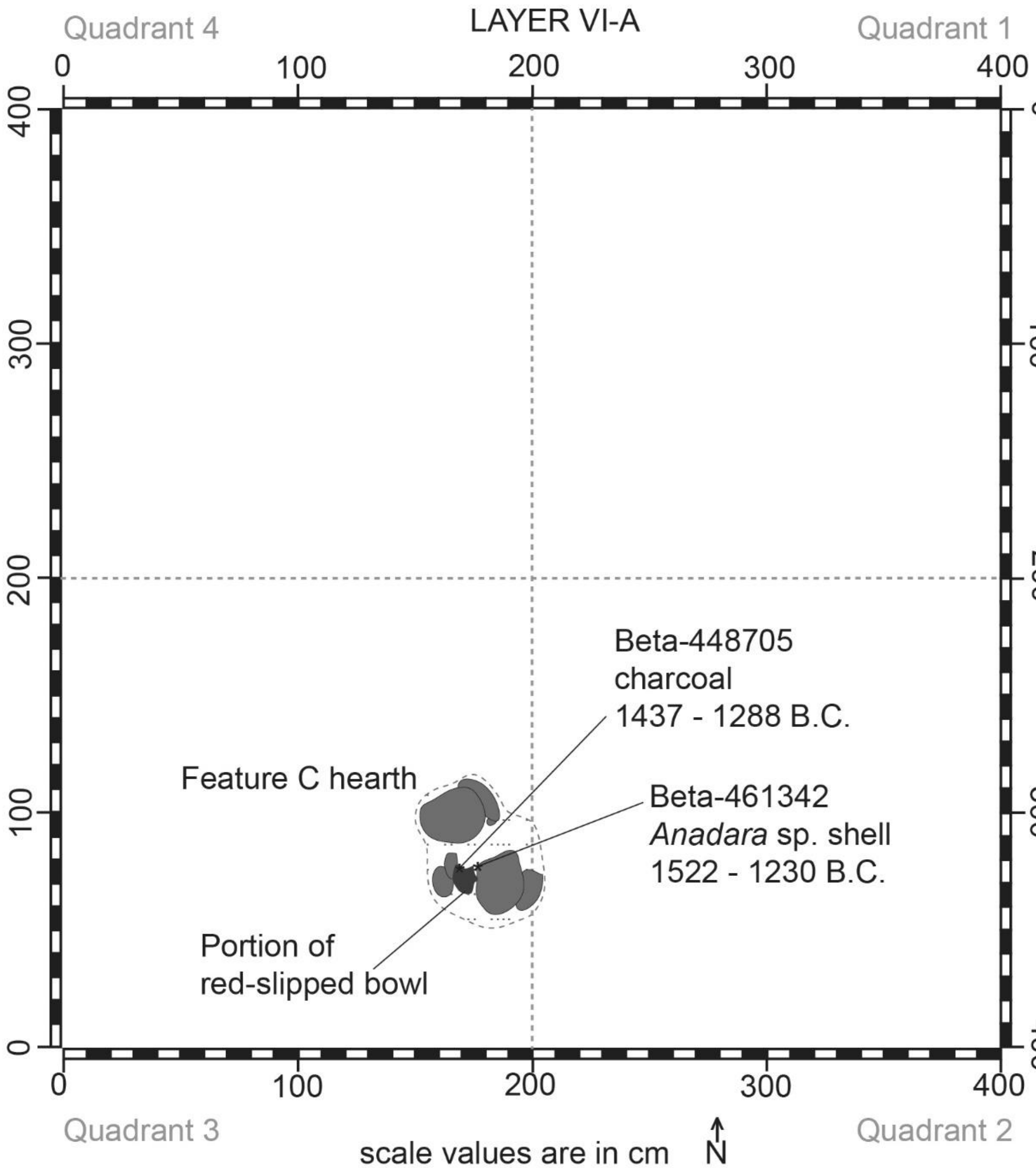

FIGURE 35. PLAN VIEW OF LAYER VI-A.

Layer V

Layer V represented the beginning of a stable backbeach, occasioned by the initiation of sea-level drawdown. As the sea level lowered, the site surface was stranded at a slightly higher elevation and landward position from the moving shoreline. Storm-surge deposits began to accumulate without being washed away during repeated tidal events.

Radiocarbon dating results of this layer and the associated stable backbeach around 1100 B.C. were consistent in both the 2005 and 2016 excavations, wherein four different charcoal dates overlapped redundantly at 1127–1056 B.C. The silty sand of Layer V contained dispersed charcoal flecking throughout its extent, and large charcoal chunks were especially well preserved in a heated-rock hearth.

Two charcoal samples from this hearth produced calibrated ages of 1220–1025 B.C. (Beta-453139) and 1127–931 B.C. (Beta-448704) (Figure 36). Charcoal flecks from a pit feature proved to retain less datable carbon, but one sample yielded a calibrated result of 1263–1056 B.C. (Beta-453140). From the 2005 test pits, a concentration of charcoal flecks provided a calibrated date of 1127–903 B.C. (Beta-214761).

Beginning in Layer V, the artefacts showed less of the diagnostic first-settlement material, while different categories emerged. The exceptionally thin-walled earthenware varieties no longer were produced. A new fashion of a narrow straight-sided cup made its first appearance. Meanwhile, black-burnished bowls drastically declined in popularity, eventually disappearing later in the sequence. Additionally, polished chert adzes had disappeared by this time, and likewise some of the specialised shell ornaments, such as the highly distinctive cut and polished *Cypraea* sp. shell beads, no longer were produced.

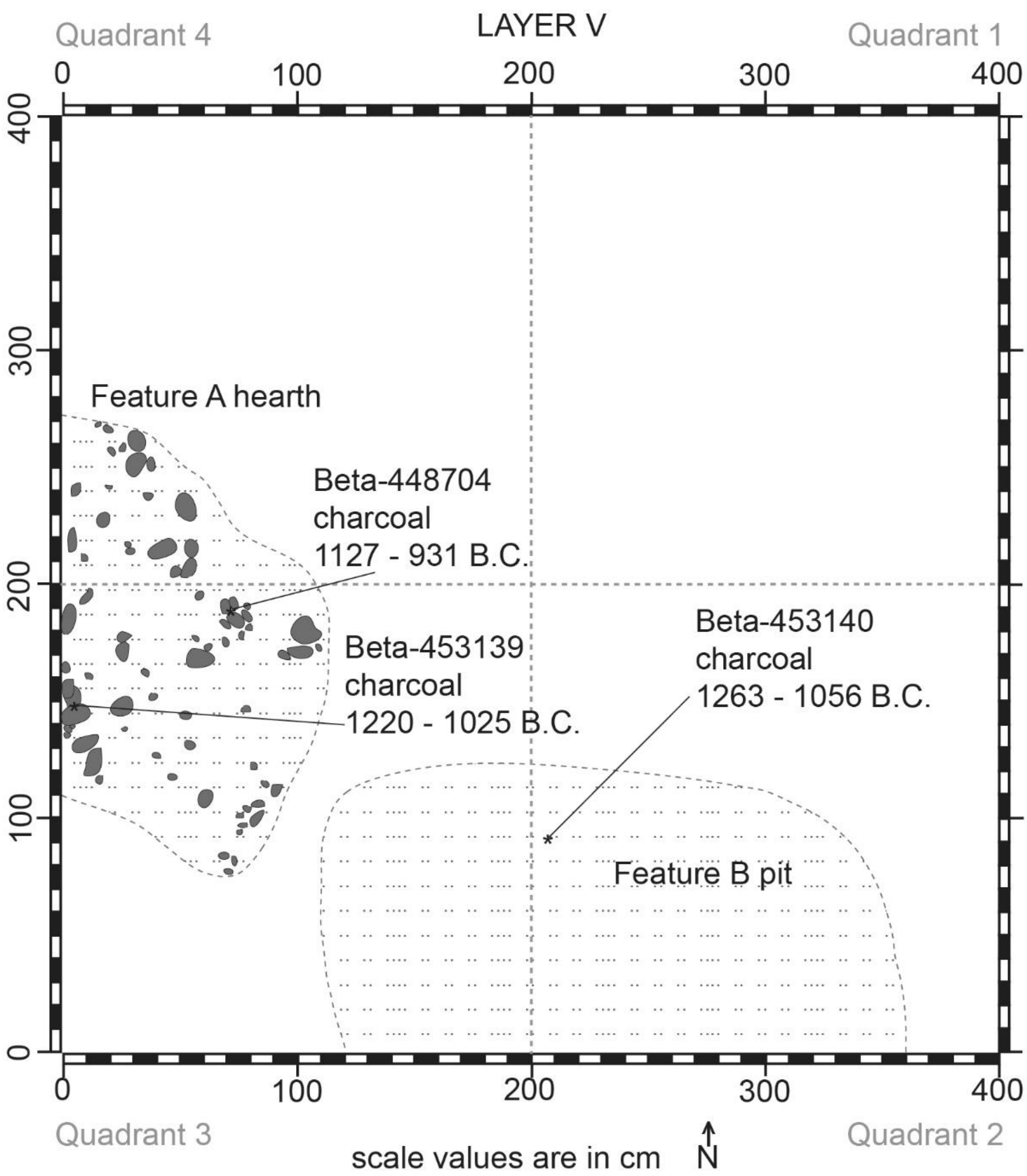

FIGURE 36. PLAN VIEW OF LAYER V.

The shellfish midden exhibited a compositional change in Layer V, interpreted as a sign of nearshore resource depression, due to the combined effects of sea-level drawdown and cultural harvesting. *Anadara* sp. began a drastic decline, followed by dwindling numbers of *Patelloida* spp. (limpets) and sea urchins soon thereafter. *Haliotis* sp. (abalone) and chiton already had disappeared entirely from the midden. In their place, *Turbo* spp. and *Trochus* spp. became more popular, and notably these gastropods could be harvested from a wider range of lagoons and reefs than was the case for the other declining taxa. Small *Gafrarium* sp. bivalves also became more popular, as they could survive in a broader range of nearshore habitats as compared to the more narrow-niche *Anadara* sp. clams.

The same chronological shifts in pottery types, shellfish midden, and beach formation were documented at the Ritidian Site in Guam (Carson 2017a, 2017b) and at House of Taga in Tinian (Carson 2014a), consistently around 1100 B.C. At Ritidian, the older paleo-lagoon layer was covered by tidal-surge detritus of broken branch coral, directly dated at 1386–1006 B.C., followed by the formation of an elongate beach ridge that had been stranded behind the lowering sea level. Cultural habitation along the newly formed beach ridge was dated at 1073–843 B.C. At House of Taga in Tinian, the shift from near-tidal zone to stable backbeach was dated by charcoal in a hearth of the stable backbeach layer, calibrated at 1264–1045 B.C. In both of these cases, the shifts in associated pottery and shellfish composition mirrored their counterparts as seen at Unai Bapot in Layer V.

The findings at Unai Bapot, as at other sites, indicated that the palaeo-seashore context of initial human presence in the Marianas already had started to transform by the time of Layer V, dated around 1100 B.C. The first-settlement context therefore pre-dated 1100 B.C., and it was characterised by the range of pottery, other artefacts, and shellfish midden as seen in Layers VII through VI-A at Unai Bapot. These parameters concurred with the Marianas regional chronology of a first-settlement period (Carson 2014a, 2016).

Layer IV

Layers IV through I all post-dated the palaeo-seashore context at Unai Bapot. These layers have not yet been dated by radiocarbon, and instead their pottery fragments and other artefacts have been assessed according to the regional chronological sequence. The details of the regional chronology and supporting radiocarbon results have been published elsewhere (Carson 2016).

The calcareous sand of Layer IV resembled a short-lived period of mostly windblown material deposition. Both the lower and upper boundaries of Layer IV were abrupt, indicating rapid change in the environment before and after the formation of Layer IV. The sandy matrix of Layer IV itself consisted of fine to medium grains of calcareous sand, wherein the medium-sized fraction suggested a stronger propelling wind than otherwise seen in windblown sand composed entirely of fine-fraction particles.

The pottery of Layer V accorded with the regional chronology in a narrow window of 700 through 500 B.C. The use of red slip had continued, but black-burnished pottery had disappeared. Narrow and straight-sided cups had gained more popularity. New forms of large flat-bottomed yet shallow pans or griddles made their first appearance.

Layer III-B

The sandy silt of Layer III represented a palaeosol, recognised with internal lower (III-B) and upper (III-A) components. The temporarily stable soil formation in this case involved the accumulation of terrigenous silt with plant material decomposition and other organic debris into a sandy matrix. The base of sandy matrix overall had continued similarly from the underlying sand of Layer IV.

Layer III-B contained pottery with red slipped and non-slipped varieties, paralleling the general regional decline of red slip after 500 B.C. The straight-sided cups and the flat-bottomed pans clearly were the most popular vessel forms, and they were made with non-slipped, rough-wiped, or sometimes red-slipped exteriors. The smaller bowls were considerably less popular than in the deeper layers, and they continued to be made exclusively with red slip.

Layer III-A

The sandy silt palaeosol of Layer III was most strongly represented in the upper component of Layer III-A of stable soil-formation horizon, and it most likely corresponded with a period of slowed sea-level drawdown. In the Mariana Islands generally, the sea-level drawdown had slowed about A.D. 1 through 200, resulting in temporarily stable beach surfaces at a number of sites, such as at Tumon and at Ypan in Guam (Carson 2011, 2016). The pottery in Layer III-A at Unai Bapot accorded with this general time frame, showing minimal usage of red slip except in rare examples of larger bowls without the older varieties of smaller-sized bowls and carinated shapes.

Layer II

The calcareous sand of Layer II represented another short-lived period of mostly windblown sandy deposition, similar to the conditions as seen in Layer IV. The lower and upper boundaries were abrupt or very abrupt, indicating a rapid change in the environmental context before and after the time of Layer II's deposition. The sand mostly was windblown, and it may have accumulated rapidly.

Pottery of Layer II suggested most likely a range between A.D. 500 and 1000. Red slip had vanished entirely by this time. The straight-sided cups and flat-bottomed pans continued to be produced, but those forms generally declined in the region after A.D. 500. They were joined by thick-walled and thickened-rim bowls that mostly became popular in the Marianas after A.D. 1000.

Layer I

The rocky silty clay of Layer I represented the most recent sedimentary unit at the site, technically still in process of formation as an organic soil horizon. It most likely formed during the time of the present-day observable coastal plain, linked with the modern sea level and coastline now more than 80 m southward from the site. The silty clay was of terrigenous origin, and it was the only sedimentary unit at the site lacking a beach-derived or marine-derived component.

Layer I contained thickened-rim pottery, a slingstone fragment, a broken piece of a stone grinding mortar, a *Spondylus* sp. shell disc, and other materials that have characterised surface-visible sites of A.D. 1000 through A.D. 1700, locally known as *latte* sites. *Latte* sites have been extremely well documented throughout the Mariana Islands (Carson 2012b), named after their unique style of houses with stone pillars and capitals. The limestone ruins of two *latte* have been preserved on the site surface, associated with Layer I.

Chapter 5

New Findings: Overall Archaeological Contents

An overview summary is introduced here for the assemblage of thousands of pottery fragments, stone and shell artefacts, marine shell and animal bone midden, and other materials. Table 6 provides the raw data of counts and weights of all individual items, found in each stratigraphic unit, sub-divided by spatial quadrant (Quadrants 1 through 4) and with notation of internal artificial level (cm depth). This summary of raw data has formed the basis for most of the presentation, discussion, and interpretation of the 2016 excavation findings.

As an important note when interpreting the raw data, the shellfish remains were examined only in Quadrant 1, as a 25% sample of the total excavation area. The reported counts and weights therefore may be viewed as representing 25% of the values for the overall excavation. Likewise, when comparing the density of shellfish remains against density of pottery or other materials, the values for the shellfish have been adjusted accordingly.

Overall abundance of past cultural activity may be approximated by the overall abundance of material findings, for instance by noting the two most abundant material categories of pottery fragments and marine shellfish remains. The raw values are shown in Figure 37, and densities per 100 litres of excavation are depicted for Figure 38. For the purpose of representing each layer overall as a unit, the potentially skewed high-density findings from hearths and other features were excluded from these summary graphics.

The density values show slightly different trends in the pottery and shellfish remains, but caution is advised with awareness of how the data were recorded. The pottery (encoded in numbers of pieces) overall declined through time, with a mild increase during the most recent Layer I, but the numerous tiny and thin fragments in the older periods could be over-represented to some extent. The shellfish remains (encoded in weights) peaked at Layer VI-A through Layer IV, but the heavier total weights here could be attributed to a lessening contribution of smaller-sized and lighter-weighted specimens (such as *Patelloida* spp. shells) that previously had been more numerous in older contexts, along with increasing contribution of larger-sized and heavier-weighted specimens (such as *Turbo* spp. shells and opercula).

While pottery was numerically the most abundant artifact material, the various stone and shell artefacts included adzes, flaked debris, beads and other body ornaments, fishing gear, and several other object categories (Figure 39). The diversity of material per stratigraphic layer generally followed the overall abundance of pottery and shellfish remains, wherein greater amount of cultural material enabled greater likelihood of discovering more rarities and thus resulted in more diversity of material categories. Many of the stone and shell objects were found as singular occurrences or in very low frequencies.

Further discussion of specific findings will refer back to the raw data and summaries as disclosed here. New observations may yet provide more details for the individual materials, but the raw data never will change. Similarly, new ideas and interpretations may yet develop, but the primary datasets will need to serve as the basis for further work. A number of such detailed studies already are in progress, for example concerning analysis of potentially preserved archaeo-botanical remains.

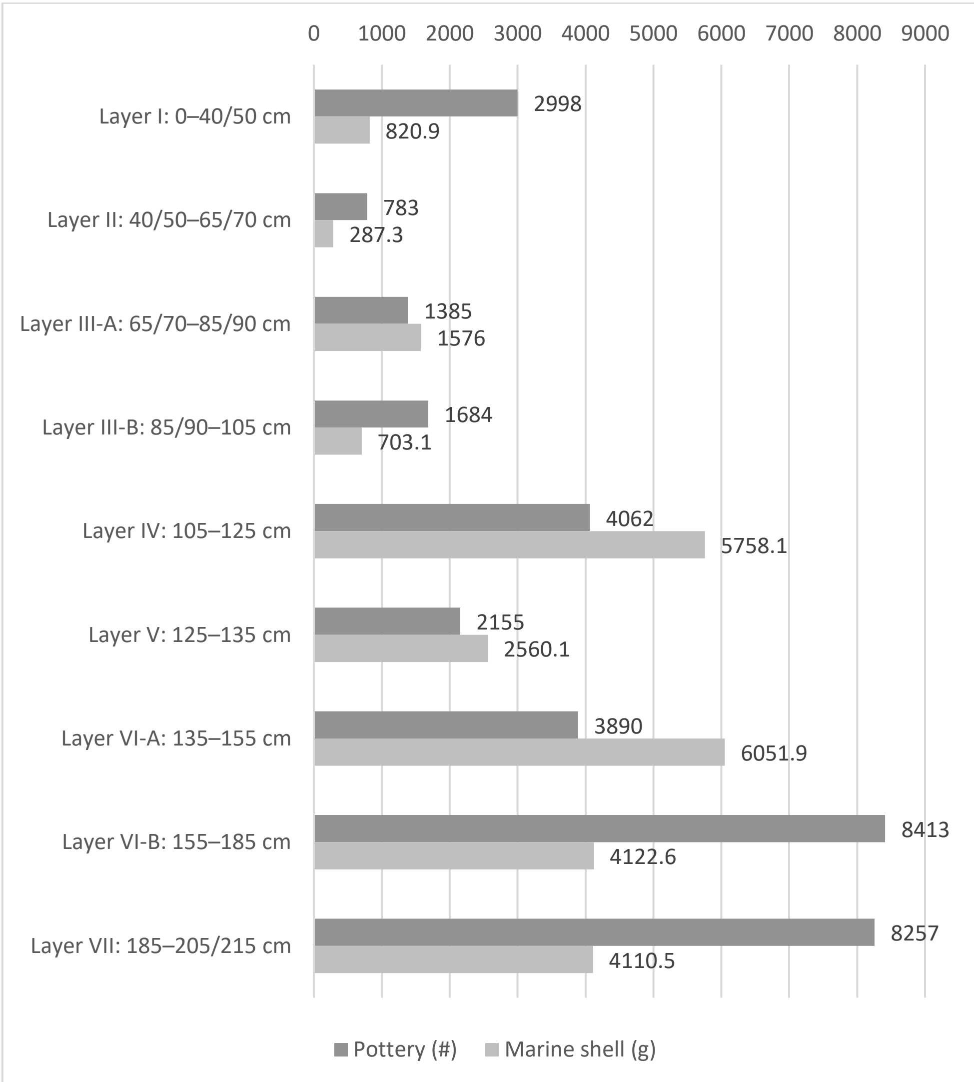

FIGURE 37. RAW COUNTS OF POTTERY FRAGMENTS AND GRAMS OF MARINE SHELL PER LAYER.

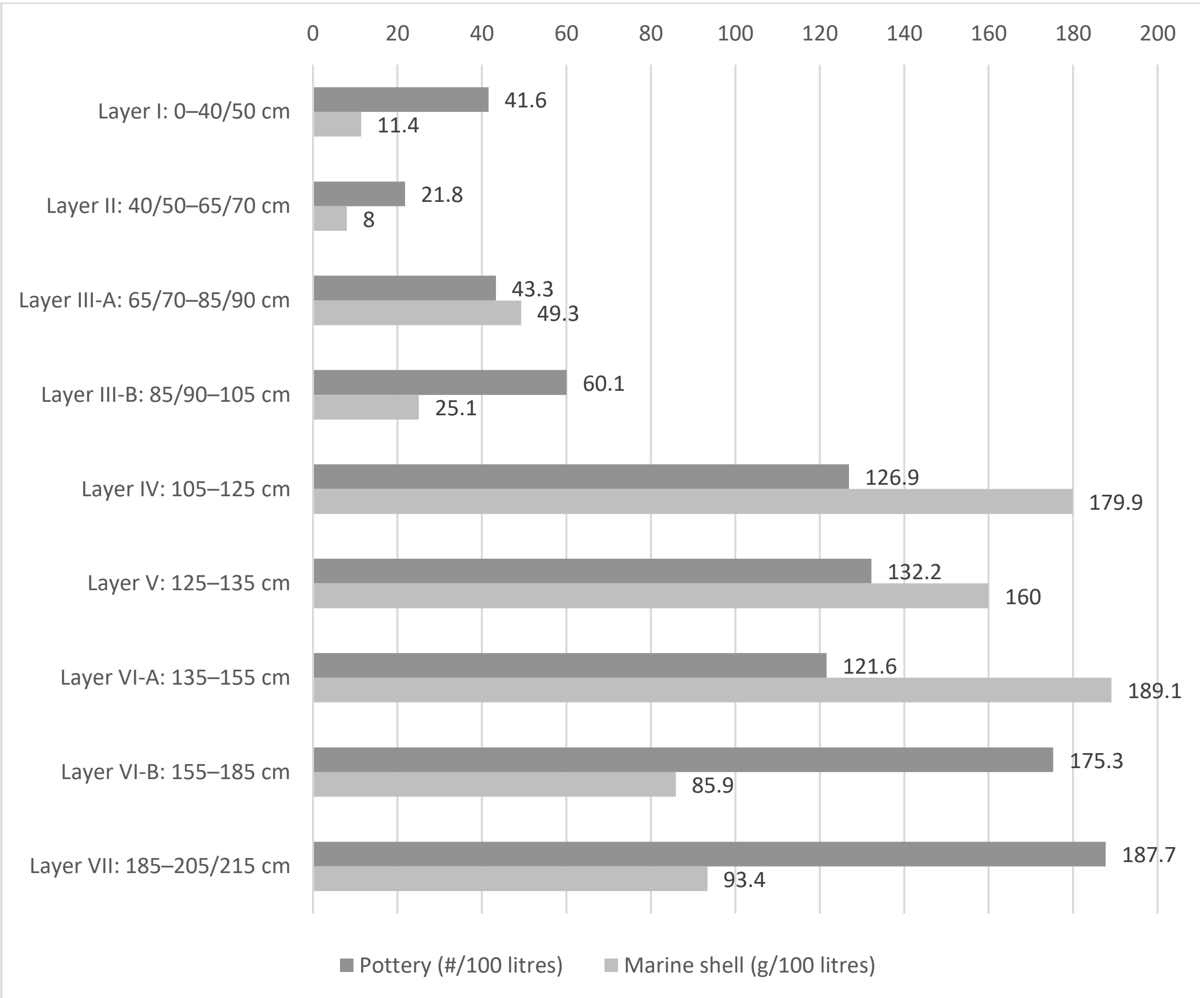

FIGURE 38. APPROXIMATE CONCENTRATIONS OF NUMBERS OF POTTERY FRAGMENTS AND GRAMS OF MARINE SHELL PER 100 LITRES OF EXCAVATED SEDIMENT IN EACH LAYER.

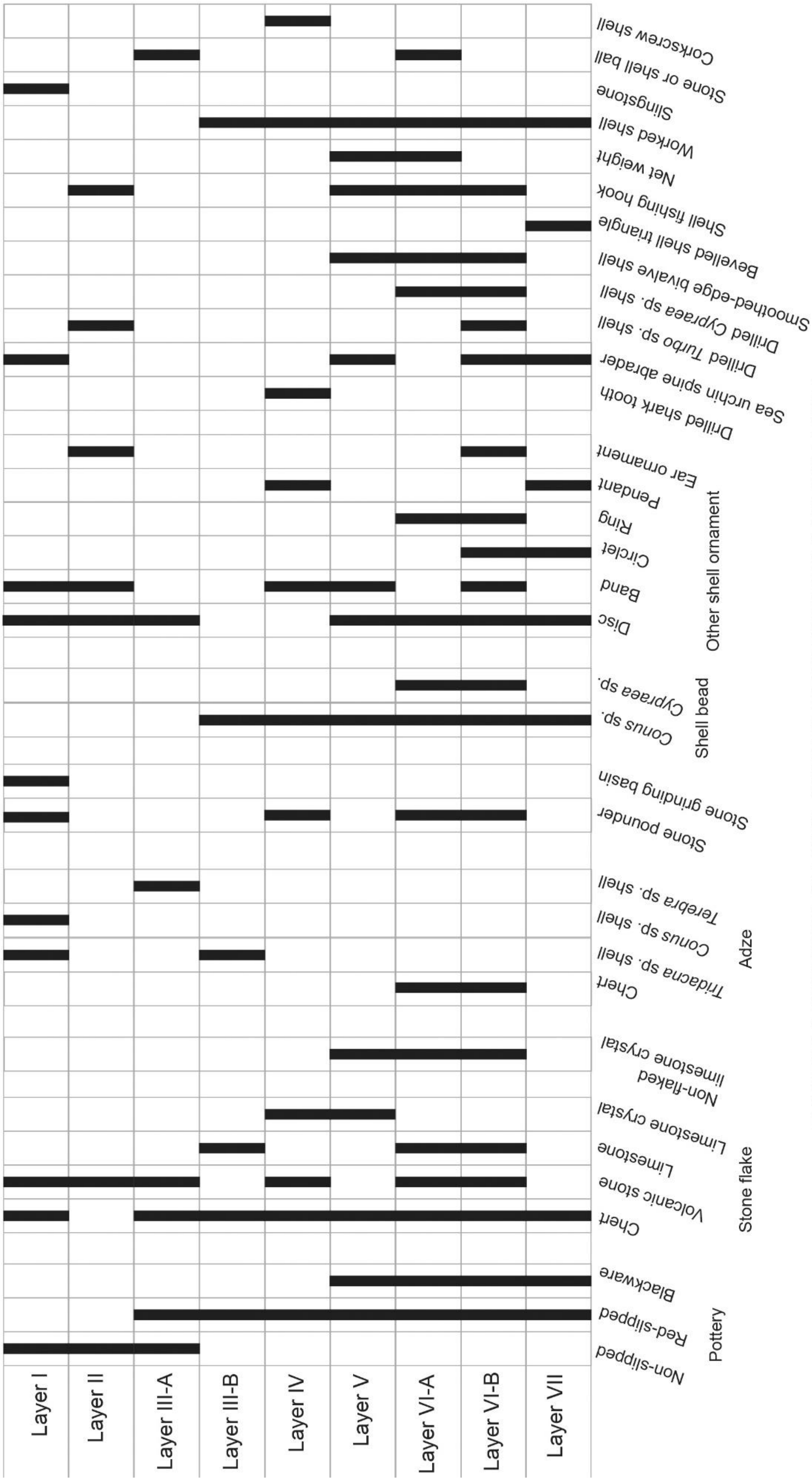

FIGURE 39. DISTRIBUTION OF MAJOR ARTEFACT CATEGORIES IN STRATIGRAPHIC LAYERS.

TABLE 6. SUMMARY OF ARCHAEOLOGICAL MATERIAL FROM THE OCTOBER 2016 EXCAVATION.

Provenience	**Pottery**	**Other Artefacts**	**Marine Shell**	**Animal Bone**
Layer I 0–20 cm				
Quadrant 1 (NE)	198 plain body, 5–15 mm thick (3037.8 g); 10 plain rims, 10–12 mm thick (138.3 g); 1 finger-impressed rim, 10 mm thick (8.2 g)	1 chert flake (41.4 g); 1 volcanic stone flake (1.8 g)	1 *Tridacna* sp. frag. (11.3 g); 1 *Cypraea* sp. (10.8 g); 6 *Gafrarium* sp. (9.2 g); 10 *Turbo* spp. frag. (41.7 g); 7 *Turbo* spp. opercula (52.7 g); 1 *Trochus* sp. frag. (13 g); 5 *Conus* spp. frag. (30.7 g); 2 *Strombus* sp. (3.4 g); 5 *Tellina* sp. frag. (16.4)	
Quadrant 2 (SE)	225 plain body, 8–18 mm thick (3319.1 g); 12 rims, 8–20 mm thick (226.g g); 2 blue-on-white porcelain body, 4 mm thick (8.8 g)	1 limestone grinding basin frag. (510.4 g); 3 volcanic stone flakes (89.4 g)	Not measured	
Quadrant 3 (SW)	261 plain body, 5–18 mm thick (3202.7 g); 9 plain rim, 8–20 mm thick (202.7 g); 1 cornered edge piece, 8 mm (11.5 g); 2 incised rims, 9–14 mm thick (141.1 g)	1 limestone slingstone frag. (61.1 g); 1 chert flake (8.3 g)	Not measured	
Quadrant 4 (NW)	299 plain body, 8–15 mm thick (3903.2 g); 12 plain rim, 8–16 mm thick (316.3 g); 1 plain base, 13 mm thick (33.7 g)	1 *Tridacna* sp. shell adze frag. (41.3 g); 1 volcanic stone flake (13.9 g)	Not measured	

Provenience	Pottery	Other Artefacts	Marine Shell	Animal Bone
Layer I 20–40/50 cm				
Quadrant 1 (NE)	464 plain body, 5–18 mm thick (5564.7 g); 27 plain rim, 10–12 mm thick (463.7 g); 1 plain base, 12 mm thick (20.3 g); 1 finger-impressed rim, 9–11 mm (9.5 g); 1 incised rim, 14 mm thick (20.1 g)	1 *Spondylus* sp. shell perforated disc (1.8 g); 1 *Conus* sp. shell band frag. (5.2 g); 1 sea urchin spine abrader (12.4 g); 1 volcanic stone flake with polish (12.3 g)	2 *Tridacna* sp. frag. (69.4 g); 10 *Gafrarium* sp. (15.3 g); 2 *Conus* sp. (12.2 g); 8 *Conus* spp. frag. (42.5 g); 4 *Cypraea* spp. (15 g); 3 *Turbo* sp. (127.2 g); 21 *Turbo* spp. frag. (252.2 g); 6 *Turbo* spp. opercula (40.3 g); 4 *Trochus* spp. (18.8 g); 1 *Vasum* sp. (6.6 g); 2 *Tellina* sp. frag. (63.5 g); 2 *Codakia* sp. frag. (9 g)	1 fish (2.1 g)
Quadrant 2 (SE)	852 plain body, 8–22 mm thick (10,595.8 g); 45 plain rims, 8–24 mm thick (1298.7 g)	1 *Tridacna* sp. shell adze pre-form (65.9 g); 1 *Conus* sp. shell adze, nearly complete (56.7 g); 1 chert flake (18.4 g)	Not measured	13 fish (1.8 g)
Quadrant 3 (SW)	304 plain body, 6–20 mm thick (5649.6 g); 7 plain rims, 9–14 mm thick (181.9 g)		Not measured	2 turtle (1.9 g); 5 fish (3.1 g)
Quadrant 4 (NW)	241 plain body, 8–18 mm thick (2098.6 g); 12 plain rims, 8–15 mm thick (302.8 g)	1 limestone pounder frag. (82.7 g)	Not measured	
Layer II 40/50–65/70 cm				

Provenience	Pottery	Other Artefacts	Marine Shell	Animal Bone
Quadrant 1 (NE)	159 plain body, 5–15 mm thick (754.9 g); 4 plain rim, 5–6 mm thick (20.8 g); 1 plain base, 20 mm thick (5.8 g)	2 nacreous marine shell ear ornaments (2.1 g)	1 *Isognomon* sp. frag. (7.6 g); 2 *Turbo* spp. frag. (31.2 g); 7 *Turbo* spp. opercula (31.3 g); 6 *Trochus* sp. (26 g); 3 *Conus* spp. (30.4 g); 3 *Conus* spp. frag. (9.6 g); 7 *Cypraea* spp. (33.1 g); 1 *Nerita* sp. frag. (2 g); 14 *Strombus* sp. (27.9 g); 1 *Terebra* sp. (13 g); 2 *Vasum* sp. frag. (6.5 g); 3 *Tellina* sp. (18.4 g); 3 *Tellina* sp. frag. (5.8 g); 29 *Gafrarium* sp. (44.5 g)	5 turtle (10.4 g); 21 bird (14.2 g); 128 fish (22.5 g)
Quadrant 2 (SE)	123 plain body, 5–10 mm thick (901.7 g); 12 plain rims, 5–10 mm thick (153.7 g)	1 *Turbo* sp. shell lime powder container (91.1 g); 1 *Conus* sp. band frag. (2.4 g); 3 volcanic stone flakes (37.1 g)	Not measured	1 bird (0.1 g); 33 fish (5.9 g)
Quadrant 3 (SW)	295 plain body, 5–14 mm thick (1847.8 g); 13 plain rims, 5–18 mm thick (226.8 g)	1 nacreous shell fishing hook, broken tip (2.4 g); 1 thick shell fishing hook frag. (5.5 g); 1 shell disc (3.8 g)	Not measured	39 fish (9.2 g)
Quadrant 4 (NW)	169 plain body, 5–22 mm thick (1502.9 g);	1 chert flake (8.6 g)	Not measured	8 fish (1.9 g)

Provenience	Pottery	Other Artefacts	Marine Shell	Animal Bone
	7 plain rims, 5–22 mm thick (201.3 g)			
Layer III-A 65/70–85/90 cm				
Quadrant 1 (NE)	516 plain non-slipped or red-slipped body, 8–144 mm thick (4828.6 g); 38 plain non-slipped or red-slipped rims, 4–20 mm thick (701.6 g); 4 plain red-slipped carination, 5–8 mm thick (209.8 g); 10 plain non-slipped or red-slipped base, 8–22 mm thick (60.2 g); 1 circle-stamped red-slipped rim, 5 mm thick (15.1 g); 1 incised rim, 5 mm thick (34.5 g)	1 limestone ball (70.9 g); 1 chert flake (52.9 g); 1 volcanic stone flake (33.2 g)	3 *Tridacna* sp. frag. (75.4 g); 2 *Turbo* sp. (92.6 g); 45 *Turbo* spp. frag. (549.4 g); 11 *Turbo* spp. opercula (81.6 g); 2 *Trochus* sp. (26.4 g); 8 *Conus* spp. (84.1 g); 12 *Conus* spp. frag. (63.8 g); 14 *Strombus* sp. (25.4 g); 4 *Tellina* sp. (39 g); 7 *Tellina* sp. frag. (41.2 g); 3 *Vasum* spp. frag. (28.3 g); 1 *Nerita* sp. frag. (0.8 g); 3 *Terebra* sp. (44.9 g); 1 *Spondylus* sp. (62.7 g); 184 *Gafrarium* sp. (360.9 g)	2 turtle (3.9 g); 1 bird (0.2 g); 39 fish (28.1 g)
Quadrant 2 (SE)	206 plain non-slipped or red-slipped body, 5–24 mm thick (2198.4 g); 23 plain red-slipped rims, 4–20 mm thick (342.4 g); 5 incised rims, 4–8 mm thick (52.6 g)	1 *Terebra* sp. shell adze (47.4 g)	Not measured	2 turtle (3.9 g); 17 fish (7.1 g)
Quadrant 3 (SW)	333 plain non-slipped or red-	2 chert flakes (25.1 g)	Not measured	13 fish (5.4 g)

Provenience	Pottery	Other Artefacts	Marine Shell	Animal Bone
	slipped body, 6–20 mm thick (2355.9 g); 26 plain non-slipped or red-slipped rims, 5–20 mm thick (412.3 g); 2 plain red-slipped base, 18–20 mm thick (63.9 g); 1 incised red-slipped rim, 12 mm thick (10.1 g)			
Quadrant 4 (NW)	212 plain non-slipped or red-slipped body, 6–15 mm thick (1989.2 g); 10 plain non-slipped or red-slipped rims, 5–14 mm thick (92.2 g); 2 plain red-slipped base, 5–20 mm thick (98.6 g)	1 shell disc (1.3 g); 1 chert flake (19.5 g)	Not measured	24 fish (19.4 g)
Layer III-B 85/90–105 cm				
Quadrant 1 (NE)	725 plain red-slipped body, 2–12 mm thick (3254.7 g); 43 plain red-slipped rims, 2–10 mm thick (298.5 g); 5 plain red-slipped base, 12–18 mm thick (58.9 g); 1 half-circle incised red-slipped rim, 8 mm thick (12.9 g); 3 circle-stamped red-slipped rims, 3–8 mm thick (15 g)	1 elongate shell pendant (1 g); 1 *Tridacna* sp. shell adze pre-form (81 g); 1 worked nacreous shell frag. (2.1 g)	1 *Tridacna* sp. frag. (3.6 g); 59 *Turbo* spp. frag. (384.5 g); 16 *Turbo* spp. opercula (50.6 g); 3 *Trochus* spp. frag. (8.8 g); 5 *Conus* spp. (28.6 g); 2 *Cypraea* spp. (8.4 g); 2 *Cypraea* spp. frag. (22.1 g); 2 *Tellina* sp. frag. (3.9 g); 104 *Gafrarium* sp. (192.6 g)	48 fish (34.2 g)
Quadrant 2 (SE)	228 plain red-slipped body, 4–26	1 *Conus* sp. shell bead (0.2 g);	Not measured	2 turtle (1.7 g);

Provenience	Pottery	Other Artefacts	Marine Shell	Animal Bone
	mm thick (2399.6 g); 25 plain red-slipped rims, 5–20 mm thick (293.6 g); 2 plain red-slipped carination, 5–7 mm thick (13.3 g); 5 plain red-slipped base, 15–20 mm thick (252.5 g)	1 limestone flake (7.8 g)		20 fish (11.4 g)
Quadrant 3 (SW)	225 plain red-slipped body, 5–20 mm thick (1815.5 g); 18 plain red-slipped rims, 5–20 mm thick (534.8 g); 8 plain red-slipped base, 16–20 mm thick (498.6 g); 1 circle-stamped red-slipped rim, 5 mm thick (7.4 g)	1 *Tridacna* sp. adze frag. (11.2 g); 3 *Conus* sp. shell bead (0.5 g); 2 chert flakes (8.4 g)	Not measured	31 fish (10.8 g)
Quadrant 4 (NW)	366 plain red-slipped body, 3–12 mm thick (2128.8 g); 27 plain red-slipped rims, 4–18 mm thick (238.9 g)		Not measured	1 bird (0.8 g); 91 fish (26.8 g)
Layer IV 105–125 cm				
Quadrant 1 (NE)	1231 plain red-slipped body, 1–5 mm thick (1075.3 g); 36 plain red-slipped rims, 2–6 mm thick (143.6 g)	1 elaborately cut *Terebra* sp. shell in "corkscrew" shape (14.2 g); 1 *Conus* sp. shell band frag. (10.5 g); 3 *Conus* sp. shell bead (0.6 g); 5 chert flakes (41.8 g); 1 drilled shark tooth frag. (2.1 g); 1 shark tooth frag. (1.9 g)	1 *Tridacna* sp. frag. (4.9 g); 1 *Isognomon* sp. frag. (2.2 g); 248 *Turbo* spp. frag. (1048.1 g); 101 *Turbo* spp. opercula (376.7 g); 41 *Trochus* spp. frag. (118.9 g); 7 *Vasum* spp. frag. (89.2 g);	2 turtle(3.1 g); 4 bird (1 g); 34 fish (9.7 g)

Provenience	Pottery	Other Artefacts	Marine Shell	Animal Bone
			11 *Tellina* sp. frag. (48.5 g); 2 *Nerita* spp. (1.9 g); 4 *Strombus* sp. (15.9 g); 8 *Conus* spp. (101.2 g); 4 *Conus* spp. frag. (25.7 g); 7 *Cypraea* spp. (22.6 g); 5 *Cypraea* spp. frag. (53.5 g); 495 *Gafrarium* sp. (790.3 g); 156 *Anadara* sp. (536.4 g); 46 *Anadara* sp. frag. (102.5 g); 4 sea urchin spine (7.4 g); 20 sea urchin spine frag. (19.9 g); 485 *Patelloida* spp. (292.3 g)	
Quadrant 2 (SE)	1048 plain red-slipped body, 1–5 mm thick (3013.6 g); 49 plain red-slipped rims, 4–18 mm thick (520.5 g); 6 plain red-slipped base, 5–18 mm thick (224.3 g)	1 limestone pounder frag. (98.7 g); 5 *Conus* sp. shell bead (1.1 g); 1 volcanic stone flake with polish (147.2 g); 3 chert flakes (29.9 g)	Not measured	5 bird (1.6 g); 50 fish (16.4 g)
Quadrant 3 (SW)	644 plain red-slipped body, 2–6 mm thick (1997.1 g); 40 plain red-slipped rims, 5–12 mm thick (200.3 g); 7 plain red-slipped base, 6–25 mm thick (335.9 g);	1 limestone pounder frag. (84.1 g); 4 *Conus* sp. shell bead (0.7 g); 2 chert flake (24.2 g)	Not measured	28 fish (7.8 g)

Provenience	Pottery	Other Artefacts	Marine Shell	Animal Bone
	1 vertically and horizontally incised rim, 12 mm thick (8.4 g)			
Quadrant 4 (NW)	946 plain red-slipped body, 2–8 mm thick (2054.4 g); 55 plain red-slipped rims, 5–12 mm thick (334.7 g)	1 nacreous shell frag. (1.8 g); 1 *Conus* sp. shell band or bangle frag. (4 g); 4 *Conus* sp. shell bead (0.8 g); 4 chert flakes (30.8 g); 1 limestone crystal (2.1 g); 1 worked nacreous shell frag. (4.2 g)	Not measured	17 fish (3.1 g)
Layer V 125–135 cm				
Quadrant 1 (NE)	868 plain red-slipped body, 1–5 mm thick (1525.3 g); 2 plain red-slipped rims, 3–5 mm thick (65.1 g); 1 circle-stamped red-slipped pottery handle, 10–12 mm thick (198.3 g); 1 conjoined circle-stamped body, 4 mm thick (50.3 g)	1 *Conus* sp. shell band frag. (3.5 g); 6 chert flakes (3.5 mm); 1 smoothed-edge nacreous bivalve shell object (3.3 g)	225 *Turbo* spp. frag. (568.4 g); 16 *Turbo* spp. opercula (86.3 g); 86 *Trochus* spp. frag. (144.6 g); 1 *Terebra* sp. (18.8 g); 3 *Vasum* spp. frag. (25.4 g); 4 *Nerita* sp. (2 g); 9 *Tellina* sp. frag. (49.7 g); 2 *Conus* spp. (23.8 g); 2 *Conus* spp. frag. (20.7 g); 2 *Cypraea* spp. frag. (14.8 g); 196 *Gafrarium* sp. (478.1 g); 82 *Anadara* sp. (840.6 g); 32 *Anadara* sp. frag. (117.8 g); 1 sea urchin body frag. (0.7 g);	2 bird (0.2 g); 16 fish (1.7 g)

Provenience	Pottery	Other Artefacts	Marine Shell	Animal Bone
			2 sea urchin spines (6.7 g); 366 *Patelloida* spp. (161.8 g)	
Quadrant 2 (SE)	523 plain red-slipped body, 1–5 mm thick (1068.5 g); 40 plain red-slipped rims, 1–5 mm thick (161.4 g); 1 circle-stamped red-slipped rim, 5 mm thick (5.4 g); 1 half-circle incised red-slipped rim, 5 mm thick (28.5 g)	1 *Conus* sp. shell band frag. (6.2 g); 4 *Conus* sp. shell bead (0.7 g); 5 chert flakes (29.7 g); 1 limestone crystal (9.3 g)	Not measured	3 bird (0.4 g); 4 fish (1.5 g)
Quadrant 3 (SW)	114 plain red-slipped body, 1–4 mm thick (309.8 g); 8 plain red-slipped rims, 2–6 mm thick (72.6 g); 5 plain red-slipped carination, 2–6 mm thick (39.4 g); 1 circle-stamped and garland red-slipped body, 4 mm thick (5.2 g)	1 red-slipped rim with notched lip, 5 mm thick (14.7 g); 4 *Conus* sp. shell bead (0.7 g)	Not measured	2 fish (0.2 g)
Quadrant 4 (NW)	574 plain red-slipped and blackware body, 1–4 mm thick (963.6 g); 19 plain red-slipped and blackware rims, 1–4 mm thick (78.4 g); 1 plain red-slipped carination, 3 mm thick (4 g); 1 circle-stamped and garland red-sipped rim, 4 mm thick (5 g)	8 chert flakes (45.2 g)	Not measured	2 bird (0.3 g); 10 fish (2.5 g)
Layer VI-A 135–145 cm				

Provenience	Pottery	Other Artefacts	Marine Shell	Animal Bone
Quadrant 1 (NE)	891 plain red-slipped body, 0.5–4 mm thick (1869.2 g); 44 plain red-slipped rims, 3–6 mm thick (171.6 g)	1 *Cypraea* sp. shell bead (0.4 g); 1 *Conus* sp. shell disc in process (5.2 g); 3 *Conus* sp. shell bead (0.5 g); 6 chert flakes (10.2 g); 7 limestone crystal (106.5 g); 1 worked nacreous shell frag. (1.6 g)	2 *Haliotis* sp. frag. (6.8 g); 1 *Tridacna* sp. frag. (24.1 g); 24 *Turbo* spp. frag. (201.9 g); 32 *Turbo* spp. opercula (177.5 g); 3 *Trochus* sp. (37.4 g); 1 *Vasum* sp. frag. (5.8 g); 3 *Nerita* spp. (5.9 g); 1 *Conus* sp. (6.6 g); 4 *Conus* spp. frag. (32.1 g); 4 *Cypraea* spp. (25.1 g); 2 *Cypraea* sp. frag. (111.6 g); 1 *Strombus* sp. (9 g); 938 *Gafrarium* sp. (247.2 g); 238 *Anadara* sp. (2017.3 g); 35 *Anadara* sp. frag. (175.2 g); 1 sea urchin body frag. (0.6 g); 4 sea urchin spines (3.8 g); 15 sea urchin spine frag. (13.7 g); 523 *Patelloida* spp. (291.6 g)	3 bird (0.6 g); 5 fish (0.4 g)
Quadrant 2 (SE)	306 plain red-slipped body, 0.5–4 mm thick (552.7 g); 11 plain red-slipped rims, 3–6 mm thick (52.8 g)	1 drilled red-slipped pottery frag., 4 mm thick (16.5 g); 1 polished ball of probable *Tridacna* sp. shell (72.5 g);	Not measured	2 bird (0.6 g); 11 fish (1.2 g)

Provenience	Pottery	Other Artefacts	Marine Shell	Animal Bone
		1 limestone pounder (45.1 g); 2 limestone crystal (12.8 g)		
Quadrant 3 (SW)	158 plain red-slipped body, 0.5–4 mm thick (322.3 g); 2 plain red-slipped rims, 2–5 mm thick (12.5 g)	1 *Conus* sp. shell disc in process (4.7 g); 1 *Conus* sp. shell bead (0.2 g)	Not measured	2 fish (0.4 g)
Quadrant 4 (NW)	374 plain red-slipped and blackware body, 0.5–4 mm thick (801.2 g); 18 plain red-slipped and blackware rims, 1–4 mm thick (108.3 g); 1 plain red-slipped carination, 3 mm thick (4.2 g)	1 cut piece of *Conus* sp. shell, probable disc debitage (9.4 g); 1 *Conus* sp. shell disc (4.1 g); 2 *Conus* sp. shell bead (0.4 g); 3 chert flakes (18.6 g); 1 volcanic stone flake (4.2 g)	Not measured	2 bird (0.6 g); 1 fish (0.3 g)
Layer VI-A 145–155 cm				
Quadrant 1 (NE)	734 plain red-slipped body, 0.5–4 mm thick (1582.8 g); 23 plain red-slipped rims, 3–6 mm thick (59.6 g)	1 *Asaphis* sp. shell with drilled hole, net weight (9.4 g); 1 cut and two-hole drilled piece of *Cypraea* sp. shell (10.1 g); 1 cut and drilled *Cypraea* sp. shell frag. (5.5 g) 2 smoothed-edge bivalve shell artifacts (7.3 g); 2 *Conus* sp. shell discs (5 g); 1 *Conus* sp. shell disc in process (4.2 g); 1 shell ring (0.1 g); 1 chert adze frag. (78.2 g); 7 *Conus* sp. shell bead (1.2 g);	1 *Tridacna* sp. frag. (5.5 g); 4 *Turbo* sp. (197.1 g); 11 *Turbo* spp. frag. (67.6 g); 31 *Turbo* spp. opercula (177.7 g); 2 *Trochus* sp. (45.2 g); 1 *Trochus* sp. frag. (16.1 g); 1 *Nerita* sp. (0.9 g); 1 *Terebra* sp. (16.8 g); 2 *Conus* spp. (17.1 g); 3 *Cypraea* spp. (27.7 g);	3 bird (0.4 g); 4 fish (2.1 g)

Provenience	Pottery	Other Artefacts	Marine Shell	Animal Bone
		3 chert flakes (21/9 g); 1 limestone crystal (1.6 g); 1 worked nacreous shell frag. (2.3 g)	1 *Cypraea* sp. frag. (4.3 g); 2 *Strombus* sp. (10.8 g); 6 *Tellina* sp. (29.2 g); 4 *Tellina* sp. frag. (16 g); 1 *Asaphis* sp. (10.7 g); 94 *Gafrarium* sp. (149.3 g); 184 *Anadara* sp. (1586.7 g); 12 *Anadara* sp. frag. (106.6 g); 1 sea urchin spine (7.2 g); 5 sea urchin spine frag. (12.5 g); 243 *Patelloida* spp. (154.3 g)	
Quadrant 2 (SE)	430 plain red-slipped body, 0.5–4 mm thick (994.8 g); 21 plain red-slipped rims, 1–5 mm thick (93.9 g)	1 *Cypraea* cp. shell bead frag. (0.3 g); 1 chert adze (184.5 g); 1 chert adze pre-form (248.7 g); 1 nacreous shell fishing hook, nearly complete (2 g); 9 *Conus* sp. shell bead (1.5 g); 1 *Conus* sp. shell bead in process (0.3 g); 1 limestone flake (6.7 g); 2 volcanic stone flakes (32.6 g)	Not measured	3 bird (0.4 g); 3 fish (0.9 g)
Quadrant 3 (SW)	533 plain red-slipped body, 05.–4 mm thick (1082.3 g);	2 *Cypraea* sp. shell bead (1 g); 1 *Cypraea* sp. shell bead frag. (0.3 g);	Not measured	7 bird (1.4 g); 3 fish (0.3 g)

Provenience	Pottery	Other Artefacts	Marine Shell	Animal Bone
	44 plain red-slipped rims, 2–5 mm thick (196.3 g); 1 plain red-slipped base, 5 mm thick (9 g); 12 incised and circle-stamped blackware (3 rims, 7 body, 2 carination), 4–5 mm thick (27.4 g); 2 circle-stamped red-slipped body, 4 mm thick (5.7 g)	1 *Conus* sp. shell disc (3.7 g); 6 *Conus* sp. shell bead (1 g); 1 shell ring (0.2 g); 2 chert flakes (13.1 g)		
Quadrant 4 (NW)	263 plain red-slipped and blackware body, 0.5–4 mm thick (681.1 g); 21 plain red-slipped and blackware rims, 1–4 mm thick (126.6 g)	1 *Cypraea* sp. shell bead frag. (0.3 g); 1 *Isognomon* sp. shell frag. with worked edges (9.3 g); 4 *Conus* sp. shell bead (0.7 g); 1 worked nacreous shell frag. (2 g)	Not measured	1 fish (0.4 g)
Layer VI-B 155–165 cm				
Quadrant 1 (NE)	1212 plain red-slipped and blackware body, 0.5–4 mm thick (2599.5 g); 52 plain red-slipped rims, 1–5 mm thick (172.2 g)	1 *Conus* sp. shell disc (1.9 g); 1 *Conus* sp. shell disc in process (3.1 g); 2 shell ring frag. (1.5 g); 1 circlet frag. (2.8 g); 2 *Conus* sp. shell bead (0.3 g); 3 sea urchin spine abraders (9.3 g); 6 chert flakes (24.2 g); 1 *Cypraea* sp. shell with drilled hole, worked frag. (4.6 g)	1 *Haliotis* sp. (6 g); 4 *Haliotis* sp. frag. (12.5 g); 1 *Isognomon* sp. frag. (3.5 g); 22 *Turbo* spp. frag. (199.2 g); 31 *Turbo* spp. opercula (242.5 g); 1 *Trochus* sp. (17.4 g); 2 *Nerita* sp. (6.5 g); 6 *Tellina* sp.(48.3 g); 4 *Tellina* sp. frag. (28.6 g);	1 fish (0.3 g)

Provenience	Pottery	Other Artefacts	Marine Shell	Animal Bone
			4 *Conus* spp. (15.5 g); 6 *Cypraea* spp. (37.1 g); 7 *Cypraea* spp. frag. (105.9 g); 55 *Gafrarium* sp. (111.1 g); 183 *Anadara* sp. (1596.8 g); 19 *Anadara* sp. frag (93.3 g); 9 sea urchin spines (24.9 g); 2 sea urchin spine frag. (3.6 g); 220 *Patelloida* spp. (173.8 g); 1 chiton plate (3.1 g)	
Quadrant 2 (SE)	644 plain red-slipped and blackware body, 0.5–4 mm thick (1173.1 g); 45 plain red-slipped and blackware rims, 1–5 mm thick (172.2 g)	1 *Conus* sp. shell bead (0.2 g); 1 limestone flake (28.6 g); 2 chert flakes (24.5 g); 1 limestone crystal (1.6 g)	Not measured	4 bird (0.9 g); 11 fish (1.6 g)
Quadrant 3 (SW)	782 plain red-slipped and blackware body, 0.5–4 mm thick (1636.3 g); 49 plain red-slipped rims, 1–5 mm thick (178.6 g); 1 plain red-slipped carination, 5 mm thick (15.2 g); 1 circle-stamped and incised with lime infill blackware body, 4 mm thick (4.9 g)	1 worked nacreous shell frag. (5.6 g); 1 *Conus* sp. shell disc in production (4.7 g); 4 *Conus* sp. shell bead (0.6 g); 1 *Conus* sp. shell bead in process (0.3 g)	Not measured	1 fish (0.2 g)
Quadrant 4 (NW)	1222 plain red-slipped and blackware body,	1 *Conus* sp. shell disc in process (5.2 g);	Not measured	4 bird (2 g)

Provenience	Pottery	Other Artefacts	Marine Shell	Animal Bone
	0.5–4 mm thick (3193.8 g); 86 plain red-slipped rims, 1–4 mm thick (498.8 g); 1 plain red-slipped carination, 4 mm thick (4 g)	1 shell ring frag. (1 g); 2 shell circlet frag. (5.9 g); 4 *Conus* sp. shell bead (0.6 g); 14 chert flakes (240.5 g)		
Layer VI-B 165–175 cm				
Quadrant 1 (NE)	705 plain red-slipped and blackware body, 0.5–4 mm thick (1257.2 g); 27 plain red-slipped rims, 2–4 mm thick (97.3 g); 2 plain red-slipped carination, 3–5 mm thick (18 g)	1 chert adze (308.6 g); 1 nacreous shell fishing hook frag. (0.7 g); 1 *Conus* sp. shell disc (3.9 g); 1 sea urchin spine abrader (5 g); 1 limestone pounder frag. (45.6 g); 5 *Conus* sp. shell bead (0.8 g); 1 *Conus* sp. shell bead in process (0.2 g); 1 limestone flake (34.6 g)	2 *Turbo* spp. frag. (17.6 g); 4 *Turbo* spp. opercula (30.4 g); 1 *Trochus* sp. (20.8 g); 2 *Trochus* spp. frag. (8.6 g); 1 *Vasum* sp. (16.6 g); 1 *Conus* sp. (10.8 g); 2 *Conus* spp. frag. (25 g); 4 *Cypraea* spp. (86.5 g); 2 *Cypraea* sp. frag. (53.6 g); 1 *Strombus* sp. (7.4 g); 3 *Tellina* sp. (19.6 g); 2 *Asaphis* sp. (27.1 g); 10 *Gafrarium* sp. (20.4 g); 28 *Anadara* sp. (213.1 g); 3 *Anadara* sp. frag. (19.8 g); 3 sea urchin spine frag. (10.6 g); 23 *Patelloida* spp. (22.6 g); 1 chiton plate (3.2 g)	

Provenience	Pottery	Other Artefacts	Marine Shell	Animal Bone
Quadrant 2 (SE)	560 plain red-slipped and blackware body, 0.5–4 mm thick (1559.8 g); 41 plain red-slipped and blackware rims, 1–4 mm thick (58.2 g); 8 plain red-slipped and blackware carination, 2–4 mm thick (54.3 g)	1 nacreous marine shell ear ornament (0.8 g); 1 smoothed-edge bivalve shell artifact (3.6 g); 6 *Conus* sp. shell bead (1.1 g); 7 chert flakes (149.2 g); 1 chert flake with polish (4.4 g)	Not measured	2 bird (0.3 g); 15 fish (2 g)
Quadrant 3 (SW)	585 plain red-slipped and blackware body, 0.5–mm thick (2115.4 g); 52 plain red-slipped and blackware rims, 1–5 mm thick (219.9 g); 1 plain red-slipped carination, 4 mm thick (8.4 g); 1 circle-stamped and incised blackware rim, 4 mm thick (4.7 g)	1 *Cypraea* sp. shell bead in process (0.8 g); 1 *Cypraea* sp. shell bead in process frag. (0.5 g); 1 shell circlet frag. (2.7 g); 1 nacreous shell fishing hook frag. (1.2 g); 2 *Conus* sp. shell bead (0.4 g); 1 chert flake (4.4 g)	Not measured	1 bird (0.1 g); 34 fish (6.7 g)
Quadrant 4 (NW)	622 plain red-slipped and blackware body, 0.5–4 mm thick (2193.9 g); 43 plain red-slipped and blackware rims, 1–4 mm thick (220.6 g); 1 plain red-slipped carination, 4 mm thick (4 g)	1 *Conus* sp. shell band frag. (1.3 g); 1 *Conus* sp. shell disc in process (5.2 g); 2 shell circlet frag. (6.2 g); 3 *Conus* sp. shell bead (0.5 g); 14 chert flakes (241.1 g)	Not measured	6 bird (1.3 g); 9 fish (2.8 g)
Layer VI-B 175–185 cm				
Quadrant 1 (NE)	590 plain red-slipped and blackware body, 0.5–4 mm thick (2001.4 g);	1 *Cypraea* sp. shell bead in process (0.8 g); 1 *Conus* sp. shell disc in process (3.2 g);	1 *Haliotis* sp. frag. (4 g); 1 *Isognomon* sp. frag. (4.4 g); 16 *Turbo* spp. frag. (64.8 g);	

Provenience	Pottery	Other Artefacts	Marine Shell	Animal Bone
	37 plain red-slipped rims, 1–5 mm thick (83.8 g); 2 plain red-slipped carination, 4–5 mm thick (9.6 g)	2 *Conus* sp. shell bead (0.4 g); 7 chert flakes (45.9 g)	16 *Turbo* spp. opercula (109.9 g); 1 *Trochus* sp. (17 g); 3 *Nerita* spp. (10.1 g); 2 *Tellina* sp. (11.4 g); 1 *Asaphis* sp. (6.4 g); 2 *Conus* spp. (25.6 g); 1 *Cypraea* sp. (1.6 g); 2 *Cypraea* sp. frag. (21.2 g); 1 *Strombus* sp. (6.7 g); 22 *Gafrarium* sp. (53.1 g); 38 *Anadara* sp. (274 g); 3 *Anadara* sp. frag. (16.2 g); 1 crab claw frag. (4.2 g); 3 sea urchin spines (14.2 g); 6 sea urchin spine frag. (10.8 g); 153 *Patelloida* spp. (134.6 g); 2 chiton plates (6.5 g)	
Quadrant 2 (SE)	1660 plain red-slipped and blackware body, 0.5–4 mm thick (4344.8 g); 98 plain red-slipped and blackware rims, 1–5 mm thick (493.2 g); 3 plain red-slipped carination, 3–4 mm thick (18.5 g)	1 *Cypraea* sp. shell bead in process (0.9 g); 1 *Conus* sp. shell disc in process (4.8 g); 1 *Conus* sp. shell disc (1.1 g); 3 *Conus* sp. shell bead (0.5 g);	Not measured	1 turtle (24.8 g); 2 bird (0.7 g); 13 fish (4.7 g)

Provenience	Pottery	Other Artefacts	Marine Shell	Animal Bone
		1 *Conus* sp. shell bead in process (0.3 g); 5 chert flakes (88.3 g); 1 chert flake with polish (4.6 g); 1 volcanic stone flake (24.4 g); 1 limestone crystal (16.1 g)		
Quadrant 3 (SW)	589 plain red-slipped and blackware body, 0.5–4 mm (2587.9 g); 56 plain red-slipped and blackware rims, 1–5 mm thick (315.6 g); 1 plain red-slipped carination, 4 mm thick (6.6 g); 1 paddle-impressed red-slipped body, 4 mm thick (5.1 g)	1 *Cypraea* sp. shell bead frag. (0.3 g); 1 complete nacreous shell fishhook, encased in hardened sand (2.7 g); 1 *Conus* sp. shell ring (0.9 g); 1 shell ring frag. (3.1 g); 1 sea urchin spine abrader (3.4 g); 1 *Conus* sp. shell band frag. (4.4 g); 1 *Turbo* sp. shell with drilled hole, worked frag. (3.2 g); 10 *Conus* sp. shell bead (1.6 g); 4 *Conus* sp. shell bead in process (1.1 g); 8 chert flakes (66.9 g); 2 volcanic stone flakes (11.8 g)	Not measured	4 bird (2.2 g); 4 fish (1.4 g)
Quadrant 4 (NW)	393 plain red-slipped and blackware body, 0.5–4 mm thick (875.7 g); 43 plain red-slipped and blackware rims, 2–4 mm thick (297.6 g);	1 *Cypraea* sp. shell bead frag. (0.3 g); 1 smoothed-edge bivalve shell artifact (3.6 g); 1 *Conus* sp. shell pendant (6.8 g);	Not measured	1 bird (0.2 g); 2 fish (0.6 g)

Provenience	Pottery	Other Artefacts	Marine Shell	Animal Bone
	1 plain red-slipped carination, 5 mm thick (13 g)	1 shell circlet frag. (3.8 g); 5 *Conus* sp. shell bead (0.8 g); 2 worked nacreous shell frag. (6.2 g); 6 chert flakes (31.6 g)		
Layer VII 185–195 cm				
Quadrant 1 (NE)	927 plain red-slipped and blackware body, 0.5–4 mm (2704.3 g); 81 plain red-slipped rims, 2–5 mm thick (284.4 g); 1 plain red-slipped carination, 3 mm thick (5.8 g)	1 *Conus* sp. shell bead (0.2 g)	1 *Haliotis* sp. frag. (4.2 g); 1 *Tridacna* sp. frag. (6.1 g); 22 *Turbo* spp. frag. (85.3 g); 25 *Turbo* spp. opercula (134.8 g); 1 *Trochus* sp. (16.8 g); 2 *Nerita* spp. (8.7 g); 4 *Tellina* sp. (22.3 g); 1 *Asaphis* sp. (10.4 g); 2 *Conus* spp. (27.2 g); 4 *Cypraea* spp. (31.4 g); 8 *Cypraea* spp. frag. (42.1 g); 1 *Strombus* sp. (7.5 g); 52 *Gafrarium* sp. (100.2 g); 138 *Anadara* sp. (1274.5 g); 13 *Anadara* sp. frag. (48.5 g); 6 sea urchin spines (21.7 g); 5 sea urchin spine frag. (18.3 g);	

Provenience	Pottery	Other Artefacts	Marine Shell	Animal Bone
			308 *Patelloida* spp. (274.1 g); 2 chiton plates (6.7 g)	
Quadrant 2 (SE)	886 plain red-slipped and blackware body, 0.5–4 mm (2509.6 g); 85 plain red-slipped rims, 1–4 mm thick (235.1 g); 1 plain red-slipped carination, 4 mm thick (4.9 g)	1 *Conus* sp. shell bead (0.2 g)	Not measured	
Quadrant 3 (SW)	963 plain red-slipped and blackware body, 0.5–4 mm (2364.7 g); 21 plain red-slipped and blackware rims, 2–4 mm thick (66.6 g)	1 nacreous shell, cut into triangle with beveled edge (2.9 g); 1 shell circlet frag. (6.1 g); 4 *Conus* sp. shell bead (0.7 g); 1 chert flake (3.5 g); 1 sea urchin spine abrader (7.1 g)	Not measured	
Quadrant 4 (NW)	983 plain red-slipped and blackware body, 0.5–4 mm (2698.5 g); 43 plain red-slipped and blackware rims, 2–5 mm thick (208.7 g); 1 plain red-slipped carination, 3 mm thick (5.1 g)	2 *Conus* sp. shell bead (0.4 g)	Not measured	
Layer VII 195–205/215 cm				
Quadrant 1 (NE)	908 plain red-slipped and blackware body, 0.5–4 mm (2523.7 g);	2 *Conus* sp. shell bead (0.4 g)	1 *Haliotis* sp. (4.9 g); 2 *Haliotis* sp. frag. (8.5 g); 1 *Tridacna* sp. frag. (5.5 g);	

Provenience	Pottery	Other Artefacts	Marine Shell	Animal Bone
	95 plain red-slipped rims, 1–5 mm thick (382.1 g); 1 plain red-slipped carination, 4 mm thick (7.2 g)		1 *Isognomon* sp. frag. (4.8 g); 2 *Turbo* sp. (38.6 g); 18 *Turbo* spp. frag. (44.7 g); 22 *Turbo* spp. opercula (121.3 g); 2 *Trochus* sp. (26.5 g); 2 *Nerita* spp. (7.5 g); 3 *Tellina* sp. (15.4 g); 1 *Asaphis* sp. (11.1 g); 2 *Conus* spp. (26.4 g); 2 *Cypraea* spp. (15.6 g); 6 *Cypraea* spp. frag. (22.3 g); 1 *Strombus* sp. (7.1 g); 58 *Gafrarium* sp. (108.5 g); 144 *Anadara* sp. (1342.8 g); 16 *Anadara* sp. frag. (54.6 g); 5 sea urchin spines (18.4 g); 8 sea urchin spine frag. (28.7 g); 351 *Patelloida* spp. (291.8 g); 3 chiton plates (9.3 g)	
Quadrant 2 (SE)	1024 plain red-slipped and blackware body, 0.5–4 mm (2422.6 g); 111 plain red-slipped rims, 1–4 mm thick (406.8 g);	3 *Conus* sp. shell bead (0.5 g); 1 chert flake (1.8 g)	Not measured	

Provenience	Pottery	Other Artefacts	Marine Shell	Animal Bone
	2 plain red-slipped carination, 3–4 mm thick (10.5 g)			
Quadrant 3 (SW)	1025 plain red-slipped and blackware body, 0.5–4 mm (2209.8 g); 18 plain red-slipped rims, 1–5 mm thick (37.7 g); 1 plain red-slipped carination, 3 mm thick (5.1 g)	5 *Conus* sp. shell bead (0.7 g); 5 *Conus* sp. shell bead in process (1.1 g)	Not measured	
Quadrant 4 (NW)	963 plain red-slipped and blackware body, 0.5–4 mm (2098.5 g); 125 plain red-slipped and blackware rims, 1–5 mm thick (592.2 g); 4 plain red-slipped carination, 3–4mm thick (19.6 g)	7 *Conus* sp. shell bead (1.2 g)	Not measured	
Feature A, Originating from Layer V Quadrants 3 (SW) and 4 (NW) 130–150/155 cm	1486 plain red-slipped and blackware body, 0.5–4 mm thick (2929.6 g); 69 plain red-slipped rims, 1–4 mm thick (292.5 g); 9 plain red-slipped carination, 2–3 mm thick (37.4 g)	8 *Conus* sp. shell bead (1.4 g); 1 sea urchin spine abrader (3.3 g); 6 chert flakes (43 g); 1 limestone crystal, flaked (2.1 g)	Not measured	2 turtle (3.9 g); 6 bird (1.8 g); 15 fish (6 g)
Feature B, Originating from Layer V Quadrant 2 (SE) 135–145/150 cm	256 plain red-slipped body, 0.5–4 mm thick (547.6 g); 11 plain red rims, 1–4 mm thick (37.3 g); 2 plain red-slipped carination (5 g)	1 limestone crystal net weight 5.8 g); 1 nacreous shell fishing hook, nearly complete (1.3 g); 1 *Conus* sp. shell band frag. (3.5 g); 2 *Conus* sp. shell bead (0.3 g); 1 worked nacreous shell frag. (1.4 g);	Not measured	3 bird (0.9 g); 2 fish (0.6 g)

Provenience	Pottery	Other Artefacts	Marine Shell	Animal Bone
		1 sea urchin spine abrader (4.2 g); 1 chert flake (13.1 g)		
Feature C, Originating from Layer VI-A Quadrant 3 (SW) 145–160 cm	151 plain red-slipped body, 0.5–4 mm thick (238.1 g); 6 plain red-slipped rims, 1–3 mm thick (47.3 g); 2 plain red-slipped shoulder, 1–3 mm thick (14.6 g)		Not measured	
Feature D, Originating from Layer VI-B Quadrant 4 (NW) 175–185 cm	329 plain red-slipped and blackware body, 0.5–4 mm thick (793.3 g); 17 plain red-slipped rims, 1–3 mm thick (66.8 g); 1 circle-stamped and incised blackware carination, 4 mm thick (8.1 g)	2 shell ring (0.2 g); 4 chert flakes (174.3 g); 2 *Conus* sp. shell bead (0.5 g)	Not measured	1 bird (0.2 g)
Feature E, originating from Layer VI-B Quadrant 1 (NE) 175–185 cm	137 plain red-slipped and blackware body, 0.5–4 mm thick (260.3 g); 10 plain red-slipped rims, 1–4 mm thick (54.5 g)	1 cut Cypraea sp. shell frag. (3.3 g)	Not measured	
Feature F, Originating from Layer VI-B Quadrant 1 (NE) 175–185 cm	71 plain red-slipped and blackware body, 0.5–4 mm (130.1 g); 3 plain red-slipped rims, 1–3 mm thick (8.4 g)		Not measured	
Feature G, originating from Layer VII Quadrant 2 (SE) 185–205/215 cm	274 plain red-slipped and blackware body, 0.5–4 mm thick (639.8 g); 31 plain red-slipped rims, 1–4 mm thick (239.8 g); 1 point-impressed and circle-stamped	1 *Conus* sp. shell bead (0.2 g); 1 chert flake (3.5 g)	Not measured	

Provenience	Pottery	Other Artefacts	Marine Shell	Animal Bone
	red-slipped body, 5 mm thick (1.6 g)			
Feature H, Originating from Layer VII Quadrant 1 (NE) 185–195 cm	53 plain red-slipped and blackware body, 0.5–4 mm thick (114.2 g); 4 plain red-slipped rims, 2–4 mm thick (25.6 g)	1 *Conus* sp. shell disc in process (3 g); 1 *Conus* sp. shell bead (0.2 g)	Not measured	
Feature I, Originating from Layer VII Quadrant 3 (SW) 185–195 cm	146 plain red-slipped and blackware body, 0.5–4 mm (270.1 g); 8 plain red-slipped rims, 1–4 mm (22.9 g)	1 worked nacreous bivalve shell, worked around all edges (6.2 g);	Not measured	1 bird (0.4 g)

Chapter 6

New Findings: Traces of Structural Features

The features will be presented for each layer in chronological order, but first the different feature forms will be described. Traces of structural features included heated-rock hearths, pits with ash and charcoal, and post moulds. Each feature was excavated separately, as its own stratigraphic unit. The layer of origin was indicated by the uppermost visible portion of a feature, interpreted as having intruded downward from that position. None of the features in the 2016 excavation showed signs of upward-building technique.

These features were documented in the lower and older stratigraphic units of Layers VII through V, in contrast to no such features in the upper and later-dated layers. The distribution of structural features apparently had shifted through time, along with a shift in the focus of habitation at the site, eventually resulting in today's surface-visible *latte* ruins physically separated from the 2016 excavation. Concentrations of broken pottery, charcoal, ash, and other materials were observed in all layers, but they did not necessarily comprise the remnants of deliberately constructed features such as considered here in terms of the heated-rock hearths, pits, and post molds.

Heated-rock hearths were identified by four characteristics. First, limestone cobbles had been heat-altered and thus transformed into grayish colour with varying degree of chalky texture. Second, ash and charcoal flecking were adhering to the cobbles. Third, concentrations of ash and charcoal tended to be clustered around the heated-rock arrangements. Fourth, the perimeter and sometimes underside of these features in most cases were fire-hardened and reddened.

Heated-rock hearths in principle could be created by digging downward or by building upward, and a combination of techniques may have been employed. Downward-dug hearths can create an advantage of a surrounding barrier for more heat retention, as well as easier re-usage. Upward-built hearths potentially could be useful in locations where downward-digging action is impractical or for some reason undesired. The individual rocks were stacked and arranged inside the pits, so they may be viewed as upward-built elements within downward-dug features.

Upward-piled features of ash had been identified in the 2005 excavations as "ash discard piles" (Carson 2008), but no such feature was observed in the 2016 excavation. The 2016 hearths all were associated with downward-dug pits, showing a narrowing angle toward the base. In contrast, the upward-piled features (as seen in 2005) showed flat bases and upward-tapering profiles.

Seven heated-rock hearths were identified in Layers VII through V. Layer VII included Features H and I. Layer VI-B included Features D, E, and F. Layer VI-A included Feature C. Layer V included Feature A. All of these hearths were associated with pits.

Pit features contained dense ash and variable concentrations of charcoal. Evidence of burning was implied by the ash and charcoal, as well as by fire-hardened and reddened perimeters and underside portions. In most cases, these pits accompanied heated-rock hearths, but the two largest pits were made evidently without hearths, as seen in Feature G (in Layer VII) and in Feature B (in Layer V).

The two largest pits (Feature G in Layer VII and Feature G in Layer V) lacked hearths and also were created at the seaward (south) portion of the 2016 excavation area. These two pits showed clear signs of refuse-disposal and burning, but they lacked the heated-rock components of hearths that otherwise would have suggested cooking. Their positions, slightly closer to the ancient seashore than seen in the other features, may offer other clues about their original functions within the larger sets of features and activity areas.

All 18 of the identified post moulds were noticed only in the lowest stratigraphic unit of Layer VII. Potentially, they could have originated from either Layer VII or Layer VI-A, later obscured after the posts had deteriorated. In each case, a post mould was identified as a vertical cylinder space, filled with dark-stained organic sediment, and lacking any surrounding fire-hardened or reddened characteristics. The organic sediment content was interpreted as the result of disintegrated or decomposed wood of a former post. Bracing cobbles were found in seven of the 18 post moulds, noticed around the edges of seven features of P-1-1, P-2-3, P-32, P-4-1, P-4-3, P4-6, and P-4-7, mostly (but not always) around the largest post moulds. Additionally, seven of the post moulds terminated on the underlying limestone of Layer VIII, as seen in post moulds P-1-1, P-1-3, P-2-1, P-2-2, P-2-3, P-3-2, and P-4-3.

The spatial patterns of the post moulds were difficult to interpret, except that they generally were installed in the landward (north) side of the 2016 excavation area, farthest from the ancient shoreline. Given the possibility that the post moulds were created at different points in time, they did not necessarily reflect the remains of a single structure at this location. Moreover, the footprints of those past structures may have extended outside the limits of the 2016 excavation area. Some of the posts may have been replaced or re-enforced at different times.

Hearths and pit features included generally denser amounts of artifacts and midden than seen in the surrounding sedimentary layer units. In some of these features, pottery fragments of 20% or more of pottery bowls were visible, for instance as seen in Feature C. In other cases of generalised sedimentary layers, occasional dense concentrations of pottery fragments did not necessarily consist of re-joinable pieces.

The hearths and pits were regarded as the most secure stratigraphic contexts for radiocarbon dating. Preference for dating was given to the pieces of charcoal and *Anadara* sp. shells from those features. Additionally, given the tendency of hearths of pits to contain dense artefacts, the categories of pottery and shell ornaments could support association within the Marianas regional artifact chronology.

Layer VII, Features G, H, I, and Post Moulds

Layer VII revealed several features (see Figure 32), including one large pit (Feature G), two heated-rock hearths (Features H and I), and 18 traces of post moulds (P-1-1 through P-4-8). The features all were contained within the matrix of the sandy loam of Layer VII, and therefore they can be attributed to the context of a palaeo-seashore about 1500 B.C. or possibly earlier. Some of the post moulds potentially could have intruded downward from the next superimposed Layer VI-B, but still they would have referred to a similar palaeo-seashore setting close to 1500 B.C. and definitely prior to 1100 B.C.

The large pit of Feature G extended outside the boundary of the 2016 excavation, such that its full dimensions and internal nuances have not yet been explored. The uncovered portion measured 85–110 cm north-south by 210–220 cm east-west. Its section-view profile showed a clear basin shape, cut downward from the upper 5–10 cm of Layer VII and terminating on the underlying limestone surface of Layer VIII. The thickness (top to bottom) measured about 30 cm, but it may have been deeper in the farther seaward (south) portion that continued outside the 2016 excavation area.

The pit of Feature G was defined primarily by a matrix of ash and scattered charcoal (Figures 40 and 41), slightly less firm than the surrounding hardened matrix of Layer VII. The edges and underside of the pit displayed patches of fire-hardened and reddened sediments. Within the pit, artefacts and midden were consistent with the findings generally in Layer VII, except for the rare occurrence of one finely decorated pottery fragment that will be described elsewhere in this report. An *Anadara* sp. shell from Feature G produced a calibrated radiocarbon dating of 1780–1425 B.C. ((Beta-448701).

Within 1 m on the west side of the Feature G pit, two heated-rock hearths were identified as Features H and I (Figures 42 and 43). Both of these hearths consisted of heat-altered cobbles inside pits of ash and charcoal. Feature H was about 85 cm north-south by 30–60 cm east-west, roughly twice the size of Feature I measured at 40 cm north-south by 45–60 cm east-west.

FIGURE 40. NEAR BASE OF PIT OF FEATURE G IN LAYER VII, DURING EXCAVATION IN QUADRANT 2, VIEW TO SOUTH-SOUTHEAST. FIRE-REDDENED AND HARDENED PORTIONS ARE VISIBLE AT THE PERIMETER OF THIS BASAL PORTION OF THE FEATURE, AND CONCENTRATIONS OF ASH RE VISIBLE IN THE INTERIOR PIT FILL. SCALE BARS ARE IN 20-CM INCREMENTS.

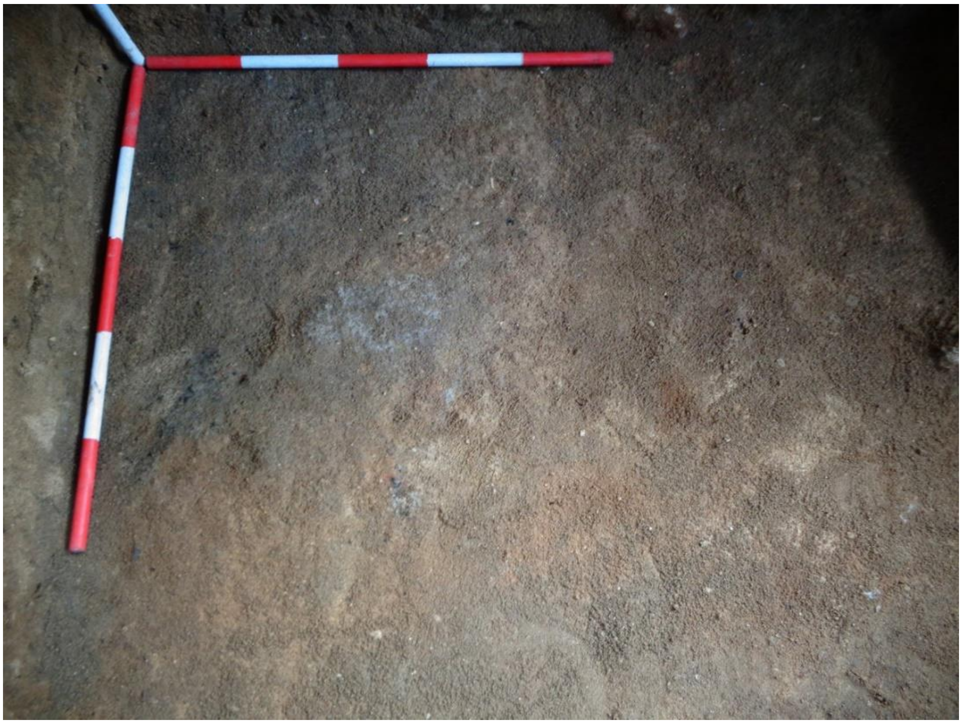

FIGURE 41. CLOSER VIEW NEAR BASE OF FEATURE G IN LAYER VII, DURING EXCAVATION IN QUADRANT 2, VIEW DOWNWARD TO SOUTH. SCALE BARS ARE IN 20-CM INCREMENTS.

FIGURE 42. INITIAL EXPOSURE OF HEATED-ROCK HEARTHS OF FEATURES H AND I IN LAYER VII, DURING EXCAVATION IN QUADRANT 3, VIEW TO SOUTHWEST. SCALE BARS ARE IN 20-CM INCREMENTS.

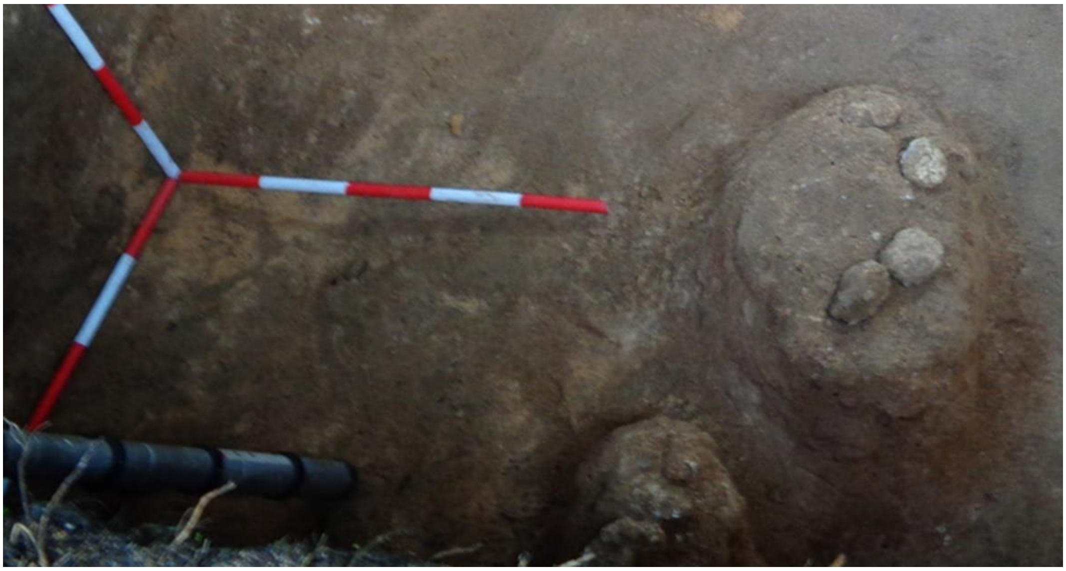

FIGURE 43. PEDESTALLED PORTIONS OF HEATED-ROCK HEARTHS OF FEATURES H AND I IN LAYER VII, DURING EXCAVATION IN QUADRANT 3, VIEW DOWN TO NORTH. SCALE BARS ARE IN 20-CM INCREMENTS.

Feature H contained an arc of three cobbles at the northwest edge of a basin-shaped pit, while the other portions of Feature H contained more generally dispersed cobbles, ash, and charcoal. The arc of cobbles may relate to the original format of heating stones along the perimeter of a pit, later disturbed or degraded into the more dispersed character of the feature as viewed today. Although the cobbles could reflect differential preservation across the hearth feature, the artefacts and midden showed no such differential patterning within Feature H.

Feature I overall met the expectations of a heated-rock hearth, containing heat-altered cobbles inside a pit of ash and charcoal, but it disclosed two rare material findings. First, this hearth contained the single preserved animal bone attributed to Layer VII, in this case identified as a bird bone fragment. Second, a nacreous bivalve shell had been worked around all of its edges. These materials will be presented in detail elsewhere in this report.

The 18 post moulds all were distributed in the middle to landward (north) portion of the excavated area, while the large pits and two hearths occupied the seaward (south) side. The post moulds were identified by their vertical cylindrical shapes, filled with dark-stained organic sediment of soft to slightly hard consistence in contrast to the surrounding cemented sandy loam of Layer VII (Figures 44, 45, and 46). Perimeter bracing cobbles were observed only in seven of the 18 cases, such as P-1-1, P-2-3, P-32, P-4-1, P-4-3, P4-6, and P-4-7. Also in seven of the 18 cases, post moulds had terminated on the underlying limestone of Layer VIII, as seen at P-1-1, P-1-3, P-2-1, P-2-2, P-2-3, P-3-2, and P-4-3.

FIGURE 44. POST MOULDS, AFTER EXCAVATION NEAR BASE OF LAYER VII, VIEW TO SOUTH. SCALE BARS ARE IN 20-CM INCREMENTS.

FIGURE 45. POST MOULDS, AFTER EXCAVATION NEAR BASE OF LAYER VII, VIEW DOWN TO SOUTHEAST. SCALE BARS ARE IN 20-CM INCREMENTS.

FIGURE 46. POST MOULDS P-3-1 (RIGHT), P-3-2 (PARTIAL IN TOP CENTER), AND P-3-3 (LOWER LEFT) IN QUADRANT 3, AFTER EXCAVATION NEAR BASE OF LAYER VII, VIEW TO NORTH-NORTHWEST. SCALE BARS ARE IN 20-CM INCREMENTS.

Although all 18 post moulds were identified within Layer VII, their downward-intrusive qualities have created ambiguities about their stratigraphic origins. The original posts may have been driven downward from a superimposed and later-aged context, but the surviving traces of post moulds have been observed only in contrast to the surrounding Layer VII. The original posts probably were not emplaced directly on an exposed limestone surface of Layer VIII, but rather they would have been driven through some amount of sedimentary build-up that began with Layer VII. Moreover, the bracing cobbles would have been most effective when wedged between the posts and the pre-existing sediment surrounding them, whereas considerably more substantial stonework construction would be necessary to hold a post resting directly on the exposed limestone terrain or other ground surface.

A cluster of six post moulds in Layer VII was identified beneath the super-imposed features of Layer VI-B, definitely pre-dating Layer VI-A and attributable most confidently to Layer VII. This cluster was identified in Quadrant 3, specifically for post molds P-4-1 and P-4-3 through -7. Four of those post molds (P-4-1, -3, -6, and -7) included bracing cobbles, and one (P-4-3) had extended all the way downward to the underlying limestone surface of Layer VIII.

Layer VI-B, Features D, E, and F

Layer VI-B disclosed three heated-rock hearths (see Figure 34), all within the landward (north) side of the 2016 excavation area in Quadrants 1 and 4. These hearths were designated as Features D, E, and F. Additionally in Quadrant 1, concentrations of pottery fragments were observed and recovered individually for potential re-joining, but they did not comprise formal structural features.

In Quadrant 4, Feature D was the largest heated-rock hearth in Layer VI-B, and it contained the largest pieces of heat-altered cobbles as well (Figure 47). Rare artefacts inside this hearth included two shell rings and one distinctively decorated blackware pottery fragment with lime-infilled circle-stamped and incised designs. These materials will be presented separately, but their association within Feature D has allowed clarity of context.

FIGURE 47. EXPOSURE OF HEATED-ROCK HEARTH OF FEATURE D IN LAYER VI-B, DURING EXCAVATION IN QUADRANT 4, VIEW DOWN TO NORTH. SCALE BARS ARE IN 20-CM INCREMENTS.

FIGURE 48. INITIAL EXPOSURE OF HEATED-ROCK HEARTHS OF FEATURES E AND F IN LAYER VI-B, DURING EXCAVATION IN QUADRANT 1, VIEW DOWN TO NORTH. POTTERY CONCENTRATION IS VISIBLE, SEPARATE FROM THE TRACES OF STRUCTURAL FEATURES. SCALE BARS ARE IN 20-CM INCREMENTS.

In Quadrant 1, Feature E was the best defined in terms of arranged cobbles, whereas Feature F consisted of only three small cobbles among diffuse ash and charcoal flecks (Figure 48). Both of these features contained broken pottery and midden as seen throughout the associated Layer VI-B. The only unusual item was a fragment of cut *Cypraea* sp. shell in Feature E. The well defined hearth of Feature E yielded no reliably datable charcoal, but an *Anadara* sp. shell was dated at 1697–1368 B.C. (Beta-461341).

Layer VI-A, Feature C

A single feature in Layer VI-A was a heated-rock hearth (Feature C) in Quadrant 3 (see Figure 35). The fragments of about 20% of a red-slipped carinated bowl were visible over the top of the hearth's internal cobbles (Figures 49 through 52). The cobbles could not have been displaced more than minimally from their original positions of the ancient usage of the hearth, or else the pottery would have been displaced as well. The associated pit of the hearth contained dense concentrations of charcoal among an ashy matrix, underlain by fire-reddened and hardened sediment (Figure 53), indicative of a burning event precisely in this spot and associated with the cobbles and pottery as preserved in situ.

Within the ashy matrix of Feature C, a charcoal concentration (Figure 54) yielded a radiocarbon date calibrated at 1437–1288 B.C. (Beta-448705), paired with an *Anadara* sp. shell (see Figure 28) calibrated at 1522–1230 B.C. (Beta-461342). This dating result aligned perfectly in the stratigraphic sequence for Layer VI-A, relative to older-aged underlying units and later-aged overlying units (see Table 5). The hearth of Feature C clearly had been overlain by the later-aged pit of Feature B in the super-imposed Layer V.

FIGURE 49. INITIAL EXPOSURE OF POTTERY CONCENTRATION AT TOP OF FEATURE C IN LAYER VI-A, DURING EXCAVATION IN QUADRANT 3, VIEW DOWN TO WEST. SCALE BARS ARE IN 20-CM INCREMENTS.

FIGURE 50. PEDESTALLED PORTION OF HEATED-ROCK HEARTH OF FEATURE C IN LAYER VI-A, DURING EXCAVATION IN QUADRANT 3, VIEW DOWN TO WEST. A PRESERVED PORTION OF A CARINATED RED-SLIPPED BOWL IS VISIBLE INSIDE THE FEATURE. SCALE BARS ARE IN 20-CM INCREMENTS.

FIGURE 51. PRESERVED PORTION OF CARINATED RED-SLIPPED BOWL IN PARTIALLY PEDESTALLED HEATED-ROCK HEARTH OF FEATURE C IN LAYER VI-A, DURING EXCAVATION OF QUADRANT 3, VIEW TO EAST. SCALE BARS ARE IN 1-CM INCREMENTS.

FIGURE 52. DETAIL OF PRESERVED PORTION OF CARINATED RED-SLIPPED BOWL IN HEATED-ROCK HEARTH OF FEATURE C IN LAYER VI-A, DURING EXCAVATION OF QUADRANT 3, VIEW DOWN TO EAST. SCALE BARS ARE IN 1-CM INCREMENTS.

FIGURE 53. FIRE-REDDENED AND HARDENED ASHY MATRIX AT THE BASE OF FEATURE C, DURING EXCAVATION IN QUADRANT 3, VIEW DOWN TO WEST. SCALE BARS ARE IN 20-CM INCREMENTS.

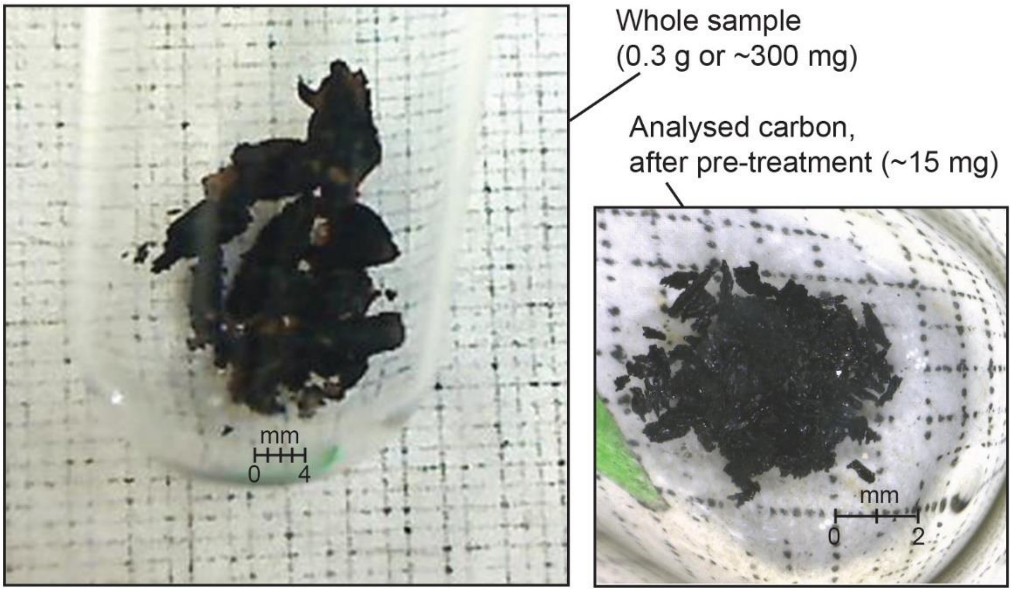

FIGURE 54. SAMPLE BETA-448705 FROM FEATURE C OF LAYER VI-A. LEFT IMAGE SHOWS THE WHOLE SAMPLE, REMOVED BY TROWEL FROM THE FEATURE. RIGHT IMAGE SHOWS THE ANALYSED CARBON AFTER PRE-TREATMENT OF ACID WASH TO REMOVE CONTAMINANTS, RETAINING A SURPLUS OF CARBON FOR RADIOCARBON DATING. IMAGES WERE PROVIDED BY BETA ANALYTIC LABORATORY.

Layer V, Features A and B

A heated-rock hearth (Feature A) and a large pit (Feature B) were identified within Layer V (see Figure 36). Both features had been cut downward from the upper portions of the silty sand of Layer V, and the base of Feature B clearly overlaid and post-dated the hearth of Feature C in the underlying Layer VI-A. Radiocarbon dating of two samples from Feature A and one sample from Feature B provided cross-confirming results all overlapping significantly at 1127–1056 B.C. (see Table 4).

The original full dimensions of Features A and B are unknown, as they had extended outside the boundaries of the 2016 excavation. The excavated portion of Feature A measured 160 cm north-south by 110 cm east-west. The excavated portion of Feature B measured 120 cm north-south by 240 cm east-west.

The hearth of Feature A displayed some apparently intact portions, while mostly its contents had been scattered through re-usage or natural post-depositional displacement. Numerous limestone cobbles were distributed throughout the pit of ash and charcoal, and only some of those cobbles appeared to retain their original placements in stacked or other organised positions (Figures 55 and 56). Many but certainly not all of 1566 pottery fragments were re-joinable or showed obvious signs of having been broken from the same vessels.

The pit of Feature B was identified by its ashy matrix with dispersed flecks and chunks of charcoal (Figure 57), as well as by a fire-reddened and hardened perimeter and underside. The pit contained mostly the same range of broken pottery and midden as seen generally in Layer V, but it also contained a two rare items that will be presented separately. A small net weight was made of limestone crystal, and a nearly complete fishing hook was made of nacreous shell.

FIGURE 55. INITIAL EXPOSURE OF HEATED-ROCK HEARTH OF FEATURE A IN LAYER V, DURING EXCAVATION IN QUADRANTS 3 AND 4, VIEW TO WEST. SCALE BARS ARE IN 20-CM INCREMENTS.

FIGURE 56. PEDESTALLED PORTIONS OF HEATED-ROCK HEARTH OF FEATURE A IN LAYER V, DURING EXCAVATION IN QUADRANTS 3 AND 4, VIEW TO WEST. SCALE BARS ARE IN 20-CM INCREMENTS.

FIGURE 57. PEDESTALLED SURFACE OF PIT OF FEATURE B IN LAYER V, DURING EXCAVATION IN QUADRANT 3, VIEW TO SOUTHEAST. SCALE BARS ARE IN 20-CM INCREMENTS.

Chapter 7

New Findings: Pottery Artefacts

Pottery was by far the most numerically abundant artefact category from the 2016 excavation, and indeed pottery has been the dominant material in most archaeological assemblages of the Marianas region. The abundance has made pottery potentially useful for studying large-scale patterns and trends. Moreover, the combinations of technical and artistic choices in pottery-making traditions have resulted in distinctively identifiable forms and styles, now comprising the categories in an overall Marianas regional pottery chronology.

In its most recent summary formulation (Carson 2016), the Marianas pottery sequence has shown several chronological trends, and these trends were noticed in the 2016 findings at Bapot (Figure 58). The oldest traditions since 1500 B.C. if not earlier were red-slipped and generally small bowls with outcurving or everted rims, accompanied by small amounts of black-burnished or blackware of the same shapes and sizes of bowls, whereas the later traditions were non-slipped and large bowls with incurving rims, most pronounced after A.D. 1000. Meanwhile, the oldest traditions were made with thin walls and fine paste, whereas the later traditions were notably thicker and made with coarse paste and large temper inclusions. In the middle of the sequence, about 500 B.C. through A.D. 500, forms of shallow and flat-bottomed pans or griddles had become popular, along with a category of narrow straight-sided jar or cup.

Decorated pieces have been rare in all time periods in the Marianas, but their distinctive patterns have allowed more precise observations of their associated contexts and traditions. The oldest designs prior to 1100 B.C. were made with fine-line incision, circle-stamping, and dentate-stamping often highlighted by white lime infill. These traditions later were modified into expressions of coarser and bolder line-incised and circle-stamped motifs, continuing in low frequency through 500 B.C. and virtually non-existent thereafter. From 500 B.C. through A.D. 500, rims sometimes were incised with lines, circles, and half-circle designs. The later-aged pottery mostly lacked decoration, except for very rare instances of simple incisions and fingertip impressions, as well as the applications of coarse exterior combing more common in Guam and Rota than in Saipan and northern islands.

The 2016 Bapot pottery sequence has shown gradational change through time (see Figure 58). The older traditions declined, simultaneously with the increasing popularity of later traditions. These gradational transitions occurred a few times over the course of more than 3000 years at the site. To an unknown extent, these cross-stratigraphy transitions could reflect post-depositional movement or displacement of pottery and other materials within the site stratigraphy, but mostly the transitions can be accepted as reflecting the actual chronological overlap of past cultural traditions.

Decorated pottery pieces comprised less than 1% of the total pottery fragments in any single layer, consistently in the 2005 and 2016 excavations. Sampling error was acknowledged as a possible reason for not having found decorated pieces in the deepest and oldest cultural layer in the 2005 test pits that had totaled 4 sq m, instead found only in the second-oldest layer and thereafter (Carson 2008). The 2016 excavation confirmed decorated pottery beginning in the lowest cultural layer, although decoration was extremely rare, even with the 2016 excavation of a contiguous 16 sq m amounting to four times (400%) of the 2005 sampling.

The 2016 excavation recovered 36,706 pottery fragments from the complete sequence of stratigraphic layers and features. This scope of material allowed clarification of some parts of the pottery sequence that had been ambiguous on the basis of the more constrained findings from the 2005 excavation, plus new information from other sites now has become available about the Marianas regional chronology (Carson 2016). The collection of 36,706 pottery fragments was more than sufficient to characterise the pottery forms, styles, and variations within each represented time period at the site.

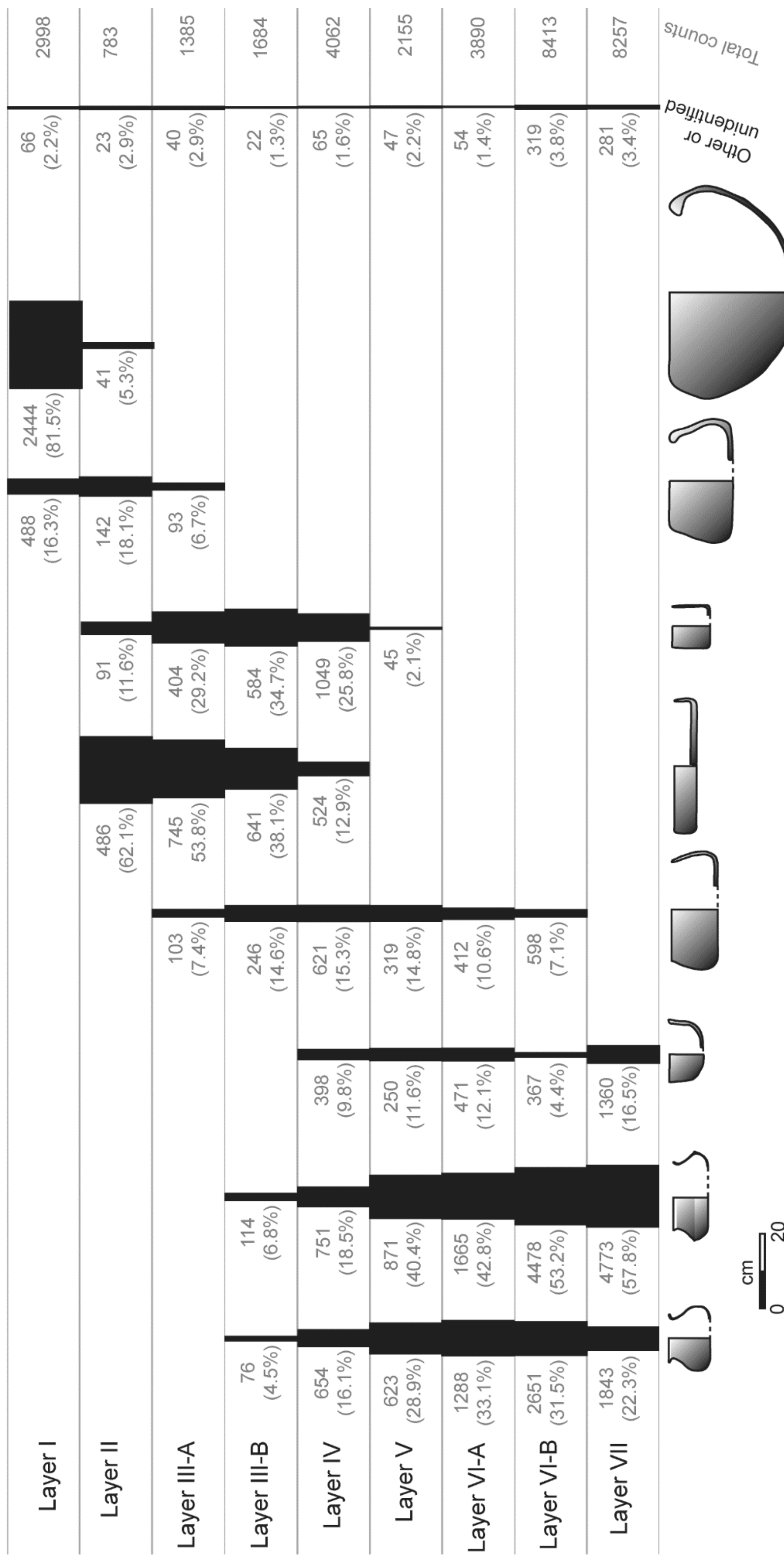

FIGURE 58. OVERALL CHRONOLOGICAL TRENDS IN MAJOR CATEGORIES OF POTTERY.
THE RAW COUNTS HERE ARE EXCLUDING THE HIGH-DENSITY CONCENTRATIONS INSIDE HEARTHS AND PITS OF LAYERS VII THROUGH V.

The 2016 pottery findings will be presented here in chronological order, from Layer VII through Layer I. The major categories and the rarities all will be identified in each context. Representative pieces will be depicted, and the corresponding vessel shapes will be approximated to the extent possible with the available fragments.

Layer VII Pottery

Layer VII yielded 8774 pottery fragments, including 8257 from the general layer itself, plus another 517 from Features G, H, and I. All pieces had been broken from red-slipped (redware) or black-burnished (blackware) vessels, made with fine paste and fine-grained sand temper inclusions. All pieces were 4 mm of less in thickness. The thinnest pieces were measured as 0.5 mm. The thickest portions were at the critical junctures of base corners, shoulders, carinations, rims, or lips.

The pieces of pottery in Layer VII mostly had been broken into fragments of less than 4 sq cm, and the few largest were up to 50 sq cm. The thin vessel walls surely contributed to the small fragmentation, further exacerbated by the weight of overlying sedimentary layers, later intrusive tree-root disturbance, and other factors. The smallest crumb-like pieces of less than 0.5 sq cm were not quantified. The thinnest pieces (0.5–1 mm) accounted for 1632 (19.8%) of the total 8257 fragments, and they generally were less than 2 sq cm.

The pottery in Layer VII represented a few varieties of small and thin-walled bowls (see Figure 58). According to the extrapolation measured from the curvatures of rim pieces, most of the bowls were about 20 cm in diameter, but a few were as small as 10 cm diameter. The small size applied equally to all of the vessel shapes.

The small bowls were made in three major shapes. First, the most popular occurrence (seen in about 57.8% of the Layer VII assemblages) displayed an outcurved rim with everted lip, extended horizontally over an angled carination (Figure 59). Second, a variant of the first shape involved a rounded shoulder without the sharply angled carination (Figure 60), seen in about 22.3% of the Layer VII assemblage. Third and least popular was a nearly straight-sided vessel, with a vertical or very slightly outcurved rim profile (Figure 61), seen in about 16.5% of the total assemblage from Layer VII. For all three of these major shape categories, the bases were made with mildly rounded bottoms, with only two instances of clearly flat-cornered base pieces (Figure 62).

A single piece of pottery from Layer VII showed a decorative design (Figure 63). The design was composed of horizontal rows of circles and impressed dots. The original red slip had been mostly eroded, and the broken edges of the potsherd likewise had been partly eroded. This piece was obtained from the large pit of Feature G. The same decorative design has been identified in early pottery at other site layers dated in the rage of 1500–1100 B.C., for instance at House of Taga in Tinian and at Ritidian in Guam (Carson 2016), also on pottery where the red slip had been mostly eroded.

Of the total 8774 pottery fragments from Layer VII, most were red-slipped, and the blackware specimens clearly were in the minority (Figure 64). Red-slipped pieces accounted for 97.9%, while blackware pieces accounted for only 2.1% of the Layer VII potsherds. The blackware products represented the same vessel categories as seen in their red-slipped counterparts of Layer VII, but they certainly were out-numbered by the red-slipped output.

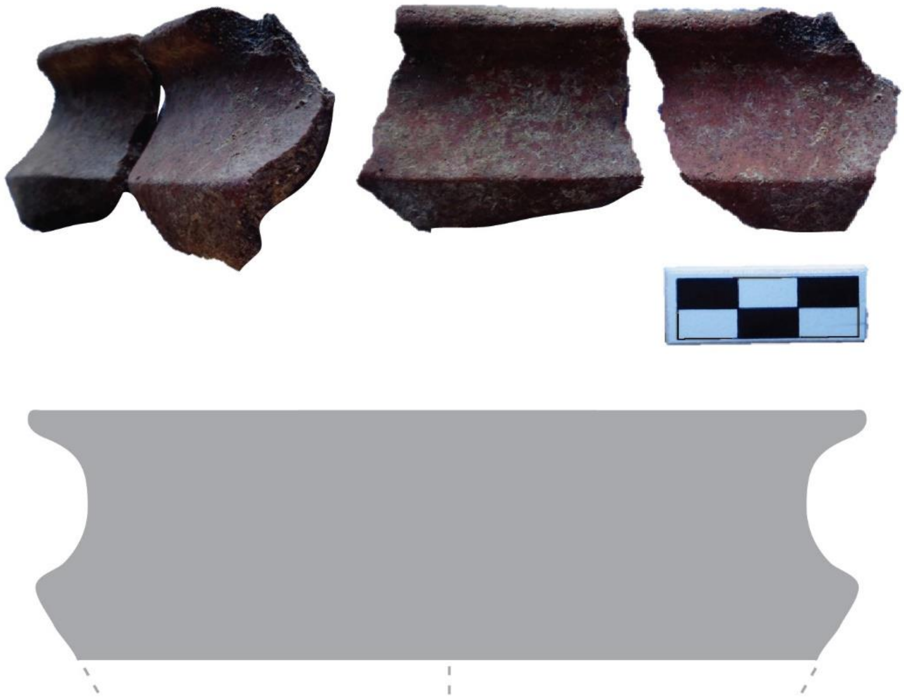

FIGURE 59. PIECES OF A CARINATED BOWL WITH EVERTED LIP, TWO PIECES SHOWN IN TWO VIEWS, RECOVERED FROM LAYER VII. SCALE BARS ARE IN 1-CM INCREMENTS.

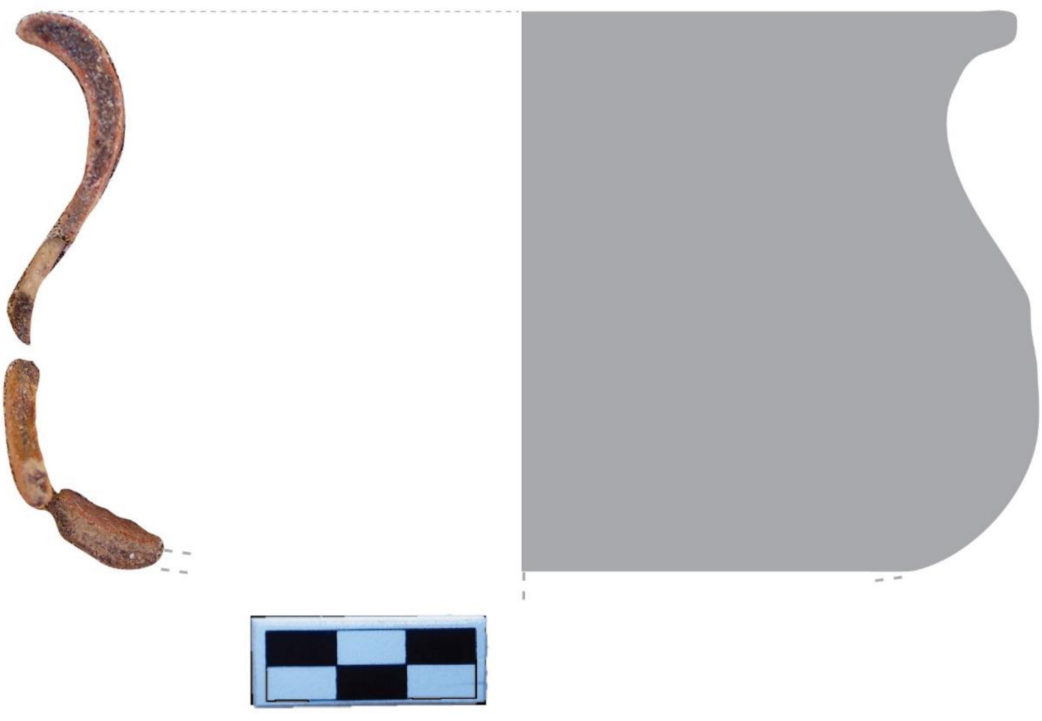

FIGURE 60. PIECES OF A ROUND-SHOULDERED BOWL WITH EVERTED LIP, RECOVERED FROM LAYER VII. SCALE BARS ARE IN 1-CM INCREMENTS.

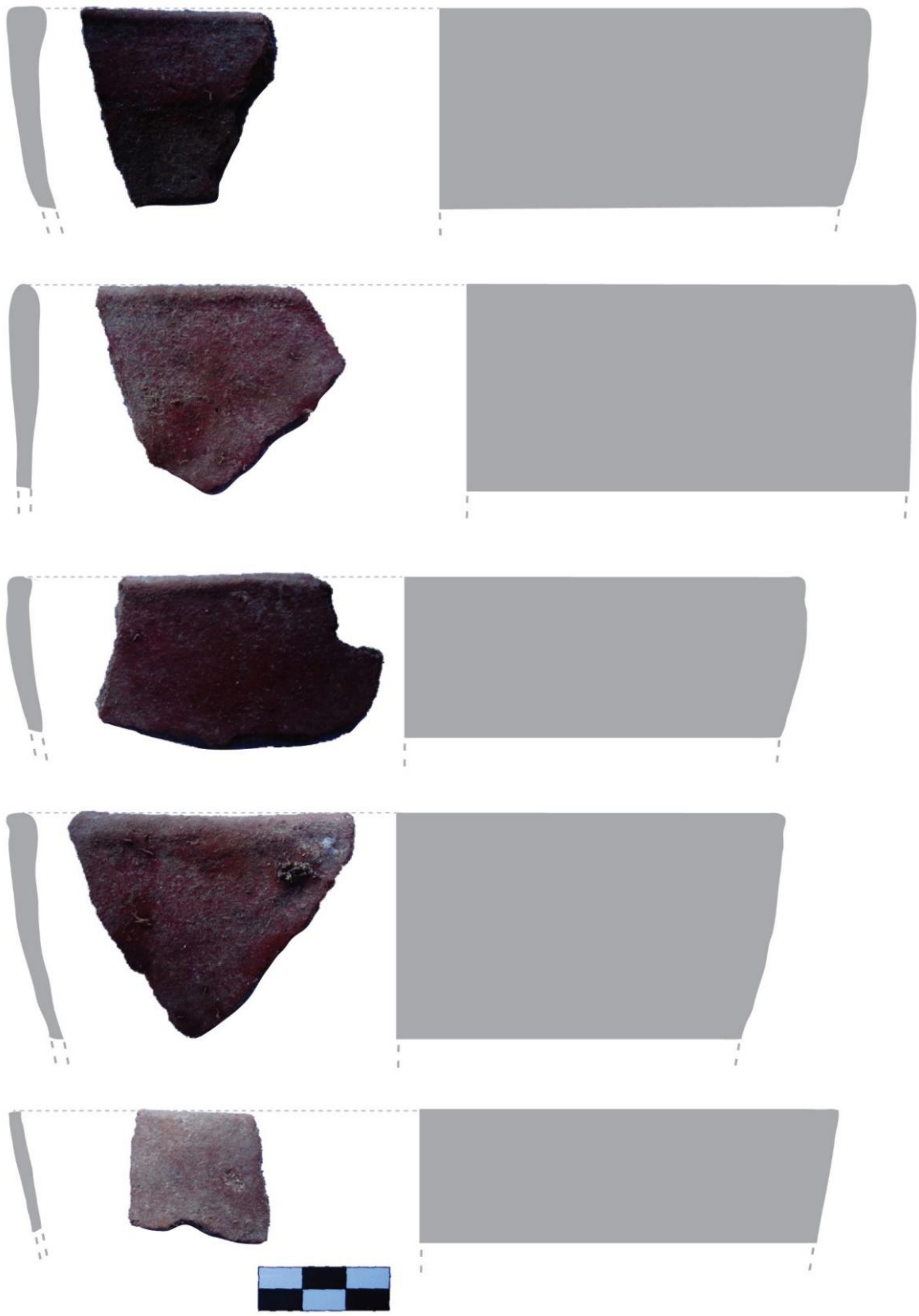

FIGURE 61. RIM FRAGMENTS OF NEARLY STRAIGHT-SIDED BOWLS, WITH SLIGHT OUTCURVING, RECOVERED FROM LAYER VII. SCALE BARS ARE IN 1-CM INCREMENTS.

FIGURE 62. RARE EXAMPLES OF FLAT-CORNERED BASE FRAGMENTS, RECOVERED FROM LAYER VII. SCALE BARS ARE IN 1-CM INCREMENTS.

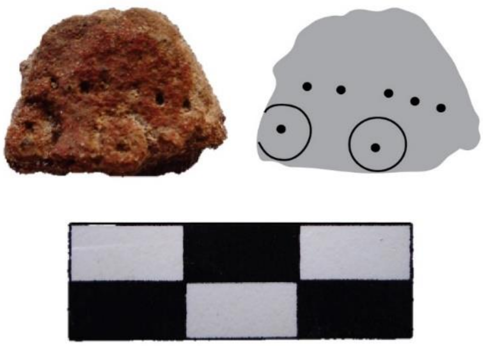

FIGURE 63. DECORATED POTTERY FRAGMENT, RECOVERED FROM FEATURE G OF LAYER VII. SCALE BARS ARE IN 1-CM INCREMENTS.

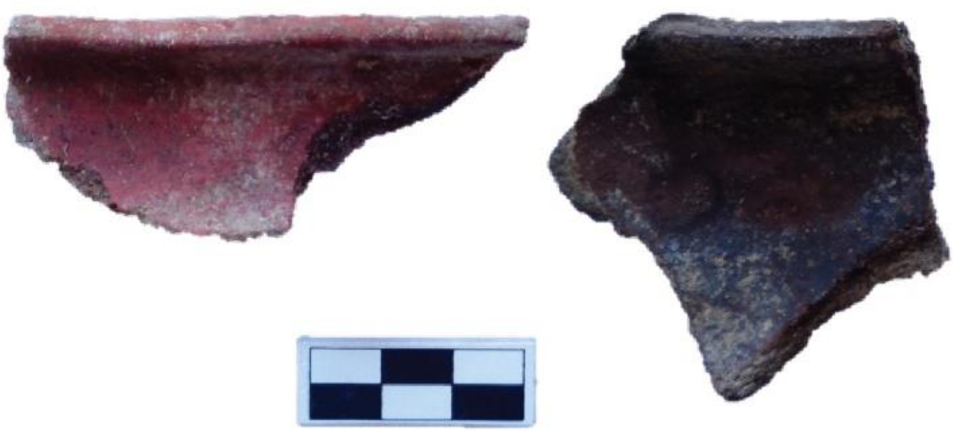

FIGURE 64. COMPARISON OF RED-SLIPPED (LEFT) VERSUS BLACKWARE (RIGHT) EVERTED RIMS, RECOVERED FROM LAYER VII. SCALE BARS ARE IN 1-CM INCREMENTS.

Layer VI-B Pottery

The 8981 pottery fragments from Layer VI-B included 8413 from the layer itself, plus another 568 from heated-rock hearths of Features D, E, and F. The overall density of pottery indicated a slight decrease from 187.7 pieces per 100 litres in Layer VII to 175.3 pieces per 100 litres in Layer VI-B (see Figure 38). This difference was minimal, calculated as a 6.6% reduction between the two layers. The thinnest (0.5–1 mm) and generally smallest (mostly less than 2 sq cm) fragments accounted for 1793 (20%) of the Layer VI-B assemblage, comparable with the proportion of 19.8% as seen in Layer VII.

The Layer VI-B pottery mostly represented continued traditions of the same categories of small bowls from Layer VII (Figures 65, 66, and 67), with four notable exceptions. First, the nearly straight-sided bowl had diminished significantly in its popularity relative to the other options at the time (see Figure 58). Second, a new form of larger bowl with slightly incurved profile began to appear in low frequency (Figure 68). Third, decorated potsherds continued to be extremely rare in just two specimens, and both were blackware pieces (Figures 69 and 70). Fourth, one pottery fragment exhibited a rare paddle-impressed exterior (Figure 71).

Regarding the appearance of a larger bowl with slightly incurved profile (see Figure 68), this category never gained much popularity overall in any stratigraphic layer at Bapot or any other site so far known in the Mariana Islands. It was made with fine paste and fine-fraction beach sand temper inclusions, with vessel walls almost uniformly 4 mm thick, and the surfaces were red-slipped. The lips rarely were decorated in later periods, but none exhibited decorations in Layer VI-B at the Bapot Site.

The two decorated blackware potsherds (see Figures 69 and 70) included one carination piece from the hearth of Feature D and a separate rim piece from the generalised layer in the upper 10 cm of Quadrant 3. Both of the decorations had been composed of fine-line incisions and circle-stamped designs, although they appeared to have been broken from vessels of different clay paste composition. White lime infilling was noticed only on the carination piece from Feature D.

The paddle-impressed piece (see Figure 71) was recovered from the lower 10 cm of Layer VI-B in Quadrant 4. The paddle marks had been produced by a paddle with parallel grooves, impressed into the wet clay during the final stages of pottery shaping prior to drying and firing. Paddle-impressed pieces so far have been observed very rarely in the early-period Marianas site layers generally prior to 1100 B.C. (Carson 2016).

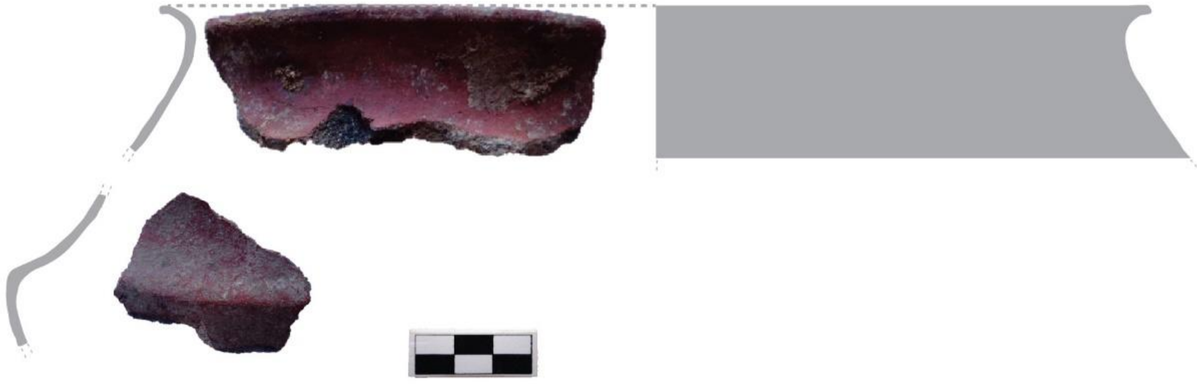

FIGURE 65. PIECES OF CARINATED RED-SLIPPED BOWL, RECOVERED FROM LAYER VI-B. SCALE BARS ARE IN 1-CM INCREMENTS.

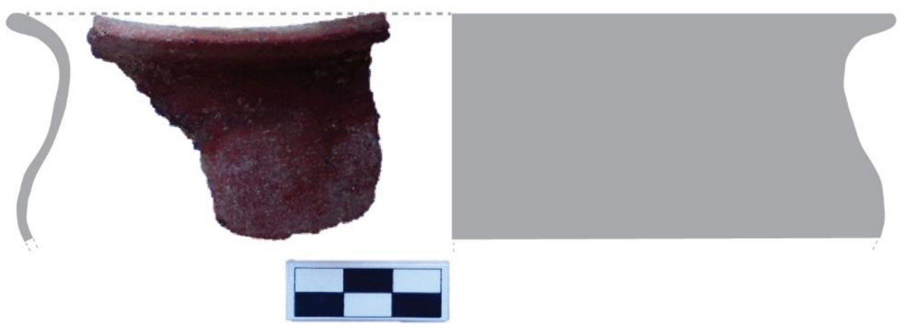

FIGURE 66. FRAGMENT OF ROUND-SHOULDERED BOWL, RECOVERED FROM LAYER VI-B. SCALE BARS ARE IN 1-CM INCREMENTS.

FIGURE 67. FRAGMENTS OF BLACKWARE RIMS, BROKEN FROM EVERTED (UPPER) AND NEARLY STRAIGHT-SIDED (LOWER) VARIANTS, RECOVERED FROM LAYER VI-B. SCALE BARS ARE IN 1-CM INCREMENTS.

FIGURE 68. RIMS BROKEN FROM SLIGHTLY INCURVED BOWLS, RECOVERED FROM LAYER VI-B. SCALE BARS ARE IN 1-CM INCREMENTS.

FIGURE 69. DECORATED BLACKWARE RIM, RECOVERED FROM LAYER VI-B. SCALE BARS ARE IN 1-CM INCREMENTS.

FIGURE 70. DECORATED BLACKWARE CARINATION, WITH PARTLY RETAINED WHITE LIME INFILL, RECOVERED FROM FEATURE D OF LAYER VI-B. SCALE BARS ARE IN 1-CM INCREMENTS.

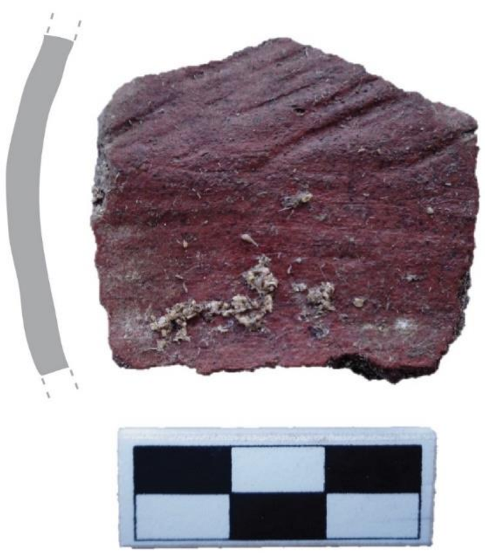

FIGURE 71. PADDLE-IMPRESSED POTTERY FRAGMENT, RECOVERED FROM LAYER VI-B. SCALE BARS ARE IN 1-CM INCREMENTS.

Layer VI-A Pottery

The pottery from Layer VI-A continued the same vessel categories as already seen in the directly preceding Layer VI-B (Figures 72 and 73), with three notable differences. First, the Layer VI-A revealed two circle-stamped red-slipped pieces (Figure 74). Second, Quadrant 3 contained a cluster of decorated blackware fragments related to a single carinated bowl (Figure 75). Third, the thinnest varieties of 0.5–1 mm were vastly reduced, seen in 311 (7.7%) of the total 4049 pieces, as compared to their values of 19.8% in Layer VII and 20% in Layer VI-B.

The total 4049 pottery fragments from Layer VI-A included 3890 from the generalised sedimentary layer, plus another 159 pieces broken from about 20% of a single bowl preserved in the hearth of Feature C (see Figures 50 through 52). The raw count of pieces had decreased from the preceding Layers VII and VI-B, but the density of fragments per 100 litres of excavation had increased (see Figures 37 and 38).

The preserved portion (about 20%) of a carinated red-slipped bowl in Feature C allowed clear definition of this vessel category in association with Layer VI-A. Overall, the carinated small bowl category had been the most popular vessel shape since Layer VII and continuing through Layer V. The particular occurrence in Feature C represented the most frequent category of a carinated bowl about 20 cm diameter, although less numerous examples were closer to 10 cm diameter or occasionally even smaller.

Two circle-stamped red-slipped pieces (see Figure 74) both showed traces of white lime infilling in their designs. One had been made with slightly overlapping circles, and points or dots had been situated in the centers of the circles. The other had been made with separate circles in a row. Both designs were reminiscent of findings at other sites for contexts over a period of several centuries from 1500 through 500 B.C. (Carson 2016).

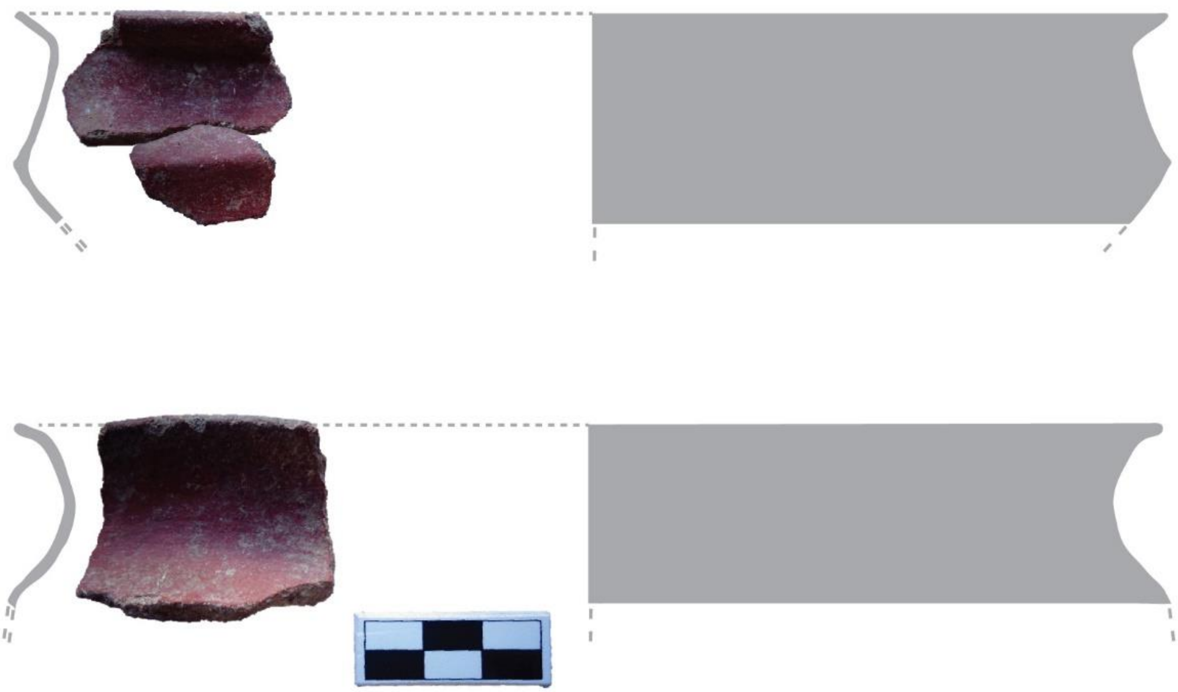

FIGURE 72. EXAMPLES OF FRAGMENTS FROM EVERTED-RIM BOWLS, WITH VARYING DEGREE OF SHARPLY CARINATED TO ROUNDED PROFILE, RECOVERED FROM LAYER VI-A. SCALE BARS ARE IN 1-CM INCREMENTS.

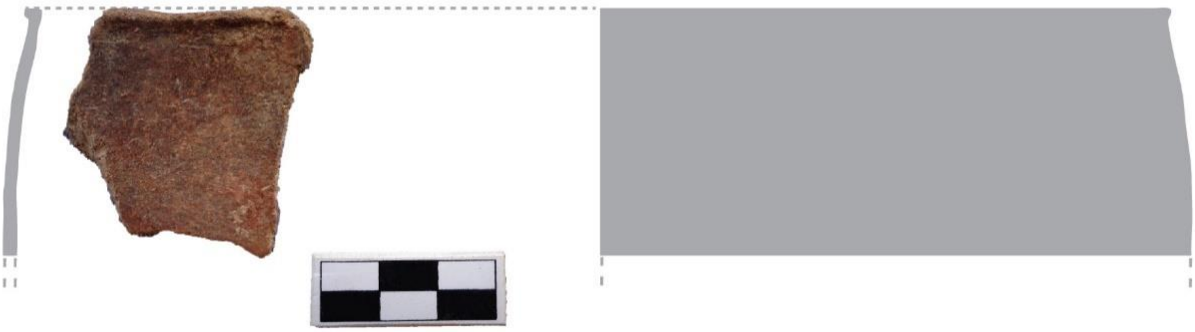

FIGURE 73. RIM OF SLIGHTLY INCURVED BOWL, RECOVERED FROM LAYER VI-A. SCALE BARS ARE IN 1-CM INCREMENTS.

FIGURE 74. DECORATED RED-SLIPPED POTTERY FRAGMENTS, WITH TRACES OF WHITE LIME INFILL, RECOVERED FROM LAYER VI-A. SCALE BARS ARE IN 1-CM INCREMENTS.

The 12 decorated blackware pieces (see Figure 75) mostly (N = 7 of 12) were retrieved from a concentration inside Quadrant 3, while others (N = 5 of 12) were distributed more broadly in Quadrant 3. All of these pieces apparently were broken from a single carinated bowl, according to the identical clay paste, temper inclusion composition, black burnishing, and decorative design. The design was composed of rows of circles alternating with rows of incised chevrons, highlighted with white lime infilling. The decorations covered the most visible upward-facing portion of the bowl, from the rim to the top of the carination.

Layer VI-A yielded an unusual fragment of red-slipped pottery that had been modified by drilling a hole through its center (Figure 76). The drilling had been achieved from two directions, resulting in a classic "bi-conical" shape of the drilled hole. The red slip had been almost entirely removed by abrasion, possibly providing a clue about how the drilled fragment was used. The drilling must have been performed after the pottery had been fired into earthenware, or else no such drilling marks could be produced in wet or leather-hard clay. The bi-conical drilling, requiring two directions of drilling, most likely had occurred after the fragment had been broken into a small piece allowing easy access to both of its sides.

FIGURE 75. DECORATED BLACKWARE FRAGMENTS, WITH TRACES OF WHITE LIME INFILL, BROKEN FROM CARINATED BOWL, RECOVERED FROM QUANDRANT 3 IN LAYER VI-A. SCALE BARS ARE IN 1-CM INCREMENTS.

FIGURE 76. DRILLED POTSHERD, SHOWN IN EXTERIOR (LEFT) AND INTERIOR (RIGHT VIEWS), RECOVERED FROM LAYER VI-A. SCALE BARS ARE IN 1-CM INCREMENTS.

Layer V Pottery

The total 3990 pottery fragments from Layer V included 2155 pieces from the generalised sedimentary layer, plus another 1835 from Features A and B. The two features occupied about 35% of the volume of Layer V, and they yielded 46% of the total pottery fragments. Other than the differential density of material, the features revealed the same range of pottery as seen in the generalised layer.

The categories of vessel shapes in Layer V overall were consistent with the trends already seen in the preceding layers at the site, but five important new transitions were noticed. First, the expected forms such as carinated bowls (Figures 77 and 78) were joined by a new appearance of very few examples of a narrow cup or jar that would become more popular in later periods (Figure 79). Second, the category of exceptionally thin red-slipped pottery, about 0.5–1 mm thickness, had disappeared entirely from the assemblage. Third, blackware was notably rare in 106 (2.7%) of the total 3990 pottery fragments. Fourth, circle-stamped designs occurred on an exceptionally rare handle fragment (Figure 80) and on another piece broken from an impressively small bowl (Figure 81). Fifth, the classic "San Roque Type" of decoration (see Butler 1994, 1995) made its first and only appearance in two fragments, displaying the diagnostic rows of circles and curvilinear garlands (Figure 82).

Layer V coincided with a shift in the environmental context, during initial sea-level drawdown and resulting newly stable backbeach terrain at the site. This transition began about 1100 B.C. throughout the Mariana Islands (Carson 2011, 2014a, 2014b, 2016). The same dating has been corroborated at the Bapot Site from the 2005 excavation (Carson 2008) and again from charcoal in Feature A of Layer V in the 2016 excavation as reported here.

An exceptional discovery in Layer V was a circle-stamped handle fragment (see Figure 80), constituting so far the only decorated handle recovered from an excavation in the Mariana Islands. The circles have been highlighted by white lime infilling, and the overall design was comprised of a row of large circles along the middle of the handle, bordered by smaller circles along the two side edges. The handle's two ends had been broken, so the complete shape and attachment to a larger vessel could not be clarified.

Handle fragments have been extremely rare at other sites, and none of those have shown decorations as seen here in Layer V. Two handle pieces from House of Taga in Tinian were from the lowest cultural layer in the range of 1500–1100 B.C. Another two handle pieces from Ritidian in Guam were from two different contexts of 1500–1100 B.C. and 1100–700 B.C.

Two conjoined earthenware body fragments showed a circle-stamped design (see Figure 81). These fragments must have been broken from a tiny vessel, less than 10 cm diameter according to the observable curvature. The interior and the apparent base of the exterior has been blackened by heat and a thin veneer of charred residue.

Two decorated red-slipped pieces displayed classic designs of the "San Roque Type" (see Butler 1994, 1995) with curvilinear garlands and circles (see Figure 82). One piece was a rim, and the other was a body piece that had been broken near the rim. These two fragments were composed of slightly different clay paste and temper inclusions, reflecting breakage from two different red-slipped bowls.

Two other red-slipped rim fragments showed decorations over their lip portions (Figure 83). One rim's design was composed of large circles. The other rim's design consisted of half-circle impressions. In both of these cases, no white lime infilling was noticed.

Another rare finding from Layer V was a red-slipped pottery rim, with triangular carved notching along its lip (Figure 84). The notching had been cut into the hard clay, after the pot had been fired. The notching had cut through the red slip, and it had exposed the inner firing core of the clay paste. Two notches were clearly visible in the middle of the lip, and a partial third notch may have been retained along one broken edge. The notching could have occurred when the pot was whole before breakage, or it may have been applied to a broken piece that subsequently underwent further fragmentation.

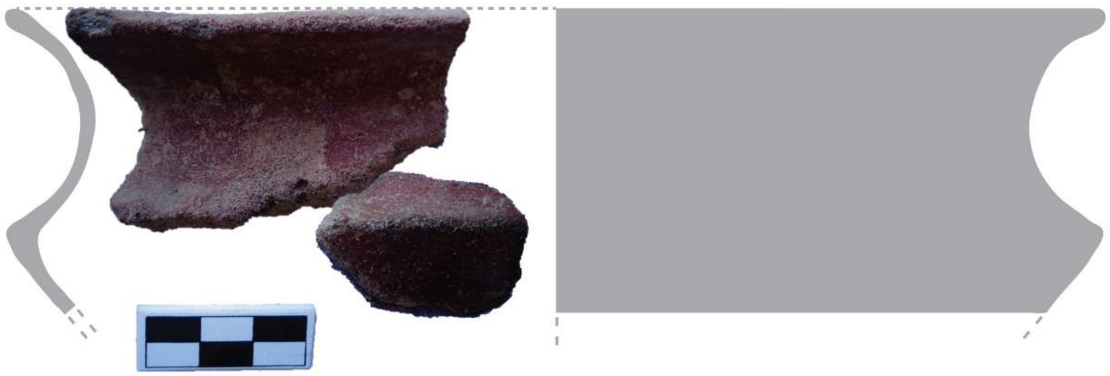

FIGURE 77. FRAGMENTS OF CARINATED RED-SLIPPED BOWL WITH EVERTED RIM, RECOVERED FROM LAYER V. SCALE BARS ARE IN 1-CM INCREMENTS.

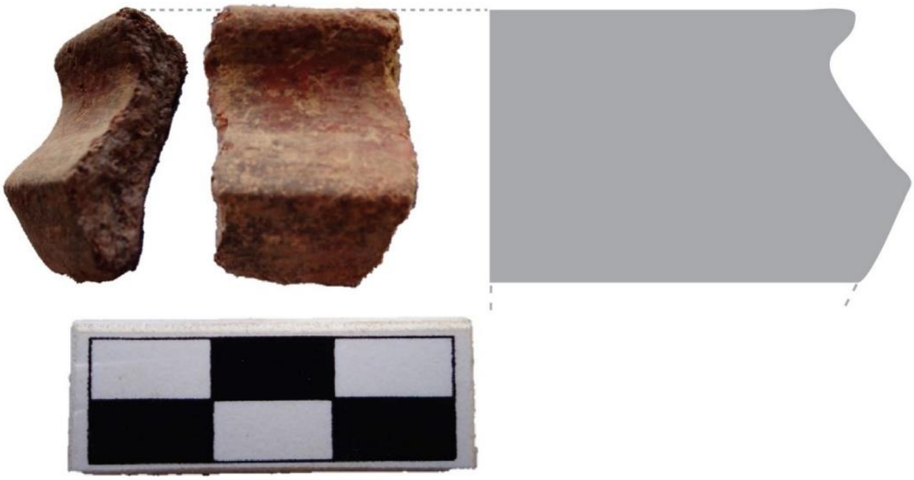

FIGURE 78. FRAGMENT OF VERY SMALL CARINATED RED-SLIPPED BOWL WITH EVERTED RIM, RECOVERED FROM LAYER V. SCALE BARS ARE IN 1-CM INCREMENTS.

FIGURE 79. RIM OF NARROW STRAIGHT-SIDED CUP, RECOVERED FROM LAYER V. SCALE BARS ARE IN 1-CM INCREMENTS.

Figure 80. Rare example of circle-stamped red-slipped handle, with traces of white lime infill, shown in three views, recovered from Layer V. Scale bars are in 1-cm increments.

Figure 81. Portion of very small circle- stamped red-slipped pottery, shown in three views, recovered from Layer V. Scale bars are in 1-cm increments.

FIGURE 82. TWO RED-SLIPPED POTTERY FRAGMENTS, WITH CURVILINEAR GARLANDS AND CIRCLES, RETAINING TRACES OF WHITE LIME INFILL, RECOVERED FROM LAYER V. SCALE BARS ARE IN 1-CM INCREMENTS.

FIGURE 83. TWO RED-SLIPPED RIMS, DECORATED OVER THE LIP, SHOWING ROW OF CIRCLES (LEFT) AND ROW OF HALF-CIRCLES (RIGHT), RECOVERED FROM LAYER V. SCALE BARS ARE IN 1-CM INCREMENTS.

FIGURE 84. RED-SLIPPED POTTERY FRAGMENT, MODIFIED BY NOTCHING OF THE RIM, RECOVERED FROM LAYER VI-A. SCALE BARS ARE IN 1-CM INCREMENTS.

FIGURE 85. FRAGMENTS OF RED-SLIPPED BOWL WITH EVERTED RIM, RECOVERED FROM LAYER IV. SCALE BARS ARE IN 1-CM INCREMENTS.

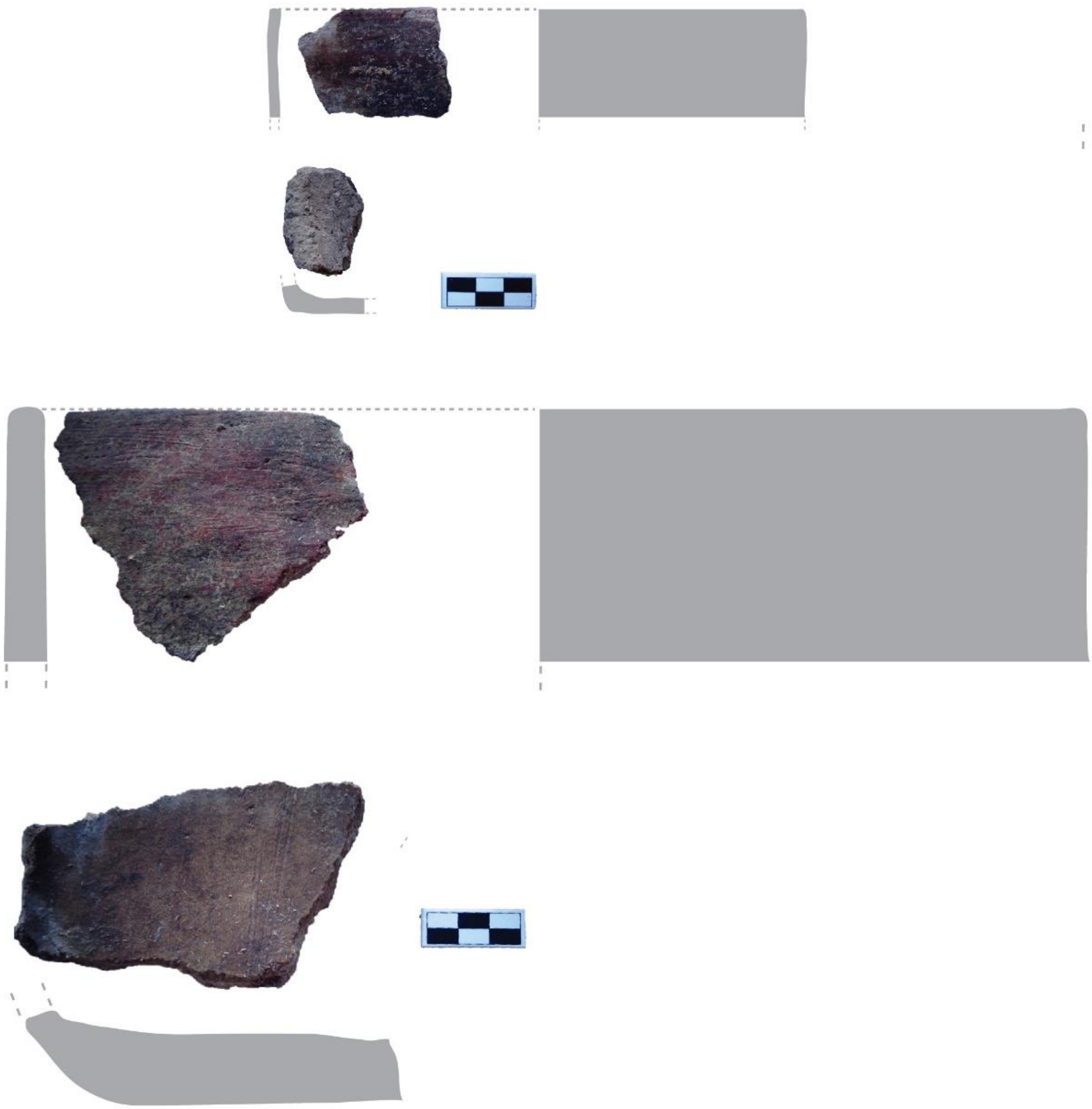

FIGURE 86. EXAMPLES OF NARROW STRAIGHT-SIDED CUP (UPPER) AND LARGE FLAT-BASED PAN (LOWER), RECOVERED FROM LAYER IV. SCALE BARS ARE IN 1-CM INCREMENTS.

Layer IV Pottery

Pottery from Layer IV was defined by 4062 fragments, overall displaying decline of older traditions simultaneously with the appearance of new traditions. The same transitions occurred in other sites of the Marianas about 700–500 B.C. (Carson 2016). The new traditions seen in Layer IV became significantly more popular in later contexts, while the older traditions eventually vanished entirely.

In Layer IV, the categories of small red-slipped bowls declined in popularity (Figure 85), while two other forms gained prominence (Figure 86). First, the narrow cup or jar, as had been seen initially in Layer V, now became more numerously represented. Second, a thick-walled, flat-bottomed, and shallow pan or griddle appeared as well. Meanwhile, blackware had disappeared from the assemblage.

The narrow cups or jars were made with a number of distinctive characteristics. The clay paste was fine and tightly compressed, and the surfaces were roughly brushed. The profiles were nearly vertical, with variation from very slightly outcurved to incurved by only a few degrees. The bases were flat, with angled edges leading up to the body walls. The rims and lips were thinning to straight, lacking decoration in Layer IV but seen in rare cases in later-aged layers.

The thick, flat-bottomed vessels were made with generally coarse clay paste and medium to large temper inclusions, easily distinguished from the finer and compacted paste of the narrow cups and jars. The vertical straight-sided walls surrounded shallow interiors of 8–11 cm depth, around spaces about 40–60 cm diameter. The lips mostly were squared around the rims. The base pieces consistently exceeded 18 mm and were made up to 24 mm in thickness, while the walls mostly were 10–14 mm thickness.

The narrow cups and the flat-bottomed pans both have been found most popularly in site layers of 500 B.C. through A.D. 500 in the Mariana Islands generally, although both of these forms were produced in low numbers earlier and later by perhaps 200 years around the most popular range (Carson 2016). The older components, as seen here in Layer IV, were made with red slip. Later variants were made without slip, while decorated rims and lips became more numerous yet still quite rare overall.

Decoration was extremely rare, seen in only a single piece with bold-line incised vertical and horizontal lines (Figure 87). This form of bold-line incision was typical of the period of 700–200 B.C. (Carson 2016). No white lime infill was visible, although it was present in similar pottery at other sites.

FIGURE 87. BOLD-LINE INCISED POTTERY RIM FRAGMENT, RECOVERED FROM LAYER IV. SCALE BARS ARE IN 1-CM INCREMENTS.

Layer III-B Pottery

Based on 1684 recovered pottery fragments, Layer III-B showed the rising popularity of narrow straight-sided cups (Figure 88) and thick flat-based pans (Figure 89), while the older forms of small red-slipped bowls strongly declined. Among those lingering traditions of small red-slipped bowls, the most popular in Layer III-B was the form with slightly incurved rim, while the other variants were greatly diminished or else entirely vanished from the assemblage. Meanwhile, non-slipped options were seen in some of the cups and pans, although most of those categories still were made with red-slipped surfaces.

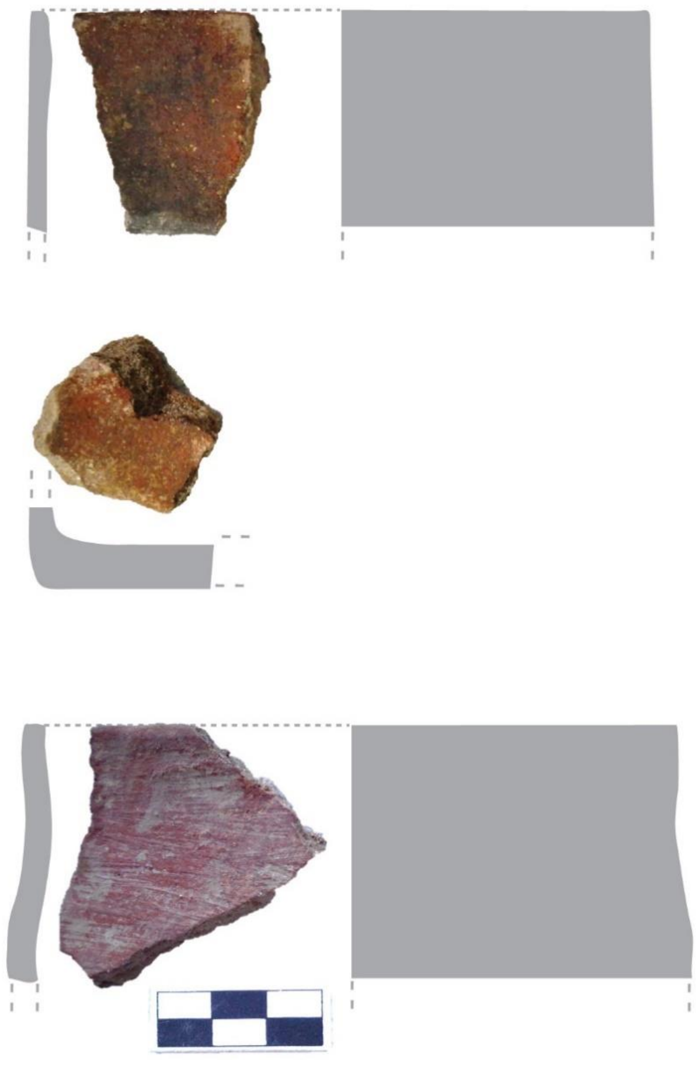

FIGURE 88. VARIATIONS OF NARROW CUPS, RECOVERED FROM LAYER III-B. SCALE BARS ARE IN 1-CM INCREMENTS.

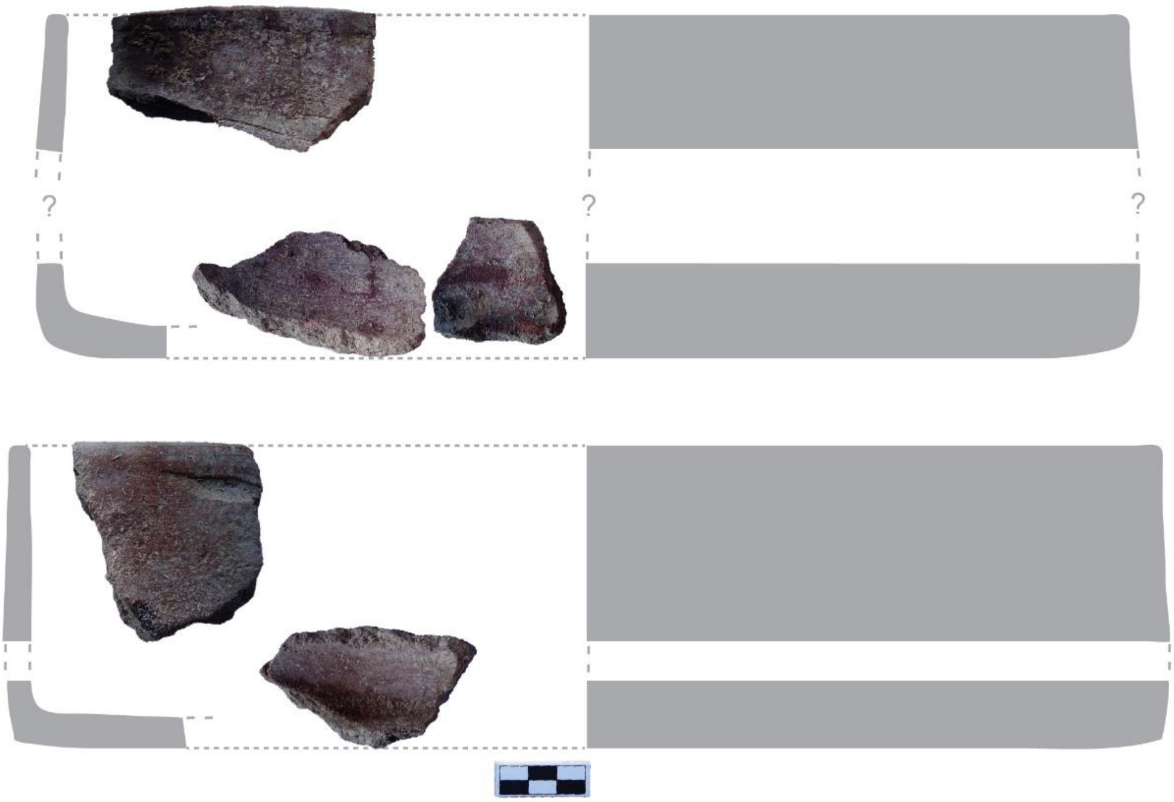

FIGURE 89. VARIATIONS OF THICK-WALLED, FLAT-BOTTOMED PANS, RECOVERED FROM LAYER III-B. SCALE BARS ARE IN 1-CM INCREMENTS.

Roughened exterior surfaces became more popular, especially in the narrow cup pieces. The roughened texture was made by rubbing or brushing generally in horizontal motions around the pottery exteriors. The same procedure was applied to some of red-slipped large bowls appearing in Layer III-B, for instance in one piece with a circle-stamped lip (Figure 90).

Within Layer III-B, the forms of rare decorations changed into simpler expressions of bold-line circles along the upward-facing lips of varied bowls, seen in the aforementioned red-slipped piece (see Figure 90) plus another four occurrences (Figure 91). Without the prior options of upper surfaces of carinated or shouldered vessels, the most visible portions for decorations were only in the upward-facing lips. If white lime infilling still was used, then it was not preserved in the surviving pieces.

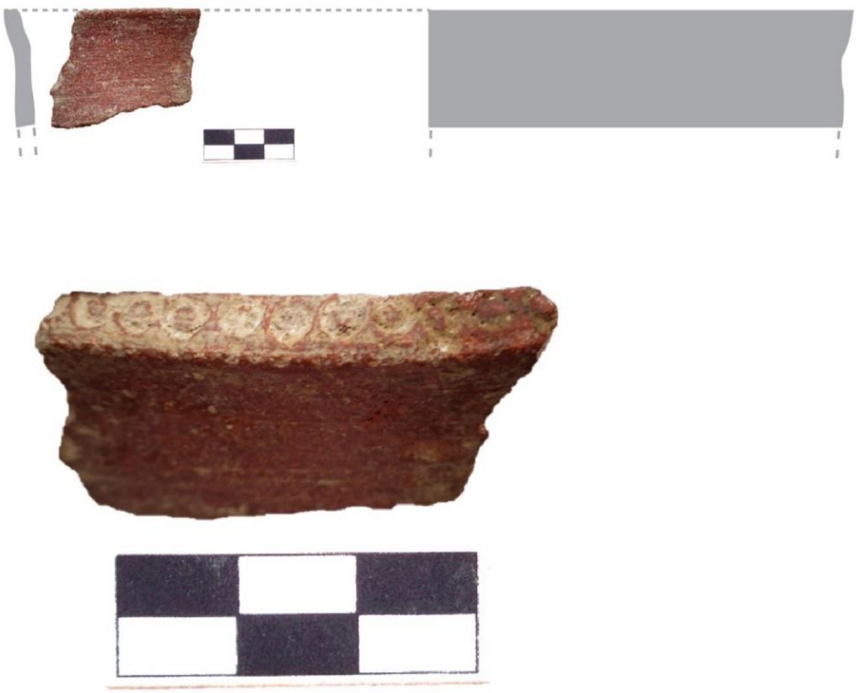

FIGURE 90. EXAMPLE OF SURFACE-ROUGHENED RED-SLIPPED LARGE BOWL FRAGMENT, WITH CIRCLE-STAMPED LIP, RECOVERED FROM LAYER III-B. SCALE BARS ARE IN 1-CM INCREMENTS.

FIGURE 91. VARIATIONS OF CIRCLE-STAMPED LIP PIECES, RECOVERED FROM LAYER III-B. SCALE BARS ARE IN 1-CM INCREMENTS.

Layer III-A Pottery

A total of 1385 pottery fragments from Layer III-A mostly showed a continuation of the same traditions from Layer III-B, with three new developments. First, the straight-sided cups (Figure 92) and the thick flat-based pans (Figure 93) continued as the most popular traditions, now made mostly with non-slipped surfaces and only rarely with red slip. Second, the older traditions of small red-slipped bowls with outcurved rims had vanished entirely, and only the variant of larger and slightly incurved red-slipped bowl had continued in very low frequency (Figure 94). Third, a form of thick-walled, non-slipped, incurved bowl made its first appearance (Figure 95) prior to its greater popularity that would develop later.

Decorated pottery pieces from Layer III-A included seven rim fragments, all showing designs on their upward-facing lip portions (Figure 96). One rim was adorned with two parallel rows of stamped circles, and another showed a row of half-circle impressions. Others displayed rows of repeated incisions or impressions, in three different patterns, including simple straight lines and curved designs.

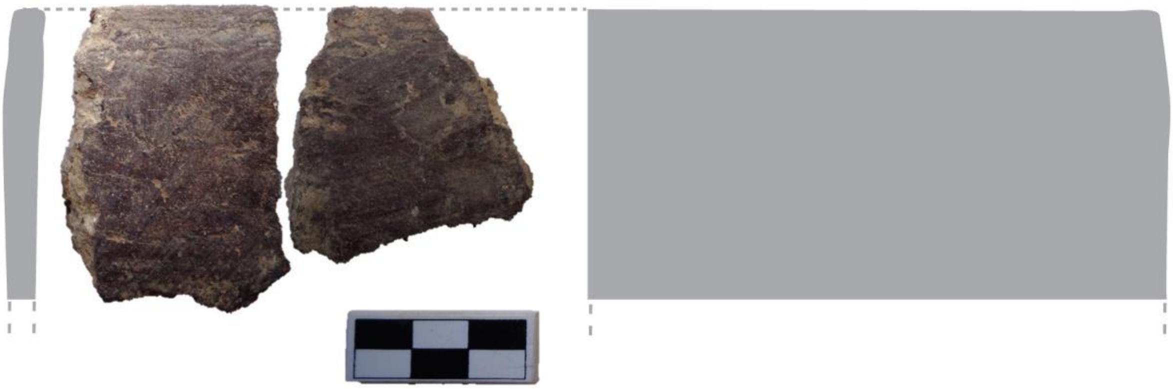

FIGURE 92. RIM FRAGMENTS OF NARROW STRAIGHT-SIDED CUP, RECOVERED FROM LAYER III-A. SCALE BARS ARE IN 1-CM INCREMENTS.

FIGURE 93. CONJOINED RIM AND BASE FRAGMENTS OF A SHALLOW FLAT-BOTTOMED PAN, RECOVERED FROM LAYER III-A. SCALE BARS ARE IN 1-CM INCREMENTS.

FIGURE 94. RIM OF RED-SLIPPED SLIGHTLY INCURVED BOWL, RECOVERED FROM LAYER III-A. SCALE BARS ARE IN 1-CM INCREMENTS.

FIGURE 95. RIM OF THICK-WALLED, NON-SLIPPED, SLIGHTLY INCURVED BOWL, RECOVERED FROM LAYER III-A. SCALE BARS ARE IN 1-CM INCREMENTS.

FIGURE 96. DECORATED LIP PIECES, RECOVERED FROM LAYER III-A. SCALE BARS ARE IN 1-CM INCREMENTS.

Layer II Pottery

Layer II yielded only 783 potsherds, likely due to the nature of the mostly windblown sandy matrix of Layer II containing overall low density of artifacts and midden. Red-slipped varieties and outcurved bowl shapes both had completely disappeared by this time, instead replaced entirely by non-slipped and either straight-sided or incurved vessels. Decoration was absent among the available 783 fragments.

The recovered potsherds included some belonging to categories that were most popular prior to A.D. 500, namely straight-sided cups and thick flat-bottomed pans (Figures 97 and 98). Meanwhile, other potsherds reflected categories that were most popular after A.D. 1000, belonging to thick-walled bowls with incurving rim profiles (Figure 99). All of these categories overlapped in lower frequencies around A.D. 500–1000 (Carson 2016).

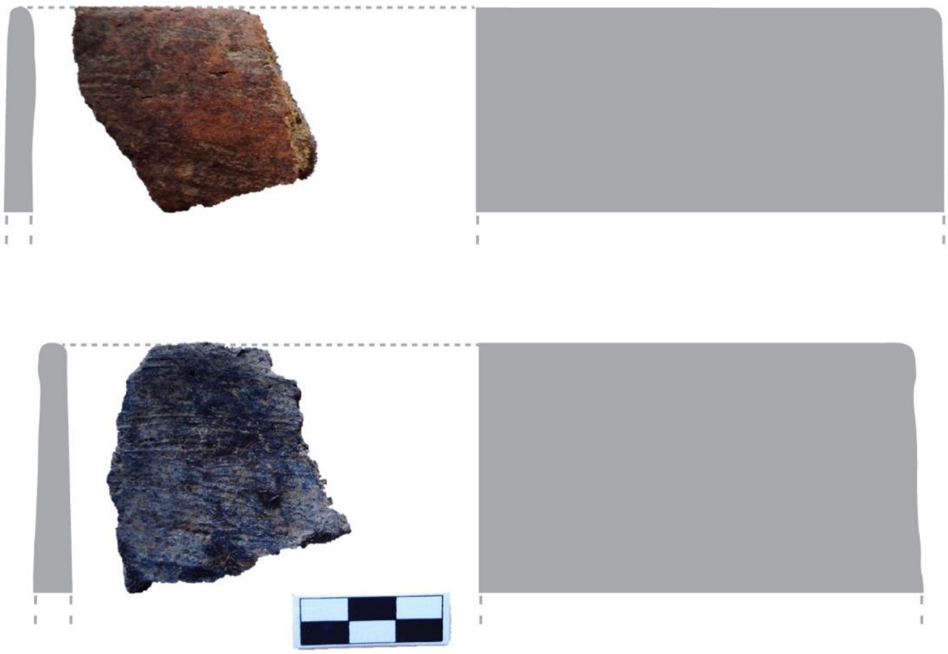

FIGURE 97. RIMS FROM STRAIGHT-SIDED CUPS, RECOVERED FROM LAYER II. SCALE BARS ARE IN 1-CM INCREMENTS.

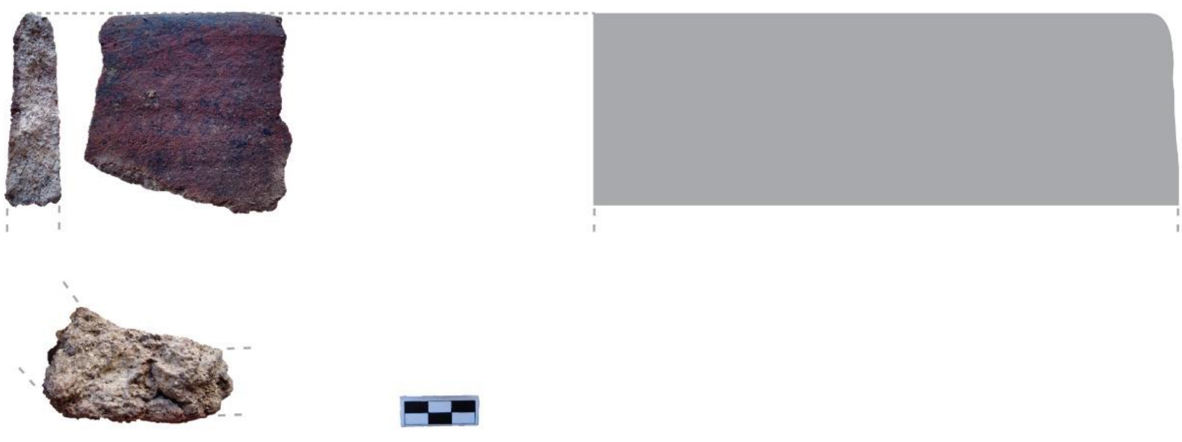

FIGURE 98. EXAMPLES OF RIM AND BASE FRAGMENTS OF TWO DIFFERENT PANS, RECOVERED FROM LAYER II. SCALE BARS ARE IN 1-CM INCREMENTS.

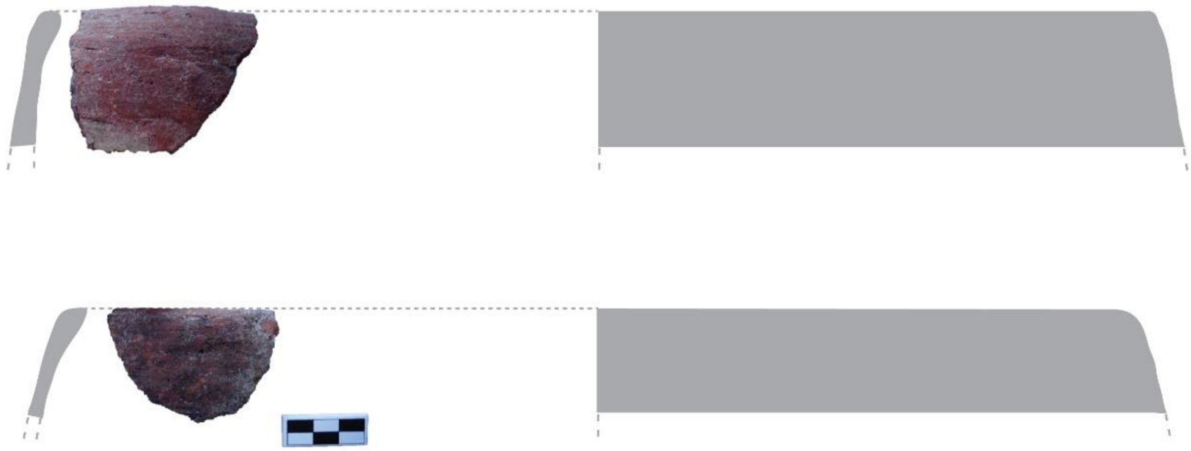

FIGURE 99. THICK INCURVING RIMS PIECES, RECOVERED FROM LAYER II. SCALE BARS ARE IN 1-CM INCREMENTS.

Layer I Pottery

Layer I revealed two major forms of pottery in 2998 fragments. One form was an incurved bowl, with thick walls and even thicker rims (Figure 100). The other form was a straight-sided to slightly incurved bowl (Figure 101). All pieces were made of coarse clay paste with medium to large temper inclusions, and none of the surfaces were slipped.

Decorations were rare, seen in two finger-impressed rims and three simply incised or impressed rims (Figure 102). These decorations all were on the upward-facing lip portions. One incised rim was broken from a thickened-rim bowl. The other decorated rims were broken from varieties of slightly incurved bowls without definite thickened-rim profiles.

The thickened-rim pottery was typical of the *latte* period in the Marianas, but the traditions seen at Bapot and generally in Saipan can be distinguished from the more abundantly documented cases in Guam. In Guam and Rota, coarse vertical combing was popular on the exteriors of most of the thickened-rim pottery, but it was overall less common in Saipan and entirely absent from the 2016 excavation findings at Bapot. Likewise, the thickened-rim characteristic was much less pronounced overall in the Bapot assemblage as generally seen in Saipan, as compared to the massively thickened rims seen most commonly in Guam.

One rim piece from Layer I was exceptionally thickened (Figure 103), and indeed this radical thickening was quite rare overall in the Mariana Islands. The thickened rim in this case protruded both inward and outward from the lip, while the rim profile itself was incurving for a constricted top of a large bowl. This particular form of rim most likely facilitated a specific function not possible with the more common shapes seen generally in the Layer I assemblage.

One unusual pottery fragment had been broken from an angled corner (Figure 104). The original shape of the associated pottery construction has not been ascertainable on the basis of this single piece. Other pieces from the Layer I assemblage have not shown the same composition of clay paste and temper inclusions, so this one piece has not yet been associated with other pieces potentially revealing more about the original product.

The pottery from Layer I was most typical of the period of *latte* structures in the Mariana Islands, dated as old as A.D. 1000 and continuing through A.D. 1700 (Carson 2012). The nearby surface-visible *latte* ruins at Bapot originally had been set into Layer I. Other findings within Layer I were typical of this same period, such as a fragment of a stone grinding basin, a broken slingstone, and a *Spondylus* sp. perforated disc that all will be described later in this report.

Layer I yielded two tiny fragments (less than 1 sq cm each) of high-fired porcelain that must have been imported ultimately from Asia but potentially passing through other places before reaching the Bapot Site in Saipan. Porcelain must have been fired in a kiln, and no kiln technology existed in the Marianas region prior to Spanish influence primarily after the late A.D. 1600s. Even then, porcelain mostly was imported from overseas, through the connections of the Spanish galleon trade. Elsewhere in the Mariana Islands, high-fired porcelain, stoneware, glass beads, and metal fragments have been found at several *latte* sites in contexts of the middle to late 1600s (Carson 2012).

FIGURE 100. VARIATIONS OF THICK INCURVING RIMS PIECES, RECOVERED FROM LAYER I. SCALE BARS ARE IN 1-CM INCREMENTS.

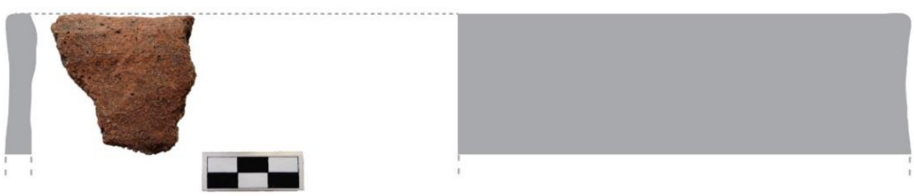

FIGURE 101. EXAMPLE OF THICK STRAIGHT-SIDED RIM, RECOVERED FROM LAYER I. SCALE BARS ARE IN 1-CM INCREMENTS.

FIGURE 102. DECORATED PORTIONS OF UPWARD-FACING LIPS OF RIM FRAGMENTS, RECOVERED FROM LAYER I. SCALE BARS ARE IN 1-CM INCREMENTS.

FIGURE 103. EXCEPTIONALLY THICKENED RIM PIECE, SHOWN IN FOUR VIEWS, RECOVERED FROM LAYER I. SCALE BARS ARE IN 1-CM INCREMENTS.

FIGURE 104. UNUSUAL CORNERED PIECE, RECOVERED FROM LAYER I. SCALE BARS ARE IN 1-CM INCREMENTS.

Chapter 8

New Findings: Non-Pottery Artefacts

The non-pottery artefacts of shell, stone, and shark tooth objects occurred in considerably lower numbers than the pottery fragments that supported a full chronological sequence. Their lesser numbers contributed to some ambiguities and occasional gaps in the chronological sequence at Bapot, as expected at any single site. Nevertheless, the 2016 excavation has generated enough material to compare with the findings known generally in the Mariana Islands.

The 2016 non-pottery findings included stone and shell adzes, stone flakes and raw materials, pounders, one grinding basin fragment, a slingstone fragment, polished balls, fishing gear, sea urchin spine abraders, assorted body ornaments, worked shell pieces, and a number of rare anomalies (see Figure 39). Each category will be presented here, following a chronological order to the extent possible. Some of the items have been identified as diagnostic of specific traditions and time periods, furthermore coordinated with a larger Marianas regional view (Carson 2016).

Adzes

Whole, partial, or in-process adzes were found in most but not all stratigraphic layers in the 2016 excavation, although adzes have been found throughout the chronological sequence in the Mariana Islands overall. Those from the Bapot 2016 excavation had been made of chert in Layers VI-B and VI-A, of *Tridacna* sp. shell in Layer III-B, of *Terebra* sp. shell in Layer III-A, and of both *Tridacna* sp. and *Conus* sp. shell in Layer I (Figure 105). Additionally, chert and volcanic stone flakes and fragments with polished surfaces may have been broken from adzes or other polished tools, considered separately here.

The chert adze materials (Figures 106, 107, and 108) included one polished adze in Layer VI-B, plus another smaller polished adze, a tip fragment, and a pre-form in Layer VI-A. The finished polished products showed roughly rectangular section views, although their overall forms were slightly rounded. The smaller of the two adzes was more rounded than the larger adze. The back ends, near the positions of hafting, were made square for the larger piece and rounded for the smaller piece. The even larger pre-form or "blank" had been prepared for a quadrangular adze, thus hinting at the possibility of initial production of quadrangular chert adzes, followed by variations of quadrangular or rounded shapes during continual stages of reduced-size maintenance and re-working throughout the use-life of the chert adzes overall.

The *Tridacna* sp. giant clam shell adze materials (Figures 109 and 110) included two fragments (one each in Layers III-B and I), plus two pre-form pieces in process of manufacture (again, one each in Layers III-B and I). Several different shapes and sizes have been described in all time periods throughout the Mariana Islands, but those seen in the 2016 excavation at Bapot resembled straight-sided adzes. They showed variable degree of curvature longitudinally, likely useful for specific modes of wood-chopping or other actions.

The *Terebra* sp. and *Conus* sp. shell adzes included one specimen each (Figure 111). Like its counterparts known at other sites, the *Terebra* sp. shell adze may have been used as a gouge or chisel, not necessarily as an adze. Its discovery from Layer III-A indicated an older age than so far has been seen for *Terebra* sp. shell adzes in the Marianas. The *Conus* sp. shell adze in Layer I was recognised as somewhat rare in the Marianas region, although one other had been recovered from the 2005 excavation at Bapot, also in a later-aged context associated with the *latte* period after A.D. 1000.

The 2016 findings accorded with the Marianas regional sequence overall, wherein chert adzes were most popular prior to 1100 B.C. and declined rapidly thereafter, while the hard shells of *Tridacna* sp. giant clams had been produced in steadily greater frequency through time. Adzes of *Terebra* sp. and *Conus* sp.

shells have been rare overall, mostly confined to the *latte* period post-A.D. 1000 with the best representation in the archaeological record. So far only a single adze of *Cassis cornuta* shell has been found in the Mariana Islands and in a context of 1500–1100 B.C. at House of Taga in Tinian (Carson 2016), whereas *Cassis cornuta* adzes have been found throughout much of Micronesia and parts of Indonesia in contexts post-pasting A.D. 100. Volcanic stone adzes have been confirmed throughout the Marianas regional sequence, although they were not represented at the Bapot Site except possibly through flaked debris and fragments.

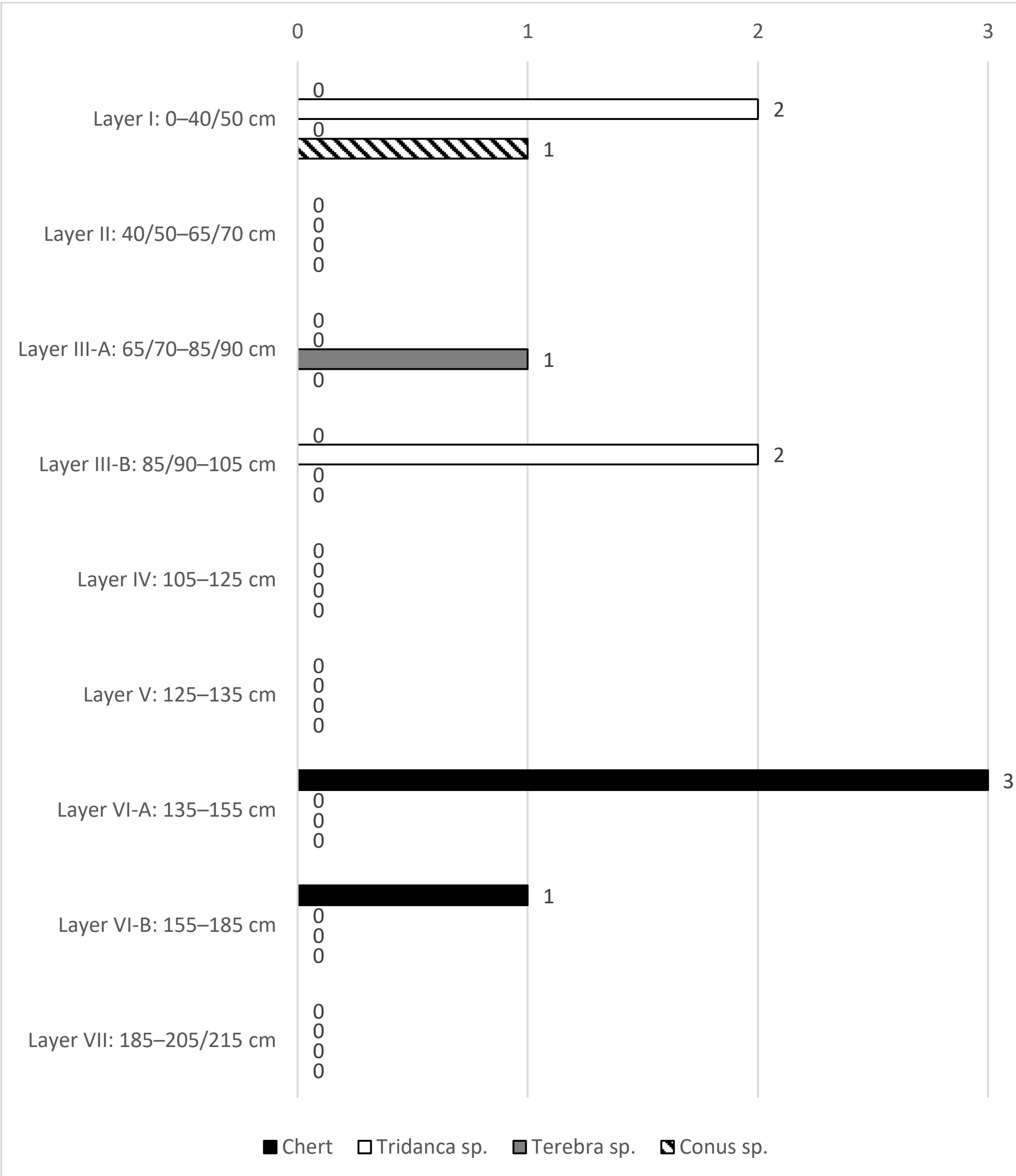

FIGURE 105. STRATIGRAPHIC DISTRIBUTION OF ADZES (WHOLE, PARTIAL, AND PRE-FORM VARIETIES) OF DIFFERENT MATERIAL CATEGORIES.

FIGURE 106. POLISHED CHERT ADZES FROM LAYER VI-B (UPPER LEFT) AND LAYER VI-B (LOWER RIGHT), SHOWN IN TWO VIEWS. SCALE BARS ARE IN 1-CM INCREMENTS.

FIGURE 107. BROKEN TIP OF POLISHED CHERT ADZE OR CHISEL, SHOWN IN THREE VIEWS, RECOVERED FROM LAYER VI-A. SCALE BARS ARE IN 1-CM INCREMENTS.

FIGURE 108. CHERT ADZE PRE-FORM, RECOVERED FROM LAYER VI-A. SCALE BARS ARE IN 1-CM INCREMENTS.

FIGURE 109. *TRIDACNA* SP. ADZE FRAGMENT (UPPER ROW, TWO VIEWS) AND PRE-FORM (LOWER ROW, TWO VIEWS), RECOVERED FROM LAYER III-B. SCALE BARS ARE IN 1-CM INCREMENTS.

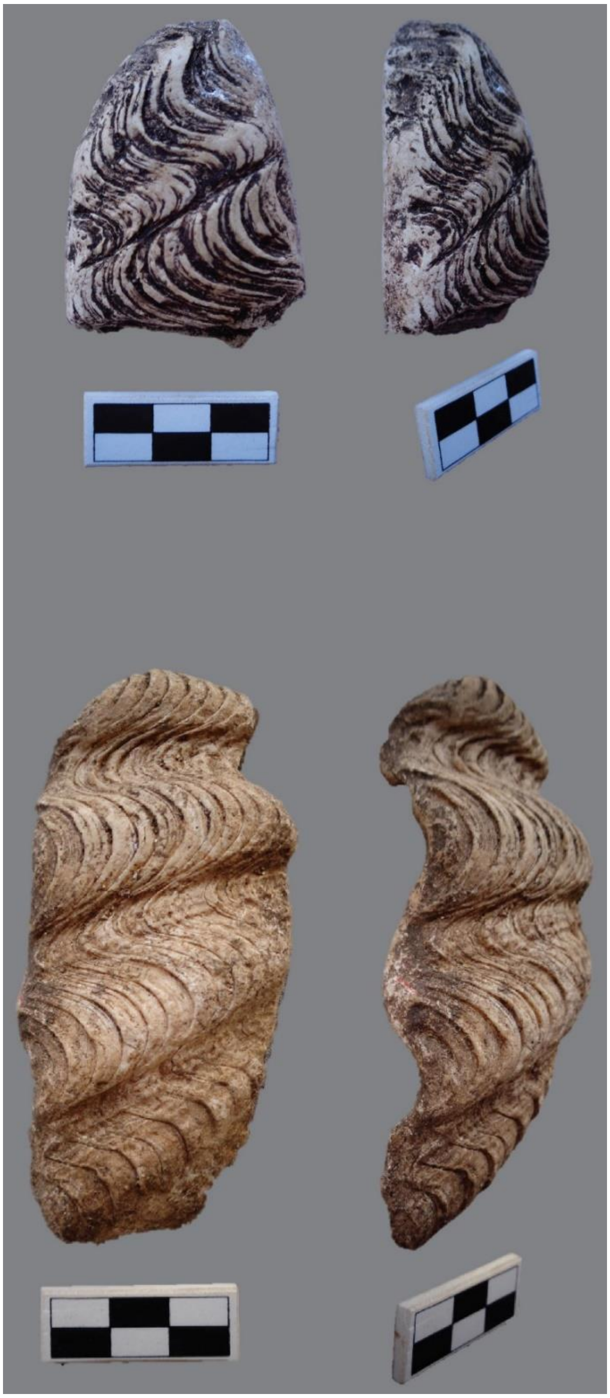

FIGURE 110. *TRIDACNA* SP. ADZE FRAGMENT (UPPER ROW, TWO VIEWS) AND PRE-FORM (LOWER ROW, TWO VIEWS), RECOVERED FROM LAYER III-B. SCALE BARS ARE IN 1-CM INCREMENTS.

FIGURE 111. *TEREBRA* SP. SHELL ADZE OR CHISEL (UPPER ROW, TWO VIEWS) FROM LAYER III-A AND BROKEN *CONUS* SP. SHELL ADZE (LOWER ROW, TWO VIEWS) FROM LAYER I. SCALE BARS ARE IN 1-CM INCREMENTS.

Stone Flakes, Fragments, and Raw Materials

Stone flakes and raw materials consisted of pieces of chert, volcanic stone, limestone, and limestone crystal (Figure 112). The flaked material included removed debitage, flaking cores, some flakes with use-wear edges, and other flakes with polished surfaces evidently removed from older finished tools. A category of "raw material" was assigned for pieces of limestone crystal that could not have entered into the sedimentary matrix naturally, although they did not disclose clear signs of flaking or other modification.

The characteristics of the raw materials facilitated production of different categories of tools. For instance, chert and volcanic stone could be polished into adzes or other tools, retaining sharp edges, but they also could be fashioned into other non-polished flake tools for general-utility cutting, slicing, or scraping. By comparison, pieces of limestone or of limestone crystal were less than ideal for polishing or for creating resilient sharp edges.

Chert flakes were found in fluctuating numbers through the stratigraphic sequence, but a coarse-scale trend depicted decline in popularity through time, corroborating the apparent restriction of chert adzes within the older layers (Figure 113). In particular, Layer VI-B contained a peak occurrence of 74 chert flakes, plus two flakes retaining polish and most likely related to adze usage or maintenance. In the later-aged layers, no formal chert adze artefacts were identified, yet the flakes may have related to any of a broad range of tools (Figure 114). Layer VII disclosed only three flakes. Layer VI-B yielded 74 flakes and two flakes with polish. Layer VI-A contained 18 flakes. Layer V generated 26 flakes. Layer IV produced 14 flakes. Layer III-B provided two flakes. Layer III-A showed four flakes. Layer II offered a single flake. Layer I contained two flakes.

Overall small numbers of volcanic stone flakes and fragments of flaked tools were found inconsistently through the stratigraphic sequence, in total comprising 20 pieces. Flakes with polish hinted at the usage or maintenance of adzes or similar tools in Layers IV and I, while overall the flakes may have been associated with a broad potential range of cutting or slicing activities (Figure 115). Layer VI-B showed three flakes. Layer VI-A revealed three flakes. Layer IV disclosed one flake with polish. Layer III-A contained one flake. Layer II yielded three flakes. Layer I five flakes and one flake with polish.

Limestone flakes were rare (Figure 116), comprised of just three examples, perhaps due to their lesser technical qualities when compared to chert, volcanic stone, and hard shell in terms of predictable and controllable flaking, sharpness retention, and other attributes. The limestone flakes included two from Layer VI-B, plus one from Layer III-B. Their original purposes have not yet been clarified.

Pieces of limestone crystal appeared only in Layers VI-B through IV (Figure 117). They may have been obtained from the re-crystallised content of the Layer VIII limestone or similar formation, or they may have been obtained from a cave interior, in any case not occurring naturally within their associated sedimentary layers at the site. They included two pieces from Layer VI-B, 10 pieces from Layer VI-A, one piece from Layer V, and one piece from Layer IV.

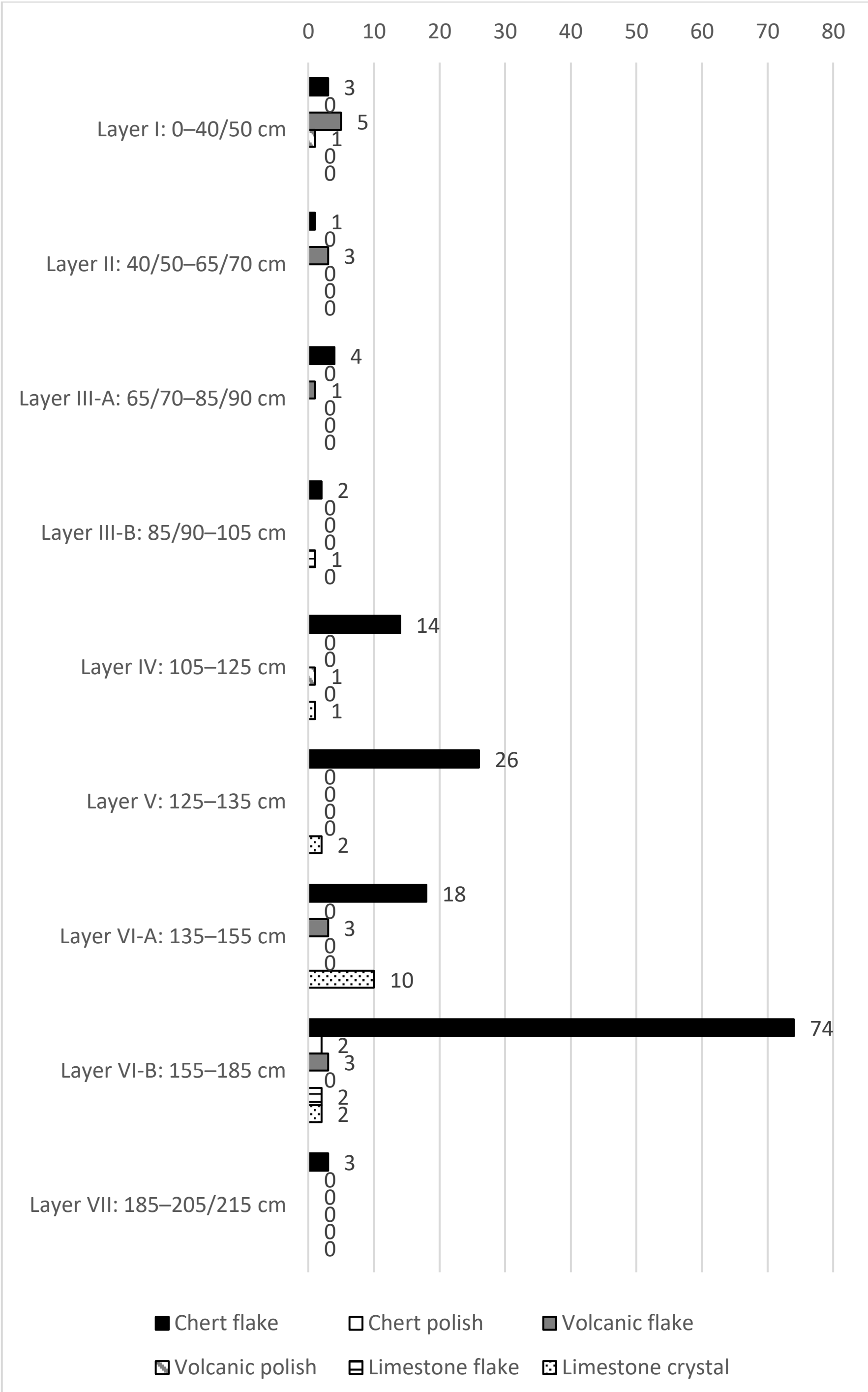

FIGURE 112. STRATIGRAPHIC DISTRIBUTION OF STONE FLAKES AND RAW MATERIALS, SHOWN IN VALUES OF RAW COUNTS PER STRATIGRAPHIC LAYER.

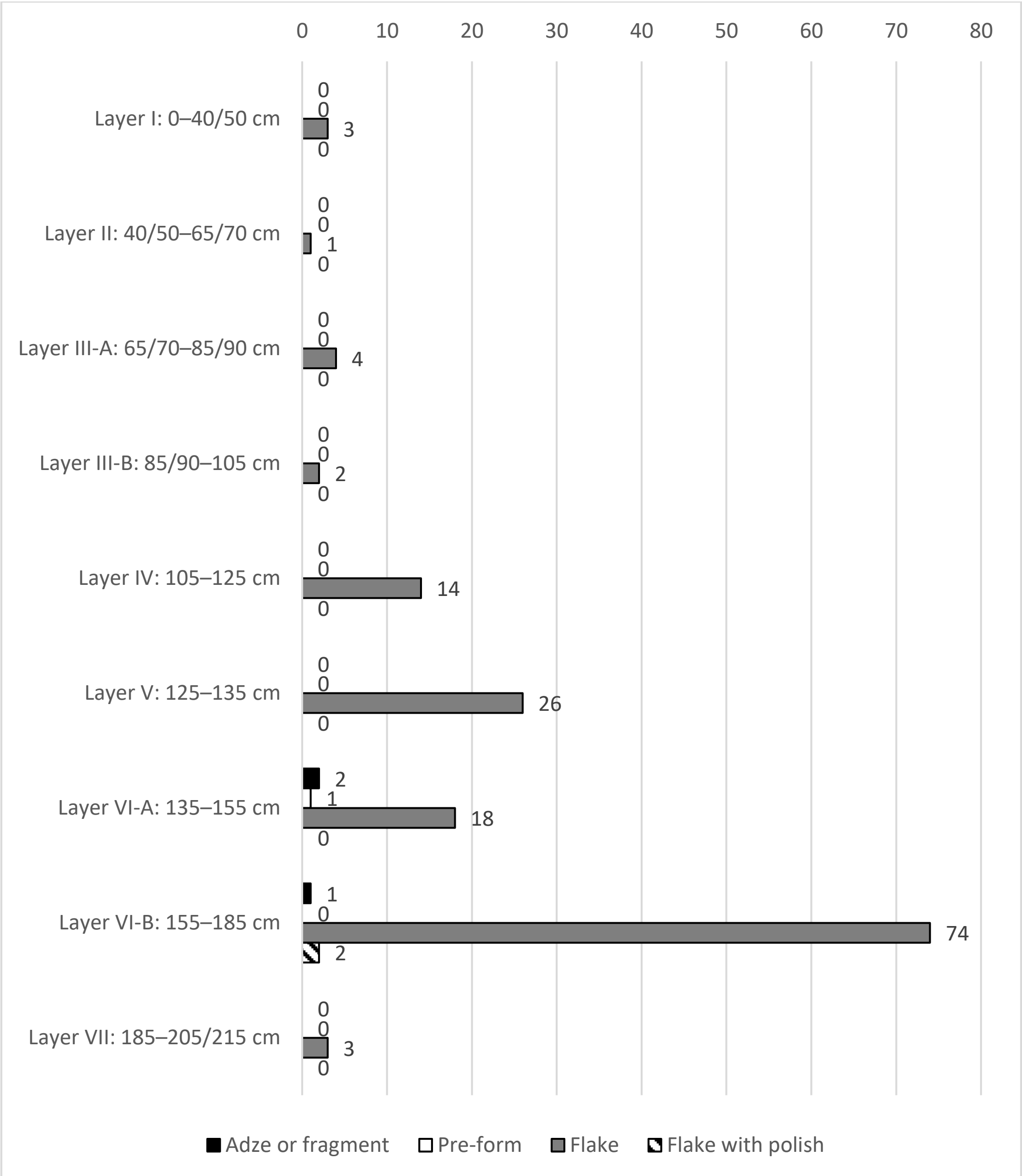

FIGURE 113. STRATIGRAPHIC DISTRIBUTION OF CHERT FLAKES, FLAKES WITH POLISH, AND ADZE-RELATED MATERIALS, SHOWN IN VALUES OF RAW COUNTS PER STRATIGRAPHIC LAYER.

FIGURE 114. EXAMPLES OF CHERT FLAKES. ITEMS ARE FROM LAYER VII (BOTTOM ROW), LAYER VI-B (TWO MIDDLE ROWS), AND LAYER VI-A (UPPER ROW). EXAMPLE OF CHERT FLAKE WITH POLISH IS IN LEFT SIDE OF SECOND ROW FROM THE TOP. SCALE BARS ARE IN 1-CM INCREMENTS.

FIGURE 115. EXAMPLES OF VOLCANIC STONE FLAKES. ITEMS ARE FROM LAYER VI –B (BOTTOM ROW), LAYER VI-A (LOWER MIDDLE ROW), LAYER IV (UPPER MIDDLE ROW), AND LAYER I (UPPER ROW). EXAMPLES OF FLAKES WITH TRACES OF POLISH ARE IN THE UPPER LEFT ROW AND THE SECOND ROW FROM THE TOP. SCALE BARS ARE IN 1-CM INCREMENTS.

FIGURE 116. EXAMPLES OF LIMESTONE FLAKES. ITEMS ARE FROM LAYER VII-B (LOWER) AND LAYER III-B (UPPER), SHOWING TWO DIFFERENT LIMESTONE COMPOSITIONS. SCALE BARS ARE IN 1-CM INCREMENTS.

FIGURE 117. EXAMPLES OF LIMESTONE CRYSTAL RAW MATERIALS, RECOVERED FROM LAYER VI-A. SCALE BARS ARE IN 1-CM INCREMENTS.

Pounders and Grinding Basins

Pieces of ground and pecked stone related to one grinding basin fragment (Figure 118) and five pounders (Figures 119, 120, and 121). The pounder artefacts included one small but complete item from Layer VI-A, plus broken pieces of one from Layer VI-B, two from Layer IV, and one from Layer I. A single fragment of a grinding basin was found in Layer I, reminiscent of the broken grinding basin seen on the present-day ground surface near the *latte* ruins of the site (see Figure 6).

The pounders from Layers VI-B and VI-A were much smaller than the others, likely reflecting differential functions in the separated time periods. Also potentially related to a differential functional context, the pounder fragment from Layer I was the only item made of porous volcanic rock, with distinctive inclusion clasts, in contrast to all other items made of different compositions of limestone. More detailed research about the variation in pounders and grinding basins has not yet been possible, given the small numbers of pieces and discontinuous stratigraphic distribution.

Stone pounders and grinding basins have been found abundantly on the surfaces of latte sites throughout the Marianas, but they have been rare in excavated contexts. So far no grinding basins have been assigned securely to contexts pre-dating A.D. 1000, but pounders have been found in varying shapes and sizes in layers of different time periods at a few sites. The pounders generally were narrower in later periods, including limestone and volcanic stone varieties as known at *latte* sites.

The discoveries from Bapot now have added to the overall knowledge of stone pounders in the regional chronology. Stone pounders definitely were among the material inventory ever since the earliest cultural periods, pre-dating the confirmed appearance of stone grinding basins. Analysis of possible preserved microscopic residues may yet reveal more about their past functions.

FIGURE 118. FRAGMENT OF LIMESTONE GRINDING STONE, SHOWN IN TWO VIEWS, RECOVERED FROM LAYER I. SCALE BARS ARE IN 1-CM INCREMENTS.

FIGURE 119. LIMESTONE POUNDER FRAGMENT FROM LAYER VI-B (LOWER ROW) AND COMPLETE POUNDER FROM LAYER VI-A (UPPER ROW), SHOWN IN TWO VIEWS EACH. SCALE BARS ARE IN 1-CM INCREMENTS.

FIGURE 120. TWO LIMESTONE POUNDER FRAGMENTS, SHOWN IN TWO VIEWS PER ROW, RECOVERED FROM LAYER IV. SCALE BARS ARE IN 1-CM INCREMENTS.

FIGURE 121. VOLCANIC STONE POUNDER FRAGMENT, SHOWN IN TWO VIEWS, RECOVERED FROM LAYER I. SCALE BARS ARE IN 1-CM INCREMENTS.

Slingstone Fragment

A single slingstone fragment was recovered from Layer I (Figure 122). It had been made from limestone. So far, slingstones in the Mariana Islands have been found only at *latte* sites in contexts post-dating A.D. 1000.

Polished Balls

Two polished balls included one of probable *Tridacna* sp. shell from Layer VI-A and another of limestone from Layer III-A (Figure 123). They may have been used as burnishing stones, for example when finishing products of wooden bowls or pottery. The ball of limestone was only roughly polished or perhaps ground, whereas the ball of probable *Tridacna* sp. shell definitely was thoroughly polished.

FIGURE 122. FRAGMENT OF LIMESTONE SLINGSTONE, SHOWN IN TWO VIEWS, RECOVERED FROM LAYER I. SCALE BARS ARE IN 1-CM INCREMENTS.

FIGURE 123. BALL OF LIMESTONE FROM LAYER III-A (LEFT) AND ANOTHER OF POLISHED PROBABLE *TRIDACNA* SP. SHELL FROM LAYER VI-A (RIGHT). SCALE BARS ARE IN 1-CM INCREMENTS.

Fishing Gear

Artefacts of fishing gear overall have been rare in Marianas archaeological sites, although they have been reported now from every time period as expected in any coastal or island setting. The items from the 2016 excavation at Bapot included two different forms of net weight, one complete fishing hook, and six fragments of fishing hooks. Additionally, pieces of worked shells may have related to fishing hooks or to other objects, presented separately here.

The two net weights reflected different usage. From Layer VI-A, half of a bivalve of *Asaphis* sp. shell had been modified with a drilled hole (Figure 124), suitable for dropping into water with medium-weight sinking. From Feature B in Layer V, a limestone crystal had been ground into an oval shape and modified with a longitudinal groove (Figure 125), suitable for tossing into water and with directed sinking.

The shell fishing hook pieces all were J-shaped pieces (Figures 126 and 127). Layer VI-B offered one complete fishing hook, plus two fragments. Layer VI-A disclosed one broken piece. Layer V yielded a mostly complete fishing hook from the pit of Feature B. Layer II provided one thin piece, plus another notably thicker and larger fishing hook fragment.

FIGURE 124. BROKEN NET WEIGHT MADE OF *ASAPHIS* SP. SHELL, SHOWN IN TWO VIEWS, RECOVERED FROM LAYER VI-A. SCALE BARS ARE IN 1-CM INCREMENTS.

FIGURE 125. NET WEIGHT MADE OF LIMESTONE CRYSTAL, SHOWN IN THREE VIEWS, RECOVERED FROM FEATURE B IN LAYER V. SCALE BARS ARE IN 1-CM INCREMENTS.

FIGURE 126. NACREOUS SHELL FISHING HOOK PIECES, RECOVERED FROM LAYER VI-B. BOTTOM ROW SHOWS THREE VIEWS OF COMPLETE HOOK, STILL PARTIALLY ENCASED IN CEMENTED SAND. UPPER ROW SHOWS TWO DIFFERENT FRAGMENTS. SCALE BARS ARE IN 1-CM INCREMENTS.

FIGURE 127. NACREOUS SHELL FISHING HOOK PIECES, RECOVERED FROM LAYERS IV-A THROUGH II. BOTTOM RIGHT WAS FROM LAYER VI-A. BOTTOM LEFT WAS FROM FEATURE B IN LAYER V. UPPER ROW SHOWS TWO DIFFERENT PIECES FROM LAYER II. SCALE BARS ARE IN 1-CM INCREMENTS.

The fishing hooks all were made of nacreous shell material, suitable for attracting fish. Although the taxa cannot be identified from observing the artifacts lacking the diagnostic parts of the whole shells, the most likely nacreous taxa included bivalves of *Isognomon* sp. or *Pinctada* sp., as well as gastropods of *Turbo* spp. and perhaps *Haliotis* sp. shellfish. Worked pieces at the site mostly were not identifiable taxonomically, but a few could be classified as *Turbo* sp. and *Isognomon* sp. specimens. Pieces of *Isognomon* sp., *Turbo* spp., and *Haliotis* sp. remains were identified in different layers of midden. *Pinctada* sp. shells were not identified at all at the site, although they have been identified at other sites and specifically as artefacts.

The fishing hooks all reflected a preference for J-shaped and rotating hooks, instead of hard-angled jabbing hooks, V-shaped gorges, or other forms. The tops of the shanks displayed variable forms of notching for line attachments, potentially revealing different purposes, fishing strategies, or preferences of the fishers. The one complete hook has been retained inside its hardened-sand matrix, pending the possibility of residue analysis. The single thick-bodied hook from Layer II reflected most likely a specialised usage for capturing large fish, whereas all others where much thinner and more suitable for catching small to medium fish.

Sea Urchin Spine Abraders

Sea urchin spine abraders were identified by worn-down tips, typically worn at an angle through abrasion (Figures 128 and 129). They may have been used for filing or abrading slightly hard material, for example for the fine-scale work of finishing a fishing hook or similar item. They most likely were abraded against material approximately of the hardness of shell.

Although the stratigraphic distribution was inconsistent and in very few total numbers, the abraders arguably were more numerous in lower layers, where coincidentally non-artefact sea urchin pieces were more prevalent among the midden compositions. Layer VII yielded one abrader. Layer VI-B provided four abraders. Layer V offered two abraders, including one apiece from Features A and B. Layer I contained one abrader.

FIGURE 128. SEA URCHIN SPINE ABRADERS, RECOVERED FROM LOWER LAYERS. BOTTOM ROW WAS FROM LAYER VII. UPPER THREE ROWS WERE FROM LAYER VI-B. SCALE BARS ARE IN 1-CM INCREMENTS.

FIGURE 129. SEA URCHIN SPINE ABRADERS, RECOVERED FROM MIDDLE AND UPPER LAYERS. BOTTOM ROW WAS FROM FEATURE B OF LAYER V. MIDDLE ROW WAS FROM FEATURE A IN LAYER V. UPPER ROW WAS FROM LAYER I. SCALE BARS ARE IN 1-CM INCREMENTS.

Shell Discs

Shell discs were identified as circular pieces, usually made with a central perforation except when found as in-process discards or debitage. A disc was defined as having a broad surface around the central perforation, while the thickness in side-view was thinner than the width of the face. Additionally, the central perforation was roughly equal or narrower than the surrounding broad face of the disc.

For general reference, examples of different categories of shell ornaments have been compiled in Figure 130. This reference may assist in clarifying the characteristics of discs, bands, circlets, and other categories. The details of each category then can be treated individually.

Different forms of shell discs showed a definite chronological sequence, including one category found in Layers VII through VI-A (Figures 131 and 132), in contrast to another single item in Layer I (Figure 133). The older tradition was represented by whole finished discs and in-process pieces, including one item from Feature H of Layer VII, 10 from Layer VI-B, and eight from Layer VI-A. The younger tradition was represented only by one item in Layer I.

Those items from Layers VII through VI-A referred to *Conus* spp. shells with polished faces, yet they retained their original perimeter surfaces with preserved shape, texture, and colour. Different sub-categories may be discerned according to shell species, size, thickness, and display or textured versus smooth perimeter. Each shell first was sliced at the top, and then it was drilled through the centre. The drilling sometimes was aided by the naturally hollow interior of the shells, although typically the top portions had been sliced just above the entirely hollow portion, as seen in the in-process pieces.

The later-aged traditions included one disc, recovered from Layer I. This disc apparently had been reduced from a non-lustrous shell, possibly of *Spondylus* sp. shell. The taxonomic identification could not be confirmed, due to the reduction of the shell to its inner portion, no longer retaining any diagnostic parts.

The apparently older forms of shell discs resembled others that have been documented in ancient site layers at House of Taga in Tinian and at Ritidian in Guam (Carson 2016). At those other sites, the *Conus* spp. shell discs were most popular prior to 1100 B.C., and a few variants were found as extreme rarities through perhaps 700 B.C. Those other sites notably yielded wafer-thin varieties that were not seen at Bapot, along with the others as documented here.

The later-aged shell discs have tended to be less finely polished, sometimes rough around the edges, and they mostly were made by reducing a shell down to its interior portion as seen here in Layer I. The later-aged discs often were made of *Spondylus* sp. shells, but other taxa have been noted in variable frequency. Similarly, the later-aged shell beads tended to be much less polished than the older variants.

The discs of the older tradition were most similar to ethnographic and archaeological parallels known in Taiwan as elements of head dressing, shoulder straps, belts, and other accoutrements (Carson 2016). The oldest known archaeological examples in Taiwan have been dated about 1500 B.C., although older examples may yet be confirmed. The termination of this tradition in the Marianas has not yet been explained, but its original contexts of cultural usage may have been linked with the counterparts that have continued into modern times in Taiwan.

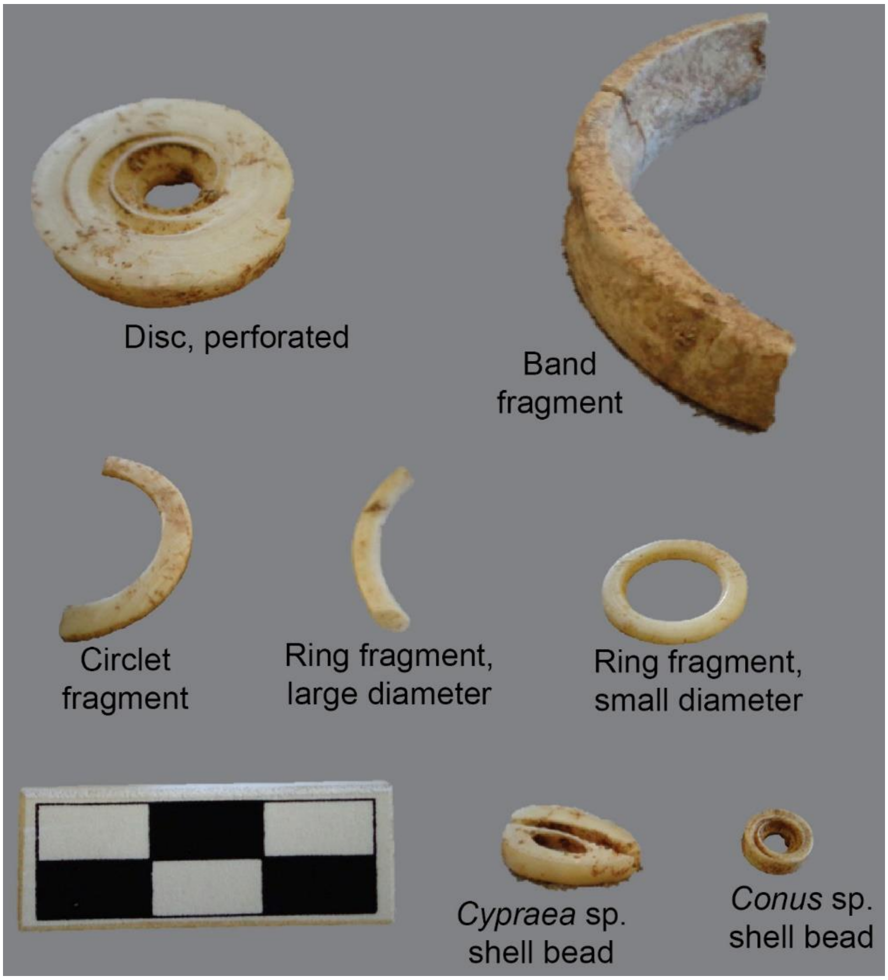

FIGURE 130. EXAMPLES OF DIFFERENT CATEGORIES OF SHELL ORNAMENTS, RECOVERED FROM 2016 EXCAVATION. SCALE BARS ARE IN 1-CM INCREMENTS.

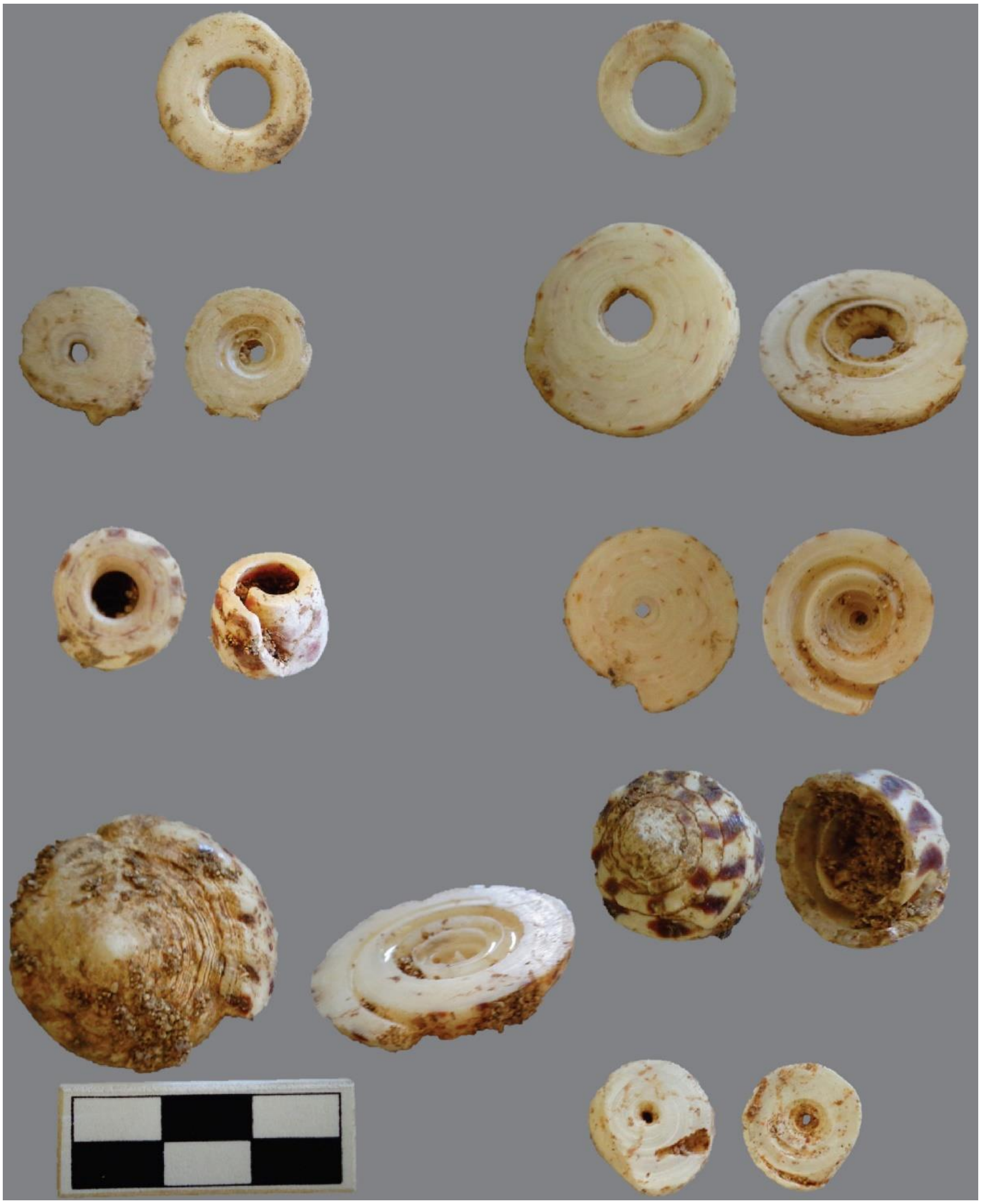

FIGURE 131. *CONUS* SPP. SHELL DISC PIECES FROM LAYERS VII AND VI-B. LOWER RIGHT ITEM WAS FROM FEATURE H IN LAYER VII, SHOWN IN TWO VIEWS. ALL OTHER ITEMS WERE FROM LAYER VI-B, SHOWN IN TWO VIEWS EACH. SCALE BARS ARE IN 1-CM INCREMENTS.

FIGURE 132. *CONUS* SPP. SHELL DISC PIECES FROM LAYER VI-A. ALL BUT UPPER LEFT ITEM ARE SHOWN IN TWO VIEWS EACH. SCALE BARS ARE IN 1-CM INCREMENTS.

FIGURE 133. *SPONDYLUS* SP. SHELL DISC, SHOWN IN TWO VIEWS, RECOVERED FROM LAYER I. SCALE BARS ARE IN 1-CM INCREMENTS.

Shell Bands

No complete shell bands were recovered, but nine fragments were identified as having been broken from circular or ring-shaped objects. In each case, the exterior presented a broad face notably thicker than the width of the shell (Figure 134). The curvatures indicated sizes of 8–18 cm in diameter, large enough to have been worn as bracelets in the smallest cases or perhaps as anklets or armlets in the largest cases. Other usage could have occurred as well. Their widths were variable, possibly indicative of sub-categories that have not yet been clarified with the limited numbers of pieces.

These fragments were found inconsistently in the site stratigraphy, including two pieces from Layer VI-B, one from Layer VI-A, three from Layer V, two from Layer IV, and one from Layer II. The observable width and thickness, along with projected diameter estimation, varied for each specimen. The older bands appeared to have been narrower or finer overall, but the small numbers so far have disallowed conclusive statements about chronological trends.

FIGURE 134. SHELL BAND FRAGMENTS. LOWER ROW, TWO ITEMS AT RIGHT WERE FROM LAYER VI-B. LOWER ROW, CENTER ITEM WAS FROM LAYER VI-A. LOWER ROW, TWO ITEMS AT LEFT WERE FROM LAYER V. UPPER ROW, ITEM AT RIGHT WAS FROM LAYER V. UPPER ROW, TWO ITEMS AT CENTER WERE FROM LAYER IV. UPPER ROW, ITEM AT LEFT WAS FROM LAYER II. SCALE BARS ARE IN 1-CM INCREMENTS.

Shell Circlets

Shell circlets were represented in three fragments, including one piece from Layer VII and two pieces from Layer VI-B (Figure 135). They were distinguished from bands due to their outer-facing exteriors that were narrower than the thickness of the shell "walls." The circlets had been cut from thick-bodied shells, most likely *Conus* spp. shells according to the retained portions. The "walls" were 5–10 mm wide, while the outer faces were 1–2 mm thick.

No complete circlets were discovered at this site, but the three identifiable fragments suggested diameters of 3–4 cm. Diameters at other sites were 3–6 cm, all so far discovered in pre-1100 B.C. contexts such as at House of Taga in Tinian and at Ritidian in Guam (Carson 2016). These items were too small to have been worn as bracelets. As seen with the older-period shell discs, parallels have been found in archaeological sites of eastern Taiwan dated at least as early as 1500 B.C., but specific cultural usage has not been clarified.

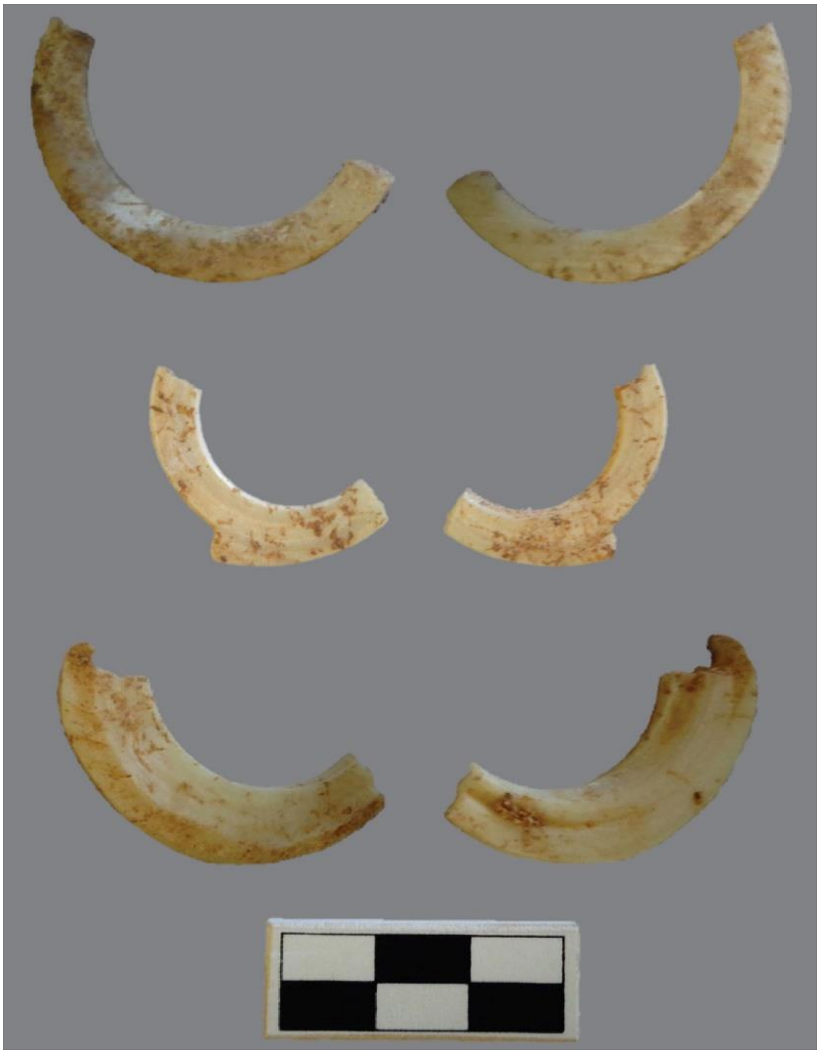

FIGURE 135. SHELL CIRCLET FRAGMENTS, EACH SHOWN IN TWO VIEWS. LOWER ROW, ITEM WAS FROM LAYER VII. MIDDLE AND UPPER ROWS, ITEMS WERE FROM LAYER VI-B. SCALE BARS ARE IN 1-CM INCREMENTS.

Shell Rings

Shell rings were identified as circular shapes, with "walls" that were equally tall and wide in section view, so far identified in two size categories. The larger category was made with walls of 3–5 mm thickness, surrounding hollow diameters of 6–8 cm, and the exterior faces often retained the original shell surfaces. The smaller category was made with walls of 2–4 mm thickness, surrounding hollow diameters of 1.2–1.4 cm, and their outer-facing perimeters had been reduced or polished down from the original shell surfaces. Smaller and thinner rings were considered separately as "beads."

All of the shell rings were found in the lowest and oldest cultural layers. The larger-diameter rings were represented only by fragments, including two from Layer VII and six from Layer VI-B (Figure 136). The smaller-diameter rings included one complete piece from Layer VII and two partial pieces from Layer VI-B (Figure 137). Their contexts accorded with dating in other sites consistently prior to 1100 B.C. at House of Taga in Tinian and at Ritidian in Guam (Carson 2016).

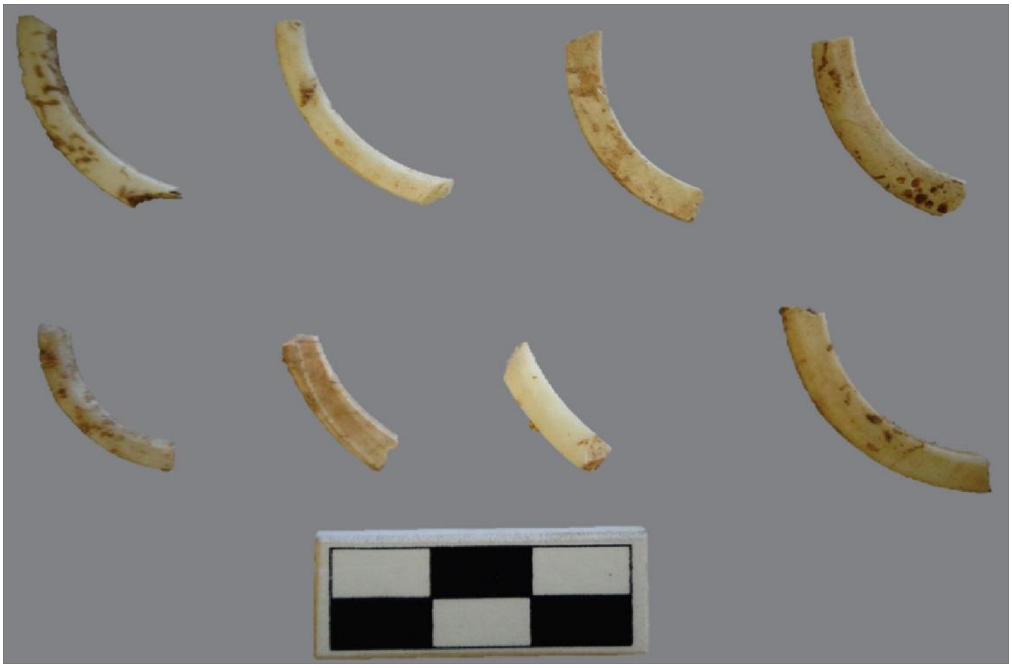

FIGURE 136. LARGER-DIAMETER SHELL RING FRAGMENTS. TWO ITEMS IN LOWER RIGHT WERE FROM LAYER VII. ALL OTHER ITEMS WERE FROM LAYER VI-B. SCALE BARS ARE IN 1-CM INCREMENTS.

FIGURE 137. SMALLER-DIAMETER SHELL RINGS. COMPLETE ITEM AT LEFT WAS FROM LAYER VII. TWO FRAGMENTS AT MIDDLE AND RIGHT WERE FROM LAYER VI-B. SCALE BARS ARE IN 1-CM INCREMENTS.

***Cypraea* sp. Shell Beads**

Cypraea sp. shell beads had been made from shells of 12–15 mm length, possibly of *Cypraea moneta* according to their size. Three in-process beads and one in-process but broken bead showed that the shells first had been sliced longitudinally on one side, then on the opposite side. The work perhaps involved a combination of slicing and follow-up polishing.

The 2016 excavation recovered three in-process beads, one in-process but broken bead, three complete and intact finished beads, and four broken pieces (Figure 138). Layer VI-B yielded three in-process beads and one in-process but broken bead. Layer VI-A disclosed three complete and four broken beads.

This distinctive form of bead has been found only very rarely at other sites, most clearly dated prior to 1100 B.C. at both House of Taga in Tinian and at Ritidian in Guam (Carson 2016), congruent with the association in Layers VI-B and VI-A at Bapot. Their original cultural usage has not been ascertained, and so far they have not been identified in any archaeological site outside the Mariana Islands. The closest tentative parallels have been ethnohistorical examples of similar but clearly not identical items sewn into vests in Taiwan or into rattan shields in Indonesia, still needing further study and more cross-regional searching.

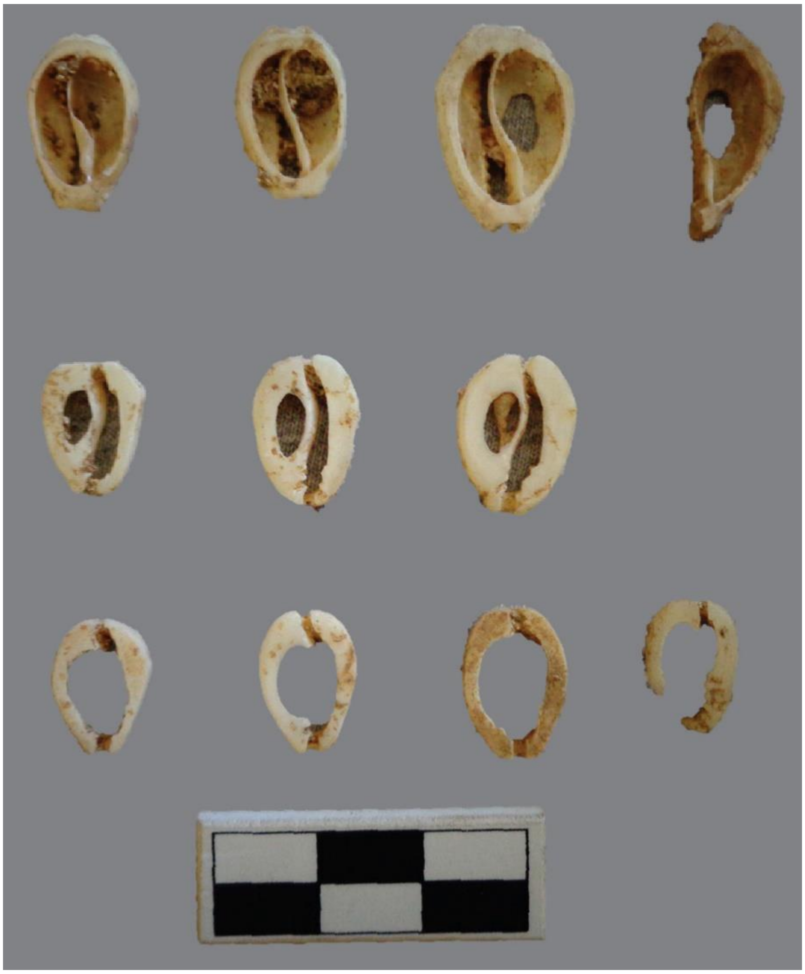

FIGURE 138. *CYPRAEA* SP. SHELL BEAD PIECES. BROKEN ITEMS IN LOWER ROW WERE FROM LAYER VI-A. COMPLETE ITEMS IN MIDDLE ROW WERE FROM LAYER VI-A. IN-PROCESS ITEMS IN UPPER ROW WERE FROM LAYER VI-B. SCALE BARS ARE IN 1-CM INCREMENTS.

Conus spp. and Other Small Round Shell Beads

Conus spp. and other small round shell beads consistently were less than 1 cm diameter, less than 3 mm thick, and with "walls" of 1.5 mm or less. In-process beads showed that they were made first by cutting the top sections of *Conus* spp. shells, then cutting the remaining side with the result of a thin "slice" that next could be polished. The final stage of polishing was not always needed if the initial stages of slicing had been sufficient to produce smooth and glossy surfaces. In some cases, the shells may have been taxa other than *Conus* spp. and not yet identifiable. The exterior outward-facing perimeters sometimes had been polished, but they often displayed the original shell surfaces. If beads were not fully cut or polished, then they were considered as "in process," with an understanding that some may in fact have been used without the complete finishing.

The small round beads and in-process beads all were found continuously from Layer VII through Layer III-B, mostly in the lower and older layers. Layer VII produced 26 beads and five in-process beads, including two of those finished beads within Feature G (Figures 139 and 140). Layer VI-B yielded 49 beads and seven in-process beads, including two of those finished beads within Feature D (Figures 141 and 142). Layer VI-A provided 27 beads and one in-process bead (Figures 143 and 144). Layer V offered 18 beads, including eight within Feature A and another two within Feature B (Figure 145). Layer IV disclosed 16 beads (Figure 146). Layer III-B contained four beads (Figure 147).

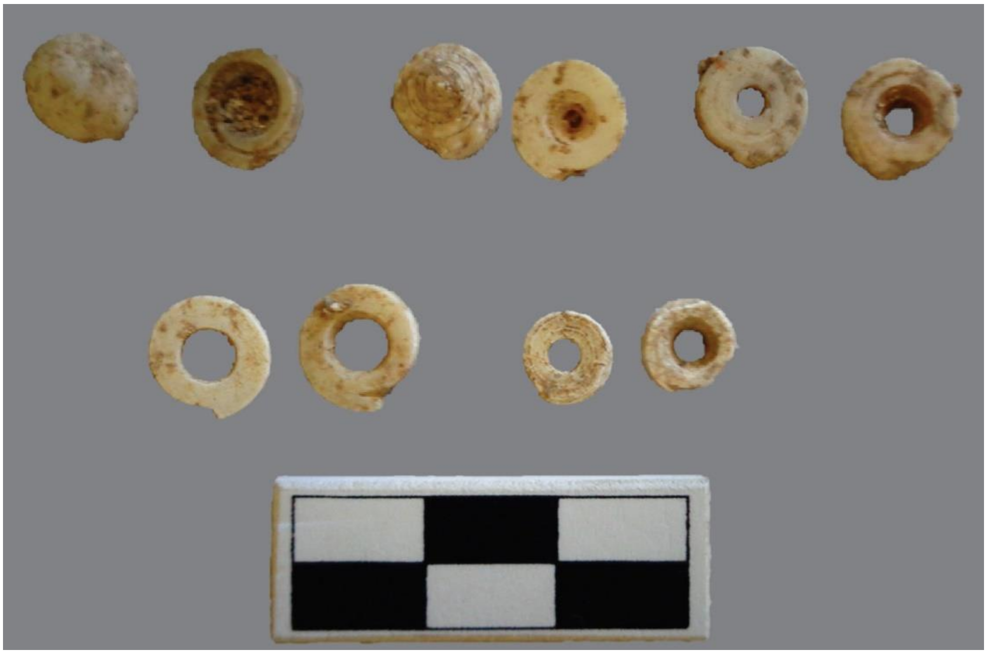

FIGURE 139. *CONUS* SPP. SHELL BEADS IN PROCESS, SHOWN IN TWO VIEWS EACH, RECOVERED FROM LAYER VII. SCALE BARS ARE IN 1-CM INCREMENTS.

The overall stratigraphic distribution of these beads at Bapot accorded with the Marianas regional chronology. Generally in the Mariana Islands, these forms of sliced small beads were most popular prior to 1100 B.C., and then they continued in much lower frequency through 500 B.C. and eventually were non-existent by A.D. 100 (Carson 2016). In later-period contexts, shell beads were larger, thicker, and less polished.

The closest ethnographic and archaeological parallels of these small beads have been seen in Taiwan, documented historically but also found in contexts dated at least as old as 1500 B.C. The examples in Taiwan have been manufactured mostly from *Tridacna* sp. shells and less commonly from *Conus* spp. shells. In contrast, the small beads at Bapot and other sites of the Mariana Islands were made often of *Conus* spp. shells, and other possible shell taxa have not yet been verified in the archaeological collections.

According to the ethnographic parallels in Taiwan, these small beads were used in great abundance in costumes, in some cases reserved for ceremonial regalia. The specific usage has been documented primarily as sewn into robes, skirts, leg coverings, and other dressing or accessories, all requiring several dozens of beads (Carson 2016). Less common instances were strung into necklaces, requiring fewer numbers of beads, and they were not associated with the same cultural contexts and potential ceremonies as implied with the other costuming.

FIGURE 140. *CONUS* SPP. AND POSSIBLY OTHER TAXA OF SHELL BEADS, RECOVERED FROM LAYER VII. SCALE BARS ARE IN 1-CM INCREMENTS.

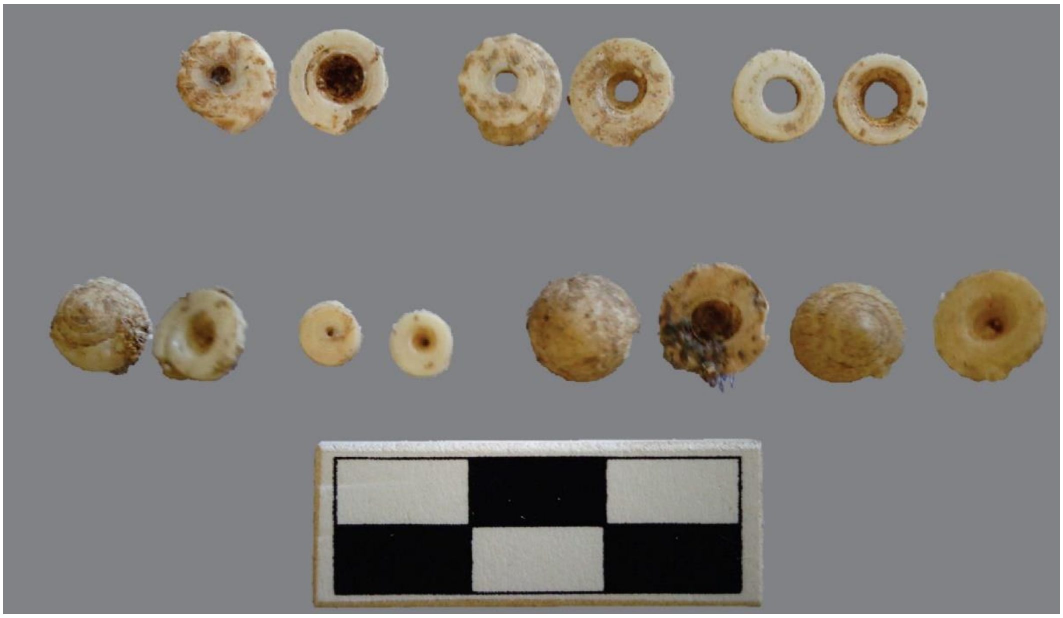

FIGURE 141. *CONUS* SPP. SHELL BEADS IN PROCESS, SHOWN IN TWO VIEWS EACH, RECOVERED FROM LAYER VI-B. SCALE BARS ARE IN 1-CM INCREMENTS.

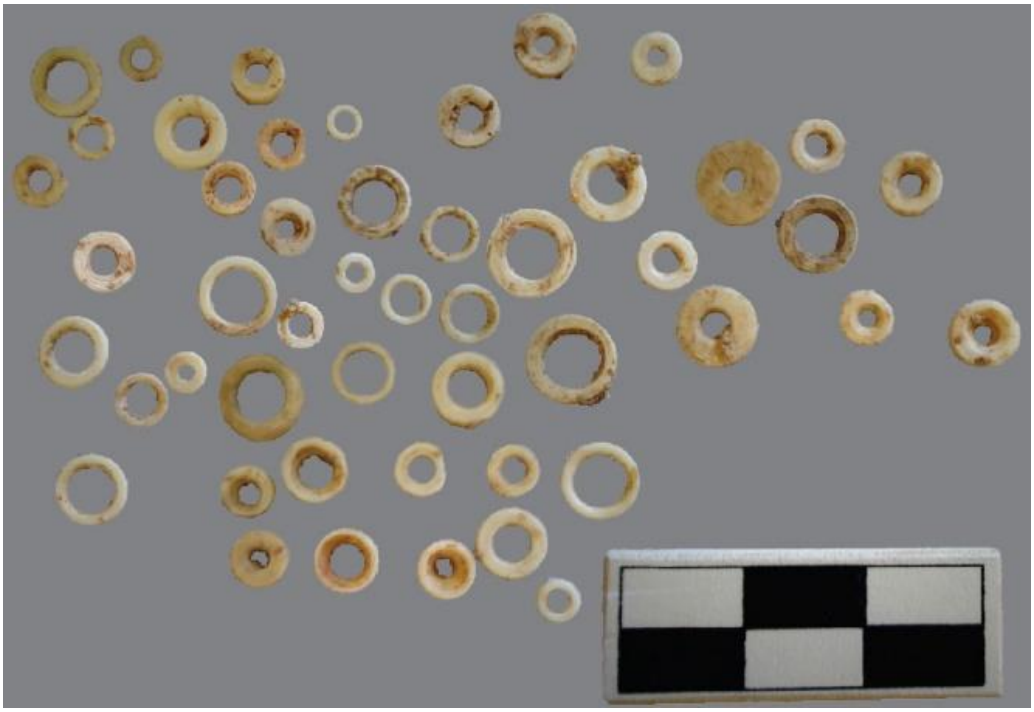

FIGURE 142. *CONUS* SPP. AND POSSIBLY OTHER TAXA OF SHELL BEADS, RECOVERED FROM LAYER VII. SCALE BARS ARE IN 1-CM INCREMENTS.

FIGURE 143. *CONUS* SP. SHELL BEAD IN PROCESS, SHOWN IN TWO VIEWS, RECOVERED FROM LAYER VI-A. SCALE BARS ARE IN 1-CM INCREMENTS.

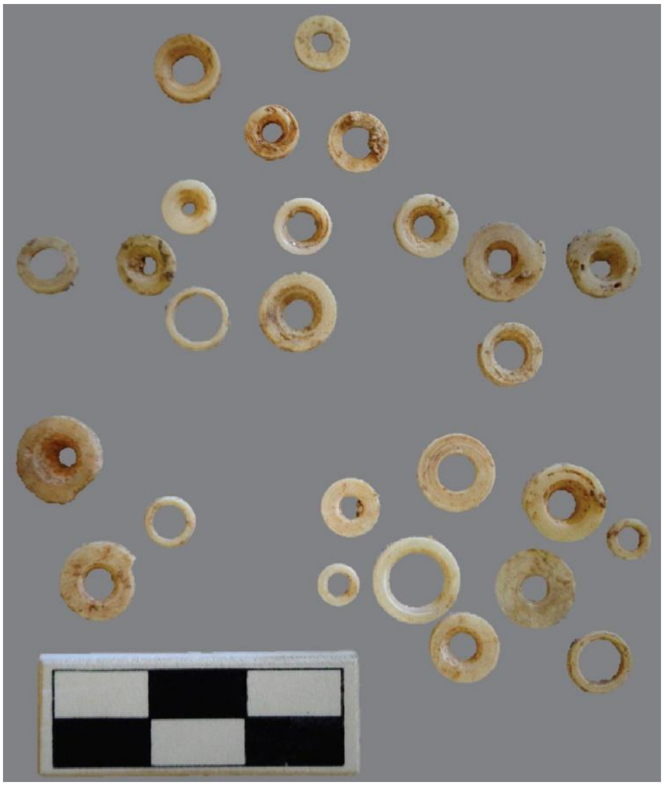

FIGURE 144. *CONUS* SPP. AND POSSIBLY OTHER TAXA OF SHELL BEADS, RECOVERED FROM LAYER VI-A. SCALE BARS ARE IN 1-CM INCREMENTS.

FIGURE 145. *CONUS* SPP. AND POSSIBLY OTHER TAXA OF SHELL BEADS, RECOVERED FROM LAYER V. SCALE BARS ARE IN 1-CM INCREMENTS.

FIGURE 146. *CONUS* SPP. AND POSSIBLY OTHER TAXA OF SHELL BEADS, RECOVERED FROM LAYER IV. SCALE BARS ARE IN 1-CM INCREMENTS.

FIGURE 147. *CONUS* SPP. AND POSSIBLY OTHER TAXA OF SHELL BEADS, RECOVERED FROM LAYER III-B. SCALE BARS ARE IN 1-CM INCREMENTS.

Shell Pendants

Pendants were identified as small-sized and light-weight objects that could be suspended by holes, hanging downward. They may have been worn singly or as parts of compound-element products. Pendants could have been made of any material, but the items from the 2016 excavation all were made of shells. All of these items were unique, so far not duplicated in other known artefacts.

The pendants were found in small numbers (only three items) and inconsistently in the site stratigraphy. Layer VII offered a pendant of *Conus* sp. shell, cut lengthwise and then modified with two holes drilled at one end (Figure 148). Layer IV disclosed a fragment of a nacreous shell pendant, and the original complete shape has not yet been ascertained (Figure 149). Layer III-B yielded an elongate piece, reduced from an unknown non-lustrous shell taxon, with a hole drilled near its centre (Figure 150).

Overall in Marianas archaeological sites, pendants were unique and non-duplicated objects, thus implying personal expressions of identity rather than parts of traditions repeated by multiple people. They were extreme rarities during all represented time periods, possibly more frequent in older periods prior to 1100 B.C. but not yet confirmable with the low numbers involved. Nearly all of the archaeological specimens were made of shells, but rare examples pre-dating 1100 B.C. included a coral pendant from the 2005 excavation at Bapot (see Figure 10) and a marine mammal tooth pendant from the Ritidian Site in Guam (Carson 2017a, 2017b).

FIGURE 148. *CONUS* SP. SHELL PENDANT, SHOWN IN FOUR VIEWS, RECOVERED FROM LAYER VII. SCALE BARS ARE IN 1-CM INCREMENTS.

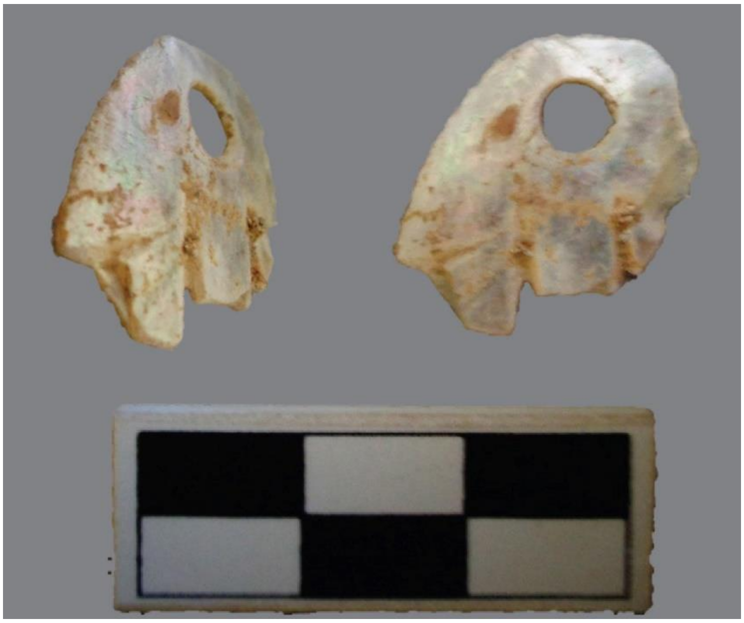

FIGURE 149. FRAGMENT OF NACREOUS SHELL PENDANT, SHOWN IN TWO VIEWS, RECOVERED FROM LAYER IV. SCALE BARS ARE IN 1-CM INCREMENTS.

FIGURE 150. ELONGATE SHELL PENDANT, SHOWN IN TWO VIEWS, RECOVERED FROM LAYER III-B. SCALE BARS ARE IN 1-CM INCREMENTS.

Shell Ear Ornaments

Two forms of apparent ear ornaments were identified (Figures 151 and 152). Both forms had been created by reducing nacreous shells into the final shapes. The shell taxa could not be identified on the basis of the reduced final products.

The older form was represented by a single piece from Layer VI-B (see Figure 151). It was made in the shape of a semi-circle, about 8 mm in diameter, with one tangential projecting point. No other similar object has been found in the Marianas region, but it most closely resembled a variation of ear ornament made of varied materials in neighbouring regions of Island Southeast Asia.

The younger form was represented by two nearly identical pieces from Layer II (see Figure 152). Each was made as an elongate shank with a semi-circle at one end. The semi-circle portions was interpreted as the hanging part that could have been suspended as an ear ornament.

FIGURE 151. SHELL EAR ORNAMENT, SHOWN IN TWO VIEWS, RECOVERED FROM LAYER VI-B. SCALE BARS ARE IN 1-CM INCREMENTS.

FIGURE 152. TWO NEARLY IDENTICALLY SHAPED EAR ORNAMENT FRAGMENTS, RECOVERED FROM LAYER II. SCALE BARS ARE IN 1-CM INCREMENTS.

Drilled *Turbo* spp. Shells

Drilled *Turbo* spp. shells were represented by one complete specimen (Figure 153) and one small fragment (Figure 154). The complete specimen was from Layer II, and it resembled most likely the shell of *Turbo setosus*. The small fragment was from Layer VI-B, and it could be identified only as *Turbo* sp. shell.

The complete specimen from Layer II (see Figure 153) corresponded with the shape of a lime powder container, known ethnographically in betelnut-chewing areas of the Asia-Pacific region. According to the ethnographic usage, the lime powder was held inside the shell, and the small hole allowed for controlled dispensing of small amounts of powder. The controlled dispenser strategy protected the user's hands from being burned by the slaked lime, while also it facilitated precise measurement of the powder. Only a small amount of lime powder was needed as one of three interactive ingredients in a chewable quid, along with the betelnut (nut of *Areca catechu*) itself and the leaf of "betel vine" (*Piper betle*).

The small fragment from Layer VI-B (see Figure 154) could not be categorised definitively as part of a lime container. The shape was consistent with the whole specimen version, but it equally could have been broken from another object made of *Turbo* sp. shell. Other possible objects may have included a pendant or the debris from fishing manufacture.

FIGURE 153. COMPLETE PROBABLE LIME CONTAINER, MADE OF *TURBO* SP. SHELL, SHOWN IN THREE VIEWS, RECOVERED FROM LAYER II. SCALE BARS ARE IN 1-CM INCREMENTS.

FIGURE 154. FRAGMENT OF DRILLED *TURBO* SP. SHELL, RECOVERED FROM LAYER VI-B. SCALE BARS ARE IN 1-CM INCREMENTS.

Drilled and Cut *Cypraea* spp. Shells

Drilled and cut pieces of larger-sized *Cypraea* spp. shells were recovered from Layers VI-B and VI-A (Figure 155). The only complete specimen was from Layer VI-A, showing an oval shape with two drilled holes. Other pieces were fragments, likely broken from similar objects as the one whole example. One piece from Feature E of Layer VI-B showed cut edges of a similar shell, but it may have been broken from a different form of artefact, as the diagnostic drilled holes were not visible on the surviving fragment in this case.

The past cultural usage of this artefact category has not yet been clarified. The colourful appearance may have been suitable for ornamentation, but the hardness of the shell may have been suitable for service as a tool. Elsewhere in the Pacific region and in later-aged contexts in the Mariana Islands, *Cypraea* spp. shells were employed in lures for catching octopus, but the context in Layers VI-B and VI-A pre-dated the expected date range of this tradition in the Marianas. The specimens from the 2016 excavation did not resemble the later forms of pieces of octopus lures.

FIGURE 155. PIECES OF DRILLED AND CUT *CYPRAEA* SPP. SHELLS. COMPLETE ITEM AT UPPER LEFT WAS FROM LAYER VI-A. FRAGMENT AT UPPER CENTRE WAS FROM LAYER VI-A. FRAGMENT AT UPPER RIGHT WAS FROM LAYER VI-B. FRAGMENT AT CENTRE BOTTOM WAS FROM FEATURE E WITHIN LAYER VI-B. SCALE BARS ARE IN 1-CM INCREMENTS.

Smoothed-edge Bivalve Shell Objects

Among the unusual artefacts from the 2016 excavation, five pieces of bivalve shell had been modified into smoothed-edge oblong shapes of 2.5–3.5 cm length. Two different variants were noticed, with a chronological difference as well. The older variant was represented by four artefacts of apparent *Anadara* sp. shells from Layers VI-B and VI-A (Figures 156 and 157). The younger variant was represented by a single example from Layer V, made of a different kind of shell and in slightly smaller dimensions (Figure 158).

The four older variants were made of apparent *Anadara* sp. shells (see Figures 156 and 157). These items showed nearly identical measurements, and they were found exclusively in Layers VI-B and VI-A. *Anadara* sp. shells dominated the shell midden during earlier periods, but they had declined and later disappeared entirely by the time of Layer III-B. For reference, Figure 28 depicts a typical *Anadara* sp. bivalve in ventral and dorsal views.

The single younger example was found in Layer V (see Figure 158). It was slightly smaller in size than the older examples. It had been manufactured from a different shell taxon with nacreous material.

The past cultural usage has not been ascertained, possibly different for the older versus younger variants. The shapes were similar to pieces of trolling lures, likely more effective when using nacreous shell as in the one example from Layer V. The older objects of non-lustrous *Anadara* sp. shells were more suitable for rough handling, and slight depressions on one side may have been suitable for thumb-pressing action, also seen in a thumb-sized depression in another curious singular artefact of *Anadara* sp. shell found in a pre-1100 B.C. context in the 2005 excavation (see Figure 10).

FIGURE 156. TWO SMOOTHED-EDGE SHELL ARTEFACTS OF PROBABLE *ANADARA* SP. SHELL, SHOWN IN THREE VIEWS EACH, RECOVERED FROM LAYER VI-B. SCALE BARS ARE IN 1-CM INCREMENTS.

FIGURE 157. TWO SMOOTHED-EDGE SHELL ARTIFACTS OF PROBABLE *ANADARA* SP. SHELL, SHOWN IN THREE VIEWS EACH, RECOVERED FROM LAYER VI-A. SCALE BARS ARE IN 1-CM INCREMENTS.

FIGURE 158. SMOOTHED-EDGE SHELL ARTEFACT OF NACREOUS SHELL, SHOWN IN TWO VIEWS, RECOVERED FROM LAYER V. SCALE BARS ARE IN 1-CM INCREMENTS.

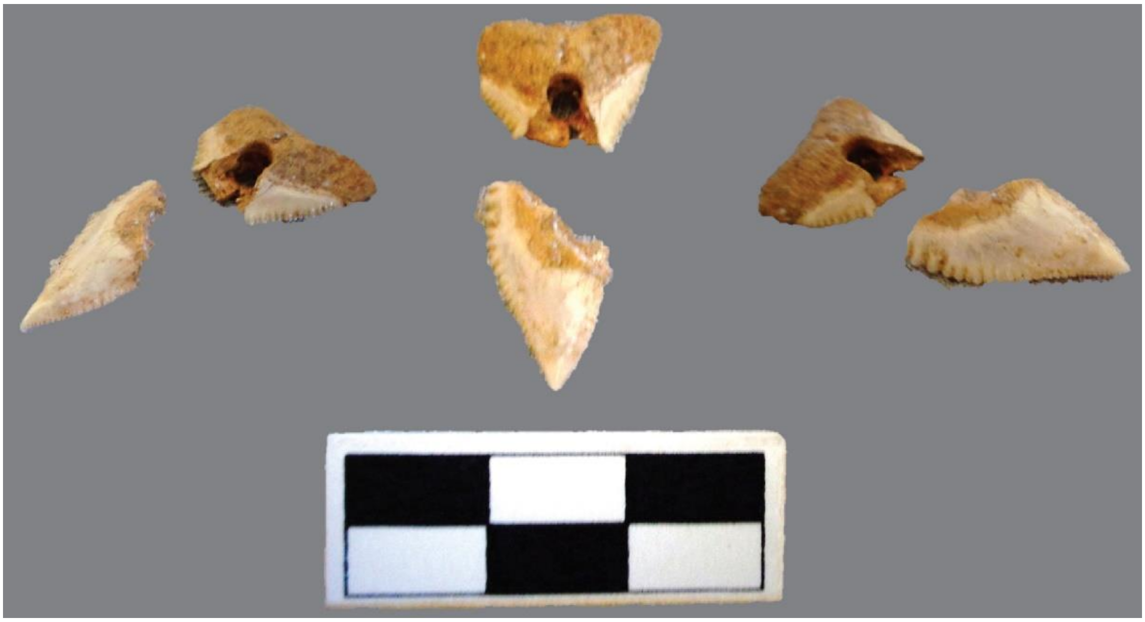

FIGURE 159. FRAGMENT OF DRILLED SHARK TOOTH (UPPER) AND ANOTHER UNMODIFIED FRAGMENT (LOWER), SHOWN IN THREE VIEWS, RECOVERED FROM LAYER IV. SCALE BARS ARE IN 1-CM INCREMENTS.

Drilled Shark Tooth

Layer IV offered a piece of drilled shark tooth, plus one other fragment of shark tooth without definite sign of modification (Figure 159). No shark bones were identified in the site midden in any layer, so the pieces of shark teeth both were regarded as artefacts. In particular, the durable and easily identifiable vertebrae of sharks and rays, both of the Elasmobranchii Subclass, were absent.

The sharp and serrated edges of shark teeth may have been used for cutting or slicing, perhaps in tools or weapons. The drilled hole most likely allowed fastening by sennit or other string, either on a strand or lashed to a handle or other object. While drilled shark teeth have been used as pendants or strung into necklaces historically and in modern times in other Pacific Islands areas, the sharpness of the teeth must have influenced the usage for those items as recovered from Layer IV.

Bevelled Shell Triangle

A single piece of nacreous shell from Layer VII has been cut and polished into a triangular shape with one bevelled edge (Figure 160). The artefact was about 22 mm long, 18 mm maximum base width, and 2–3 mm thick. In section view, it was nearly flat.

This form of artefact so far has not been seen in any other known example, and its original function has not yet been ascertained. The bevelled edge, other finished edges, and thorough polishing all indicated the intended final form of the artefact, except for the possibility of adding a drilled hole for usage as a pendant. The bevelled edge, however, suggested a potential usage as a tool, similar to an adze or chisel, although nacreous shell generally was less suitable than the typically harder shells of *Tridacna* sp. and others. The overall small dimensions implied ornamental or decorative context, except for the possibility of very fine-scaled work.

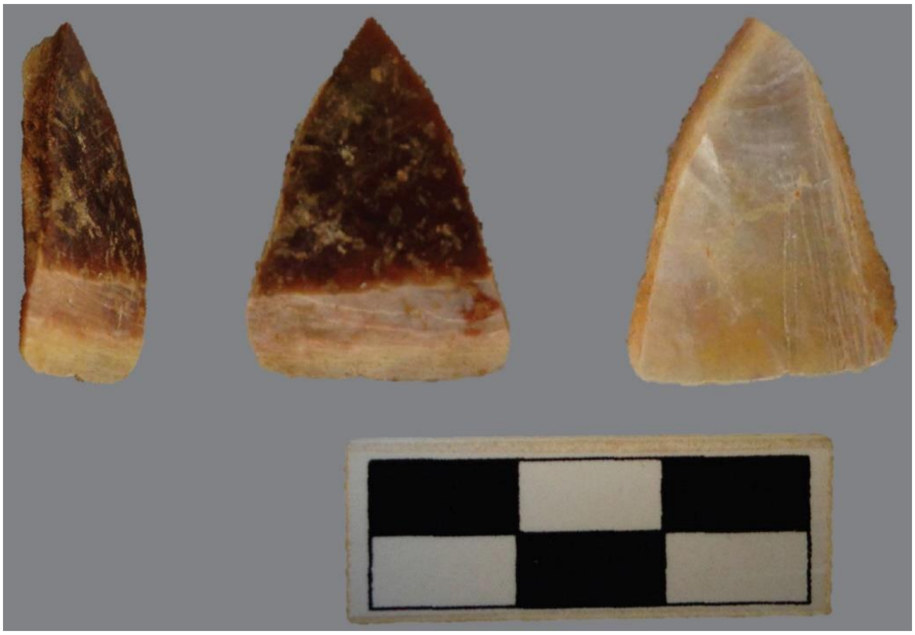

FIGURE 160. BEVELLED NACREOUS SHELL TRIANGLE, SHOWN IN THREE VIEWS, RECOVERED FROM LAYER VII. SCALE BARS ARE IN 1-CM INCREMENTS.

FIGURE 161. "CORKSCREW" SHAPED *TEREBRA* SP. SHELL ARTEFACT, RECOVERED FROM LAYER IV. SCALE BARS ARE IN 1-CM INCREMENTS.

"Corkscrew" Shell

Found in Layer IV, a singular piece of apparent *Terebra* sp. shell was cut into a "corkscrew" shape (Figure 161). No other object of this design has been found in the Marianas or elsewhere, and the past function has not been identified. The narrow "tip" end did not reveal visible signs of use-wear, but future microscope inspection may yet reveal micro-patterns or residues.

Edge-worked Nacreous Bivalve Shells

Two edge-worked nacreous bivalve shells included one piece from Feature I of Layer VII (Figure 162) and another from Layer VI-A (Figure 163). The piece from Layer VI-A was made of *Isognomon* sp. shell, identifiable by the diagnostic ligature marks as retained on one edge, and this edge may have served as the gripping side while the other worked edges were applied for cutting or other action. The piece from Feature E of Layer VII had been worked around all edges, possibly for a different function or not yet finished.

Past functions of these objects have not yet been ascertained, and they may have been different for the two objects. The apparently finished product from Layer VI-A resembled a "shell harvesting knife" as known in coastal China and Taiwan, generally interpreted as related to the harvesting of rice or millet, although other functions were possible. Both of the shell objects may have been used for scraping or grating action, perhaps for grating the interiors of coconuts or in similar fashion.

FIGURE 162. THOROUGHLY EDGE-WORKED NACREOUS SHELL, SHOWN IN TWO VIEWS, RECOVERED FROM FEATURE I WITHIN LAYER VII. SCALE BARS ARE IN 1-CM INCREMENTS.

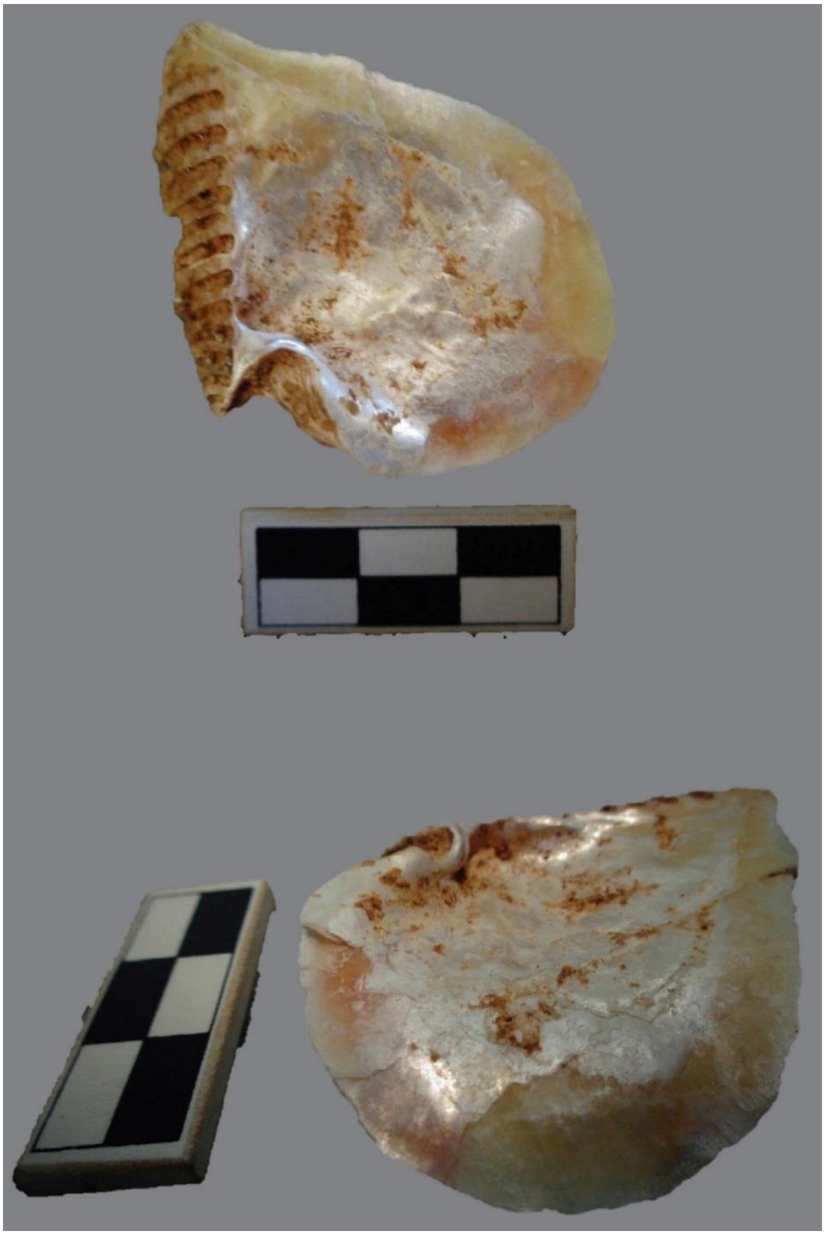

FIGURE 163. EDGE-WORKED *ISOGNOMON* SP. SHELL, SHOWN IN TWO VIEWS, RECOVERED FROM LAYER VI-A. SCALE BARS ARE IN 1-CM INCREMENTS.

Worked Nacreous Shell Debitage

Scattered fragments of worked nacreous shell were recovered from Layers VI-B through III-B (Figure 164), apparently as the by-products or debitage of manufacturing fishing hooks, pendants, or other objects. Layer VI-B disclosed one piece. Layer VI-A provided three pieces. Layer V contained one piece. Layer IV yielded one piece. Layer III-B offered one piece.

FIGURE 164. EXAMPLES OF PIECES OF WORKED NACREOUS SHELL. ITEM AT LOWER RIGHT WAS FROM LAYER VI-B. ALL OTHER ITEMS WERE FROM LAYER VI-A. SCALE BARS ARE IN 1-CM INCREMENTS.

Chapter 9

New Findings: Midden of Animal Food Remains

A category of "midden" referred to animal food discard, including invertebrate marine shellfish remains and vertebrate animal bones. These pieces were considered as "midden" if they showed no signs of deliberate modification as artefacts. The shellfish remains were by far more numerous than the animal bones, and these two different types of materials underwent different analysis.

Shellfish Remains

The shellfish remains were impressively dense in all of the site layers, as expected for any coastal site. Given the prior 2005 detailed documentation (Carson 2005, 2008), the 2016 effort focused on the shellfish remains from Quadrant 1 as a representative 25% sample of the total 16 sq m excavation area. The shellfish remains were examined from each layer separately, and those findings from subsurface features were combined with their associated layers.

Every piece from Quadrant 1 was identified taxonomically, counted, and weighed (see Table 6). The major categories of chronological significance were included in a summary chronological diagram (Figure 165). These results may be compared with the prior 2005 findings (see Figure 10).

Overall in the Mariana Islands, the compositions of shellfish middens changed according to the effects of cultural harvesting, altered sea-level and coastal ecology, and perhaps local culinary preference. Prior research has noted an early preference for *Anadara* sp. clams and a later preference for *Strombus* sp. gastropods (Amesbury 1998, 2007). More fine-grained chronological sequences have illustrated more complexity in the relative amounts of different shellfish taxa through time (Carson 2014a, 2016).

During earlier periods of higher sea level, *Anadara* sp. clams dominated the food middens, but they rapidly declined with sea-level drawdown after 1100 B.C. and eventually became either non-existent or extremely rare in later periods. Meanwhile, whenever people first inhabited any particular area, they harvested rock-clinging taxa such as *Patelloida* spp. (limpets), Polyplacophora (chitons), and Echinodermata (sea urchins) overall adding to the impact of sea-level change in the cases of sites where people had been living prior to 1100 B.C. as at Bapot.

The same region-wide patterns of early-period targeting of *Anadara* sp. clams and the noted rock-clinging taxa were seen in the Bapot midden, both in 2005 and again in 2016. The Bapot case, however, involved an additional rock-clinging taxon of *Haliotis* sp. (abalone) exclusively in Layers VII through V that so far has not been identified in any other archaeological site in the Mariana Islands. These shells most closely resembled *Haliotis asinina* (Figure 166), recognised as existing naturally in the Marianas region along with several other species (Geiger 1999), although historically abalone have not been known popularly in the region.

A major shift in the shellfish midden started with Layer V and continued through Layer VI or III-B, concurrent with the larger regional occurrence of a "nearshore resource depression" (Carson 2014a, 2016). This resource depression involved the combined effects of lowering sea-level, changing coastal ecology, and impacts of cultural harvesting in the nearshore zones. These factors resulted in notable decline or total disappearance of *Anadara* sp., chitons, sea urchin, *Patelloida* spp., and *Haliotis* sp. that in fact already had begun to decline or disappear earlier.

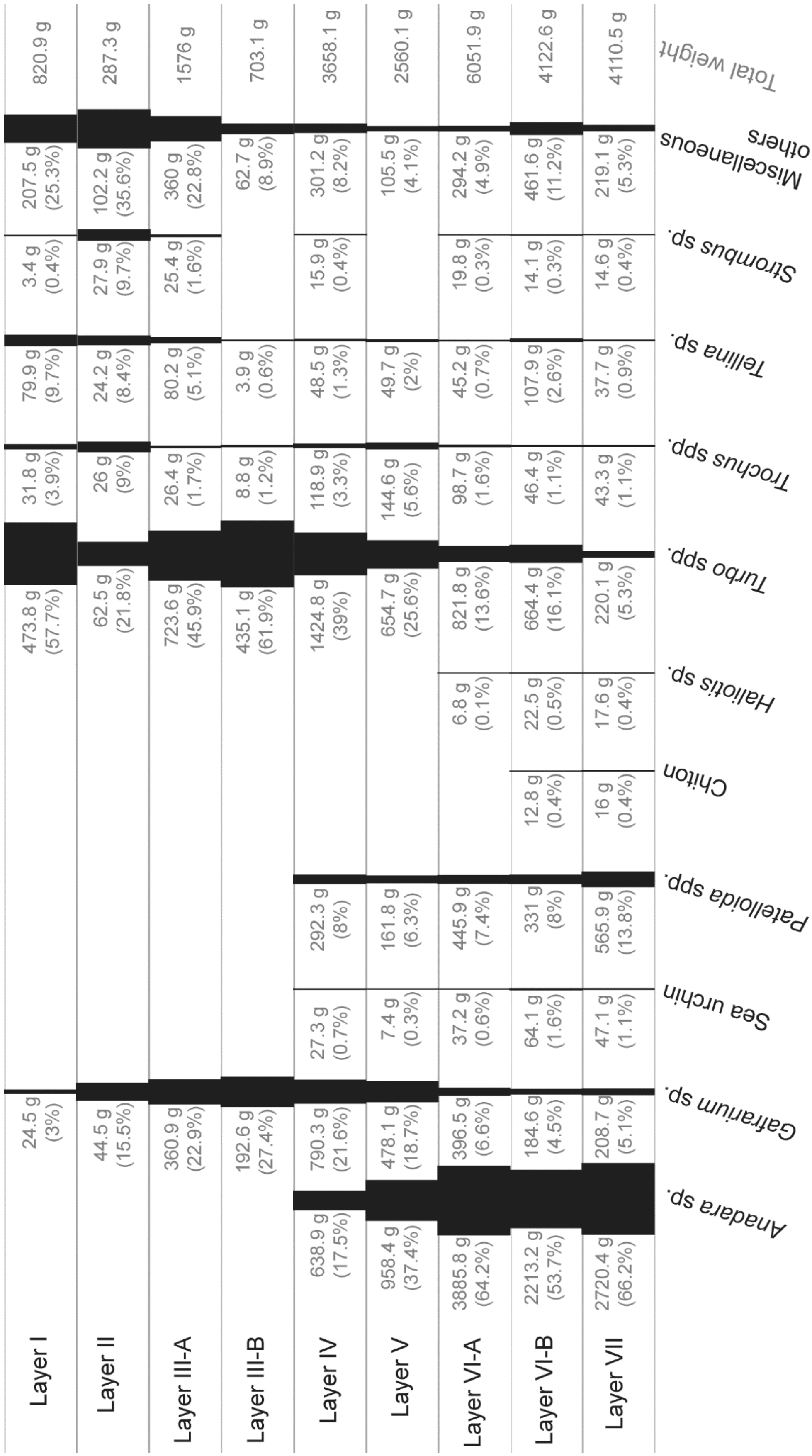

FIGURE 165. MAJOR CHRONOLOGICAL TRENDS IN MARINE SHELLFISH REMAINS, BASED ON COLLECTIONS FROM QUADRANT 1.

FIGURE 166. EXAMPLE OF NEARLY COMPLETE *HALIOTIS* SP. SHELL, SHOWN IN DORSAL (LEFT) AND VENTRAL (RIGHT) VIEWS, RECOVERED FROM LAYER VII. SCALE BARS ARE IN 1-CM INCREMENTS.

With the decline or loss of the earlier-preferred shellfish taxa, the shellfish midden showed increasing amounts of *Gafrarium* sp., *Turbo* spp., and others. These taxa generally could be found in the middle to outer portions of lagoons and reefs, although *Gafrarium* sp. and a few others could be harvested from nearshore zones. The complete sets of taxa were not all depicted in the summary graphic of Figure 165, but they included *Trochus* spp., *Tellina* sp., *Conus* spp., *Cypraea* spp., and others as detailed in Table 6. Evidently most abundant, however, were *Turbo* spp. gastropod remains.

In the later-aged contexts, especially at *latte* sites post-dating A.D. 1000, *Strombus* sp. shells often dominated site middens, but such was not the case in the 2016 excavation area at Bapot. In particular, *Strombus gibberulus* often comprised more than 90% of many later-aged site middens (Carson 2012). Although *Strombus* sp. shells were numerous in the 2005 excavation findings, they were infrequent in the 2016 excavation area, thus reflecting differential activity areas at the site.

Animal bones

Bones of fish, bird, and turtle were found through the site stratigraphy (Figure 167). The sparse numbers so far have revealed only tentative speculation of possible chronological trends. In addition to the overall picture seen in Figure 167, counts and weights were recorded for each occurrence (see Table 6).

Pending two cautionary notes, bird bones apparently declined through time from Layer VI-B through Layer III-A, then peaked again at a later point in Layer II. First among the cautionary notes, Layer VII yielded only a single bird bone and no other animal bone material, likely due to the poor preservation of bone material overall in the ancient seashore context, so the apparent trend of bird decline has not yet accounted for the initial years of human presence. Second, the later peak in Layer II may have been over-represented by the mostly windblown sand of this layer, incorporating more light-weight bone material than usually expected.

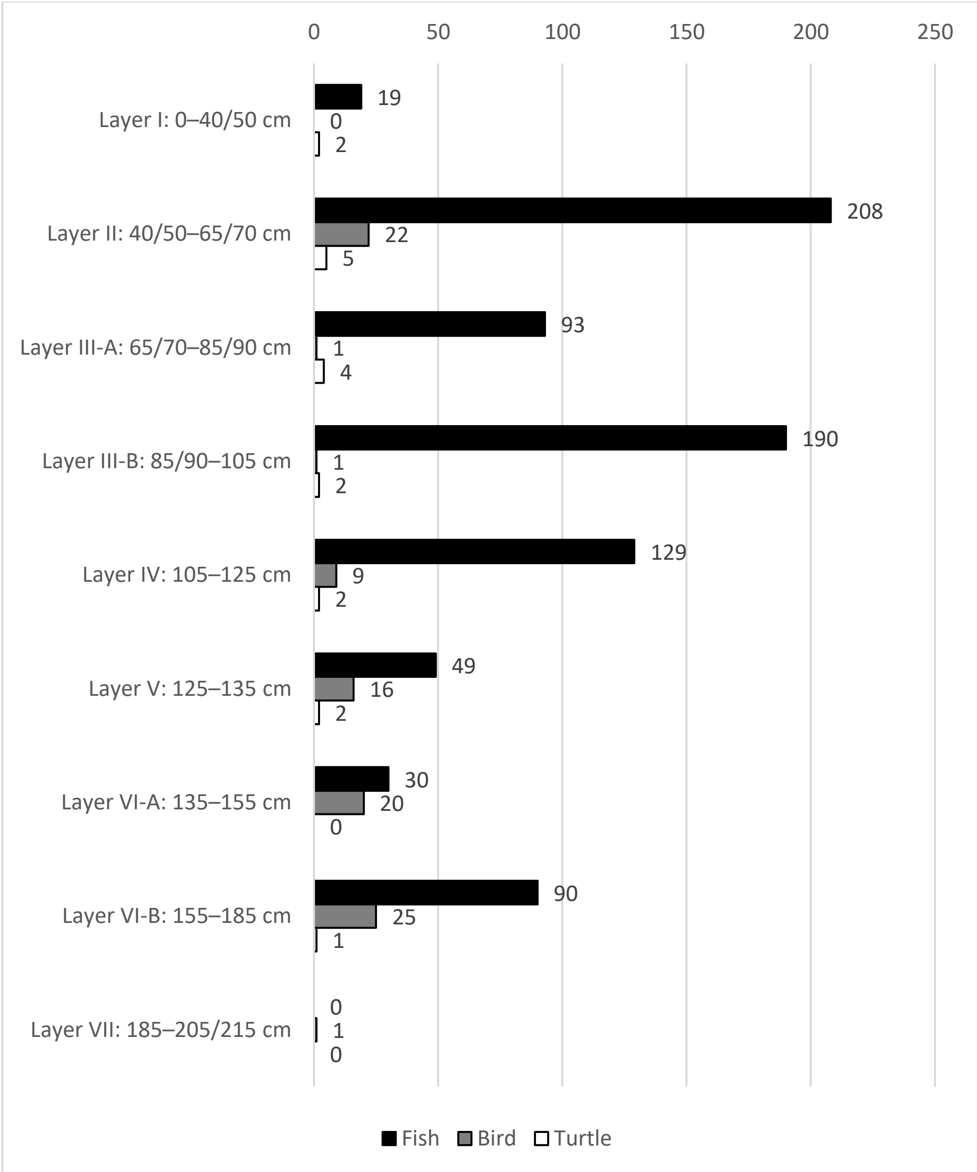

FIGURE 167. STRATIGRAPHIC DISTRIBUTION OF VERTEBRATE ANIMAL BONES, SHOWN IN RAW COUNTS PER STRATIGRAPHIC LAYER.

If indeed people consumed more birds during early periods and then less through time, then the impact on bird populations may have been greater than so far has been documented in the Marianas region. In most Remote Oceanic settings, the initial episodes of human presence resulted in massive de-population of the native birds and sometimes of other animals, but so far this record has not been confirmed in the early-period Marianas sites (Carson 2016). Toward addressing these issues, the bird bones from the 2016 excavation will need to be examined for the possibility of identifying bird taxa that became extinct after human impacts, but realistically the observed bird bones showed very few of the anatomical parts that could diagnose their taxonomy.

As expected of a coastal site, the fish specimens consistently were the most numerically represented in the vertebrate remains of each stratigraphic layer. The observed anatomical parts mostly were vertebrae and spines of varied small, medium, and large fish. Very few diagnostic mouth parts were noted, such as the easily identified grinding plates and teeth of Scaridae (parrotfish).

Turtle bones were identified in very low numbers and inconsistently through the stratigraphic sequence. Possible chronological trends have not been identifiable. Future analysis potentially could assess if the individual pieces had belonged to single or multiple animals in each stratigraphic layer, but the fragmentary pieces have not revealed any obvious signs of how they may have inter-related.

Future analysis may be attempted for the possibility of finer-scale taxonomic identifications. For instance, the mouth parts of some fish potentially can be identified, and the epiphyseal ends of bird bones potentially can be identified as well. These particular elements, however, were not retained in most of the surviving bones or fragments, so further analysis may need to consider other kinds of observations in order to refine much more than already seen in the initial categories of fish, bird, and turtle.

Chapter 10

Answering the Initial Research Questions

The current research has focused on five primary research questions, each reiterated here and discussed with reference to the new excavation findings.

1) What was the date of initial human presence at this site?

The 2016 findings validated an earliest cultural presence slightly older than 1500 B.C. at this particular site, previously suggested from the 2005 excavations but regarded as needing confirmation or refinement. A confident result was possible through radiocarbon dating of material from the interior of a large pit feature (Feature G) in the deepest and oldest cultural layer (Layer VII) that had not been identified in the areas of the prior excavations, instead found only in the currently excavated area. The dating was corroborated by multiple samples from different contexts, all in stratigraphic order.

2) How did the oldest layer at Unai Bapot relate to the dating of other earliest settlement sites in the Mariana Islands?

The pre-1500 B.C. dating was slightly older than the usual findings of 1500 B.C. generally in the sites bearing first-settlement layers in the Mariana Islands (Carson and Kurashina 2012). The confirmed results now allow greater confidence about 1500 B.C. as the timing of when people definitely were living in the region. The site records prior to 1500 B.C. now can be acknowledged and explored further, although the most convincing material records at multiple sites have been evidenced after 1500 B.C.

3) What was the ecological context of the site during different time intervals?

The changing ecological context at the site has been studied through at least three lines of evidence. First, a slightly refined elevation map allowed precise measurement of the ancient living surfaces of the observed stratigraphic layers during their specific time periods, in coordination with the sea-level history. Second, the stratigraphic sequence was documented in finer detail, given the advantages of a larger excavation and the ability to excavate precisely at the location of the ancient seashore where it had existed prior to 1100 B.C. Third, the shellfish remains offered clues about the changing environment, including the effects of both cultural harvesting and alteration due to sea-level drawdown.

The new findings have clarified that the first inhabitants at the site had lived in a palaeo-seashore setting, during a time of higher sea level and different coastal ecology than seen today. This earliest period now has been outlined as beginning just prior to 1500 B.C. and continuing through 1100 B.C. The artefacts, midden, and traces of structural features all have shown new information about this ancient context, and moreover this ancient context involved a degree of internal chronological variation as seen in at least three separate stratigraphic units of Layers VII, VI-B, and VI-A.

While the sea level lowered during later periods, people adjusted to the different conditions, inhabitable land surfaces, and habitat zones of shellfish and other resources. These different contexts were noted since 1100 B.C. with Layer V, followed by continual change all the way through the most recent surface-associated context of Layer I. The combined effects of lowering sea level, altered coastal ecology, and increasing human impacts all contributed to the developments of different natural and cultural landscape contexts in each identifiable time period.

4) What was the cultural setting at the site during different time intervals?

The findings from each distinguished cultural layer now can be compared with an overall Marians regional chronology (Carson 2016), in particular adding more detail and a number of unique site-specific findings that otherwise could not have been known. The excavation of 16 sq m significantly increased the amount of material known from all of the time periods represented at the site, especially valuable for the earliest periods that have been accessed in few sites overall in the Mariana Islands. Most of the current work focused on the oldest cultural layers pre-dating 1100 B.C., but the exposed stratigraphy showed a complete chronological sequence continuing through approximately A.D. 1700.

The findings already have been presented in chronological order, not repeated here. Each material category has been described, and relations with regional patterns have been noted mostly as following the regional findings yet with a number of site-specific discoveries. Future studies may yet clarify some of the apparent anomalies, as well as refine some portions of the chronological sequence dating.

5) What can be ascertained of spatial patterns of site use during different time intervals?

The exposure of 16 sq m allowed more opportunity to examine potential spatial patterns than otherwise had been possible through smaller-sized test pits at the site. Especially informative were the arrangements of heated-rock hearths, pits, and post moulds in the lower cultural layers, previously not detected in the smaller-sized 2005 test pits. Additional information was gained through examining concentrations of artefacts and midden, not only internally within the 2016 excavation area but also in comparison with the prior findings in slightly different portions of the site.

The lower layers revealed deliberate cultural investment in living in formalised structures at the site, evidenced in several hearths, pits, and 18 post moulds of Layers VII through VI-A all pre-dating 1100 B.C. These features must have been constructed close with the ancient seashore setting of that time period. While the shapes and sizes of individual houses could not be ascertained, due to the limits of the 4 by 4 m excavation window into these ancient layers, the substantial investment in the site habitation can be acknowledged.

After 1100 B.C., Layer V disclosed portions of one large hearth (Feature A) and one large pit feature (Feature B). Although only tentative as a working hypothesis, pending further exploration of the site, the larger-sized features in Layer V could reflect a shift in the stability of the beach surface following the initiation of sea-level drawdown. Beginning with Layer V, considerably more charcoal was preserved in situ in all of the site layers, indicative of greater site stability in contrast to the shoreline-oriented contexts in the deeper and older layers pre-dating 1100 B.C.

The upper units of the stratigraphy, in Layers IV through I, did not disclose the same kinds of structural features as were seen in the lower and older layers. In later periods, the focus of cultural activity most likely had shifted to a slightly different location. For instance, the surface-visible *latte* structures were positioned slightly to the east from the 2016 excavation, and furthermore the associated shell midden (in Layer I) emphasised *Strombu*s sp. closer to the *latte* but not in the area of the 2016 excavation.

Chapter 11

Larger Research Implications

Archaeological excavation at Unai Bapot has confirmed first Remote Oceanic settlement just prior to 1500 B.C. and in a palaeo-seashore setting, in this case dated at least as early as 1697–1531 B.C. according to the redundant overlap of radiocarbon dating from the two lowest cultural layers. The material signature of the first-settlement period involved red-slipped pottery, polished chert adzes, assorted shell ornaments, reliance on *Anadara* sp. shellfish and other nearshore resources, and shoreline-oriented habitation that continued through 1100 B.C. The same artefact assemblage has been documented at other early sites such as Ritidian and House of Taga in the range of 1500–1100 B.C. (Carson 2014a), in particular noting the identical finely decorated pottery motifs with dentate-stamped and circle-stamped designs of a highly distinctive tradition. The deepest cultural layers of Unai Bapot specifically can be situated at the earliest end of this context, substantively expanding our understanding of the world's first successful settlement in the Remote Oceanic region.

The results just prior to 1500 B.C. for the pottery-bearing horizon at Unai Bapot now enable a confident redefinition of the larger regional cultural chronology, specifically in terms of when and where people first successfully inhabited the Remote Oceanic region. The region-wide pottery-bearing horizon in the Marianas definitely was established by 1500 B.C. (Carson 2014a, 2016; Carson and Kurashina 2012), and the dating at Unai Bapot in fact was slightly earlier than 1500 B.C. as documented here. The occurrence in the Marianas therefore was prior to any of the known archaeological layers in other parts of Remote Oceania, for instance in the areas of Southern Melanesia and West Polynesia where layers of dentate-stamped Lapita pottery have been dated as early as 1100 B.C. (Denham et al. 2012).

The findings at Unai Bapot just prior to 1500 B.C. now leave no doubt of first cultural settlement in Remote Oceania having occurred in the Mariana Islands and pre-dating the Lapita-associated dispersal into Southern Melanesia and West Polynesia about 1100 B.C. At the time of first Marianas settlement, the only possible homeland source with a similar pottery-making tradition and other related artefact assemblage was in Island Southeast Asia, most probably in the northern to central Philippines. This connection has been indicated in the cross-regional pottery trail (Carson et al. 2013), and it has been highlighted as indicating the world's longest ocean-crossing migration of its time in excess of 2000 km (Craib 1999; Hung et al. 2011). Although these implications have been mentioned previously as cited here, the new material evidence and dating from Unai Bapot now enable greater confidence as well as more refined statements.

The first settlers at Unai Bapot and other sites of the Marianas around 1500 B.C. apparently were targeting certain kinds of palaeo-seashores that existed prior to the effects of sea-level drawdown and other factors following 1100 B.C. Post-raised houses were installed close to the former shoreline, likely for direct access to shallow-water mangroves or seagrass beds as the preferred habitats of *Anadara* sp. shellfish that dominated the food middens, but this food resource was not the only concern of the site's first inhabitants. *Anadara* sp. shellfish were the most abundant items in the early-period diet in the Marianas and elsewhere in the western Pacific (e.g., Amesbury 2007; Carson 2014a, 2016), but people at the Bapot Site also harvested rock-clinging taxa such as limpets, chiton, sea urchins, and abalone that all declined rapidly within a few centuries.

In addition to the targeting of preferred shellfish habitat zones, the palaeo-seashore settlement must have been situated with access to a freshwater source. This access differed from one site to another, but at Unai Bapot a stream drainage was situated about 1 km to the west. Coastal seepage flows of fresh water may have been available just above sea level in several low-elevation locations such as around the Bapot Site. Water pools were accessible in caves just above the mid-Holocene sea level at the Ritidian Site in Guam

(Carson 2017a, 2017b), but so far this unique situation at Ritidian appears to be different from the ancient use of freshwater sources at Bapot and other sites.

The palaeo-seashore context at the Bapot Site now can be framed within the conditions of the higher mid-Holocene sea level and attendant factors of ancient coastal morphology and nearshore ecology, definitely pre-dating 1100 B.C. and extending at least as early as 1500 B.C. During those centuries, people targeted certain kinds of palaeo-seashores as the basis of the first ever successful human settlement of Remote Oceania, but then their descendants after 1100 B.C. needed to adapt to a set of changing conditions precisely in those same seashore-oriented zones. The reasons are not yet clarified in regards to why people targeted those specific first-settlement locations, rather than other possibilities in different seashores around the Mariana Islands, but the documentation of the palaeo-seashore context now substantiates a necessary beginning toward this larger research.

With the refined understanding of the palaeo-seashore habitation context, at least two avenues of research can be explored in terms of how people adapted to their given configurations of coastal landforms and nearshore habitat zones. First, the defined site contexts can be examined as chosen deliberately for their access to specific kinds of shellfish and other resources, playing roles in shaping the world's longest-distance ocean-crossing migration of its time. Notions of ancient people seeking faraway islands may need to be revised, instead now accommodating the apparent targeting of specific seashore niches that happened to be situated in remote islands. Second, the evident change in coastal ecology after 1100 B.C. signaled the termination of the palaeo-seashore context as defined here, and it coincided with a deep structural change in the cultural inventory of pottery, shell ornaments, and food midden compositions. Consistently at all of the known first-settlement sites, the niche-targeting of the first settlers was sustained for at least 400 years in the Marianas, such that the re-structuring after 1100 B.C. necessitated a departure from long-established traditions, instructive today for our modern situation of coping with another major event of environmental change due to global warming and sea-level rise.

References

Amesbury, Judith R.

1998 Changes in species composition of archaeological marine shell assemblages in Guam. *Micronesica* 31: 437–366.

Amesbury, Judith R

2007 Mollusk collecting and environmental change during the prehistoric period in the Mariana Islands. *Coral Reefs* 26: 947–958.

Bonhomme, Theresa, and John L. Craib

1987 Radiocarbon dates from Unai Bapot, Saipan – Implications for the prehistory of the Mariana Islands. *Journal of the Polynesian Society* 96: 95–106.

Bronk Ramsey, Christopher

2013 Recent and planned developments of the program OxCal. *Radiocarbon* 55: 3–4.

Butler, Brian M.

1994 Early prehistoric settlement in the Mariana Islands: New evidence from Saipan. *People and Culture in Oceania* 10: 15–38.

Butler, Brian M. (editor)

1995. *Archaeological investigations in the Achugao and Matansa areas of Saipan, Mariana Islands*. Micronesian Archaeological Survey Report No. 30. Division of Historic Preservation, Saipan, Commonwealth of the Northern Mariana Islands.

Carson, Mike T.

2005 National Register of Historic Places nomination for the Unai Bapot Latte Site (Sp-1-0013) in Laulau, Saipan, Commonwealth of the Northern Mariana Islands. International Archaeological Research Institute, Inc., Honolulu.

Carson, Mike T.

2008 Refining earliest settlement in Remote Oceania: Renewed archaeological investigations at Unai Bapot, Saipan. *Journal of Island and Coastal Archaeology* 3: 115–139.

Carson, Mike T.

2010 Radiocarbon chronology with marine reservoir correction for the Ritidian Archaeological Site, northern Guam. *Radiocarbon* 52: 1627–1638.

Carson, Mike T.

2011 Palaeohabitat of first settlement sites 1500–1000 B.C. in Guam, Mariana Islands, western Pacific. *Journal of Archaeological Science* 38: 2207–2221.

Carson, Mike T.

2012 An overview of latte period archaeology. *Micronesica* 42: 1–79.

Carson, Mike T.

2014a *First settlement of Remote Oceania: Earliest sites in the Mariana Islands*. Springer Briefs in Archaeology Series, Volume 1. Springer, New York.

Carson, Mike T.

2014b Paleo-terrain research: Finding the first settlement sites of Remote Oceania. *Geoarchaeology* 29: 268–275.

Carson, Mike T.

2016 *Archaeological landscape evolution: The Mariana Islands in the Asia-Pacific region*. Springer International, Cham, Switzerland.

Carson, Mike T.

2017a Cultural spaces inside and outside caves: A study in Guam, western Micronesia. *Antiquity* 91: 421–441.

Carson, Mike T.

2017b Inhabiting remote tropical seashores at 1500–1100 B.C.: Water, practicalities, and rituals in the Mariana Islands. *Journal of Field Archaeology* 42: pages forthcoming in 2017.

Carson, Mike T., and Hsiao-chun Hung

2015 On the beach in Remote Oceania. In *Field Archaeology from around the World: Ideas and Approaches*, edited by Martin Carver, Bisserka Gaydarska, and Sandra Monton-Subias, pp. 133–136. Springer, New York.

Carson, Mike T., and Hiro Kurashina

2005 Re-envisioning long-distance Oceanic migration: Early dates in the Mariana Islands. *World Archaeology* 44: 409–435.

Carson, Mike T., and John A. Peterson

2011 Calcrete formation and implications for buried archaeological deposits in the Mariana Islands, western Pacific. *Geoarchaeology* 26: 501–513.

Carson, Mike T., and David J. Welch

2005 Archaeological survey, mapping, and testing of Bapot Latte Site (SP-1-0013) in Laulau, Saipan, Commonwealth of the Northern Mariana Islands. Report prepared for Division of Historic Preservation, Commonwealth of the Northern Mariana Islands. International Archaeological Research Institute, Inc., Honolulu.

Carson, Mike T., Hsiao-chun Hung, Glenn Summerhayes, and Peter Bellwood

2013 The pottery trail from Southeast Asia to Remote Oceania. *Journal of Island and Coastal Archaeology* 8: 17–36.

Clark, Geoffrey, Fiona Petchey, Olaf Winter, Michael Carson, and Patrick O'Day

2010 New radiocarbon dates from the Bapot-1 Site in Saipan and Neolithic dispersal by stratified diffusion. *Journal of Pacific Archaeology* 1: 21–35.

Cordy, Ross

1979a Laulau Bay Archaeological Survey, Field Report 1. Unpublished manuscript on file at Division of Historic Preservation, Department of Community and Cultural Affairs, Commonwealth of the Northern Mariana Islands.

Cordy, Ross

1979b Laulau Bay Archaeological Survey, Field Report 2. Unpublished manuscript on file at Division of Historic Preservation, Department of Community and Cultural Affairs, Commonwealth of the Northern Mariana Islands.

Cordy, Ross

1979c Further Archaeological Investigations at Laulau, Saipan. Unpublished manuscript on file at Division of Historic Preservation, Department of Community and Cultural Affairs, Commonwealth of the Northern Mariana Islands.

Craib, John L.

1999 Colonisation of the Mariana Islands: New evidence and implications for human settlement in the western Pacific. In *Le Pacifique de 5000 à 2000 avant le Présent: Suppléments à l'Histoire d'une Colonisation*, edited by Jean-Christophe Galipaud and Ian Lilley, pp. 477–485. Institut de Récherche pour le Développement, Paris.

Denham, Tim, Christopher Bronk Ramsey and Jim Specht

2012 Dating the appearance of Lapita pottery in the Bismarck Archipelago and its dispersal to Remote Oceania. *Archaeology in Oceania* 47:39–46.

Dickinson, William R.

2000 Hydro-isostatic and tectonic influences on emergent Holocene paleoshorelines in the Mariana Islands, western Pacific Ocean. *Journal of Coastal Research* 16: 735–746.

Driver, Marjorie (translator)

1987 *Navigational Data for the Mariana Islands* (1863). Originally published by the Hydrographic Office, Madrid. Translation published by Micronesian Area Research Center, University of Guam, Mangilao.

Geiger, Daniel L.

1999 Distribution and biogeography of the recent Haliotidae (Gastropoda: Vetgastropoda) world-wide. *Bollettino Malacalogico* 35: 57–119.

Hornbostel, Hans

1925 Notes and records of archaeological investigations in the Mariana Islands. Documents on file at Micronesian Area Research Center, University of Guam.

Hung, Hsiao-chun, Mike T. Carson, Peter Bellwood, Frediliza Z. Campos, Philip J. Piper, Eusebio Dizon, Mary Jane Louise A. Bolunia, Marc Oxenham, and Zhang Chi

2011 The first settlement of Remote Oceania: The Philippines to the Marianas. *Antiquity* 85: 909–926.

Kopp, Robert E., Frederik J. Simons, Jerry X. Mitrovica, Adam C. Maloof, and Michael Oppenheimer

2013 A probabilistic assessment of sea level variations within the last interglacial stage. *Geophysical Journal International* 193: 711–716.

Laguana, Andrew, Hiro Kurashina, Mike T. Carson, John A. Peterson, James M. Bayman, Todd Ames, Rebecca A. Stephenson, John Aguon and Harya Putra

2012 Estorian i latte: A story of latte. *Micronesica* 42: 80–120.

Marck, Jeffrey

1978 Interim report of the 1977 Laulau excavations, Saipan, NMI. Unpublished manuscript on file at Division of Historic Preservation, Department of Community and Cultural Affairs, Saipan, Commonwealth of the Northern Mariana Islands.

Olmo, Richard K.

1992a Phase I archaeological inventory survey, Shimizu Laulau Resort project area, Saipan, Commonwealth of the Northern Mariana Islands. Report prepared for the Northern Islands Company. International Archaeological Research Institute, Inc., Honolulu.

Olmo, Richard K.

1992b Phase I archaeological inventory survey, Kanaya Property, Laulau Bay, Saipan. Report prepared for the Northern Islands Company. International Archaeological Research Institute, Inc., Honolulu.

Reimer, Paula J., Edouard Bard, Alex Bayliss, J. Warren Beck, Paul G. Blackwell, Christopher Bronk Ramsey, Caitlin E. Buck, Hai Cheng, R. Lawrence Edwards, Michael Friedrich, Pieter M. Grootes, Thomas P. Guilderson, Halfidi Haflidason, Irka Hajidas, Christine Hatté, Timothy J. Heaton, Dirk L. Hoffmann, Alan G. Hogg, Konrad A. Hughen, K. Felix Kaiser, Bernd Kromer, Sturt W. Manning, Mu Niu, Ron W. Reimer, David A. Richards, E. Marian Scott, John R. Southon, Richard A. Staff, Christian S. M. Turney, and Johannes van der Plicht

2013 INTCAL13 and MARINE13 radiocarbon age calibration curves 0–50,000 years cal BP. *Radiocarbon* 55: 1869–1887.

Reimer, Ron W., and Paula J. Reimer

2017 An online application for ΔR calculation. *Radiocarbon* 59: pages forthcoming in 2017.

Russell, Scott

1987 Laulau: Its history and historic resources. Report prepared for the Northern Islands Company. Division of Historic Preservation, Department of Community and Cultural Affairs, Saipan, Commonwealth of the Northern Mariana Islands.

Spoehr, Alexander

1957 *Marianas Prehistory: Archaeological Survey and Excavations on Saipan, Tinian and Rota*. Fieldiana Volume 48. Chicago Natural History Museum, Chicago.

Thompson, Laura M.

1932 *Archaeology of the Marianas Islands*. Bernice P. Bishop Museum Bulletin 100. Bishop Museum Press, Honolulu.

1940 The function of latte in the Marianas. *Journal of the Polynesian Society* 49: 447–465.

Tomonari-Tuggle, M. J.

1991 Preliminary assessment of cultural resources, Laolao, Saipan, Commonwealth of the Northern Mariana Islands. Report prepared for the Northern Islands Company. International Archaeological Research Institute, Inc., Honolulu.

Topping, Donald M., Pedro M. Ogo, and Bernedita C. Dungca

1975 *Chamorro-English dictionary*. PALI Language Texts: Micronesia. University of Hawaii Press, Honolulu.

Ward, Graeme, and John L. Craib

1985 Preliminary report on archaeological research at Unai Bapot, Saipan, during January 1985. Unpublished manuscript on file at Division of Historic Preservation, Department of Community and Cultural Affairs, Saipan, Commonwealth of the Northern Mariana Islands.

Young, Fred J.

1989 *Soil Survey of the Islands of Aguijan, Rota, Saipan, and Tinian, Commonwealth of the Northern Mariana Islands*. United States Department of Agriculture, Soil Conservation Service, Washington, D.C.